# Investigation of the Stabilization of a Selected Expansive Soil in North Cyprus Using an Aqueous Polymer

**Mohammadreza Golhashem**

Submitted to the
Institute of Graduate Studies and Research
in partial fulfillment of the requirements for the degree of

Doctor of Philosophy
in
Civil Engineering

Eastern Mediterranean University
September 2019
Gazimağusa, North Cyprus

Approval of the Institute of Graduate Studies and Research

Prof. Dr. Ali Hakan Ulusoy
Acting Director

I certify that this thesis satisfies the requirements as a thesis for the degree of Doctor of Philosophy in Civil Engineering.

Assoc. Prof. Dr. Serhan Şensoy
Chair, Department of Civil Engineering

We certify that we have read this thesis and that in our opinion it is fully adequate in scope and quality as a thesis for the degree of Doctor of Philosophy in Civil Engineering.

Asst. Prof. Dr. Eriş Uygar
Supervisor

Examining Committee

1. Prof. Dr. Huriye Bilsel
2. Prof. Dr. İlknur Bozbey
3. Prof. Dr. Zalihe Nalbantoğlu Sezai
4. Prof. Dr. Yüksel Yılmaz
5. Asst. Prof. Dr. Eriş Uygar

# ABSTRACT

In this research, co-polymer of Butyl Acrylate and Styrene (CBAS) is utilized to improve volume change behaviour, undrained shear strength and internal stability of a cohesive soil obtained from Famagusta Bay, Cyprus. CBAS has low viscosity improving its adsorption in the soil microstructure and its ionic structure enhances its interaction within the soil fabric. The ease of application of CBAS, by shallow mixing or direct spraying onto soils, makes it favorable for engineered fills or just to be used as a wind or water erosion measure. Treatment of the soil samples with CBAS indicated significant improvement in the shrinkage and compressibility characteristics when it is added up to 5% of dry mass of soil, whereas the swelling behaviour is improved with further addition. The secondary compression rate is reduced down to approximately a quarter of the rate obtained from untreated specimens. The unconfined compressive strength is increased significantly even at low percentages of treatment. A similar efficacy is also observed from the results of internal stability tests. The mode of the collapse of specimens in the internal stability tests changed from being `gradual cracking and slaking` to `explosive` when CBAS is used. The cyclic wetting and drying behaviour is also tested, which indicated delay in the drying periods and a reduced swelling potential for the treated specimens. Microstructural changes in the soil fabric are observed with the use of scanning electron microscopy, which indicated that an effective formation of polymer soil interaction is achieved. X-Ray Diffraction analysis and Fourier Transform Infrared Spectroscopy are performed for observation of the effect of CBAS on microstructural interactions such as electrostatic bonding and changes in soil fabric.

**Keywords:** Aqueous polymer, Compressibility, Expansive clay, Internal stability, Stabilization, Unconfined Compressive Strength

# ÖZ

Bu araştırmada Mağusa Körfezi kıyılarında mevcut yüzeysel alüvyon tabakalarından elde edilen kohezyonlu zemin üzerinde uygulanan ‘co-polymer of Butyl Acrylate and Styrene’ (CBAS) isimli polymerin, bu zeminin hacim değiştirme, kayma dayanımı ve içsel stabilitesine olan etkisi değerlendirilmiştir. CBAS düşük viskositeli ve ionik yapısı sebebi ile hem mikroyapıya daha kolay emilimi olabilen hem de zemin içerisinde interaktivitesi yüksek bir katkı malzemesidir. Sığ zemin karıştrması veya püskürtme yötemleri ile uygulamada kolaylık sağlayabilen CBAS, mühendislik dolgularında veya sadece rüzgar ve su erozyonuna karşı koruma sağlamak için uygun bir seçenektir. Ağırlıkça %5’e kadar uygulanan CBAS katkısı, deney numunelerinin büzülme ve oturmaya karşı davranışını yüksek derecede iyileştirmesine rağmen, şişmeye karşı iyileşme bu seviyeden daha yüksek katkılarda sağlanabilmiştir. İkincil oturma hızı katkılı numunelerde dörtte bir oranında azalmıştır. Drenajsız kayma dayanımında çok düşük katkı oranlarında dahi çok yüksek seviyede iyileştirme sağlanmıştır. Buna benzer bir iyileştirme etkinliği içsel stabilite deneylerinde de elde edilmiştir. Bu deneylerde elde edilen göçme şekli ‘düzenli çatlama ve dağılma’ dan ‘ani göçme’ şekline değişmiştir. Tekrarlı ıslatma ve kurutma davranışı deneyleri katkılı numunelerde kuruma davranışını geciktirmiş ve şişme potansiyelini de azaltmıştır. Mikroyapıdaki değişimler taramalı electron mikroskopu ile gözlemlenmeye çalışılmıştır, ki bu sonuçlar efektif bir etkileşimi onaylar niteliktedir. X-ışınlı difraktometre ve Fourier Transform Infrared Spektometre deneyleri yine katkılı numunelerde mikroyapı etkileşimlerini gözlemlemek için uygulanmış ayrıca elektrostatik bağlar ve zemin yapısı incelenmiştir.

**Anahtar Kelimeler:** Şişen kil, Su bazlı polimer, Stabilizasyon, Oturma, Drenajsız kayma dayanımı, İçsel stabilite

To My Beloved Family

# ACKNOWLEDGMENT

Firstly, I would like to express my sincere gratitude to my supervisor Asst. Prof. Dr. Eris Uygar for the continuous support of my Ph.D. study and related research, for his patience, motivation, and immense knowledge. His guidance helped me throughout the research and writing of this thesis. I could not have imagined having a better advisor and mentor for my Ph.D. study.

Similar, profound gratitude goes to Prof. Dr. Huriye Bilsel, who has been a truly dedicated mentor. I am particularly indebted for her guidance and care.

My sincere thanks also goes to the board of Civil Engineering Department of Eastern Mediterranean University, for offering me the assistantship opportunity and leading me working as an assistant on diverse exciting courses.

I am also hugely appreciative to Mrs. Sandra Ghavam Shirazi, especially for sharing her English expertise so willingly.

Special mention goes to Mr. Ehsan Bahramzadeh, for his helping to get microstructure test results from Pharmacy Department of Eastern Mediterranean University.

Finally, but by no means least, thanks go to my Mother, Father and my sisters for almost unbelievable support and love.

# TABLE OF CONTENTS

# LIST OF TABLES

# LIST OF FIGURES

# LIST OF SYMBOLS AND ABBREVIATIONS

| | |
|---|---|
| $a_i$ | Number of Samples that Collapsed |
| $a_\propto$ | Number of Samples Which Remained Stable |
| $Al_2Si_2O_5(OH)_4$ | Kaolinite |
| ASTM | American Society for Testing and Materials |
| $CaCO_3$ | Calcite |
| $C_c$ | Compression Index |
| $c_i$ | Percentage Weight of Number of Collapses Observed |
| $C_r$ | Rebound Index |
| $C_u$ | Coefficient of Uniformity |
| CEC | Cation Exchange Capacity, meq/100g |
| CBAS | Copolymer of Butyl Acrylate and Styrene |
| $c_v$ | Coefficient of Consolidation, $m^2$/Year |
| $D_{10}$ | Effective Grain Size, mm |
| $D_{50}$ | Median Grain Size, mm |
| DDL | Diffuse Double Layer |
| DR | Ductility Ratio |
| e | Void Ratio |
| FT-IR | Fourier Infrared Spectronomy |
| $G_s$ | Specific Gravity |
| $K_{10}$ | Water Stability Index Based on 10 min |
| $K_{20}$ | Water Stability Index Based on 20 min |
| $K_{30}$ | Water Stability Index Based on 30 min |
| $K_f$ | Water Stability Index in Percentage |

| | |
|---|---|
| LL | Liquid Limit, % |
| $m_v$ | Coefficient of Volume Compressibility, $m^2/MN$ |
| $NaAlSi_3O_8$ | Albite |
| $p_{s'}$ | Swell Pressure, kPa |
| PI | Plasticity Index, % |
| PL | Plastic Limit, % |
| SEM | Scanning Electron Microscope |
| $SiO_2$ | Quartz |
| $t_{90}$ | Time Required to Complete 90% Consolidation, min |
| $t_i$ | Time in Minutes |
| $t_f$ | Time at Which the Water Stability Index Is Calculated. |
| UCS | Unconfined Compressive Strength |
| USCS | Unified Soil Classification System |
| w | Gravimetric Water Content, % |
| XRD | X-Ray Diffraction |
| $\Delta H/H_0$ | Axial Strain |
| $\Delta V/V_0$ | Volumetric Strain |
| $\Delta D/D_0$ | Diameteral Strain |
| $\Delta w$ | Change in Water Content, % |
| $\gamma_w$ | Unit Weight of Water, $g/cm^3$ |
| $\theta$ | Volumetric Water Content, % |
| $\sigma_{p'}$ | Effective Pre-Consolidation Pressure, kPa |

# Chapter 1

# INTRODUCTION

## 1.1 Expansive Soils

Working with expansive clays has been a very important issue in geotechnical engineering as they are considered to be problematic due to their depositional history and the nature of source rock characteristics. Some of these soils may also have a high-volume change character with an affinity to attract moisture. The volume change characteristics of cohesive soils (swelling and compressibility) in presence of water in arid and semi-arid regions has led to many constructional damages and challenged engineers over the years.

The volume changes and cracking of natural soils and engineered fills can occur with the seasonal moisture changes and lead to distress in the structures such as natural or man-made slopes, building foundations and highway embankments (Al-Homoud et al., 1995; Basma et al., 1998; Inyang et al., 2007; Akay et al., 2012; Miao et al., 2017). The magnitude of the damages on the civil engineering structures and infrastructures interfacing with expansive soils can be significant and sometimes become unrepairable (Langroudi and Yasrobi, 2009; Yazdandoust and Yasrobi, 2010).

The mineralogy of these soils can greatly influence their behaviour in periodic changes of the environmental conditions leading to moisture changes (Glenn et al., 1963; Rogers and Zane, 1997). Therefore, in a soil stabilisation method employing shallow

soil mixing, effective improvement of expansive soils can be achieved if the additive used can be adsorbed into the soil microstructure improving the stability of the soil fabric and the pore structure together.

North Cyprus is located in an arid and semi-arid region which contributes to the cyclic swell and shrinkage behaviour of expansive clays due to significant moisture changes throughout the seasons in a year. Although, there is extensive research carried out in the past (Bilsel and Tuncer, 1998; Nalbantoğlu and Tuncer, 2001; Nalbantoğlu, 2004; Nalbantoğlu and Tawfiq, 2006; Atalar and Das, 2009) for expansive clays of Cyprus, there are no research on improvement of expansive clays with aqueous polymers.

## 1.2 Background

Various methods have been considered by geotechnical engineers for surficial stabilization of clays. Amongst all methods used in practice, it is common to utilize shallow mixing with a stabilizing agent (pozzolanic or chemical admixture) followed by compaction. The intent is to improve the interactions within the clay fabric and interactions of these with other ions present in the medium such that permeability, shear strength, and overall durability of the compacted clay are improved (Lahalih and Ahmed, 1998; Guneya et al., 2007; Inyang et al., 2007; Yazdandoust and Yasrobi, 2010; Maaitah, 2012; Soltani, 2016; Tajdini et al., 2017). Based on the properties of a particular clay and the surrounding environmental conditions, various stabilization agents might be considered. The main goal of the stabilization is to ensure the internal stability of the clay fabric by controlling the water adsorption (Hudyma and Avar, 2006; Anagnostopoulos, 2007; Estabragh et al., 2011; Seco et al., 2011; Huang and Liu, 2012; Miao et al., 2017).

The internal stability of clay is strongly correlated with the stability of the fabric and agglomerations, which can be achieved by the stabilization of the macropores with a filler or by provision of cementitious (chemical or electrostatic) reactions in macro and micropores. The use of stabilizing agents such as cement, fly ash, and lime for improvement of clay internal stability has been well documented, successfully providing stability through both mechanisms. The use of other nontraditional stabilizers such as enzymes, resin, and other types of polymeric fibers has also been reported (Anagnostopoulos, 2007; Estabragh et al., 2011; Liu et al., 2011; Arasan et al., 2017; Ganapathy et al., 2017; Öncü and Bilsel, 2017; Pu et al., 2019).

## 1.3 Aqueous Polymers

Aqueous polymers are especially important from the environmental perspective, and also in recent years, as the awareness of sustainability concerns has increased, there has been a growing interest amongst researchers to pursue investigation about the use of waterborne polymers in the stabilisation of engineered fills. Waterborne polymers are generally harmless to the environment and can help provide internal stability of the soil fabric against water absorption. (Gamble, 1971; Bae et al., 2006; Seco et al., 2011; Yılmaz et al., 2012; Zezin et al., 2015; Soltani, 2016; Tajdini et al., 2017; Xiao et al., 2017).

Aqueous polymers, in particular, can easily be diluted in water and applied in shallow mixing and compaction of clays for provision of engineered fills (Azzam, 2014; Rezaeimalek et al., 2018). Compared to the method of applying traditional additives in dry form, a diluted aqueous polymer has the advantage of being effectively absorbed by the clay. This eases the mixing process prior to compaction and eliminates the need

for a curing period after application (Inyang et al., 2007). Aqueous polymers can also provide effective dust control (Bae et al., 2006; Ding, 2018; Xu et al., 2018).

One of the common aqueous polymer products used in the industry is called the `copolymer of butyl acrylate and styrene` (here onwards will be referred as CBAS for simplicity). CBAS is generally used in the industry as part of the treatment for decorative coatings and as an effective adhesive. It has high alkali resistance, low water adsorption. It is non-hazardous and inert.

Interaction between CBAS chains and clay particles is considered to be based on two different mechanisms; a) by forming chains or membrane of CBAS around clay agglomerations in macrospores, b) by forming continuous or discontinuous chains within the clay fabric in micro scale. It is also important to note that, depending on the ion concentration around clay double diffuse layer, CBAS is likely to be adsorbed in between clay particles by electrostatic interaction.

The performance of the chain formation of CBAS, notwithstanding it increases the flexibility, tends to hold the clay agglomerations and clay associations together against internal forces that will be developed upon water adsorption. As a result, it can be expected that there would be a reduction in the volume change potential of the clay and an improvement against softening, wind and water erosion. CBAS would support clay structure in both microspores and macrospores which are key for wind and water erosion resistance (Williams et al., 1968; Barthes and Roose, 2002; Niewczas and Witkowska-Walczak, 2005; Xiao et al., 2017).

## 1.4 Aims and Scope of the Study

The purpose of this research is to study the effect of aqueous polymer as an environmental friendly additive on stabilization of expansive clay in arid and semi-arid regions such as North Cyprus. In order to evaluate the performance of CBAS, an extensive set of experiments are performed to measure the volume change, unconfined compressive strength, water stability (internal stability of clay) and durability of a selected expansive clay soil. As the performance of the CBAS treated soil is likely to be affected from moisture changes, a special testing program is arranged. Test groups involving specimens with varying initial water content are formed. In this way, the impact of water adsorption potential and the rate of water adsorption on the performance of treated specimens are also observed.

The CBAS treatment is applied at various percentages by dry mass of soil. Some of the testing methods required only a minor addition whereas others needed more treatment to show the impact of the stabilisation.

The microstructural effects are observed using Fourier Infrared Spectronomy (FT-IR), X-Ray Diffraction and Scanning Electron Microscopy. Limited data obtained showed that there is effective interaction between the CBAS and the soil, which is mostly in the form of electrostatic bonding.

## 1.5 Outline of the Thesis

In this thesis, the results of the testing and analysis of the effect of CBAS stabilisation on a selected cohesive soil are presented. The treated specimens' performances with respect to internal stability (water stability), unconfined compressive strength, one-dimensional swell, compressibility and cyclic wetting and drying are measured. In

addition, microstructural interaction of the CBAS with soil is investigated using FTIR, X-Ray Diffraction and Scanning Electron Microscopy.

The following is an outline of the thesis contents:

- Chapter 2 introduces a brief review of basic concepts of clay physics relevant to the study of clay-polymer interactions. The concepts of clay particle structures, interactions between water and solid particles and parameters affecting the volume change in clays such as cation exchange capacity and diffuse double layer are presented. A review of the behaviour of expansive clays, different methods of soil stabilization i.e. mechanical stabilization and chemical stabilization, different type of soil stabilizers such as traditional and non-traditional chemical stabilizers are presented in this chapter. A summary of the literature survey on soil water stability (internal stability), different types of polymer i.e. natural polymers, synthetic polymers, resins and water-soluble polymers and their effect on soil stabilization is included. The factors affecting the soil-polymer reaction are explained and the role of polymers on the internal stability of the clay structure is reviewed.

- Chapter 3 introduces the materials and methods used in this research and explains the approach taken for the testing strategy. The methodologies used in specimen preparation and whilst conducting the experiments are explained in detail. The methods used in the analysis of test results are also presented.

- Chapter 4 presents data analysis, tables and comparative graphs of the results obtained from various tests. In this chapter, a thorough review and analysis of the results are presented, discussions on the behaviour observed are provided.

- Chapter 5 summarises the outcomes of this research with emphasis on significant findings. The limitations of the research and recommendations for further studies are also included in this chapter.

# Chapter 2

# LITERATURE REVIEW

## 2.1 Introduction

In this chapter, a summary of literature gathered from past research on soil stabilization using aqueous polymers is presented. The nature of clay-water electrolyte system is reviewed and parts related to this thesis are repeated briefly to provide a background to the laboratory work and the interpretations carried out using the test results.

The common types of polymers used recently for soil stabilization and the mechanisms through which they interact with the soil are discussed briefly.

In order to aid comparisons to be carried out in the discussion and analysis chapter (Chapter 4), the outcomes of selected similar studies are presented.

## 2.2 Basic Concepts of Clay Physics Relevant to Clay-Polymer Interactions

### 2.2.1 Clay Structure

Clays can very useful in some of the construction projects due to their water retention characteristics and elasticity, i.e. ability to shear without significant disintegration of their mass characteristics. Such construction project might involve provision of an impervious core for an earth dam, a landfill liner or a capping layer. However, the very same characteristics can also prove to be problematic, for example when a layer of

clay underlays a building foundation, due to ability to change in volume with respect to moisture changes even during natural seasonal variations.

The main component of clays are crystalline minerals, formed of silicon, aluminum, magnesium, iron, hydroxyl groups and atoms. Clays also have a net negative electrical charge. The structure of clay minerals is formed from two different structural units namely: silicon tetrahedron and aluminium or magnesium octahedron. The structure of clay minerals plays an important role in the behaviour of clays upon changes in the soil moisture. The negative charge of clay particles is due to the isomorphous substitution of silica by aluminium which enables the soil to attract and hold the positively charged cations. When the isomorphic substitutions occur in a crystal the properties of the clay mineral can also change (Grim, 1968; Craig, 2004).

### 2.2.2 Soil Water

The surface of clay particles interacts with the soil water. Due to strong affinity of oxygen in the water molecule, the bonding between hydrogen and oxygen atoms is a polar covalent bond hence water has a dipolar nature. Clay water can be double layer water, adsorbed water or free water. Adsorbed water is a very thin layer of water with more viscosity than free water that is attached to the negative surface of the particle. The movement of adsorbed water is only parallel to the surface of the clay particles. Double layer water molecules are held by attraction forces. This layer of water is formed between the surface of the particles and the soil solution. The plastic properties of clay soils depend on the orientation of the water surrounding the particles (Mitchell and Soga, 2005).

### 2.2.3 Diffuse Double Layer

The area around the particle where the cations from the solution and negative surface of the clay interact is called diffuse double layer. The chemistry of the pore water plays an important role in the properties of diffuse double layer. One of the parameters that influences the properties of the clays is the nature and the number of exchangeable ions. The negative charge of the clay particle tends to cause attraction for the cations present in the soil water. The total quantity of cations that are held by clay surface through electrostatic forces is called cation exchange capacity (Park and Seo, 2011).

As a result of the above interaction in the soil microstructure a soil-water-electrolyte system is formed, characteristics of which are important in the analysis of performance of any additive used in the stabilization of fine grained soils.

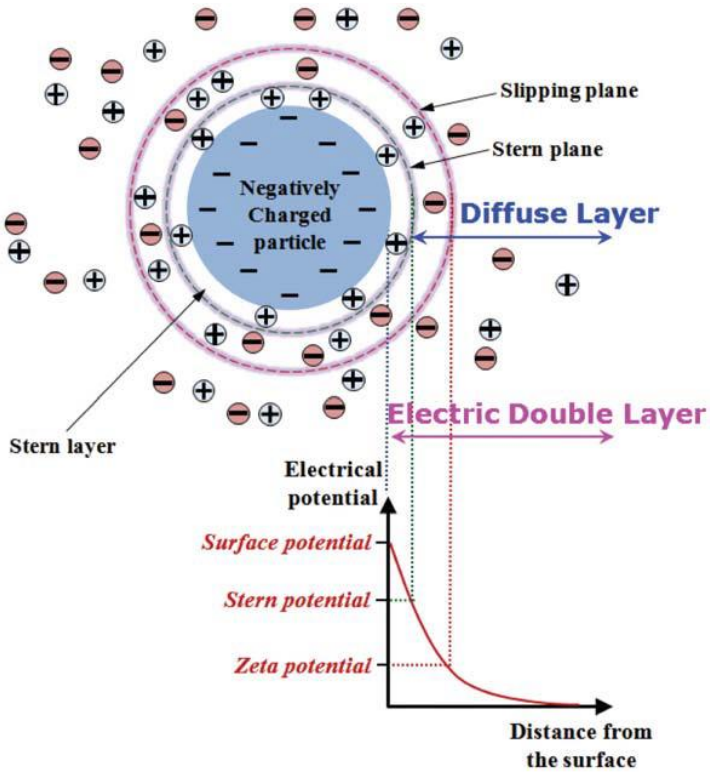


Figure 2.1. Diffuse double layer around clay particle (Park and Seo, 2011)

In Figure 2.1 an illustration of clay diffuse double layer and depiction of this within the context of soil-water electrolyte system is presented.

## 2.3 Expansive Soil

Swelling of expansive clays in presence of water in arid and semi-arid areas has led to many constructional damages and challenged engineers over the years. The magnitude of the damages in the structures that are built in expansive soils can range from minor cracks on the interior of the building to irrecoverable displacements in infrastructures (Langroudi and Yasrobi, 2009; Yazdandoust and Yasrobi, 2010). Weathering conditions play an important role in wetting and drying cyclic process and significantly affect the swelling and shrinkage characteristics of the expansive soil (Basma et al., 1996; Guneya et al., 2007). The nature of the clay minerals and their composition combined with the physicochemical reactions between the particles is the main cause for the swelling behaviour of expansive clays. Internal crystallographic configuration of the soil minerals determines their hydration characteristics which will affect the soil's swelling potential (Inyang et al., 2007). Another factor that influences the volume change in clays is the colloidal surface interactions. Therefore, to improve or eliminate the problematic properties of the soil several stabilization methods are used by engineers.

## 2.4 Soil Stabilization

Soil stabilization aims at improving some of the soil characteristics in order to enhance the performance of these soils. The leading forms of stabilization are mechanical or chemical stabilization. If there is a need to accelerate the process of stabilization or extra strength and stiffness is required, the two types of stabilization can be combined. Hence, the appropriate method must be chosen based on the nature and surrounding environment of the soil (Naeini and Ghorbanalizade, 2010; Estabragh et al., 2011).

### 2.4.1 Mechanical Stabilization

In the mechanical stabilization, a physical process takes place to improve the soil properties. In the process of physical stabilization, the environmental conditions and physical nature of the soil will be changed. There are different methods of mechanical stabilization such as shallow soil compaction, deep soil mixing, lime piles, stone columns etc. (Fannin and Raju, 1993; Lima, 2000; Shukle, 2002; Jafari et al., 2013). The application of these techniques depends on the purpose of the project, soil type, the surrounding environmental conditions, and the degree of improvement needed.

Soil Compaction is a mechanical stabilization method, which is commonly used in most of the earthworks projects. The ability of soil to be compressed by elimination of part of the void volume leads to an increase in the dry density of the soil and enhances the shear strength and compressibility behaviour. However, sometimes compaction may not be sufficient alone to improve the soil properties to the required degree, hence in conjunction to this, soil is also mixed with chemical or pozzolanic additives to create additional bonding in the soil structure (Dotto et al., 2004; Barbhuiya et al., 2009; Kalkan, 2011; Goodarzi et al., 2015; Ghavam Shirazi et al., 2017).

According to Abiodun and Nalbantoglu (2014) stabilization of expansive clay with lime pile method increases the optimum water content and maximum dry density of the clay in long curing periods (Figure 2.2).

Bell (1996) studied the effect of lime as a stabilizer for clay soil. The results obtained from this research suggests that addition of lime to the expansive soil increases the optimum water content and the soil hat to be compacted in wetter condition than its

original state. Bell (1996) also stated that compaction curves tend to flatten whereas in cement stabilized soils this trend is not observed (Figure 2.3).

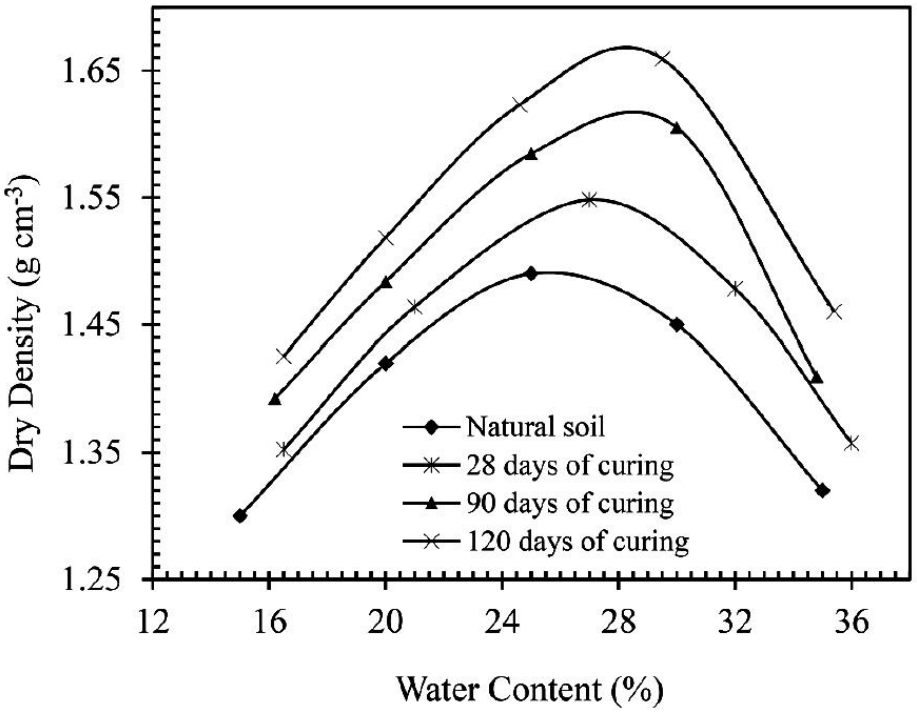


Figure 2.2. Compaction characteristics of the soil blocks treated with lime piles (Abiodun and Nalbantoglu, 2014)

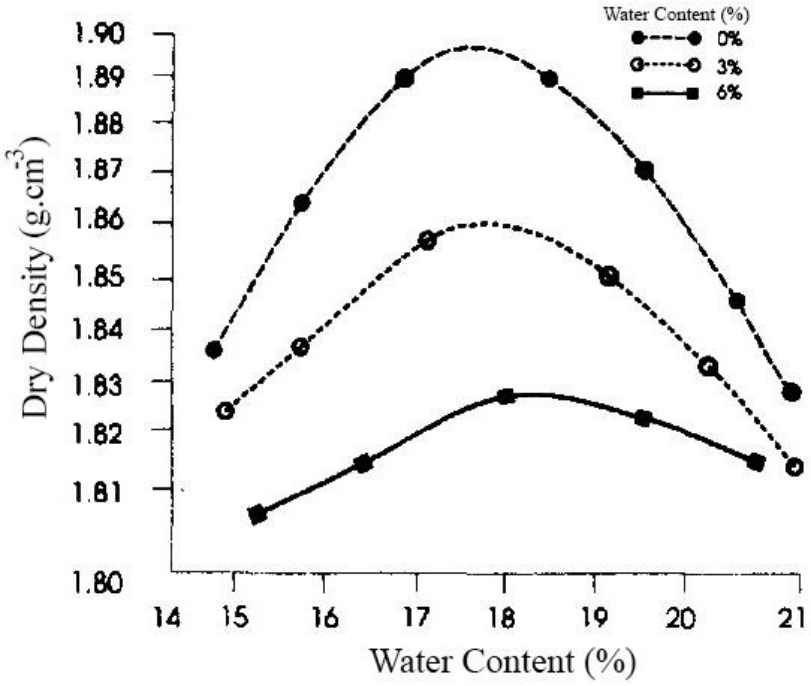


Figure 2.3. Compaction characteristics of the soil treated with lime (Bell, 1996)

### 2.4.2 Chemical Stabilization

Abiodun and Nalbantoglu (2014) assessed the effect of lime pile technique on improvement of engineering properties of expansive clay. Their results showed that this method of deep ground chemical stabilization has positive effect on engineering properties of expansive clay such as unconfined compressive strength and stiffness (Figure 2.4).

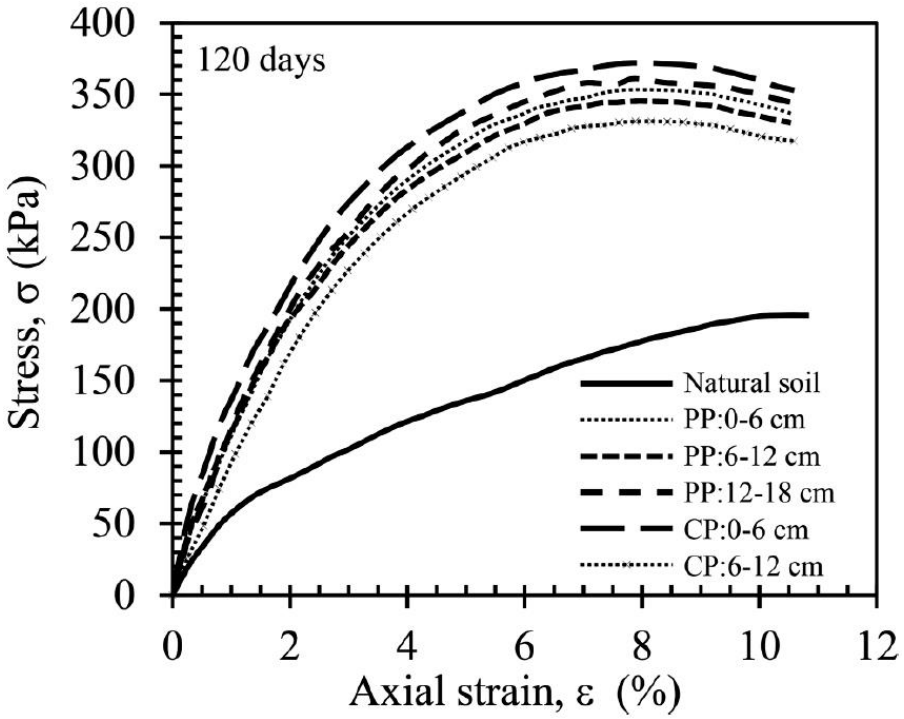


Figure 2.4. Unconfined compressive strength of soil treated with lime piles (Abiodun and Nalbantoglu, 2014)

The results found by Goodarzi et al. (2015) exhibits that although the addition of lime to the highly expansive soil reduces the soil expansion however, stabilizing the soil with lime-silica fume mixture has an even more significant results on reducing the swelling potential (Figure 2.5). It was also discovered that when lime-silica fume combination is used to stabilize the soil, the reduction in swelling occurs in shorter curing periods. Also, comparing to the results of stabilization with lime alone, less

amount of lime (approximately half) is required to achieve the same results when lime-micro silica fume mixture is used.

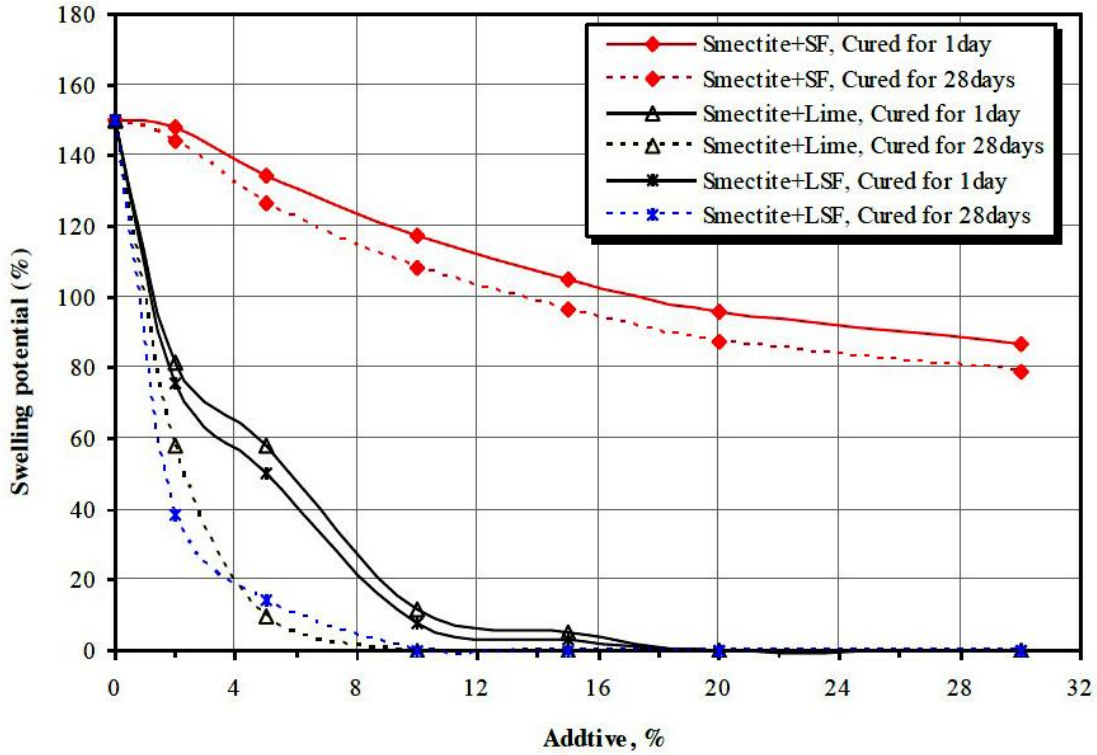


Figure 2.5. Effect of curing time and stabilizer addition on the swelling potential of smectite sample (Goodarzi et al., 2015)

Al-Mukhtar et al. (2010) assessed the effect of lime on behaviour of expansive clay (Table 2.1). The results showed that the addition of lime reduces the plasticity of the soil and the swell pressure after short curing periods. It was observed that with the increase in the amount of lime the swell pressure dramatically decreases. 4% of lime reduced the swelling pressure by 72% and 10% of lime reduced the swell pressure to 0 after 7 days of curing period.

Maaitah (2012) also reported that addition of sodium silicate and lime as stabilizing agent to the soil reduces the swell potential (Table 2.2). The findings indicate that the

addition in sodium silicate also reduces the swelling however lime has a more significant effect on the swell potential.

Table 2.1. Evolution of swelling pressure (SP) of Impersol with curing time and lime added (Al-Mukhtar et al., 2010)

| Lime (%) | 0% | 4% | 6% | 10% |
|---|---|---|---|---|
| Curing time, day | SP (kPa) | SP (kPa) | SP (kPa) | SP (kPa) |
| 0.0625 | 1060 | 293 | 106 | 9 |
| 7 | | 196 | 33 | 0 |
| 28 | | 142 | 6 | 0 |

In the process of chemical stabilization, the structure of the ions and the inter particle bonding forces will be altered by introducing the stabilizing agent to the soil mixture. Cement, lime and fly ash are traditionally used when chemical stabilization is performed (Nalbantoglu and Gucbilmez, 2002; Barbhuiya et al., 2009; Kalkan, 2011; Maaitah, 2012; Abiodun and Nalbantoglu, 2014; Li et al., 2018; Mahrous et al., 2018). However, in recent years nontraditional stabilizers like polymers, enzymes and resins has attracted much attention from researchers.

Table 2.2. Effect of lime and sodium silicate on swelling (Maaitah, 2015)

| $CaCO_3$ | $NA_2Sio_3$ | Free swelling (%) | Swelling pressure (kPa) |
|---|---|---|---|
| 0 | 0 | 10.5 | 240 |
| 0 | 1 | 9.1 | |
| | 2 | 8.7 | |
| 2 | 1 | 6.7 | |
| | 2 | 4.2 | |
| 4 | 1 | 3.3 | |
| | 2 | 1.5 | 2.3 |
| 6 | 1 | 2.8 | |
| | 2 | 0.2 | 0 |

Lime is one of the most commonly used soil stabilizers in geotechnical engineering, especially when the end goal is to improve the soil's strength, stiffness and stability

(Eades and Grim, 1960; Eades et al., 1962; Glenn and Handy, 1963; Basma and Tuncer, 1991; Bell, 1996; Basma et al., 1998; Bozbey and Garaisayev, 2010). Lime can be added to the soil directly or can be used in the lime pile technique to improve the soil (Broms and Boman, 1979; Agus and Hung, 2006; Abiodun and Nalbantoglu, 2014). In stabilization with traditional chemical stabilizers such as lime, the exchangeable ions from clay surface are replaced with lime's divalent calcium ions. Due to the double positive charge of calcium ions, they form a good bond with the clay surface. This interaction between calcium ions in the lime and negatively charged surface of clay colloids leads to reduction of diffuse double layer (DDL) and hence reduction in double layer water and swelling potential of the clay soil (Diamond and Kinter, 1965). This process occurs in two steps. The first step is known as soil modification, at this stage the exchange of ions rapidly takes place. The second step is known as soil stabilization, at this stage which can take months or even years to complete the pozzolanic reaction takes place between soil particles and lime. In some cases, depending on the type of the soil it is required to use additional pozzolanic materials such as silica fume to enhance and accelerate the pozzolanic process (Kalkan, 2011).

Fly ash is another traditional chemical stabilizer that is used as a pozzolanic material for soil stabilization (Nalbantoglu, 2004; Koteng and Chen, 2015). Flay ash is a by-product of coal combustion and contains calcium, silica and alumina oxides. The amount and ratio of these oxides determines the reactivity of fly ash. Therefore, fly ash can demonstrate a slow pozzolanic reaction rate in stabilization process in these cases the strength development might take place at longer curing periods (Barbhuiya et al. 2009). However, by mixing fly ash with other additives such as lime, bio-cement

and geopolymers, this traditional stabilizer improves the physical and chemical properties of the soil (Cokca, 2001; Nalbantoglu, 2004; Li et al., 2018; Mahrous et al., 2018). Nalbantoglu, (2004) assessed the effect of class C fly ash on behaviour of expansive clay, Figure 2.6 and 2.7 demonstrates how fly ash can be used effectively in the stabilization of the expansive soil characteristics. The results show that with the increase in the amount of fly ash and also with longer periods of curing time, the swell potential decreases. The decrease is associated with the ability of fly ash added to form new minerals through pozzolanic reactions, also leading to new mineral formation.

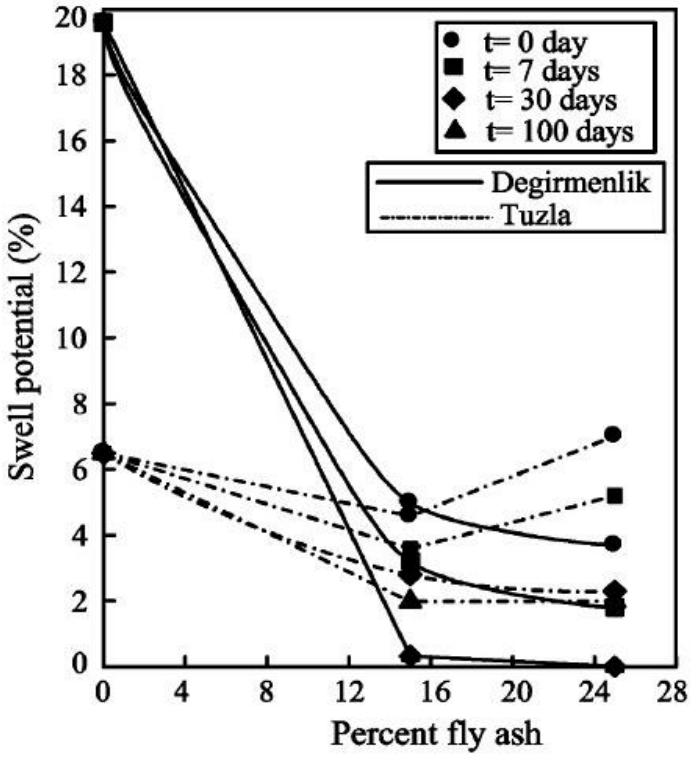

Figure 2.6. Variation of swell potential with percent fly ash and curing time for Degirmenlik and Tuzla soils (Nalbantoglu, 2004)

One of the major draw backs of utilization of traditional stabilizers is that often a lengthy curing time is required for the stabilization process to take place and in most cases relatively large quantities of additives are needed in order to achieve the desired strength. Thus, these additives are not suitable for certain projects such as military

operations that cannot afford the shipment of large quantities of construction materials or delaying the projects due to the long stabilization process (Naeini and Ghorbanalizade, 2010).

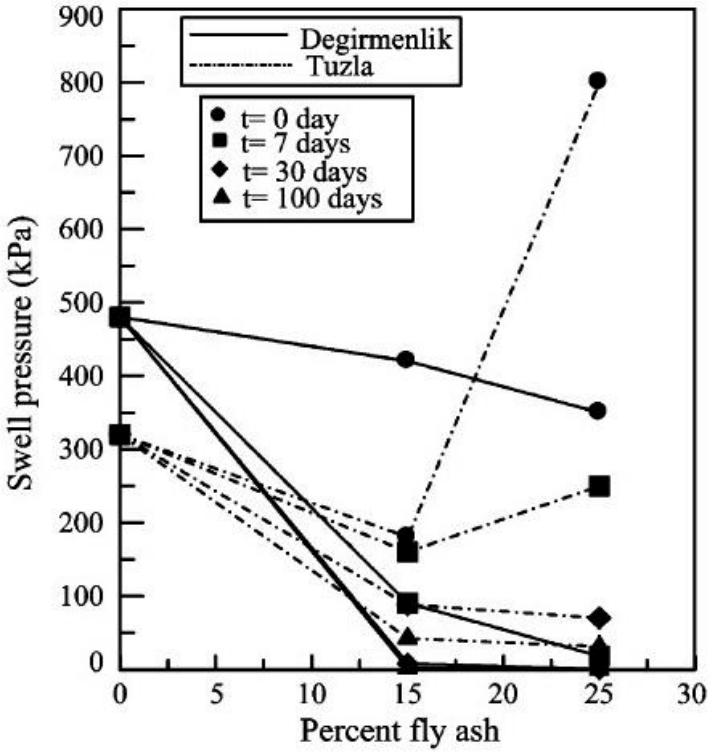


Figure 2.7. Effect of fly ash and curing time on the swell pressure values of Degirmenlik and Tuzla soils (Nalbantoglu, 2004)

There is relatively little research covering the stabilization method with nontraditional chemical additives. Ionic stabilizers, resins and polymers are some of the nontraditional chemicals that are used in soil stabilization. Ionic stabilizers change the concentration of the electrolytes in the soil solution and by doing so the process of the cation exchange in the pore fluid will be altered and clay minerals attract the cations with higher valance. Due to these reactions the affinity of the clay surface for cations reduces which leads to the reduction in thickness of DDL and potential flocculation of clay particles.

As result of this method of stabilization the plasticity and swell potential will be reduced however, the drawback of this method is that due to the alterations between acidic and basic phases of electrolyte pore fluid the changes in particle structures occur over long period of time as presented in Figure 2.8 and 2.9, using data from Tingle et al. (2007).

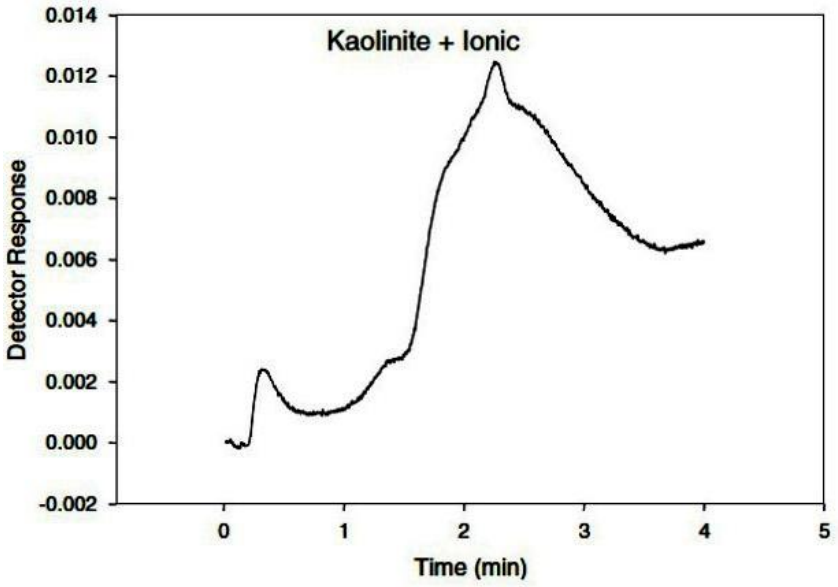


Figure 2.8. data showing time dependency of the pore fluid interaction for ionic stabilizers (Tingle et al., 2007)

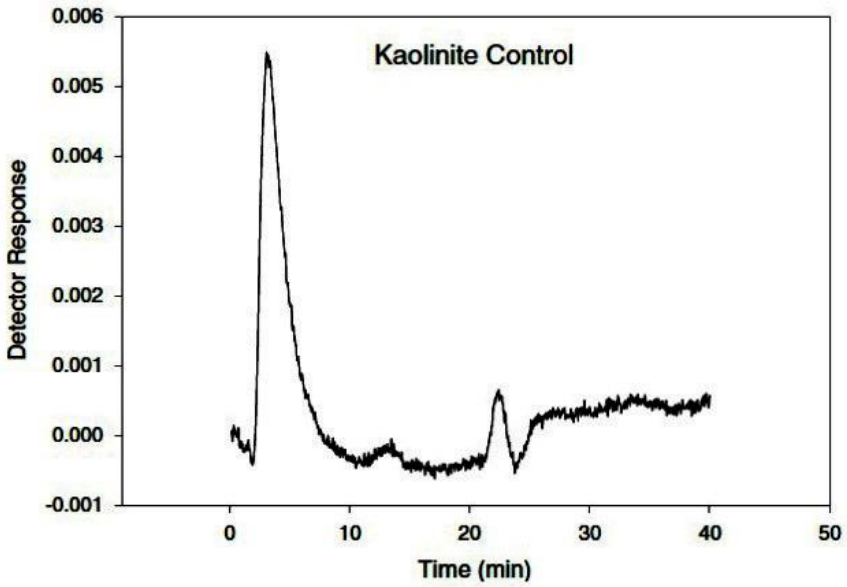


Figure 2.9. data showing time dependency of the pore fluid interaction for control sample (Tingle et al., 2007)

### 2.4.3 Polymer

The structure of polymers is mainly made of large molecules or macro molecules known as monomers. The composition of the polymer consists of multiple repetitions of these subunits. Different monomers participate in the polymerization process to create polymers however, different arrangement of molecule compounds creates unique physical properties such as viscoelasticity, toughness and tendency to form crystalline or semi crystalline structures. Due to their broad range of properties polymers have different classifications. Polymers can be categorized in to two groups: Natural Polymers and Synthetic Polymers. Figure 2.10 illustrated a general structure of a copolymer.

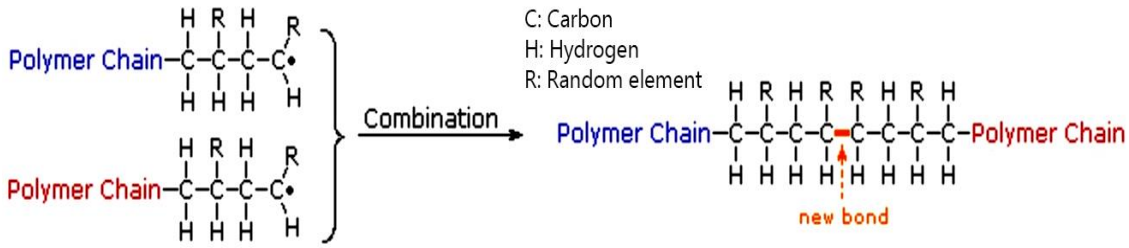


Figure 2.10. Example structure of a copolymer (Orts et al., 2007)

Polymers are also among nontraditional chemical stabilizers. When polymer is used as the stabilizing agent, the soil particles will be coated by the polymer and physical bonds will start to form after the evaporation of the emulsion water. If the polymer is able to coat the soil particles properly the primary physical bonding will be stronger thus as result the soil strength will be improved. Therefore, it is very important to make sure that the soil and polymer emulsions are thoroughly mixed. The polymers that are used in soil stabilization must have high tensile strength. The specification of the polymer depends on the environmental conditions, type and characteristics of the soil and the project. For example, the type of the polymer that is used to improve the

properties of the soils that are utilized in road constructions must be resistant to water in order to create a water-resistant layer around the soil particles (Tingle et al., 2007). Or to control the swelling in expansive soils, chemical stabilizer must affect the attractive and repulsive forces between positive counter-ions and negative ions in the diffuse DDL in order to reduce the expansion of the interlayer space while enhancing the bonding between clay particles. Aqueous polymers can achieve these functions (Inyang et al., 2007).

#### 2.4.3.1 Natural Polymers

In general, the process of soil stabilization with natural polymers consists of 3 phases of filling, chemical reaction and enwrapping. Natural polymers have gained worldwide importance as a stabilizing additive to the soil. (Lahalih and Ahmed, 1998; Liu et al., 2011).

Biopolymers are a type of natural polymer that are obtained from non-edible parts of plants. Natural polymers have long chain structures therefor they form different chemical groups based on their structure. Once polymers are mixed with the soil the physiochemical attraction between soil surface and the gel, bonds the particles together. Natural polymers can be used as soil stabilizers in different civil engineering projects. For example, Khatami and O'Kelly (2012) tested different concentration and combinations of two biopolymers to improve the strength properties of the sand. One of the tested materials was Agar. Agar is known to give the highest improvement in mechanical strength among biopolymers. However, agar molecules are negatively charged thus to further enhance the effect of agar the researchers added a positively charged biopolymer as an intermediate agent which also has good compatibility with agar, named modified starch.

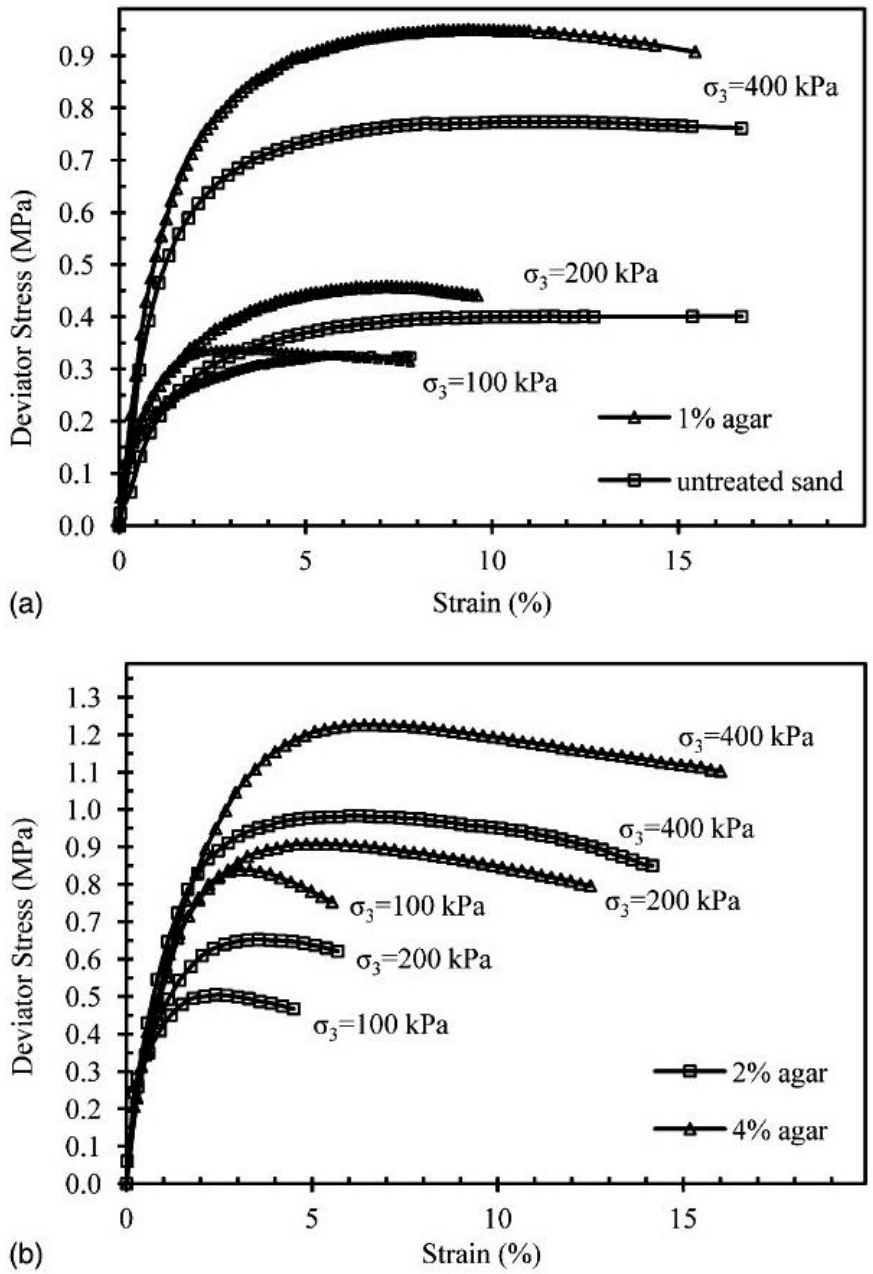


Figure 2.11. The improvement attained using Agar (Khatami and O'Kelly, 2012)

The results obtained by Khatami and O'Kelly (2012) show that the combination of agar and modified starch had positive effect on sand's strength characteristics and the combination of both materials encouraged the inter particle electrostatic reactions and enhanced stiffness. The results also indicated that the compressive strength and stiffness increased when higher concentration of agar is used (Figure 2.11).

In addition to this, Liu et al. (2011) investigated the potentials of a new type of organic polymer named STW (acetic-ethylene-ester polymer) as a soil stabilizer. As the other natural polymers, when STW is mixed with soil, the voids will be filled with the polymer then the rest the polymer will engage in a chemicals reaction with the clay surface which results in the formation of hydrogen, van der waals or ionic bonds. Due to the formation of these bonds soil particle surface will be enwrapped and interlink with the polymer molecules. This will result in a membrane like structure that is viscous and elastic. However, the process filling the voids and physicochemical reaction requires time therefore it has been observed that unconfined compressive strength increases with a higher rate at the first 24 hours and then the rate drops until it reaches a constant value. Also, the amount of STW added affects the unconfined compressive strength up to a percentage addition of 5% to 30%, with significant influence of curing time. It is shown that the addition of up to 30% of STW increases the amount of voids filled as well as increasing the interlocking forces between polymer and clay particles. However, further increasing the amount of STW (more than 30%) might not have the desired effect because the soil particles and polymer molecules will have fully reacted by this point. The findings of this study show that the addition of STW changes the soil fabric and positively affects the water stability, strength and erosion resistance of the soil. These improvements are resulted by the formation of membrane structure and physiochemical bonds between soil particles and polymer molecules. Due to improving the erosion resistance of STW treated soil, this natural polymer can be successfully used for clay slope surface stabilization.

Galán-Marín et al. (2010) used alginate as a natural polymer. Alginate is a plant based polymer that is extracted from seaweed and brown algae. Alginate gel contains 98

wt.% of water and is considered a hydrophilic material. In this research wool fibers were also added to the soil matrix as a natural fiber which prevented the visible shrinkage cracks in the drying process. The results showed that the addition of wool alone did not sufficiently affect the performance of the soil-fiber composites however, addition of alginate increases the compressive strength of the soil by 69%. When two natural additives were used together significant improvements were observed in soil's mechanical characteristics. However, the results showed that lower quantities of wool (0.25%) yields to better results. The addition of alginate as a natural polymer and wool as a natural fiber are found to result to higher strength than the traditional stabilizers such as cement and lime.

#### 2.4.3.2 Synthetic Polymers

In the recent years synthetic polymers are rapidly replacing the traditional stabilizers. In the stabilization process, synthetic polymers bind clay particles together and act as a strengthening agent. Different researches conducted on synthetic polymers as a soil stabilizer and their effect on binding the soil particles.

Heller and Keren (2002) investigated the effect of anionic polyacrylamide (PAM) on soil suspensions and its effectiveness on binding the bridging clay particles and overall clay structure stability. PAM is a synthetic polymer with long molecular chain. The tests were conducted on the sodium-montmorillonite that contained various concentrations of NaCl. The results showed that higher electrolyte concentration positively affects the ability of the polymer to bridge between adjacent clay flocs also molecular weight and degree of hydrolysis of the anionic polymeric more effective in stabilization of soil aggregates.

Concentrated flow and rain fall can cause erosion in exposed soils. When exposed soils are located in large areas of construction the erosion will increase the sedimentation which can flow through neighboring streets, surrounding developments and finally contaminated rivers or lakes. Orts et al. (2007) discussed the effect of synthetic polymer on controlling erosion during construction and controlling dust clouds in helicopter landing pads. It is stated that, dust clouds can be highly affected by the wind velocity and soil type. Authors suggested that PAM is an effective synthetic polymer for reduction of sediment loss that is caused by erosion by more than 90%. PAM keeps the constructional waste and other chemical and biological contaminants at the construction site, it also prevents top soil run of and sediment run off to enter waterways of costal zones.

Iyengar et al. (2012) used synthetic polymer to stabilize the pavement subgrade. As the majority of roads have asphalt-based pavements the authors suggested to use the polymer-based binders as a stabilization method instead of traditional binders such as Portland cement. They used three different polymers as binders and compared the results with untreated soil and soil stabilized with Portland cement. The results show that polymer-stabilized subgrades have higher toughness, stiffness and unconfined compressive strength compared to the untreated and cement-treated soils. For example the unconfined compressive strength measured for polymer treated specimens is observed to be approximately 1.5 to 2.0 folds of the results from other specimen groups. The results also indicate that the polymer-stabilized soil distributed the applied load better, resulting in reduction of cracking in the pavement and providing an extended service life for the roadway.

As mentioned before polyacrylamide is a synthetic polymer with long chain molecular structure. By binding the soil particles together polyacrylamide is mostly used as a strengthening agent which holds the soil in place. Maghchiche et al. (2010) examined a mixture of soil, synthetic polymer (polyacrylamide) with cellulose and plastic waste with the purpose of retaining water and humidity for plants at arid and semi-arid areas. The results demonstrate that the blend of synthetic and natural polymers improves the physical properties of the soil. The findings show that the mixture of polyacrylamide and cellulose increased the water retention ability of the soil against evaporation losses which will enhance the plant growth when the crops use the retained water by the polymer. Also, synthetic polystyrene can be used as a barrier in the sub layer to control the water loss. These founding can be especially important in desert regions where retaining the water by using polymers to bind the soil particles together and enhance the physical properties of the soil can tremendously help the agriculture system.

#### 2.4.3.3 Resins

Resins can be classified as a nontraditional chemical stabilizer. Resins are used to stabilize different types of soil such as sands, silty sands and clays (Lahalih and Ahmed, 1998; Naeini and Ghorbanalizade, 2010).

Production of resins are the same as polymers in which large number of monomers will be combined in the polymerization process and form long-chain molecules. According to their polymerization process resins can have two main types: thermoplastic resins and thermosetting resins. In thermoplastic resins the long-chain molecules are held together by van der waals forces which are relatively weak. This will cause the chains to separated therefore they can slide over each other. Although the chains are held by relatively weak bonds however, along the chain there are strong

chemical bonds. Therefore, when thermoplastic resins are heated, the intermolecular forces will be weakened and the material softens and becomes flexible and when it is cooled it will solidify again. But in thermosetting resins, the chains are cross linked. The cross-linking process can take place under the application of heat and pressure or in the room temperature therefore due to the strong chemical bonds the product of thermosetting resins will not flow and cannot be softened (Estabragh et al., 2011).

In General resins show higher resistance in alkaline and humid environments (Aggarwal et al., 2007). There are different types of resins which are used for different stabilization projects. Some resins such as asphalt emulsions which fall under petroleum resins category, are not soluble in water therefore, in the projects that are sensitive to moisture these resins can be used as waterproofing agents. Synthetic isoalkane fluids are another type of resin that does not have the ability to dry and form a reaction with soil particles even after long curing periods. This type of resin effects the inter particle friction and causes the soil particles to disperse therefore it can reduce the compaction effort. These types of resins do not form a significant bond between soil particles which results in minimal enhancement in strength characteristics of the soil (Tingle et al., 2007).

However, some resins have the ability to improve the physical and mechanical properties of the soil such as compaction strength and also increase the unconfined compressive strength and tensile strength in cohesive soils (Estabragh et al., 2011; Anagnostopoulos and Papaliangas, 2011). Resins can be anionic or cationic thus due to negatively charged surface of clays, cationic resins are typically used soil stabilization purposes. When resins are applied to the soil, the emulsion water will be adsorbed by the clay surface and the resin will coat the particles therefore the strength

improvement depends on the mixing process to ensure that the soil particles are adequately coated with the resin.

Naeini and Ghorbanalizadeh (2010) used the combination of resin and polyamide to stabilize the silty sand soil under wet and dry conditions. Polyamide worked as a hardening agent in this mixture providing a very high compression and tensile resistance, due to the bond strength attained in the microstructure of the stabilised soil. The researchers found that by increasing the amount of polymer and resin mixture, the cross linking between the particles does increase which will lead to increment of unconfined compressive strength of the specimens. The results indicate that the unconfined compressive strength of specimens in wet condition increased after 7 days. In contrast, under dry condition the specimens resulted to higher unconfined compressive strength. In addition, the inclusion of silt particle size range in the specimen groups resulted to a loss in the unconfined compressive strength due to prevention of effective cross linking in the microstructure attained by polymer addition.

Estebragh et al. (2011) studied the effect of two resins on the strength of soil cement mixture. The two resins that were used were both thermoplastic product of acrylic resin. They found that addition of resin to the soil-cement mixture increases the strength. Due to the reaction of resin with the soil particles and the effect of cement as a filler, the rigidity of the soil structure was increased. They also observed that the higher percentage of resin and longer curing time increases the strength of the mixture.

#### 2.4.3.4 Water-Soluble Polymers (Aqueous Polymers)

Water- soluble polymers have the ability to dissolve in water and disperse through the voids. The presence of hydrophilic groups in the water-soluble polymers puts them in

the category of hydrophilic polymers. The hydroxyl, carboxyl, ether, amine, amide and other hydrophilic groups in a water-soluble polymer can result in good adhesion, flocculation, formation and filming properties in the polymer (Huang and Liu, 2012). When the process of sorption takes place a very high level of energy is required to break the developed bonds between polymer molecules and soil particles. Therefore, the sorption of water soluble polymers on clay particle is an irreversible process which greatly contributes to the durability of the stabilized soil (Inyang and Bae, 2005; Inyang et al., 2007). Typical interaction of an aqueous polymer in soil is illustrated in Figure 2.12.

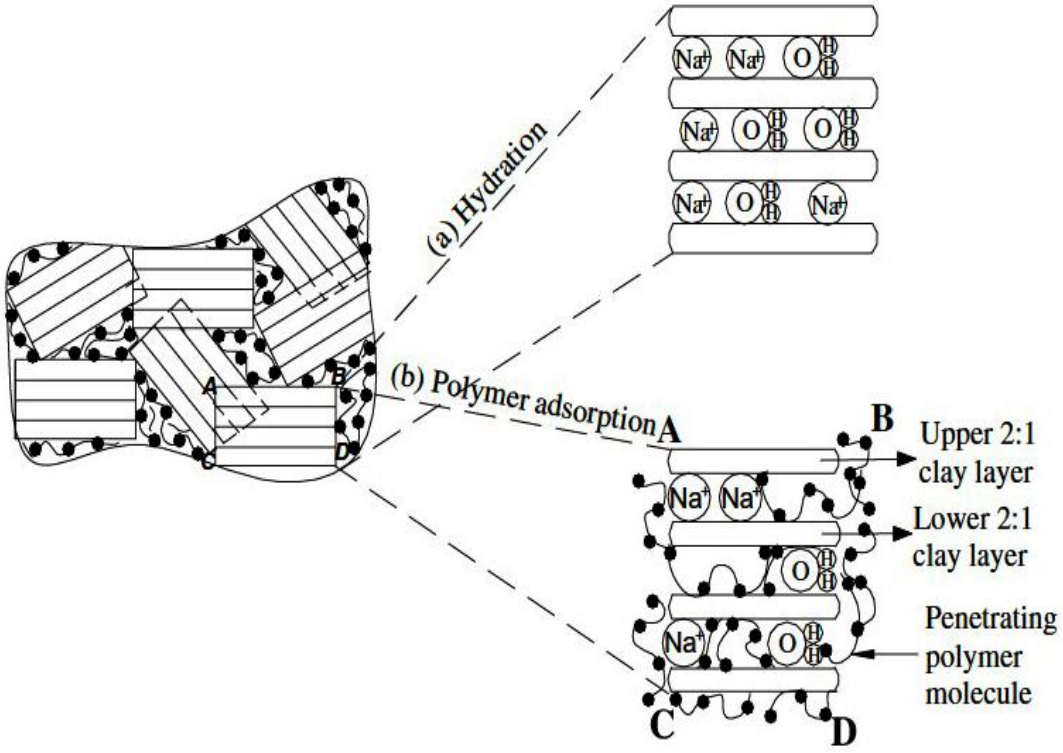


Figure 2.12. Illustration of typical interaction of an aqueous polymer is soil (Inyang and Bae, 2005)

Liu et al. (2009) used two aqueous polymers as soil stabilizer agents in order to improve the water stability of clay aggregates. By adding the aqueous polymer to the soil, the long-chain polymer molecules enwrap the particles and develop a new

structure similar to membrane on the surface of the clay. The structure of this membrane is elastic and viscous. Therefore, the polymers form and strengthen the membrane structure around the soil aggregates by bonding the soil particles together. Molecular weight of the polymer plays an important role in the stabilizing the soil particles, polymers with higher molecular weight have the higher probability of winding around the particles and bond them together. The results showed that after stabilization with polymer when the water penetrates into the pores, the membrane structure will be stronger than the expansion pressure. This goes to show that used water-soluble polymers have a positive effect on improving the water-stability of the soil.

Huang and Liu (2012) investigated the effect of a water-soluble polymer (namely STW) on the erosion resistance and expansion of expansive soils. According to the findings of their research the water-soluble polymer formed a mesh membrane between the particles of the expansive soil which reduces the expansion of the soil. The results also showed that the efficiency of the treated soil significantly improved with regard to erosion resistance.

Inyang et al. (2007) studied the effect of three aqueous polymers on volumetric swelling of Na-montmorillonite. The three polymers were cationic, anionic and neutral polymers. Based on their results the anionic and neutral polymer did not have a significant effect on reducing the swell of the soil. However, the positively charged polymer was the most effective stabilizer (Figure 2.13). The reason is due to the electrostatic interactions between negatively charged surface of the soil particles and polycations of the polymer.

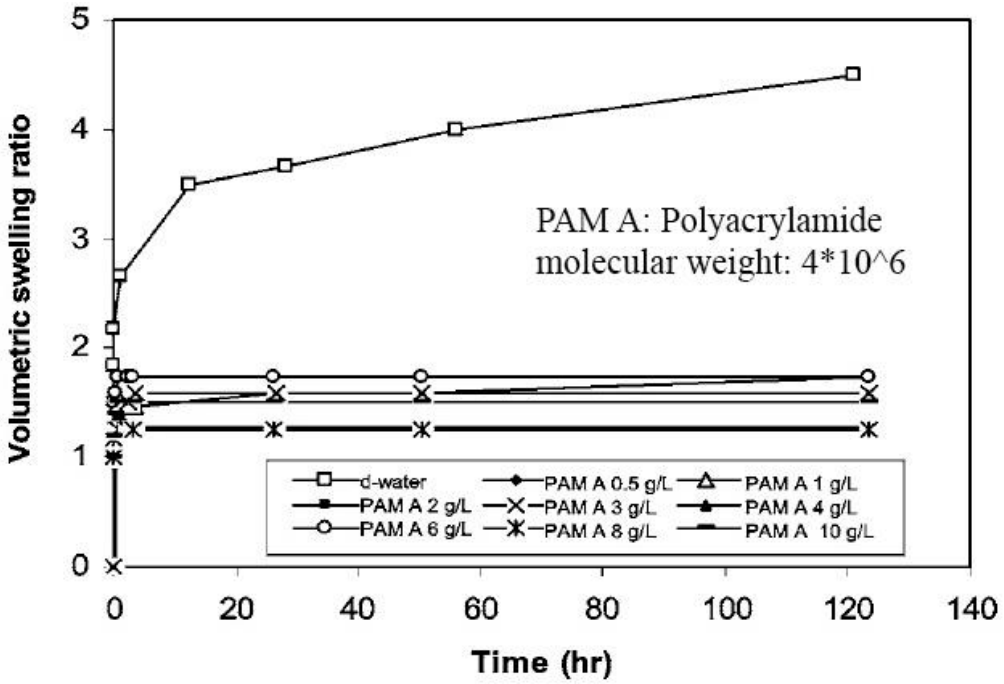


Figure 2.13. Volumetric swelling of Na-montrmorillonite (Inyang et al., 2007)

Azhar et al. (2017) used an aqueous polymer to stabilize kaolin clay soil. Due to the fact that kaolinite structure has a low coefficient of expansion in this research the polymer was used to improve the shear strength of the soil. Therefore, the kaolin soil was mixed with different percentages of liquid polymer and were cured for 4 different periods. They found that although the strength increased with the addition of aqueous polymer to a certain percentage however, a constant increase in compressive strength was not observed during the curing period.

Soltani-Jigheh and Azarnia (2017) used the combination of an anionic liquid polymer and lime as a stabilizer to study the strength of fine-grained soil at two weathering conditions: unfrozen and freeze-thaw condition. They found that the liquid polymer increases the unconfined compressive strength of the soil in the unfrozen condition however, the addition of the polymer to the lime-stabilized soil changes the soil structure to a flocculated form hence, leads to significant increment in the strength.

The results also showed that the volume change of polymer-stabilized soil decreases due to freeze-thaw cycles and addition of lime notably increases the tolerance of volume change during the freeze- thaw condition. The researchers concluded that the use of the liquid polymer has a detrimental effect on the soil behaviour in the permafrost regions and recommended that its utilization as a soil stabilizer should be limited to areas with warm or mild weather and be voided in frozen conditions.

### 2.4.4 Factors Affecting Soil-Polymer Reaction

#### 2.4.4.1 Chemical Bonding

Chemical bonding is one of the important factors that affects the stabilization process. One of the factors that affects formation of chemical bonds is the molecular weight. Higher molecular weight increases the possibility of formation of inter particle bond configurations. Different interface bonding can occur between soil particles and polymer including: ionic bonds, hydrogen bonds, van der waals bonds or covalent bonds.

In ionic bond an atom loses their electrons while the other atom gains the electron. In stabilization of soil with polymers ionic bonds occur between cationic polymers and the surface of the soil particle. However, the effectiveness of anionic polymers is influenced by the natural electrolytes in the soil. The interparticle bonds that are forming by the addition of anionic polymers can lead to flocculation of clay particles. Although, molecular weight and charge density can affect the flocculation process (Heller and Keren, 2002).

In case of using nonionic polymers as a stabilizer with the soil, adding a chemical additive can lead to formation of hydrogen bonds which is a strong intermolecular chemical force. Although van der waals bond is one of the important sources of

cohesion in fine grained soils but in the long range it can develop a weak bond between soil particles and polymer (Khatami and O'Kelly, 2013).

#### 2.4.4.2 Crystallinity of Polymer

Polymers with high crystallinity degree are strong, have high melting point and are less affected by solvent penetration. One of the factors that can affect the crystallization of polymer is the molecular weight. Polymers with higher molecular weight are more likely to undergo crystallization (Khatami and O'Kelly, 2013).

#### 2.4.4.3 Cross-Linking of Polymer

Cross-linking refers to where a polymer chain is linked to another chain by covalent or ionic bonds. This process decreases the flexibility of the polymer while increasing the melting point and strength. Changes in pressure, increase of temperature and variation in soil pH are the factors that can initiate the process of cross-linking when polymer enters the soil matrix. Cross-linking process starts after polymer infiltrates the soil void or in the curing period. Cross-linking process forms a large lattice in the soil which results in increase of the mechanical strength of the soil structure (Khatami and O'Kelly, 2013).

## 2.5 Cyclic Swelling and Shrinkage of Aqueous Polymer Stabilized Soils

The research shows that the periodic swell-shrink process of the soil affects the swelling potential after the first cycle of swelling. Yazdandoust and Yasrobi (2010) studied the influence of cyclic wetting and drying on the swelling behaviour of polymer-stabilized expansive clays. The chosen polymers were non-ionic and water soluble. When the polar polymer molecules come in contact with soil particles they collapse and are adsorbed by exchangeable cations that are on the surface of the clay particles. Hydrogen bonding, van der waals or other physical forces might occur during

the ion-dipole molecules interactions. Therefore, the adsorbed polymers coat the clay particles and link them together which will prevent the inter-crystalline swelling. The results showed that the swelling potential and axial deformation decreased in polymer-stabilized soils (Figure 2.14 and 2.15).

Yazdandoust and Yasrobi (2010) concluded that, the presence of polymer helps clay mineral layers to move closer together after each swell-shrink cycle. The micrographs of scanning electron microscopy tests demonstrated that the soil particles rearranged continuously during the cyclic wetting and drying process however the movement of particles in the specimens that were treated with polymer were closer to each other which will lead to formation of aggregates and reduction of swelling potential.

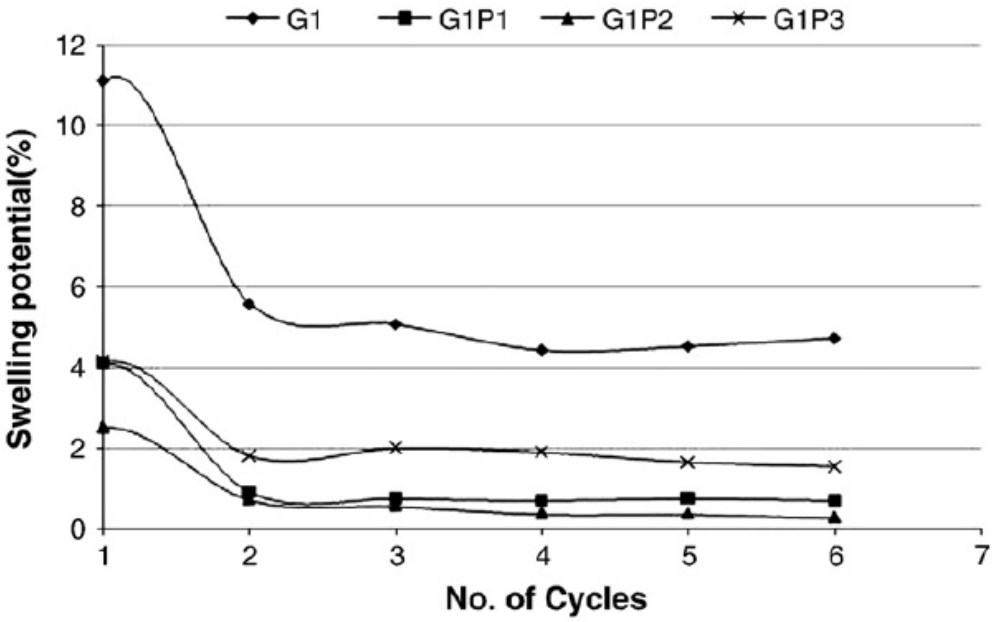


Figure 2.14. Change in swelling potential of polymer stabilized soil in cyclic swelling shrinkage test (Yazdandoust and Yasrobi, 2010)

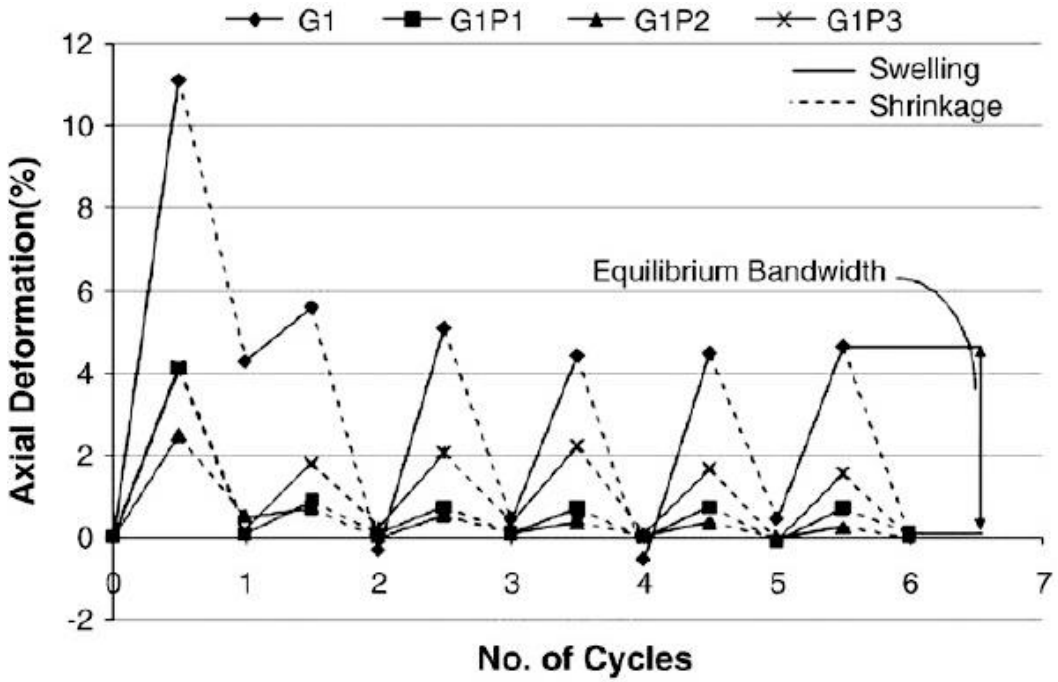

Figure 2.15. Change in axial deformation of polymer stabilized soil in cyclic swelling shrinkage test (Yazdandoust and Yasrobi, 2010)

## 2.6 Soil Water Stability

Water stability of an expansive clay treated with aqueous polymers is studied by Liu et al. (2009). They observed considerable improvement on the integrity of raw clay aggregates treated with sprayed polymer solution. Liu et al. (2009) also reported that, when external enwrapping of treated crumbs by polymer is attained, it is likely that an explosive collapse could be observed upon adsorption of water molecules during the water stability test (Figure 2.16). Hence, the ability of aqueous polymer to restrain clay aggregate during adsorption of water is key in assessing its effectiveness. With the control of the water adsorption of the clay aggregates, stability of the clay structure upon inundation is improved, however it is also important to note that the behaviour of the clay in the reverse mechanism is also important, i.e. when there is significant loss of moisture. Inyang and Bae (2005) studied the adsorption mechanism of clay treated with aqueous polymer indicating that, the drying rate of a clay treated with aqueous polymer will reduce, also reducing the rate of crack formation.

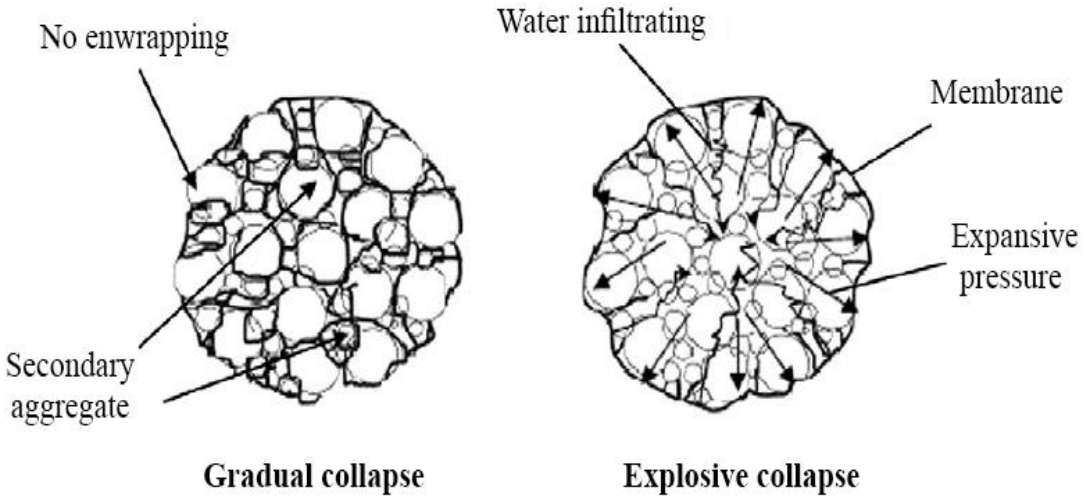


Figure 2.16. Mode of collapse for specimens (Liu et al., 2009)

# Chapter 3

# MATERIALS AND METHODS

## 3.1 Introduction

In this chapter, information about the soil sample used and the aqueous polymer utilized in the stabilization of the test specimens are provided. In addition, the testing program and strategy used in arranging the test groups for research purposes are presented. The standard laboratory testing methods used are referred and any deviations from these methods adopted for the purposes of this research are explained in detail.

## 3.2 Soil Sampling

The soil samples used in this research are obtained from surficial alluvial fan deposits, which are extensively present in the south campus of the Eastern Mediterranean University (EMU), Famagusta, North Cyprus. The approximate location of sampling is presented in Figure 3.1.

## 3.3 Copolymer of Butyl Acrylate and Styrene (CBAS)

Polymer stabilizers tend to be characterized by commercial brand names. This makes it difficult to recognize similarities between different polymer stabilizers due to the fact that the chemical composition of each stabilizer is generally undisclosed by the individual suppliers. The brand names often become inconsistent due to the alteration of names based on different marketing strategies implemented by suppliers (Rowe et al., 2009).

Emulsion of a synthetic elastic chemical substance that increases significantly the bonds within the substrate as well as the strength. It improves also the durability against chemical attack, the impermeability and finally the durability in cycles of freezing and thawing (Anagnostopoulos, 2007).

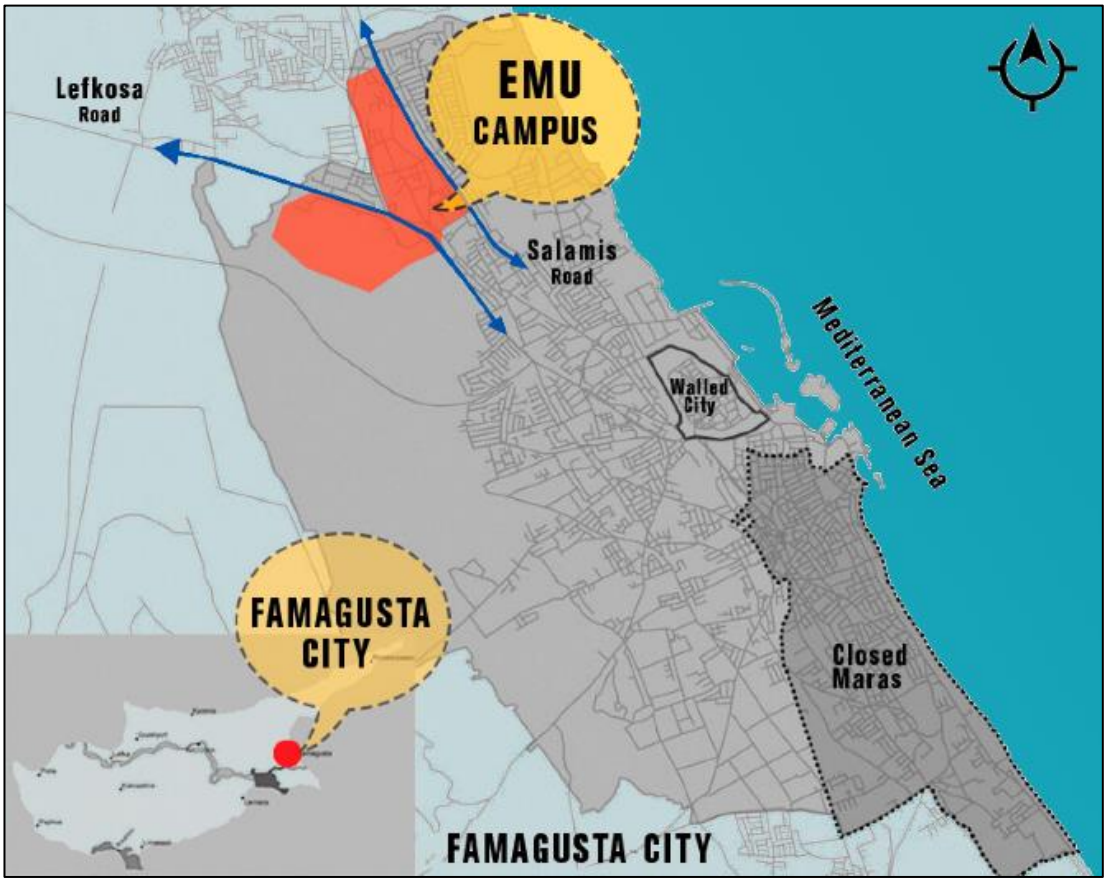

Figure 3.1. The approximate sampling location

The aqueous polymer used in this research is called Copolymer of Butyl Acrylate and Styrene (CBAS). CBAS is generally used in the industry as part of the treatment for decorative coatings and as an effective adhesive. It has high alkali resistance, low water adsorption, it is non-hazardous and inert.

CBAS is considered to be an effective admixture that can interact within the clay through two mechanisms; a) by forming films or webs around clay agglomerations in

macropores, b) by forming continuous or discontinuous films or webs within the clay fabric when it is thoroughly adsorbed into clay microstructure as shown previously in Figure 2.11. It is also important to note that, depending on the ion concentration around clay double diffuse layer, CBAS is likely to be absorbed in between clay particles by electrostatic interaction.

The influence of the resulting film or web of CBAS, despite being flexible, is likely to help keep the clay agglomerations and clay fabric together against internal forces that will develop upon water adsorption. This can reduce and slow down the volume change (potential) of the clay and it can also be expected that there would be improvements against softening as well as wind and water erosion. CBAS would improve accumulation of clay agglomerations and promote aggregate formation, the stability of which are key for wind and water erosion resistance (Williams et al., 1968; Barthes and Roose, 2002; Niewczas and Witkowska-Walczak, 2005; Xiao et al., 2017).

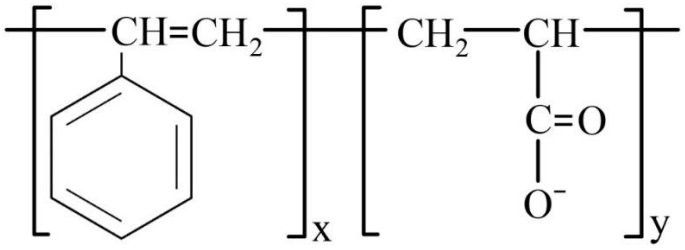


Styrene unit Acrylate unit

The amount of x and y will depend on polymer special formulation.

Figure 3.2. Copolymer of Butyl Acrylate and Styrene (Golhashem and Uygar, 2019)

The general chemical formulation of CBAS is presented in Figure 3.2. CBAS is not a hazardous synthetic waterborne (aqueous) polymer. It has a solid content of 50±1 %, pH value 7.0-9.0, viscosity of 2400-4600 mPa.s and density of 1.02 g/cm$^3$. It has

medium viscosity compared to other polymers of similar type and as it is a copolymer comprised of hydrophilic and hydrophobic blocks, it has higher penetrability into and around clay agglomerations, providing effective adsorption onto these surfaces (Panova et al., 2017).

## 3.4 Testing Strategy

The performance of the aqueous polymer selected to be used for this study is measured in terms of the engineering characteristics, long term durability (erodibility, internal stability) and the microstructural behaviour. For engineering characteristics, one-dimensional swelling and compressibility, and unconfined compressive strength are measured. For one-dimensional swelling and compressibility tests, specimens are subjected to free swell followed by standard oedometer testing.

The internal stability is measured by means of 'Water Stability Test'. A time-dependent stability index is evaluated for each specimen which defined the behaviour of the test specimens with respect to how resistant they were when exposed to inundation by distilled water.

In order to investigate the micro level interaction between polymer and the soil specimens, X-ray diffraction analysis (XRD), Fourier Infrared Spectronomy (FT-IR), Scanning Electron Microscopy (SEM), Electrical Conductivity (EC), Total Dissolved Solids (TDS) and Salinity measurements are performed.

The test groups are arranged in a form that the effect of variation of the initial moisture content is also investigated. The general testing strategy and test groups are presented in Table 3.1.

Table 3.1. Testing Strategy

| | | | | | |
|---|---|---|---|---|---|
| Tests for physical properties: | Specific gravity (GR-1)<br>Particle size distribution (GR-1,4)<br>Optimum water content (GR-1)<br>Atterberg Limits (GR-1,2,3,4,5) | | | Test Groups | Initial specimens condition |
| Tests for engineering properties: | Volume change: | Swelling (GR-1,4,5,6) | GR - 1 | Control specimens | Specimens prepared at Plastic limit (32%) |
| | Compressibility : | One dimensional consolidation test (GR-1,4,5) | GR - 2 | Treated specimens with 0.5% polymer | based on ASTM D698 |
| | Shear strength : | Unconfined Compressive test (GR-1,2,3,4,5) | GR - 3 | Treated specimens with 1% polymer | ↓ |
| | Erodibility : | Water stability test (GR-1,2,3,4) | GR - 4 | Treated specimens with 2% polymer | Vacuum Drying with Silica gel |
| | Durability : | Volume change based on wetting and drying cycles (GR1,6) | GR - 5 | Treated specimens with 5% polymer | ↓ |
| Tests for microstructure measurements: | X-Ray diffraction analysis (XRD) (GR-1,5)<br>Fourier Infrared Spectronomy (FT-IR) (GR-1,2,3,4,5,6)<br>Scanning Electron Microscopy (SEM) (GR-1,6) | | GR - 6 | Treated specimens with 10% polymer | Initial test condition |
| | Conductivity: (GR-1,2,3,4,5,6) | Electrical Conductivity | | | water content = 28% |
| | | Total Dissolved Solids | | | water content = 22.5% |
| | | Salinity | | | water content = 16% |
| | | Resistivity | | | water content = 11% |

## 3.5 Preparation of Test Specimens for Measurement of Engineering Characteristics and Durability

### 3.5.1 Mixing and Compaction

In this research the behaviour of untreated and treated soil between plastic and solid to semi solid phases are investigated. Therefore, the performance of all specimens are measured for a range of initial conditions controlled by variation of their initial moisture contents. All specimen groups are first produced at the plastic limit and then dried to water contents in between the plastic limit and shrinkage limit range.

For the treatment of the soil samples, CBAS is diluted in distilled water with the percentage concentration required based on the dry mass of soil solids. The diluted CBAS is then mixed with oven dry soil at the plastic limit water content and left in a sealed plastic bag for 24 h prior to compaction, so that a homogenous distribution of the moisture is attained in the mixture. The specimen preparation process is then continued with compaction using Standard Proctor Energy in accordance with ASTM D698, standard test methods for laboratory compaction characteristics of soil using standard effort.

Finally, test specimens are extruded from compacted samples through care using thin walled stainless steel specimen molds to minimize disturbance and achieve identical shape and dimensions as much as possible for a particular test.

### 3.5.2 Vacuum Drying

All test specimens are placed in a vacuum desiccator (Figure 3.3) for drying to the target initial condition prior to any testing. For controlled drying, the test specimens are subjected to vacuum in the desiccator at room temperature (approximately 22±2°C

in Soil Mechanics Laboratory, Civil Engineering Department, EMU) and repeatedly weighted at regular intervals of one hour to two hours, so that their moisture loss can be observed closely to obtain groups of specimens having various water contents.

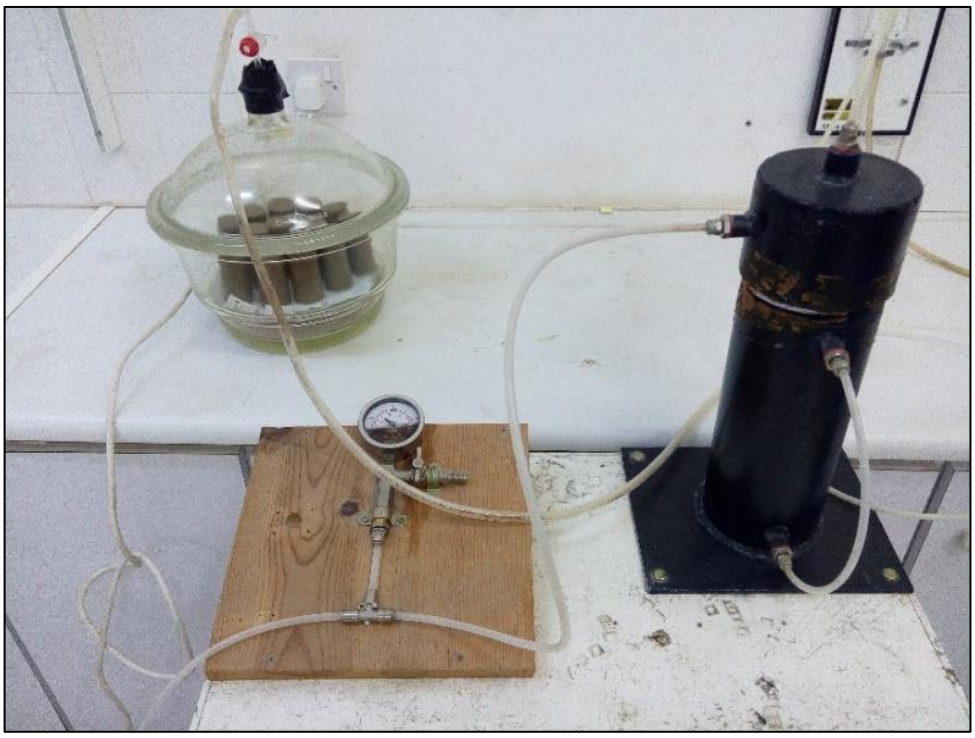

Figure 3.3. Vacuum drying setup

Figure 3.4. Deactivated silica gel

Figure 3.5. Activated silica gel

During vacuum drying in the desiccator, activated silica gel is also placed in the desiccator to help absorb the moisture uniformly from the specimens. Activated silica gel is one which is almost dry and available to absorb moisture and has a blue color. Silica gel becomes pink, when it can no further absorb water due to saturation (Figure 3.4 and Figure 3.5). The observation of change in color of the silica gel helps in predicting changes in the moisture content of the test specimen groups, which are then weighed to control the change. The deactivated silica gel is immediately replaced with active silica gel to allow a continuous drying process to be attained. The deactivated silica gel is reused after heating in oven until its blue color reappears, which normally took less than 24 hours.

At the end of this process, five sub-groups of test specimens for the untreated and CBAS treated groups are formed with the following initial water contents prior to testing; 11%, 16%, 22.5% and 28%. This provided a range of initial water contents between plastic phase and solid to semi-solid phase, which is considered to be representative of the moisture variation of a superficial soil layer through seasonal changes.

## 3.6 Laboratory Tests

### 3.6.1 Specific Gravity

Specific gravity is measured based on ASTM D854-92 standard. The soil specimen is placed in oven at 50℃ for 24 hours prior to testing. 10 g of dry soil specimen is used in each test for a pycnometer of volume 25 ml. The specimen is soaked in distilled water for 24 hours in each test and a vacuum pump is employed for 10 minutes to eliminate all the air inside the soil. This step is carried out three times within an additional time period of approximately 24 hours, after which the pycnometer is filled

up to top with distilled water. The average results indicated that the specific gravity for the soil sample used is approximately 2.69±0.01. The additional results are presented in Appendix A.

### 3.6.2 Atterberg Limits

The Atterberg limits tests are performed in accordance with ASTM D4318-98. The detailed results of plasticity tests are presented in Figure 3.6 to 3.8 and a summary of the results is presented in Table 3.2. The additional results are presented in Appendix A.

Table 3.2. Summary of Atterberg Limit test results

| | |
|---|---|
| Specific Gravity (Gs) | 2.69 |
| Liquid Limit (%) | 64 |
| Plastic Limit (%) | 30 |
| Shrinkage Limit (%) | 15 |

The test groups are formed of a control group and groups of test specimens treated with 0.5%, 1%, 2% and 5% CBAS added by dry mass of the soil. The plasticity of the treated soil is considered to be important as it affects the workability whilst mixing and compacting. Hence, the treated soil is tested for the change in its plasticity properties with the increase in the percentage of CBAS added.

The results generally indicate an unclear variation with no trend for the low concentration of CBAS, however, as the CBAS content is increased a clear trend in the plasticity behaviour is observed. The results indicate a modest change in the plasticity of the soil when CBAS is added up to approximately two percent by dry

mass of soil, beyond which there is a smooth rise in both the Liquid Limit and Plastic Limit.

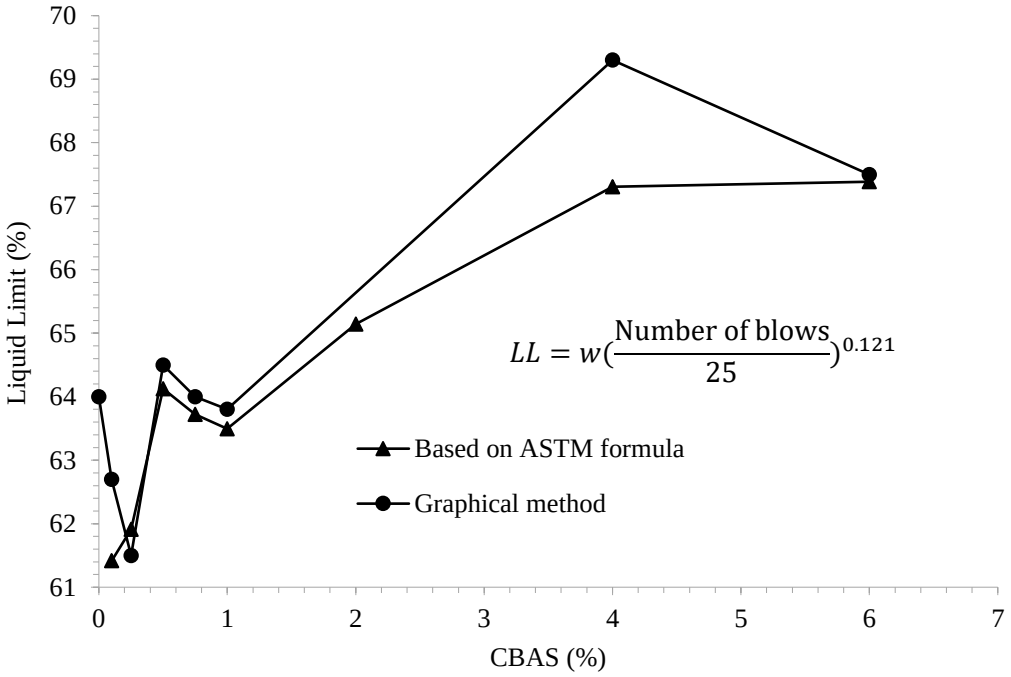


Figure 3.6. Change in Liquid Limit due to addition of CBAS

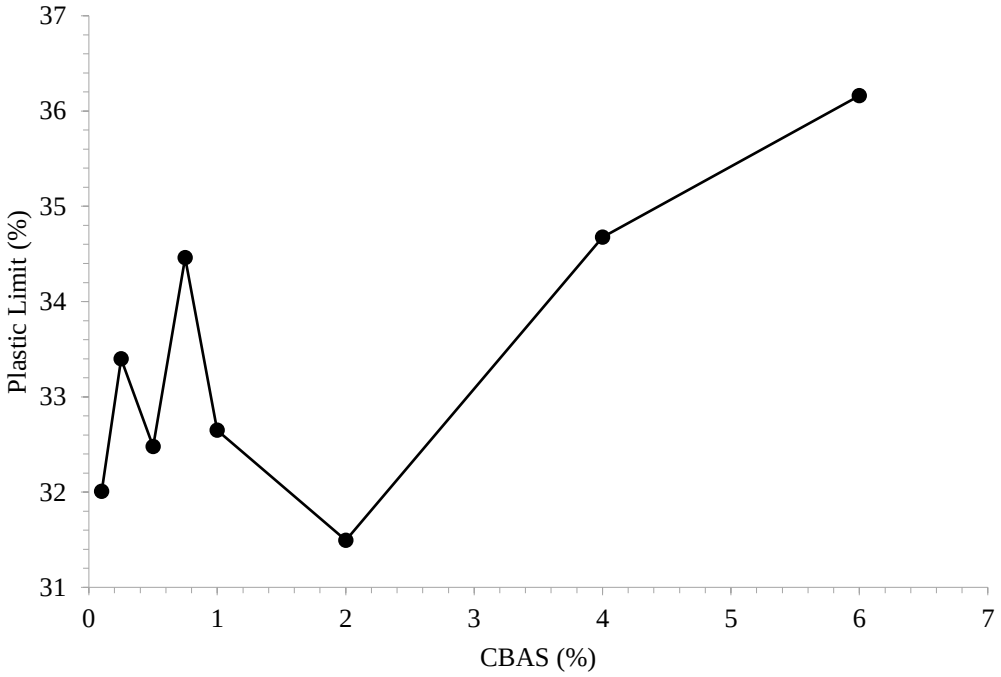


Figure 3.7. Change in Plastic Limit due to addition of CBAS

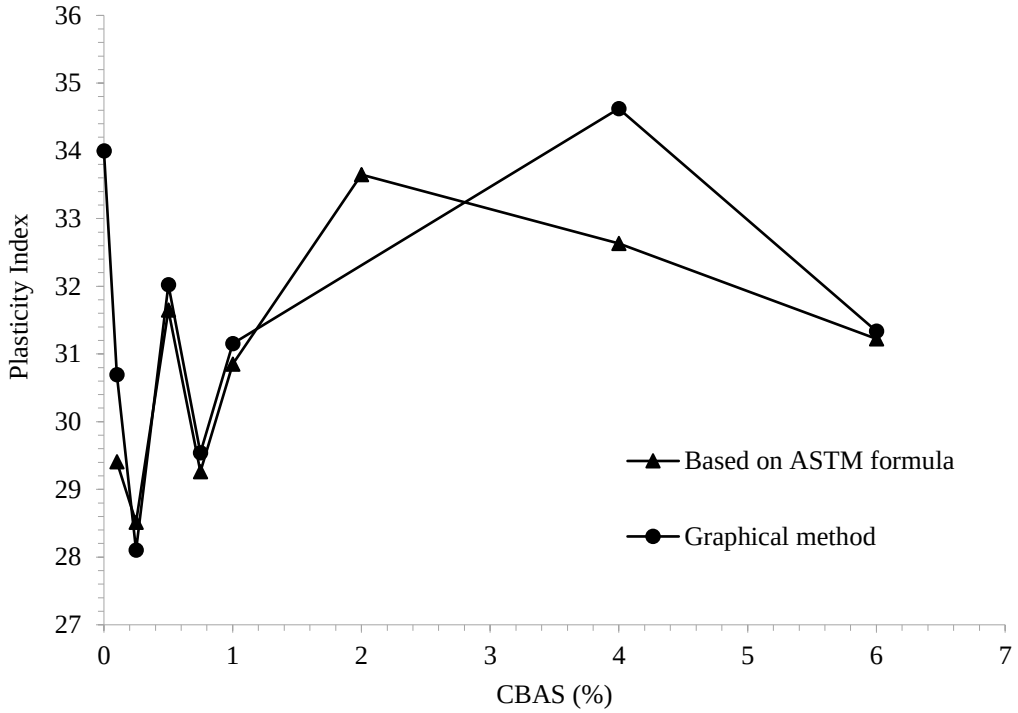


Figure 3.8. Change in Plasticity Index due to addition of CBAS

### 3.6.3 Particle Size Distribution

The particle size distribution is evaluated by the hydrometer test in accordance with ASTM D422. The soil sample is wet sieved through ASTM sieve #200 prior to testing, which indicated that 100% of the soil is fine grained. A dry mass of 50 g forming the soil specimen is treated with 125 ml of dispersing agent (hexametaphosphate and sodium bicarbonate solution, 40 g/L) prior to testing to deflocculate the silt and clay particles. The results of particle size distribution and Atterberg limits tests, indicated that the soil sample can be classified as silty clay (CH, highly plastic clay) based on the Unified Soil Classification System (USCS). The average particle size distribution obtained is presented in Figure 3.9.

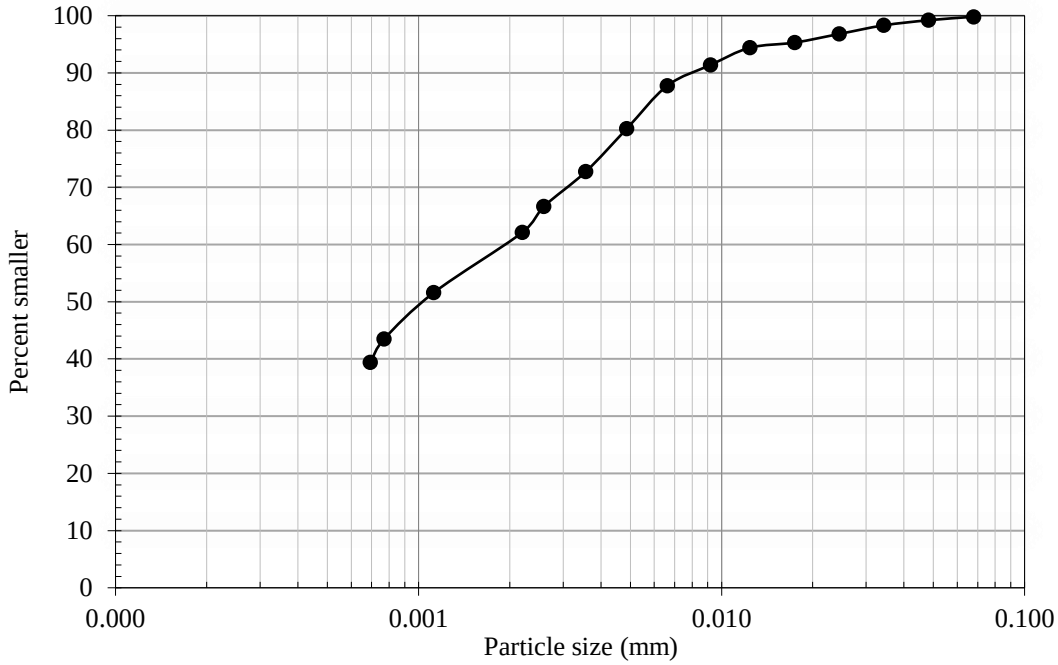


Figure 3.9. The average particle size distribution of the soil sample used

### 3.6.4 Compaction Characteristics

The Standard Proctor test is performed based on standard effort in accordance with ASTM D698-91 standard. The results are presented in Figure 3.10. The maximum dry density and optimum water content are obtained as 1.57 g/cm$^3$ and 25%, respectively.

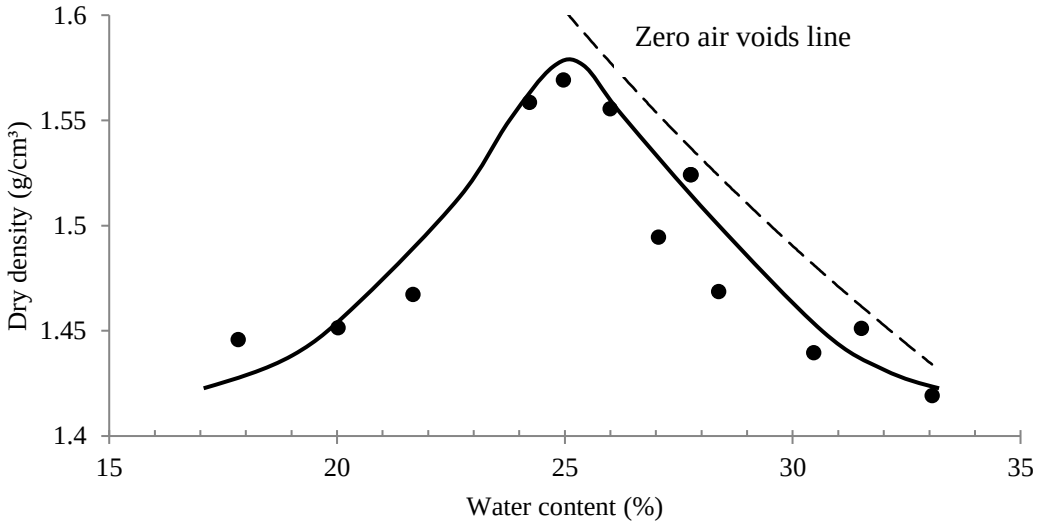


Figure 3.10. Dry density versus water content curve obtained from standard proctor compaction test

### 3.6.5 US Soil Conservation Service Laboratory Dispersion Test (Double Hydrometer Test)

Double hydrometer test is applied for measurement of the effect of CBAS addition in the soil dispersiveness which can be regarded as one of the methods of measurement for internal erosion resistance (or internal stability) of clays. This test is performed in accordance with the test method outlined in the ASTM D4221-18, Standard Test Method for Dispersive Characteristics of Clay Soil by Double Hydrometer. In this test, two specimens from each test group is taken for measurement of clay content. The standard hydrometer test is carried out on one of the specimens based on the test procedure outlined in ASTM D422, whereas on the second specimen the standard test procedure is modified by preventing mechanical stirring and the use of dispersing agent. The resulting particle size distribution curves are compared to obtain the ratio of percentage of clay smaller than 5μm in the two test specimens, which is defined as "percentage dispersion". An example of a double hydrometer test result is illustrated in Figure 3.11 and the results obtained for this research are presented in Chapter 4.

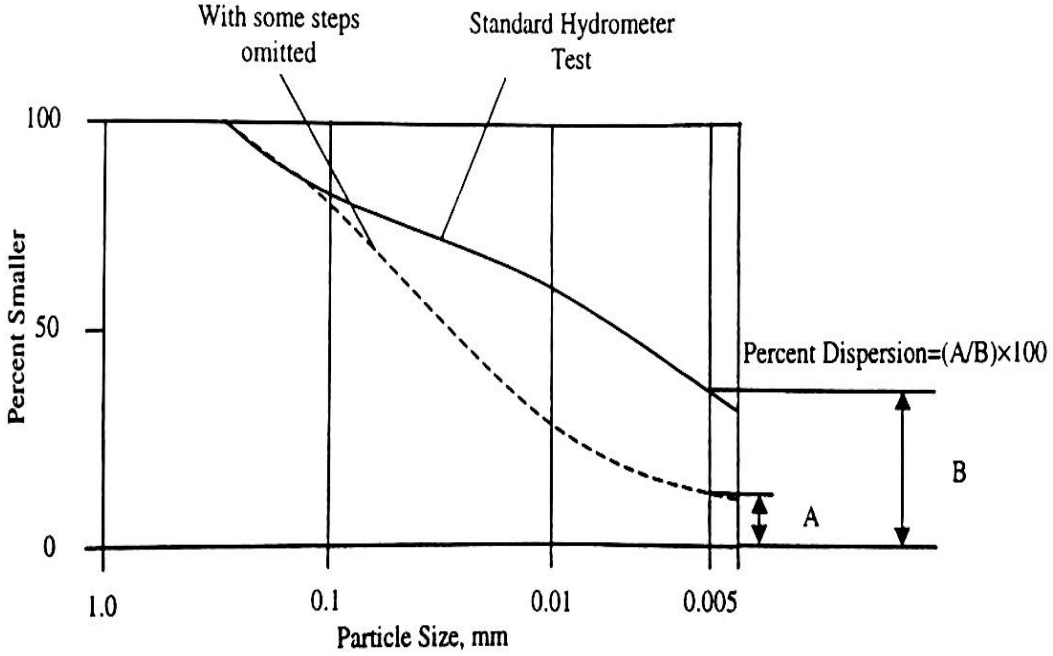


Figure 3.11. Illustration of a double hydrometer test result (Uygar, 1999)

### 3.6.6 Electrical Conductivity, Total Dissolved Solids, Salinity and Resistivity

In order to analyse the interaction between the clay and CBAS, test specimens are produced in slurry form and tested for the resulting electrical conductivity and the concentration of total dissolved solids (total dissolved anions and cations, TDS), using Bante900 Multi parameter Water Quality Meter instrument. The specimens are prepared as, one part of dry clay in grams to five parts of distilled water in millilitres including CBAS added as a percentage of the dry weight of clay up to 5%. The results are presented in Figure 3.12.

Time based measurements showed that the interaction between the soil and CBAS is formed almost instantly. Due to anionic character of the CBAS, it is considered that there is electrostatic interaction between CBAS and the readily soluble cations in clay and water molecules. The interaction is such that, even with the slightest addition of CBAS of 0.5%, there is a significant reduction of electrical conductivity and TDS. The drop in electrical conductivity is considered to be due to formation of polymer chains leading to an increase in the tortuosity of the specimens. However, with further increase in the CBAS, it is observed that there is a smooth rise in the measurements, which can be interpreted to be due to the increase in the overall volume of ions in solution, increasing conductivity.

Based on the results obtained at this stage of the research, it is decided that a period of curing is not required as the interaction between the soil and CBAS is almost instant, even in slurry form. All measurements are performed at controlled room temperature, which varied in the range 22°C to 24°C. The effect of temperature on the interaction between the soil and the CBAS is not investigated.

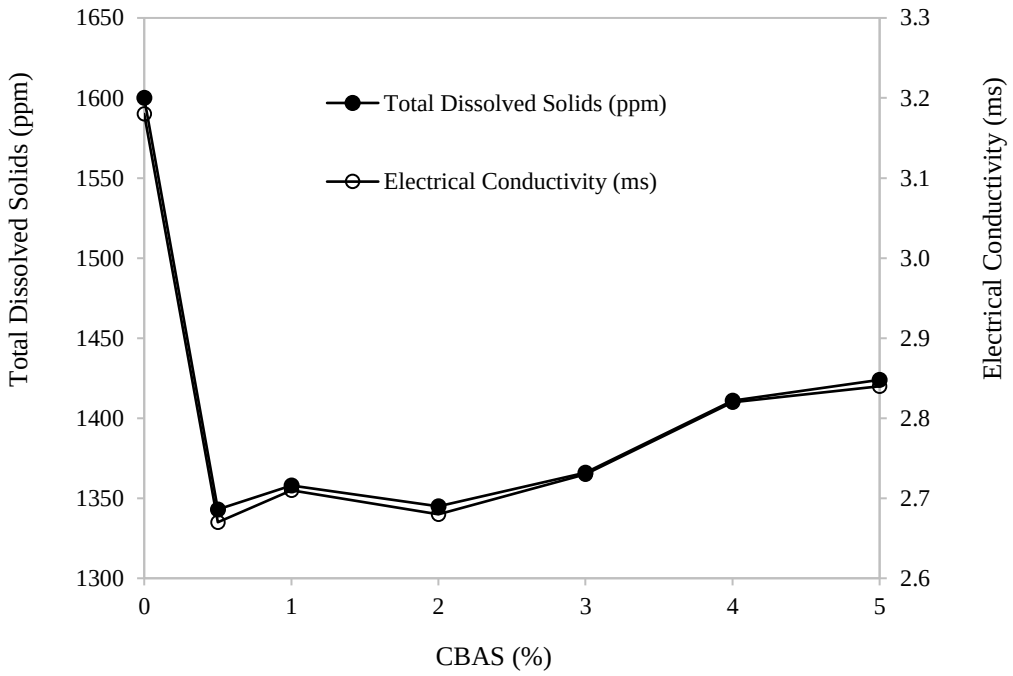


Figure 3.12. Change in electrical conductivity and total dissolved solids of specimens with respect to CBAS

### 3.6.7 Microstructure

#### 3.6.7.1 X-Ray Diffraction Analysis (XRD)

The X-Ray Diffraction test was applied by Bruker D8 XRD instrument with a copper sealed tube X-Ray source producing Cu. kα radiation at a wavelength of 1.5406 Å from a generator operating at 40 keV and 40 mA. A parallel beam of monochromatic X-Ray radiation is produced by the use of a Göbel mirror optic (primary optic). The diffracted X-Rays are recorded on a scintillation counter detector located behind a set of long Soller slits/parallel foils. All specimens are produced at wet condition and after drying process XRD test is applied. The results of the XRD test is used to examine the natural clay mineralogy and also determine whether new crystals are formed upon treatment of the clay with CBAS.

As the XRD apparatus is not available at EMU, the soil specimens from selected groups are taken to the Semnan University, Iran, and the analyses are conducted with the help of qualified engineer in this institution.

#### 3.6.7.2 Fourier Infrared Spectronomy (FT-IR)

Change in the clay mineral crystallite size is highly related to the bonding and structure of the minerals, and can be caused by the changes in clay mineral specific surface charge as a result of bond formation between clay mineral and CBAS. This is likely to happen due to potential attraction between the cations in clay and the anionic CBAS, resulting in formation of electrostatic bonds.

In order to further investigate these bonds, FT-IR test is conducted on untreated and treated test specimens by PerkinElmer UATR Two instrument, all test specimens are prepared at wet condition. This test is also performed for CBAS diluted with distilled water only for comparison with the other test results. The FT-IR tests are conducted in the laboratories of the Department of Pharmacy at EMU.

#### 3.6.7.3 Scanning Electron Microscopy (SEM)

In order to carry out visual assessments on the soil microstructure, analysis with scanning electron microscopy (SEM) is performed. The equipment model used for SEM analysis was Philips XL30 scanning electron microscope (Figure 3.13) with high vacuum pressure. A qualitative analysis of the SEM results is provided based on direct comparison of the untreated and treated test specimens. As the SEM apparatus is not available at EMU, the soil specimens from selected groups are taken to the Semnan University, Iran, and the analyses are conducted with the help of qualified engineer in this institution.


Figure 3.13. Scanning electron microscopy apparatus used (Semnan University, Iran)

### 3.6.8 Water Stability Test

The method used in this study for water stability test is based on Liu et al. (2009). The methodology contained herein is slightly modified as the observations during the test is carried out for a longer period of time. This is considered to enable for the long term stability of the treated clay to be assessed.

The test is performed on twenty-five approximately identical specimens for each group (where, GR-1: untreated clay, GR-2: clay treated with 0.5% CBAS, GR-3: clay treated with 1% CBAS, GR-4: clay treated with 2% CBAS). CBAS is diluted in distilled water by percentage added based on dry mass of the raw clay. The diluted CBAS is mixed with oven dry raw clay at the water content percentage required for sample preparation. For ensuring that the test specimens are approximately identical, they are extruded from samples compacted to the plastic limit using Standard Proctor Energy in

accordance with ASTM D698, with optimum moisture content and maximum dry density of 25% and 1.56 g/cm$^3$, respectively.

The test specimens are prepared cylindrical in shape and trimmed to a diameter of 38 mm and a height of 10.5 mm. After trimming to the test size, all test specimens are placed in a vacuum desiccator for 24 h. The initial condition of the test specimens has an influence on the rate of water adsorption, hence water stability at a given time. Therefore, in order to investigate this influence, the test specimens are subjected to vacuum drying in the desiccator and repeatedly weighed at regular intervals of one hour to two hours, so that their moisture loss can be controlled to obtain groups of specimens having various water contents. At the end of this process, four sub-groups of test specimens for the above groups are formed with the following approximate initial water contents prior to testing; 11±2%, 16±2%, 22.5±2% and 28±2%.

The test setup is presented in Figure 3.14. The test method involves immersion of the twenty-five test specimens in distilled water and recording of observations on the stability of the test specimens with respect to time. In the tests carried out for this research, the observations are carried out both real-time and also a review is performed by observing the tests for a second time from video recordings for a fair evaluation of the collapse behaviour observed.

In order to enable calculation of water stability index for a longer period of time, observations at time periods 10 min, 20 min, and 30 min are noted. The observations included recording of the number of collapsed samples within each set of twenty-five samples. This data provided an opportunity to define a water stability index based on time, which are referred to as $K_{10}$, $K_{20}$ and $K_{30}$. It is considered that measurement of

the water stability index at various time periods enables evaluation of the change of water stability with time, which can be regarded to be representative of the durability of the test specimens in the long term.

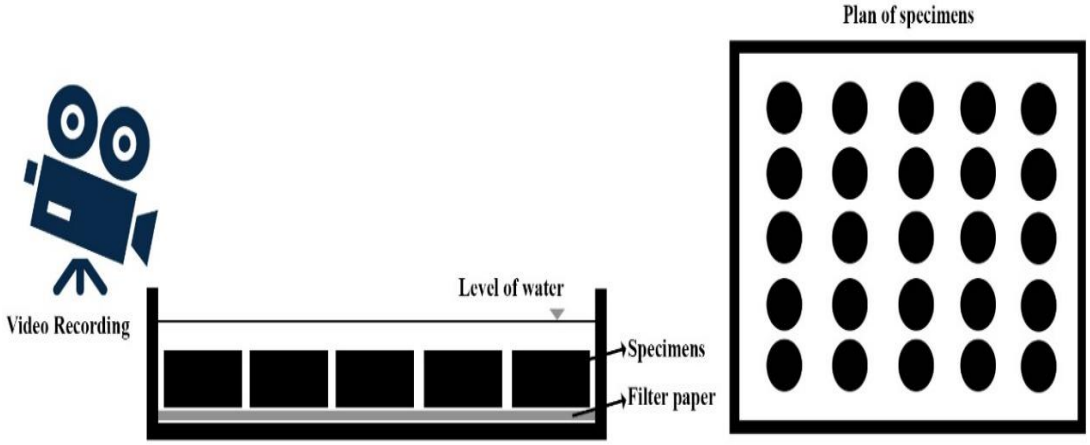


Figure 3.14. Schematic representation of water stability test setup

The equation suggested by Liu et al. (2009) is modified to allow calculation of the water stability index for various time periods as provided in the following equations;

$$K_f = \frac{\left(\sum_{i=1}^{f} a_i c_i\right) + 100 a_\alpha}{\text{total number of specimens}} \quad (3.1)$$

$$c_i = \frac{100}{2t_f} + \frac{100}{t_f}(t_i - 1) \quad (3.2)$$

where:

$K_f$ = is the water stability index in percentage, and f is the time at which the water stability index is calculated.

$t_i$ = time in minutes, and increases with one minute intervals from $t_1$= 1minute to the time at which the water stability index is calculated.

$t_f$ = time at which the water stability index is calculated.

$a_i$ = are the number of samples that collapsed at time interval between $t_{i-1}$ $and$ $t_i$.

$a_\alpha$ = is the number of samples, which remained stable at the end of the test at time $t_f$.

$c_i$ = percentage weight of number of collapses observed at time interval between $t_{i-1}\ and\ t_i$, in the water stability index calculated at time $t_f$.

The stability index, $K_f$ is calculated as a function of the percentage of samples, which remain stable at the time when it is calculated. A drop in the value of $K_f$ with time at which it is calculated shows that, as the test progressed less number of test specimens could remain stable. As it can be observed from Eq 3.1, as the time period at which the water stability index is calculated increases, the impact of the collapses observed at earlier stages of the test on the water stability index reduces. In other words, the water stability calculation starts to take account of the number of collapses in the later stages of the test as well. For the same data, if water stability index was calculated for 10 minutes, 20 minutes and 30 minutes using Eqs 3.1 and 3.2, assuming no change in the stability of the specimens after 10minutes, the results would reflect a drop in the stability with time period. This is due to the fact that the observation of collapse of test specimens are regarded to be earlier with increase in the time period. Hence, it can be concluded that earlier collapse is reflected with a lower water stability index. Addressing time of collapse for an extended period is especially important when evaluating the stability of the treated groups, as almost all of the test specimens are likely to remain intact early in the test.

The mode of collapse of individual specimens observed during the test is also noted for each time period. Two modes of collapse are considered in accordance with Liu et al. (2009): 1- gradual cracking, and 2- explosive collapse. The former is considered to be the case when a specimen cracks and disperses or slakes around gradually, with a

tendency to keep resemblance of its original shape even after collapse. Whereas, the latter mode of collapse is considered to be the one which does not show a clear indication of collapse until it happens, with sudden major cracking and release of air bubbles, often followed by complete disintegration. From the test results collected, the mode of collapse observed is quantified by calculating the percentage of specimens collapsed by explosive mode within the total specimens collapsed.

### 3.6.9 Unconfined Compressive Strength Test

The improvement on the unconfined compressive strength of the test specimens is measured by means of unconfined compressive strength test (ASTM D2166). The specimen size used in these tests is 38 mm (diameter) and 76 mm (height) and all the specimens produced from standard proctor compaction test.

As it is carried out in the specimen preparation for other tests, in order to provide uniform drying, the specimens are placed in a vacuum desiccator and silica gel is used to extract moisture from the specimens as evenly as possible. With the use of extra identical specimens of the tested specimens, which are splitted and tested for moisture content from at least five locations, the uniform drying process is controlled and ensured effectively. The test specimens are compacted at a water content equal to the plastic limit using standard Proctor energy, allowing for a controlled drying to be applied. In this way, various target initial water contents (28%, 22.5%, 16% and 11%) prior to testing are attained. In addition to the target initial water contents, subgroups of various degrees of treatment are also considered in terms of polymer addition by dry mass of soil as; 0.5%, 1%, 2% and 5%.

The loading rate used in the tests is 0.76 mm per minute. The data is collected using electronic data acquisition to allow for detailed observations on the results to be carried

out such as the assessments for the average elastic modulus and ductility behaviour. The tests are conducted until at least 25% axial strain is achieved, unless the specimen failure mode lead to a sudden shear failure in which the shear stress mobilization had almost dropped to zero.

The average undrained modulus ($E_{50}$), evaluated for the treated and untreated specimens based on Das and Sobhan, (2013) (Figure 3.15). The average elastic modulus is calculated by considering the slope of the compressive stress versus axial strain curve corresponding to the initial tangent line drawn through the half of the peak compressive stress.

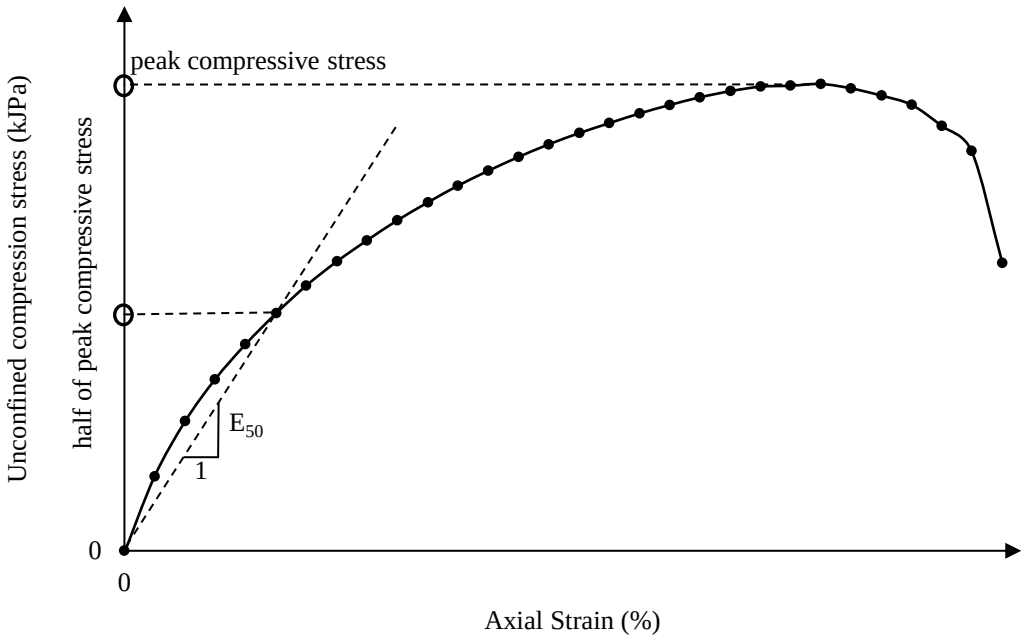


Figure 3.15. Evaluation of the average undrained modulus (Das and Sobhan, 2013)

### 3.6.10 One Dimensional Swell Test

One dimensional swell test was conducted according to ASTM D4546-14 in order to determine the swelling characteristics of both treated and untreated specimens. All the

specimens were produced at plastic limit then dried in vacuum drying condition to a specific amount of water content and molded into consolidation rings with 20 mm in diameter and 50 mm in height. For assessment of the role of CBAS in volume change of polymer stabilized specimens, three groups of treated specimens are selected. The specimens were mixed with 2%, 5% and 10% of CBAS by dry mass of clay. Figure 3.16 illustrates an example of a swelling curve.

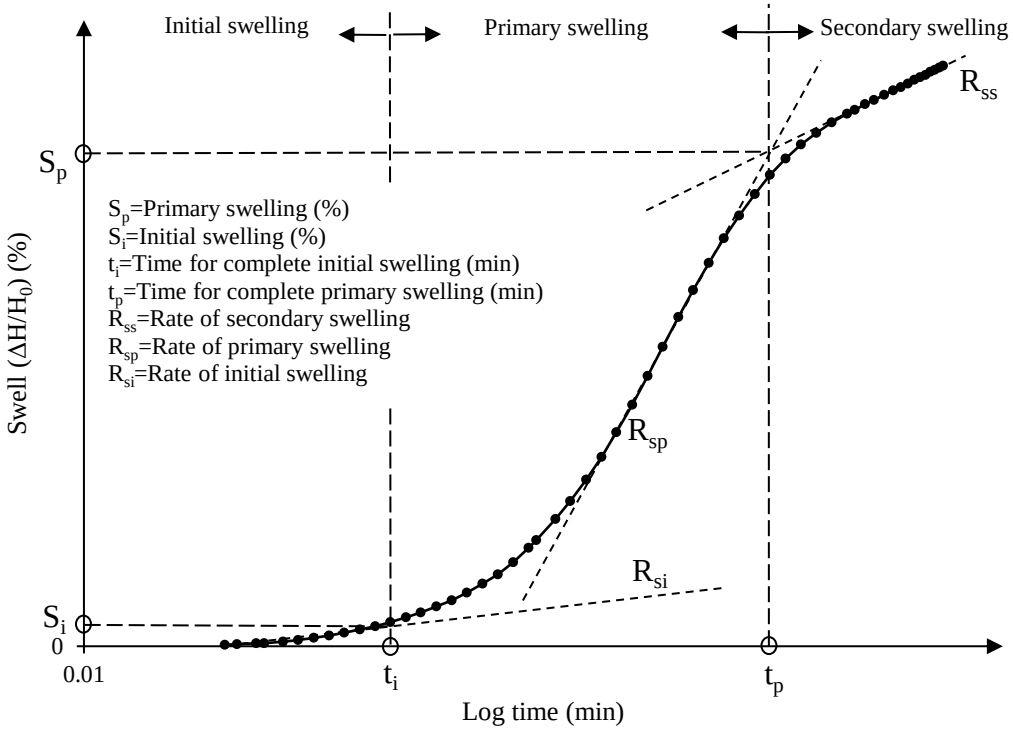


Figure 3.16. Swelling parameters (Nagaraj et al. 2010)

The one-dimensional swelling tests are conducted under a constant total stress of 7 kPa. As part of this test, change in the specimen height upon inundation is measured with respect to time and plots of the ratio of change in height ($\Delta H$) to original height ($H_0$) versus logarithm of time (log t) is studied for quantification of the performance of the treatment with CBAS. The swelling percentage is assessed by considering the

swelling process to take place in three stages; 1- initial swell, 2- primary swell and 3- secondary swell, as described by Nagaraj et al. (2010).

### 3.6.11 One Dimensional Consolidation Test

One dimensional swell and consolidation tests are conducted on a specimen size of 15mm in height and 50mm in diameter based on ASTM D2435-11. The test specimens are allowed to swell under a surcharge of 7 kPa during saturation stage based on ASTM D4546-14, allowing initial and primary swelling to be completed by observation of the test curves obtained. These tests are followed by loading and unloading steps of; 55 kPa, 110 kPa, 220 kPa, 440 kPa, 880 kPa 1760 kPa, 3520 kPa, 1760 kPa, 880 kPa and 440 kPa.

One dimensional consolidation parameters are computed accordance with Das and Sobhan, (2013) illustrated in Figure 3.17. and the preconsolidation pressure is evaluated in accordance with the Casagrande's method (Das and Sobhan, 2013), as illustrated in Figure 3.18. For determination of coefficient of consolidation, the logarithm of time method is used to obtain time required for 50% consolidation to take place following Cassagrande's method, as illustrated in Figure 3.19. The drying stages prior to testing in this stage of the study have led to a reduction of sample diameter due to shrinkage, causing a problem in the swelling measurements as these were carried out in one-dimensional method. Therefore, the initial specimens are prepared with the dimensions of 75 mm in diameter and 20 mm in height, from which sub-specimens are extracted to meet the dimensions given above for testing in the oedometer.

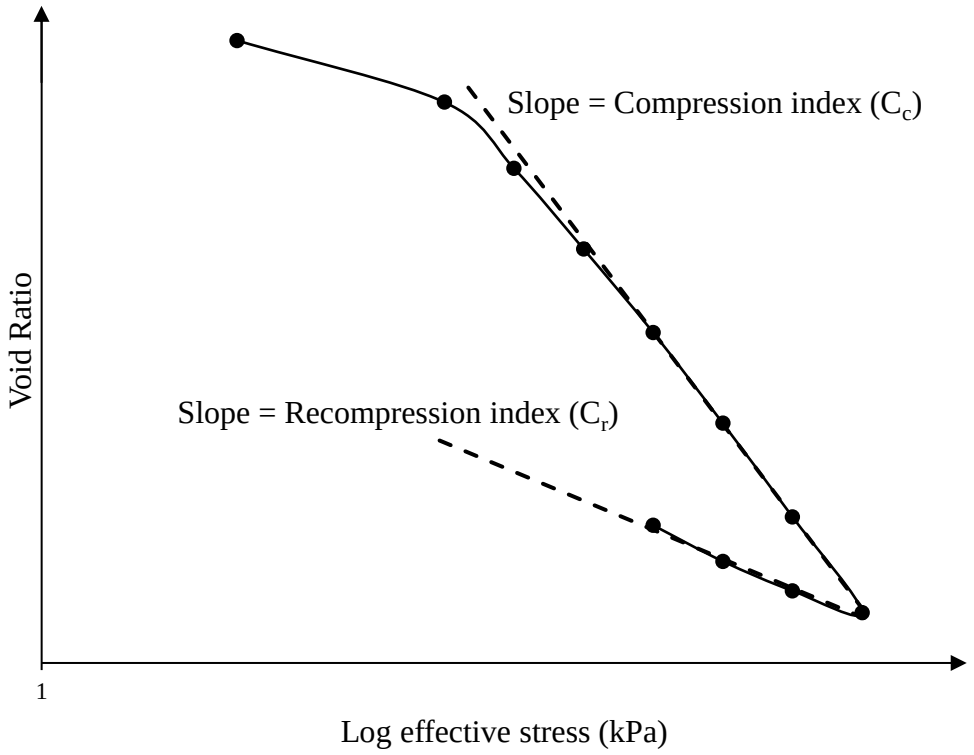


Figure 3.17. Evaluation of compressibility parameters (Das and Sobhan, 2013)

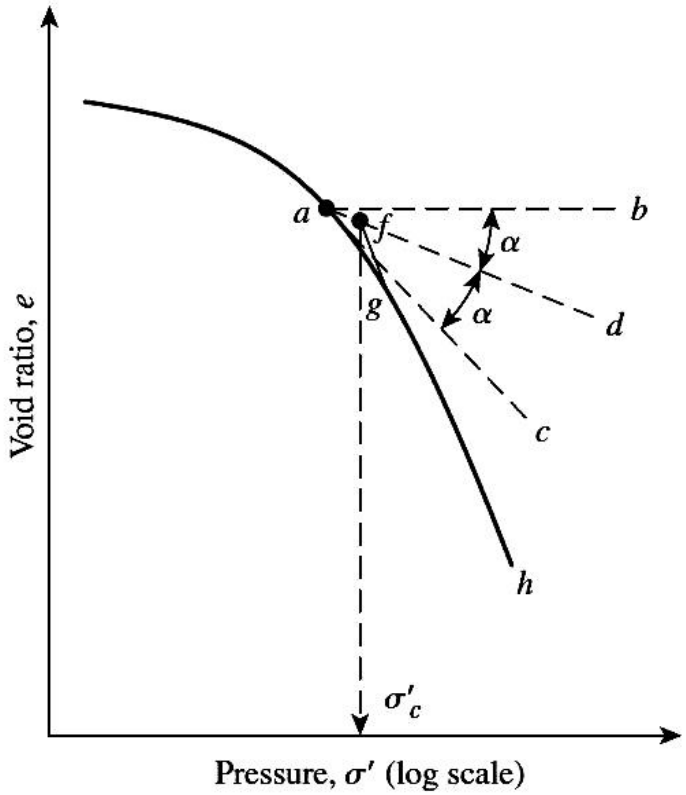


Figure 3.18. Evaluation of preconsolidation pressure by Casagrande's method (Das and Sobhan, 2013)

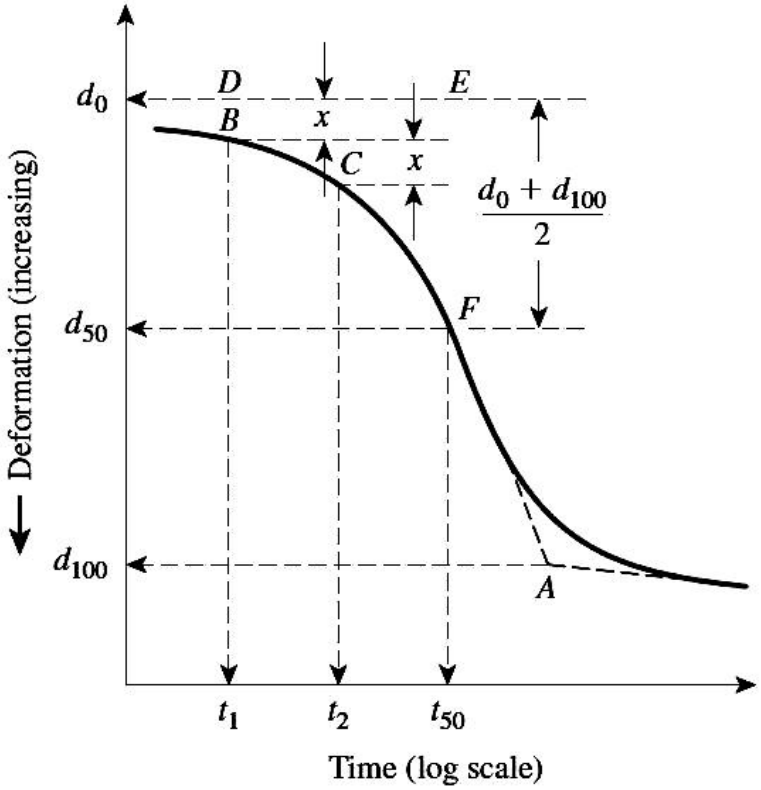


Figure 3.19. The logarithm of time method for determining coefficient of consolidation (Das and Sobhan, 2013)

Three percentages of CBAS (0.5%, 2% and 5%) were selected for the assessment of the role of CBAS stabilization on clay compressibility. In addition, to investigate the effect of initial moisture content, the CBAS was mixed by dry mass of clay and then placed in vacuum drying desiccator and dried to a specific amount of water content.

### 3.6.12 Cyclic Wetting and Drying (Swell and Shrink) Tests

In order to evaluate the durability of the CBAS treatment and also its performance upon moisture changes, cyclic wetting drying tests are performed. This test program involved application of controlled wetting drying in an oedometer with a close inspection for the change in volume of the specimens and crack development upon shrinkage.

The swelling behaviour upon inundation of the specimens in distilled water is monitored until the completion of the primary swelling stage, called as the wetting stage, at which the specimen is regarded to be approximately fully saturated. The wetting stage is followed by extraction of the fully saturated specimen and placement in a vacuum desiccator for controlled drying, called as the drying stage. In the drying stage, the moisture changes in the specimen is frequently monitored by measuring the weight of specimen until its moisture content is approximately equal to the initial moisture content. After this is achieved, the specimens are placed back in oedometer for the next cycle of wetting. Whenever possible, the cycles of wetting and drying are repeated up to 6 times. For untreated specimens and specimens with low level of treatment, the treatment cycles could not continue for more than two cycles due to formation of large cracks and disintegration. In addition, due to various reasons, some specimens are observed to dry faster than others, which meant they were subjected to a greater volume reduction due to shrinkage, affecting their swelling behaviour in the following wetting cycles. The analysis of results from such specimens are carried out accordingly, as presented in Chapter 4.

# Chapter 4

# DISCUSSION AND ANALYSIS OF LABORATORY TEST RESULTS

## 4.1 Introduction

In this chapter, results of the laboratory tests are presented. Detailed analysis and discussion on the erodibility, volume change behavior and unconfined compressive strength characteristics of the tested soil groups are provided. The role of CBAS as a soil stabilizing agent is emphasized.

## 4.2 Drying (Shrinkage behaviour) of the Test Specimens

In addition to the standard data recording (on the water content, density etc), the data on time dependency of the drying behaviour for the test specimens were also collected. The performance of the silica gel in providing uniform drying is evaluated thoroughly by taking moisture content measurements from at least five different parts of each specimen; superficially and also by cutting through to reach the core from top, bottom and middle. A representative set of data on the average water content of the specimens prepared are presented in Table 4.1 to demonstrate the effect of silica gel on uniformity of the drying water content of the specimens.

The efficacy of the silica gel used in terms of the time dependency of the drying period is also studied to enable planning of the time for collection of the specimens for testing.

The results of the water content measurements during the drying process with respect to time are presented in Figure 4.1.

Table 4.1. Water content measurement with vacuum drying

| CBAS (%) | Water content (%) | | | | | Average water content (%) |
|---|---|---|---|---|---|---|
| 0 | 28.88 | 29.25 | 28.57 | 28.74 | 28.18 | 28.72 |
| 0 | 21.31 | 22.37 | 22.68 | 22.58 | 21.05 | 22.00 |
| 0 | 16.28 | 17.86 | 17.07 | 15.22 | 16.98 | 16.68 |
| 0 | 11.29 | 10.00 | 12.20 | 10.42 | 10.71 | 10.92 |
| 0.5 | 27.27 | 28.81 | 28.40 | 27.07 | 28.28 | 27.97 |
| 0.5 | 22.81 | 20.45 | 22.54 | 22.22 | 22.34 | 22.07 |
| 0.5 | 16.39 | 16.00 | 15.91 | 17.91 | 17.31 | 16.70 |
| 0.5 | 8.82 | 8.16 | 9.52 | 8.47 | 10.00 | 9.00 |
| 1 | 26.67 | 26.25 | 26.32 | 26.32 | 26.75 | 26.46 |
| 1 | 22.74 | 22.70 | 22.61 | 22.72 | 22.66 | 22.68 |
| 1 | 16.67 | 16.78 | 16.58 | 17.09 | 17.20 | 16.86 |
| 1 | 10.00 | 10.53 | 10.89 | 11.11 | 10.62 | 10.63 |
| 2 | 27.11 | 27.27 | 25.93 | 27.07 | 27.27 | 26.93 |
| 2 | 21.67 | 22.45 | 22.09 | 22.07 | 22.77 | 22.21 |
| 2 | 16.00 | 14.29 | 14.29 | 15.69 | 15.63 | 15.18 |
| 2 | 9.52 | 11.11 | 9.46 | 10.94 | 9.80 | 10.17 |
| 5 | 28.52 | 27.70 | 27.29 | 27.34 | 28.39 | 27.85 |
| 5 | 20.27 | 21.14 | 22.22 | 20.17 | 21.35 | 21.03 |
| 5 | 16.25 | 15.18 | 15.87 | 16.18 | 16.94 | 16.08 |
| 5 | 10.64 | 11.11 | 10.06 | 10.42 | 11.44 | 10.73 |

The data obtained on the change of void ratio of specimens with respect to change in water content during drying process is presented in Figure 4.2. As observed from the data, the drying characteristics of the specimens varied due to the addition of CBAS, such that the increase in the percentage CBAS resulted in a decrease in the change of void volume as the specimens are allowed to dry. Hence at the same water content, this change in behavior allowed for a greater volume to be occupied by voids within the specimens. In other words, this measurement shows indirectly that the addition of polymer reduces the shrinkage of clay during drying by supporting the void volume

(macropores) internally within the fabric of the clay. This provides a positive practical implication such that the reduced shrinkage would also mean fewer desiccation cracks and increased erosion resistance and stability upon inundation.

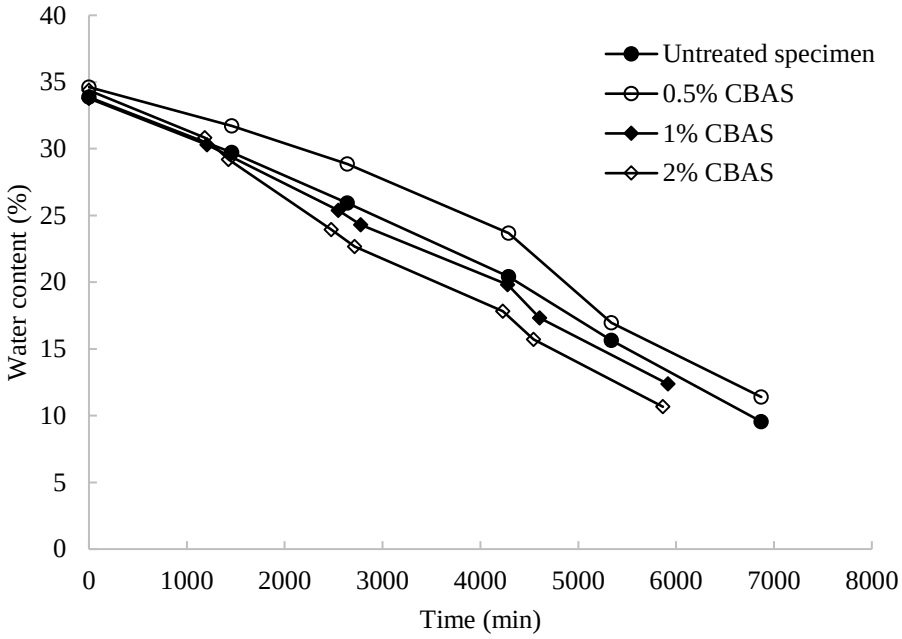


Figure 4.1. Water content of the specimens versus time

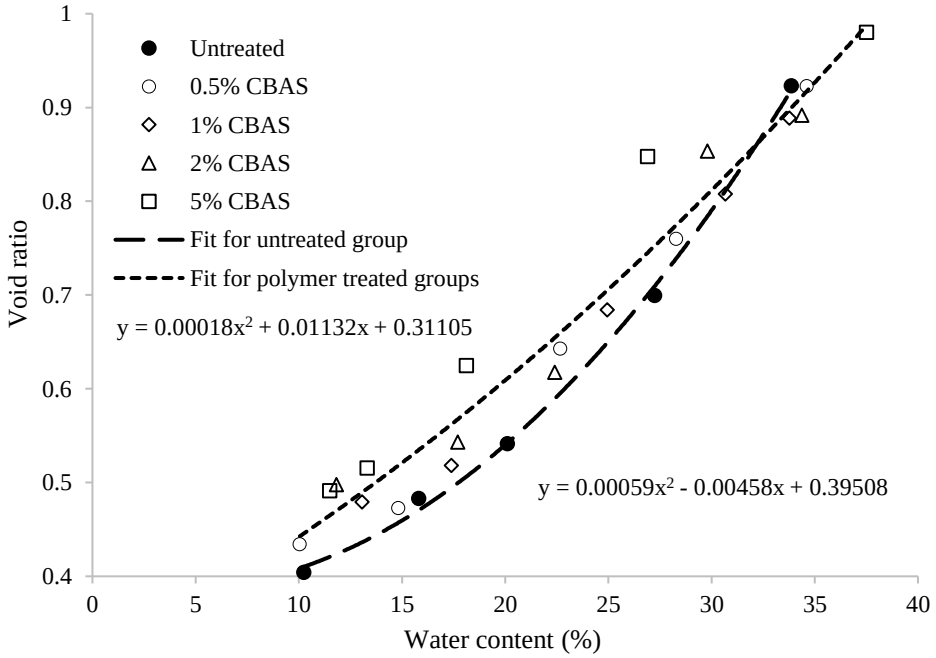


Figure 4.2. Change in void ratio with respect to water content during drying process

## 4.3 One-Dimensional Swelling

### 4.3.1 General Comments on the One Dimensional Swelling Behaviour Data

The stages observed from a typical one-dimensional swell test on clay soil (initial, primary and secondary swell) are defined by Nagaraj et al. (2010). For assessment of the role of CBAS in volume change of polymer stabilized specimens, 3 groups of treated specimens are selected. Two groups are treated with low percentage of CBAS (2% and 5%) and another group is treated with high percentage of CBAS (10%). In addition, to investigate the effect of drying on volume change, all the specimens are placed in vacuum drying desiccator. The initial water content is controlled by measuring the weight of specimens and swelling test is carried out at certain amount of initial moisture content. The results for initial swelling, primary swelling and time to complete primary swelling are presented in Table 4.2.

Table 4.2. One dimensional swelling parameters

| Group specimen | Initial water content (%) | $S_i$ (%) | $S_p$ (%) | $T_p$ (min) |
|---|---|---|---|---|
| Untreated specimen | 28±2% | 0.2 | 3.5 | 400 |
| 2% CBAS | | 0.3 | 3.6 | 200 |
| 5% CBAS | | 0.3 | 3.8 | 200 |
| 10% CBAS | | 0.05 | 0.6 | 200 |
| Untreated specimen | 22.5±2% | 0.8 | 12.8 | 700 |
| 2% CBAS | | 0.8 | 11.8 | 800 |
| 5% CBAS | | 0.8 | 10.2 | 1050 |
| 10% CBAS | | 0.2 | 5.2 | 600 |
| Untreated specimen | 11±2% | 1 | 18.5 | 750 |
| 2% CBAS | | 1 | 18.5 | 700 |
| 5% CBAS | | 1 | 18.8 | 900 |
| 10% CBAS | | 0.5 | 10.5 | 600 |

$S_i$: Initial swelling, $S_p$: Primary swelling, $T_p$: Time required for complete primary swelling

The data obtained from swelling curve in 28% of moisture content is presented in Figure 4.3. The results indicate that the initial swelling of untreated sample and low percentages of CBAS are quite similar while the initial swelling in 10% CBAS

dropped significantly. The results also showed that there is a slight change in primary swelling in untreated specimen from 3.5% to 3.6% for 2% CBAS and 3.8% for 5% CBAS but there is a significant drop to 0.6% in 10% CBAS. Assessment of primary swell time indicate that the time for primary swelling dropped from 400 minutes in untreated specimen to 200 minutes for all CBAS treated groups.

From results illustrated in Figure 4.3. It can be concluded that at 28% initial water content, when low percentages of CBAS is used, the cross-linking process does not develop properly due to insufficient intrusion of polymer into the soil matrix. When higher percentage of CBAS is added to the soil it is observed that the swelling behaviour is improved significantly.

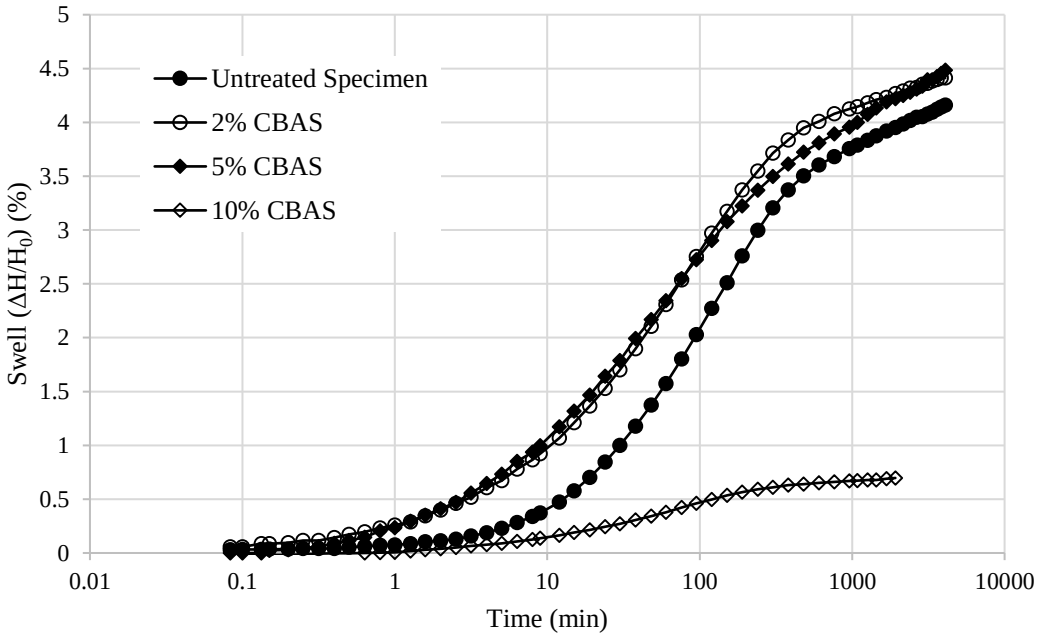


Figure 4.3. One dimensional selling curve at 28% of initial water content

The results for 22.5% initial water content is presented in Figure 4.4. In these results, it is seen that, there is an increased swelling potential due to the reduction of initial moisture content, hence primary swelling percentage is increased for all groups. In this

water content, the other effect is also the process of an improved cross-linking owing to the reduction of water content (also basal spacing and spacing within the macropores of the soil fabric). Hence, as a result, the polymer could form itself more efficiently within the soil matrix, performing better even at low percentages of treatment. The results indicate that initial swelling is 0.8% for untreated specimen and low percentage of CBAS, whereas it drops to 0.2% with further addition of CBAS. This improvement is due to the formation of an effective web around the particles, which helps to reduce initial swelling percentage.

The primary swelling behaviour is observed to be improved most efficiently in the specimens with an initial water content of 22.5%. Compared to the untreated specimens, primary swelling is reduced by; 7.8% for 2% CBAS, 20.3% for 5% CBAS and 59.4% for 10% CBAS addition. The reduction in the primary swell seemed to require greater addition of CBAS, as the swelling pressure generated by the soil specimens at this stage is greater (as also reflected commonly with a greater slope in the swelling percentage versus time plots). It can also be observed that the time for completion of primary swelling is reduced as the percentage addition of CBAS is increased. This is considered to be due to formation of a seal around the particle clusters and soil fabric overall, restricting adsorption of water molecules by the soil.

Figure 4.5 presents the results for 11% initial water content. It is notable that there is a significant increase in the overall swelling potential of the specimens due to the reduction in the initial water content. The behaviour observed during the initial swelling stages is comparable with the other test groups with different higher initial water content. The degree of improvement obtained for initial swelling is observed to be up to 50% with increase in the CBAS addition. However, the behaviour observed

for the primary swelling is not in line with the other groups. The degree of improvement is quite low even at high percentages of addition of CBAS.

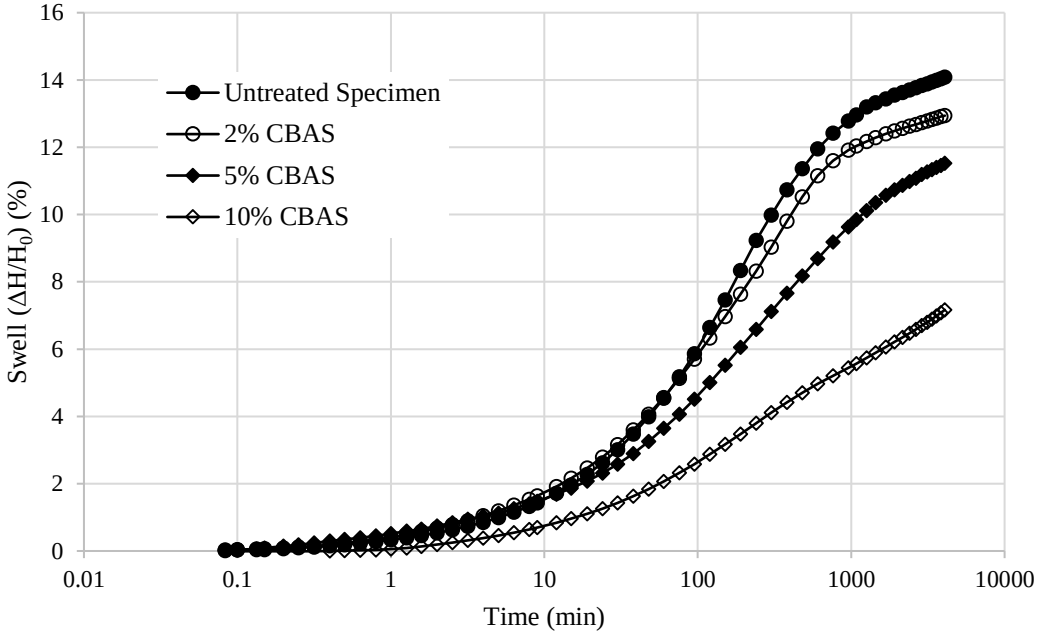


Figure 4.4. One dimensional swelling curve at 22.5% of initial water content

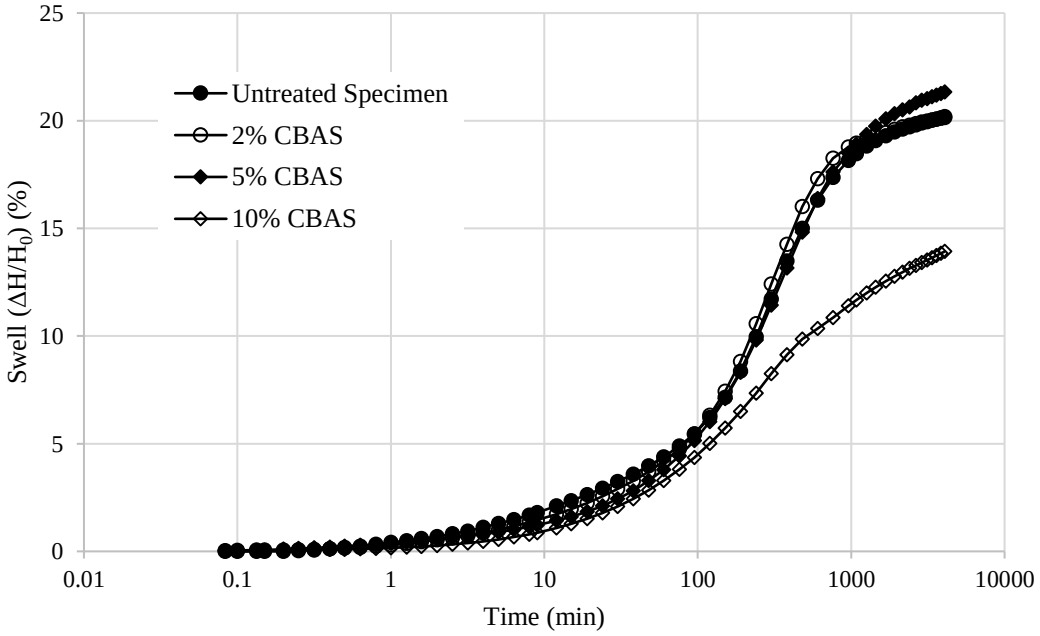


Figure 4.5. One dimensional swelling curve at 11% of initial water content

This implies that the CBAS chains are not strong enough to reduce the primary swelling potential significantly (improvement only up to 10%). Hence, it can be stated that as the initial water content of the specimens is reduced, due to the significant increase in the swelling potential, a considerably greater addition of CBAS might be required to achieve a comparable improvement in the overall swelling behaviour.

### 4.3.2 Evaluation of the One Dimensional Swelling Behaviour

The overall data obtained on one-dimensional swelling indicate that the initial swelling of untreated specimens and specimens with low percentages of CBAS (2% and 5% CBAS) are quite similar, whilst the initial swell of the high percentage CBAS group is significantly less. This initial difference in the swelling behaviour corresponds to the stages where the macropores start to become saturated and indicates that the response of the film or web of CBAS to the internal stresses created by water adsorption is not as stiff unless CBAS is introduced beyond a certain level which, in this case, is measured to be approximately 10%. However, during the primary swell stage, there is an increasing trend in the improvement observed with respect to the percentage of CBAS added. It is interesting to note that the percentage of improvement measured in the swell is approximately equal in both stages of swell for the high percentage CBAS group (approximately 50% with respect to the untreated specimen). It is also notable that as the percentage of CBAS is increased, the primary swell stage started to become less obvious, which means that the rate of primary swell is reduced. The high percentage CBAS curve (10% CBAS) indicates similar primary and secondary swell rates, both of which seem to be similar with the secondary swell rate of the untreated specimen. These observations indicate that the CBAS is fairly effective overall after the initial stages of the swell, at the end of which the specimens can be regarded as fully saturated. However, after this stage there seems to be little or

negligible improvement during secondary swelling. This is due to the high overall internal swelling stresses created by the water adsorption during swelling, which is likely to have caused exceedance of the strength of the film or web of CBAS formed. As a result of this, the rate of secondary swell remained similar to the rate observed for the untreated specimen. Another reason for this may be that; the secondary swelling stage (which is the part of swelling that occurs after saturation of the macropores, through water adsorption into the micropores) is not improved efficiently, as the CBAS is not effectively adsorbed into the micropores.

### 4.3.3 Cyclic Swell Shrink Test

The effect of CBAS treatment on cyclic swelling and shrinkage behaviour of specimens are presented in Figure 4.6 and 4.7. The addition of CBAS has a marked effect on the shrinkage characteristics such that, when a similar drying pattern led to major cracking and disintegration in the control specimens, the CBAS treated specimens managed to survive without disintegration for five cycles of wetting and drying. As the drying process (shrinkage) was well controlled, i.e. applied as gently as possible using silica gel method outlined in Chapter 3, the improvement attained with respect to the control specimens is considered to be significant.

The swelling potential is observed to be highly related with the initial water content prior to wetting. The water content at the end of drying period is tried to be kept as consistent as possible throughout the whole set of the specimens, however, due to the position of the specimens in the dessicator and variation in the homogeneity of the specimens, there were differences observed in the water content for the same waiting periods. The variation in the initial water contents obtained prior to wetting however helped observation of the fact that, as the specimens are dried to lower intial water

contents, the swelling potential increased. The control specimens responded to this variation much more compared to the CBAS treated specimens, which tended to stabilise after a few cycles regardless of their initial water contents.

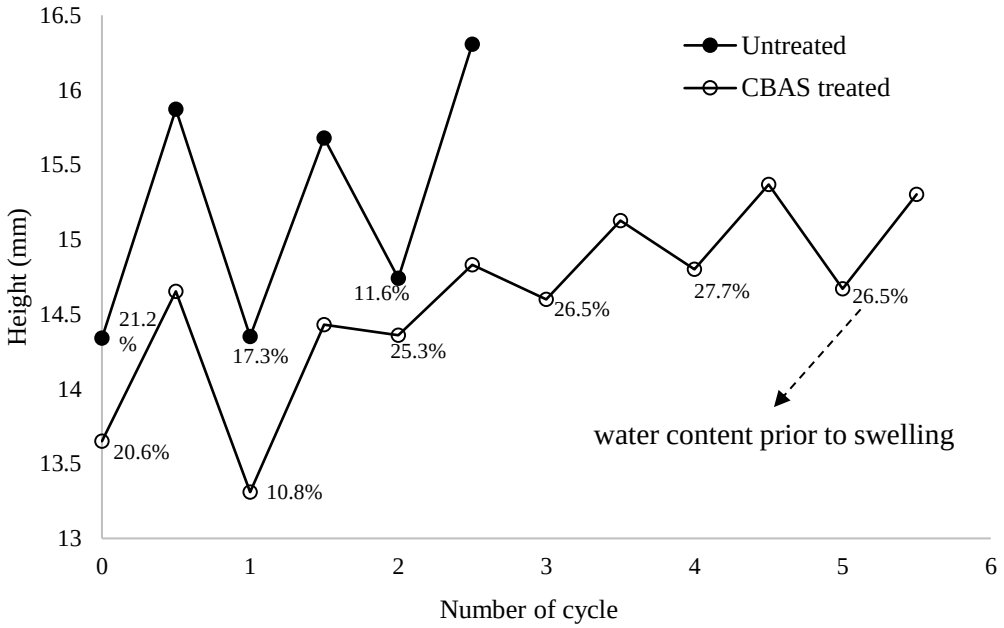


Figure 4.6. Changing height with respect to number of cycles

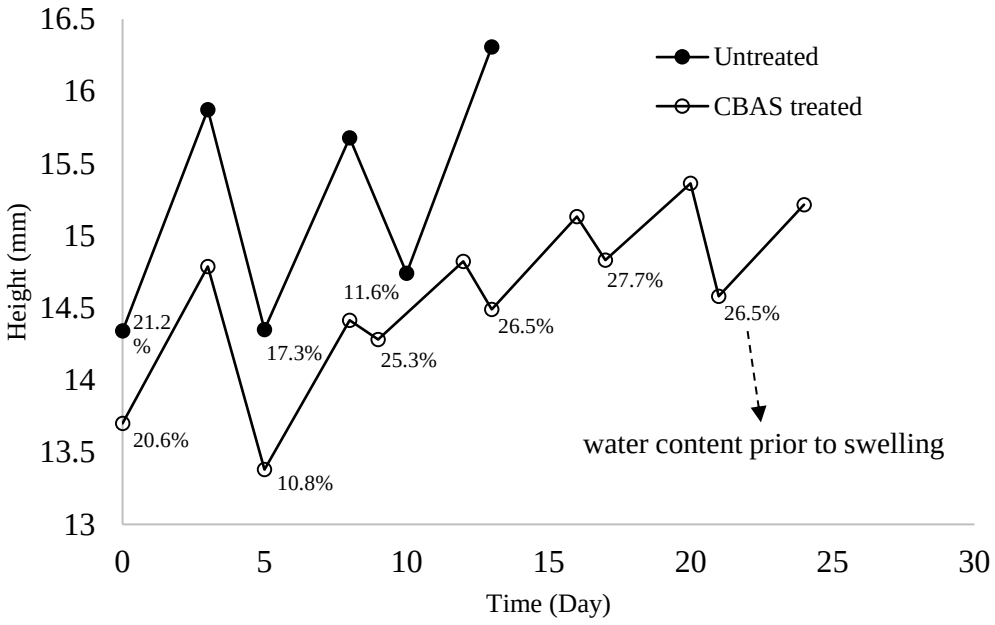


Figure 4.7. Changing height with respect to time

The rate of drying was the other aspect of the specimens observed during wetting and drying cycles. It is observed that the CBAS treated specimens have an improved ability to retain moisture as for the same drying period their water content was noticeably greater compared to the control specimens. This is due to the electrostatic bonding between the polymer chains and the water molecules making it more difficult to draw moisture out of the specimens.

## 4.4 One Dimensional Consolidation

In this part of the thesis program, compressibility of the untreated and treated specimens are investigated. Three groups of CBAS are selected for a focused assessment of the role of CBAS stabilization on clay compressibility. The CBAS treatment groups are selected to be 2% and 5%. In order to investigate the effect of initial moisture content on the efficacy of stabilization, a similar procedure is followed to prepare test specimens of initial water contents; 28%, 22.5%, 16% and 11%. The results are presented in Figure 4.8 to 4.11. The additional results are presented in Appendix D.

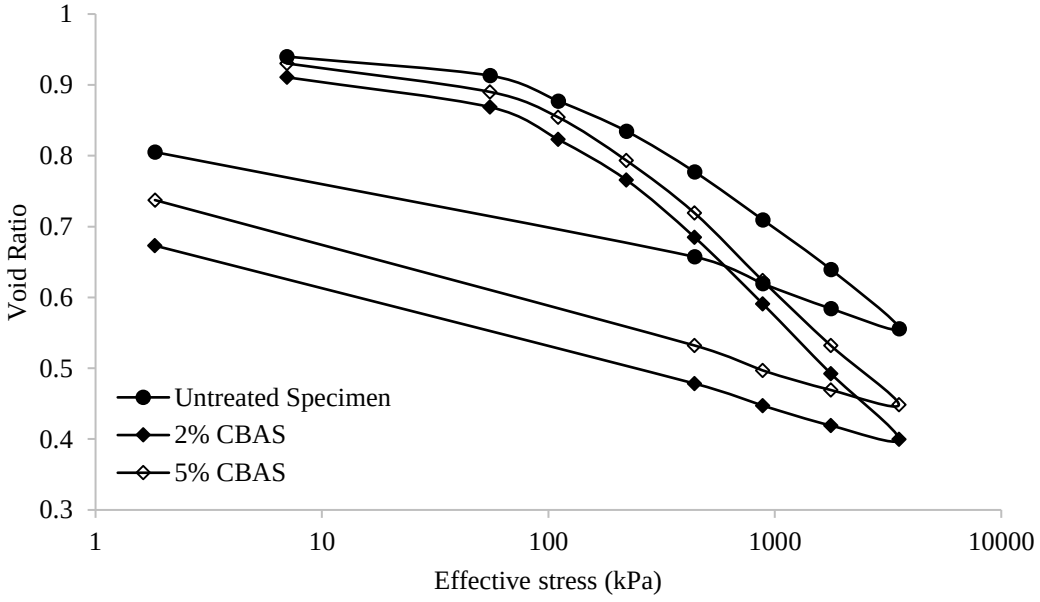


Figure 4.8. One dimensional consolidation curves at 28% initial water content

The compressibility behaviour of the polymer treated specimens are found to reflect a mixed character in terms of the degree of improvement attained at various initial water contents. The same set of curves are also presented in Figure 4.12 to aid comparison of the results.

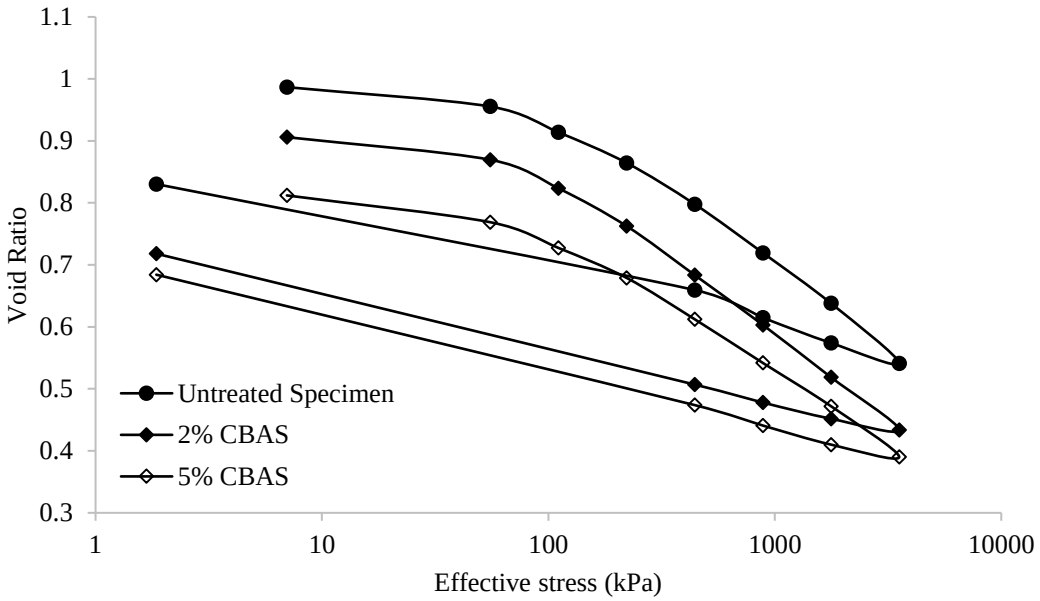


Figure 4.9. One dimensional consolidation curves at 22.5% initial water content

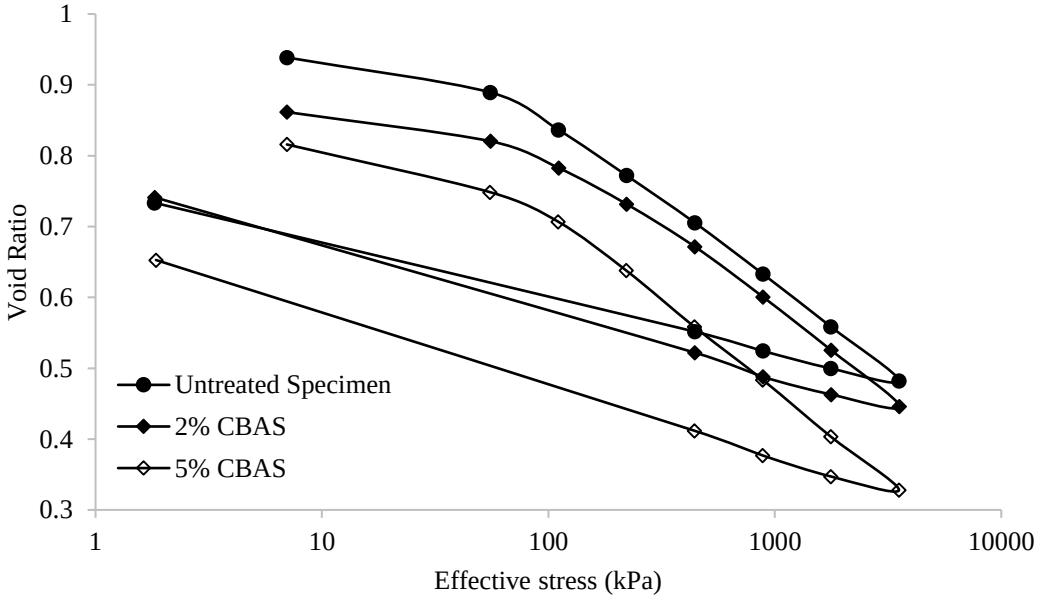


Figure 4.10. One dimensional consolidation curves at 16% initial water content

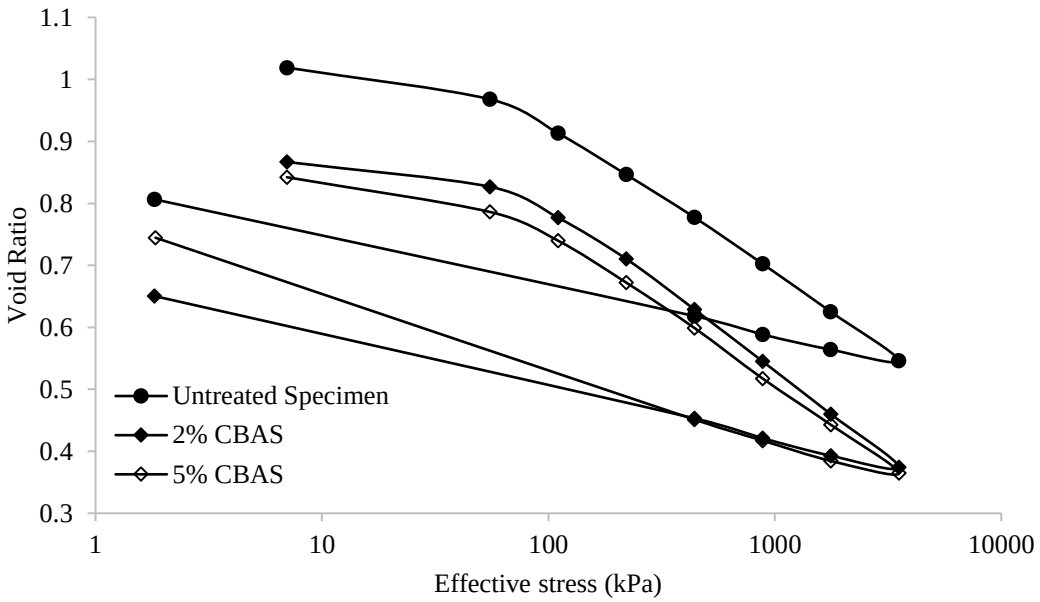


Figure 4.11. One dimensional consolidation curves at 11% initial water content

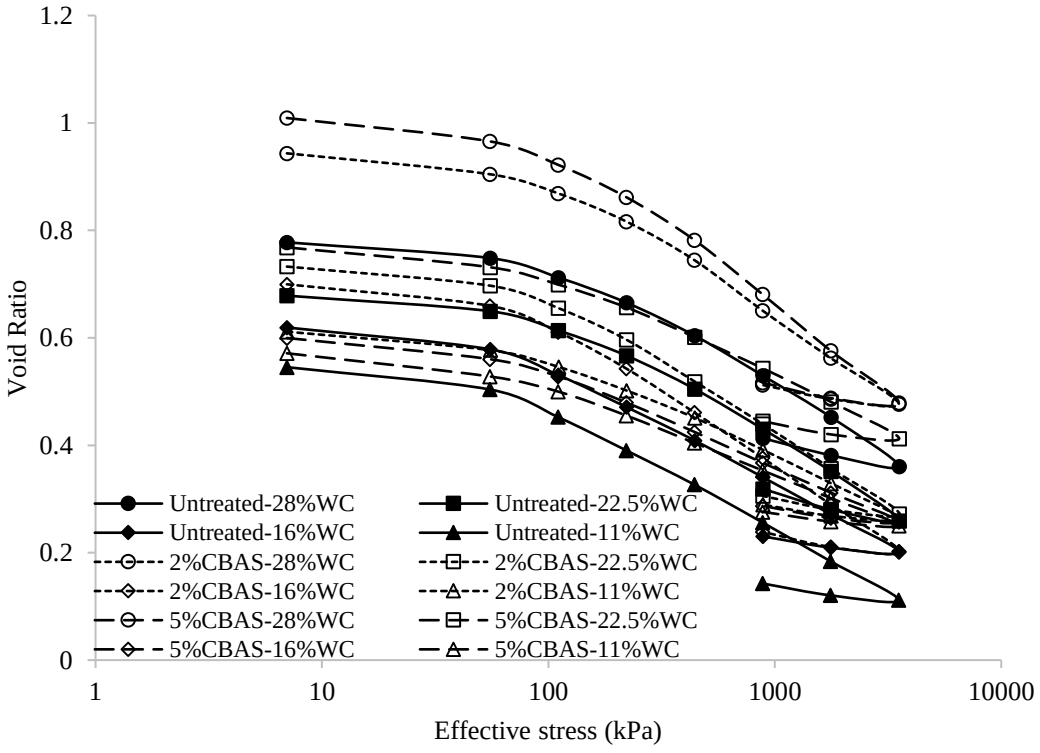


Figure 4.12. One dimensional consolidation curves for untreated and treated specimens

The testing program is organised to allow for a comparison of the compressibility characteristics of the specimens during one-dimensional consolidation. In order to

precisely assess the compressibility characteristics, a normalization is performed by calculating the ratio of the void ratio corresponding to each loading stage in the one dimensional compression test to the initial void ratio of the specimens measured prior to any effective stress increase. The initial conditions varied significantly due to drying and resaturation of the specimens as also depicted previously by the swelling curves. Therefore, the normalization applied, which is based on the states of the specimens at initial condition after saturation (prior to loading) is crucial to provide a fair evaluation of the results as presented in Figure 4.13

The results show that the compressibility of the treated specimens is improved as the initial water content prior to saturation is reduced, indicating that the polymer has interacted with soil effectively throughout the drying process prior to resaturation and loading. The results also indicated that, although there is an increased compressibility due to the softening effect caused by drying and resaturation (restructuring of the soil fabric), there is still improvement in the compressibility of the treated specimens.

In order to evaluate the degree of improvement attained in the compressibility of the specimens, the coefficient of compression ($C_c$), recompression index ($C_r$), secondary compression ($C_\alpha$), coefficient of consolidation ($C_v$) and also preconsolidation pressure ($\sigma_{p'}$) are also obtained from the test results, which are presented in Table 3. The coefficient of consolidation is calculated using time taken for 50% of consolidation and for a loading range of 7-55kPa, which is considered to be the most applicable effective stress increase for superficial fills.

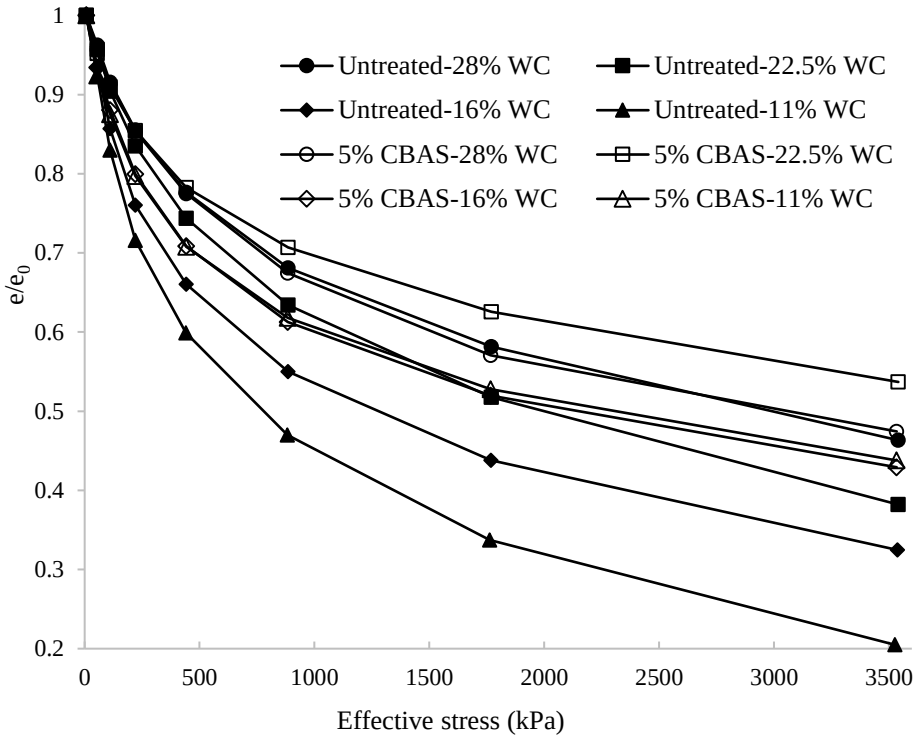


Figure 4.13. Modified one dimensional consolidation curves for untreated and treated specimens

The results in Figure 4.13, also indicate that the degree of improvement is increasing as the effective stress is increased, such that there is an improvement of almost 55% in the best case for the maximum effective stress applied (between 11% water content group of untreated and treated specimens). As the drying water content of the 11% water content group is below the shrinkage limit, upon resaturation this group is observed to have an increased compressibility, such pheonomenon is previously explained by Popescu (1980). Based on Popescu (1980), there is a critical dry density for each soil related to the characteristics of that soil, which can be attained during shrinkage. If any soil is dried to have a moisture content below its shrinkage limit, which would mean that its dry density is now above that critical dry density, upon resaturation a greater volume change potential is bound to be observed for that soil. As a result of greater swelling, 11% water content group of untreated specimens are swollen more yielding a greater initial void ratio (softer and more compressible state)

and reflected a considerably greater compressibility behavior compared to the specimens of other groups.

Table 4.3. One dimensional consolidation test results

| Group | w (%) | $C_c$ | $C_r$ | $\sigma_{p'}$ (kPa) | $C_\alpha$ * Both parameters are calculated for the loading stage of 7 to 55kPa. | $C_V$ ($m^2$/year) |
|---|---|---|---|---|---|---|
| Untreated | 28.26 | 0.265 | 0.090 | 205 | 0.0004 | 1.112 |
| 2% CBAS | 27.39 | 0.276 | 0.060 | 155 | 0.0004 | 0.708 |
| 5% CBAS | 26.9 | 0.302 | 0.053 | 145 | 0.0004 | 0.620 |
| Untreated | 22.96 | 0.260 | 0.087 | 171 | 0.0008 | 1.118 |
| 2% CBAS | 20.61 | 0.251 | 0.051 | 129 | 0.0007 | 0.743 |
| 5% CBAS | 20.12 | 0.200 | 0.044 | 125 | 0.0004 | 0.700 |
| Untreated | 16.32 | 0.253 | 0.060 | 129 | 0.0022 | 3.460 |
| 2% CBAS | 16.76 | 0.246 | 0.046 | 115 | 0.0011 | 0.857 |
| 5% CBAS | 16.76 | 0.175 | 0.041 | 110 | 0.0005 | 1.052 |
| Untreated | 10.72 | 0.226 | 0.055 | 121 | 0.0028 | 3.970 |
| 2% CBAS | 10.41 | 0.198 | 0.041 | 110 | 0.0012 | 1.149 |
| 5% CBAS | 11.56 | 0.173 | 0.039 | 100 | 0.0007 | 1.187 |

Water content (w), coefficient of compression ($C_c$), recompression index ($C_r$), secondary compression ($C_\alpha$) and coefficient of consolidation ($C_v$), preconsolidation pressure ($\sigma_{p'}$)

A similar trend of improvement is also observed in the secondary compression rates measured. However, this parameter is observed to be more sensitive to the drying water content, which is applied prior to one-dimensional consolidation testing. The reduction in the creep rate of specimens dried to a moisture content of 11% is observed to be as low as 25% of the initial estimate for their corresponding untreated group specimens. The coefficient of consolidation, which is an indirect measure of the

drainage characteristics of the specimens is observed to drop with the addition of CBAS, which is due to the support provided by the CBAS in the soil microstructure restraining the flow of water through the specimen. However, as the drying water content is dropped, due to higher swell potential upon resaturation, a slight modification in the coefficient of consolidation is observed.

## 4.5 Unconfined Compressive Strength Test (UCS)

The results of unconfined compressive strength for all groups are presented in Figure 4.14 to 4.17. Figure 4.18 illustrate the unconfined compressive strength for all groups with respect to initial water content. It can be seen from the results that there is a consistent increment in the unconfined compressive strength with increase in the degree of treatment. It is also notable that the improvement in the unconfined compressive strength is observable for all treated specimens regardless of their initial water content. The additional results and photos are presented in Appendix C.

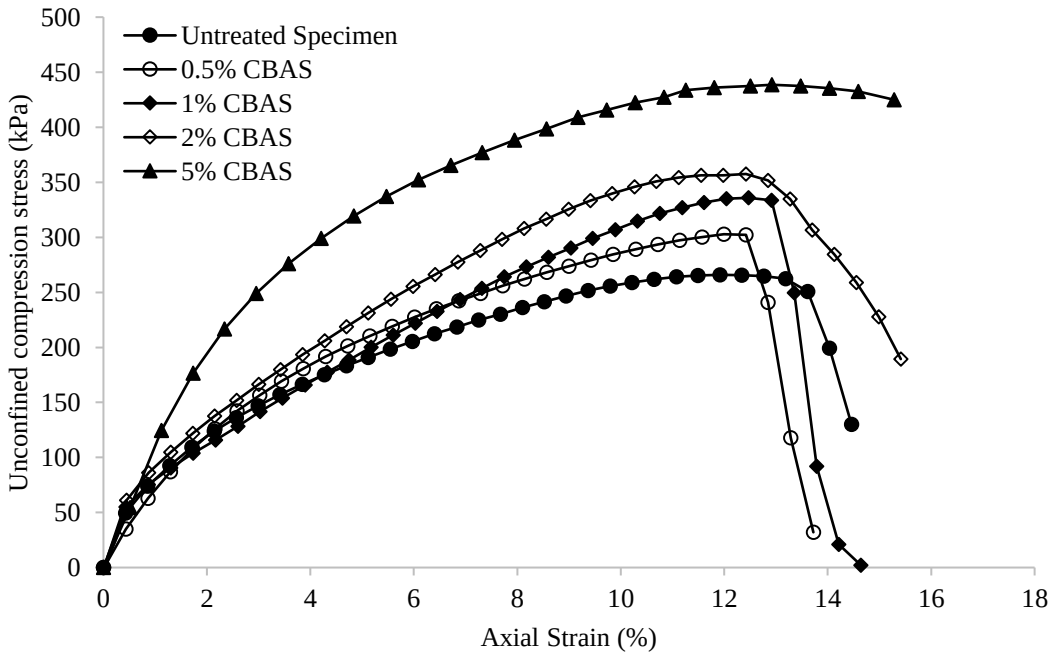


Figure 4.14. Unconfined compressive strength for all groups at 28% initial water content

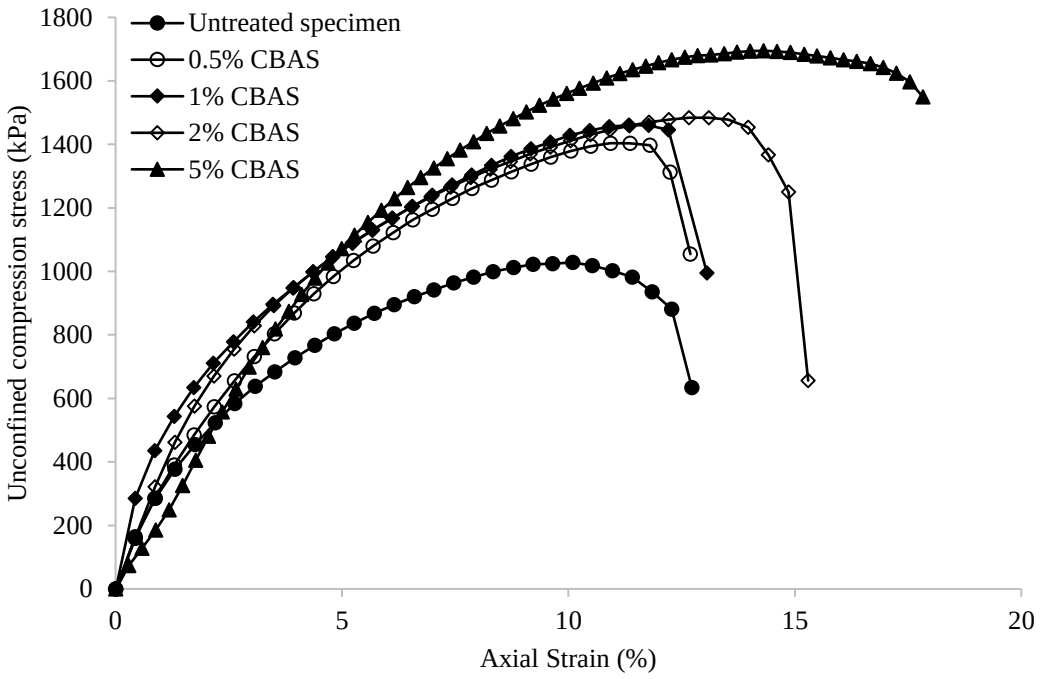


Figure 4.15. Unconfined compressive strength for all groups at 22.5% initial water content

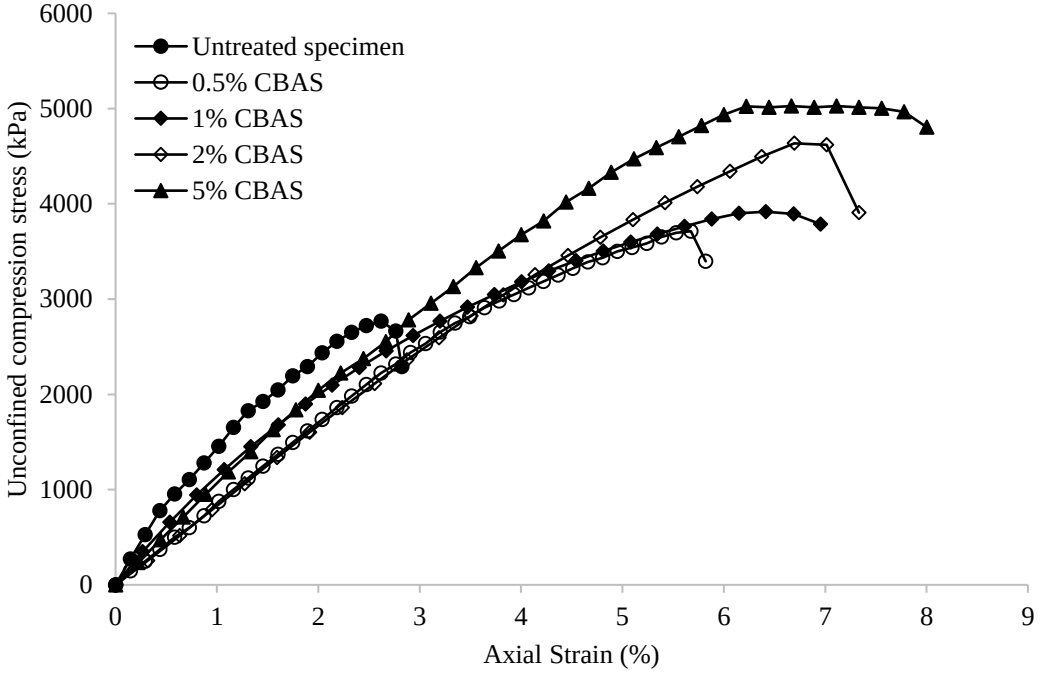


Figure 4.16. Unconfined compressive strength for all groups at 16% initial water content

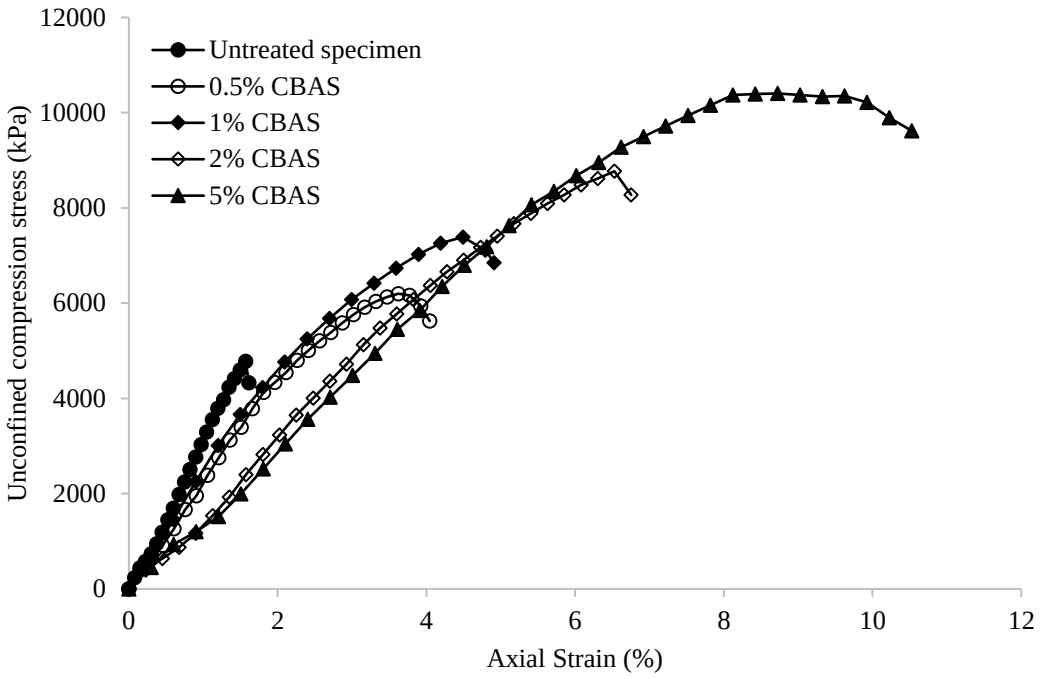


Figure 4.17. Unconfined compressive strength for all groups at 11% initial water content

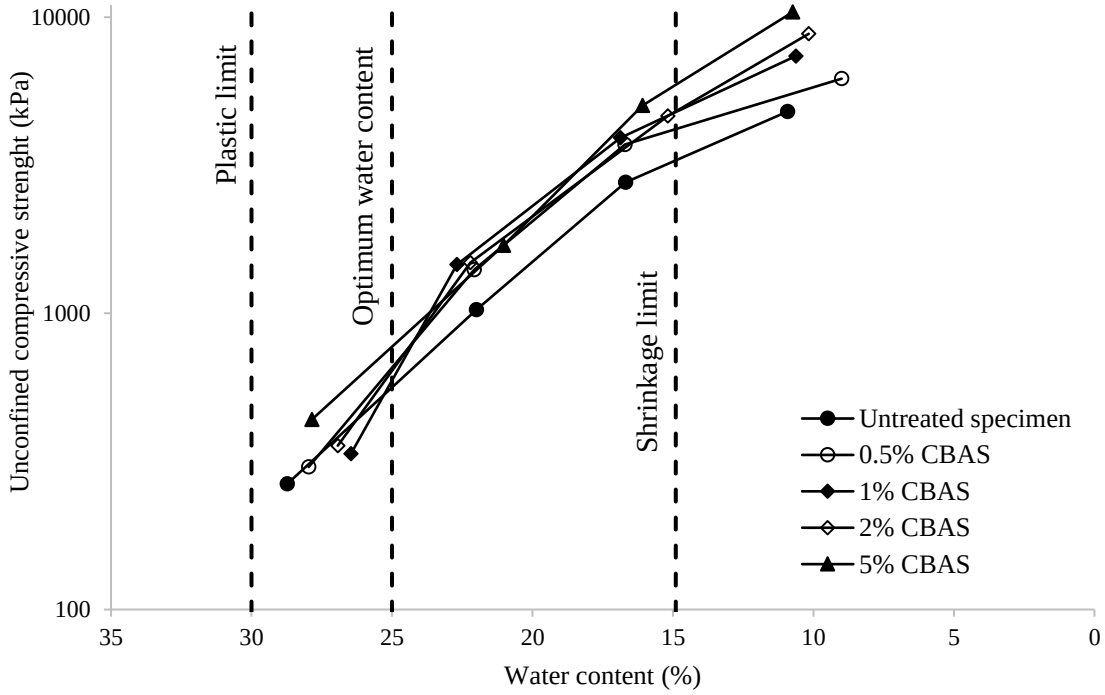


Figure 4.18. Unconfined compressive strength for all groups with respect to initial water content

In Figure 4.19, the comparison of the unconfined compressive strength of any group to the unconfined compressive strength of control group ($q_u$ ratio) is presented.

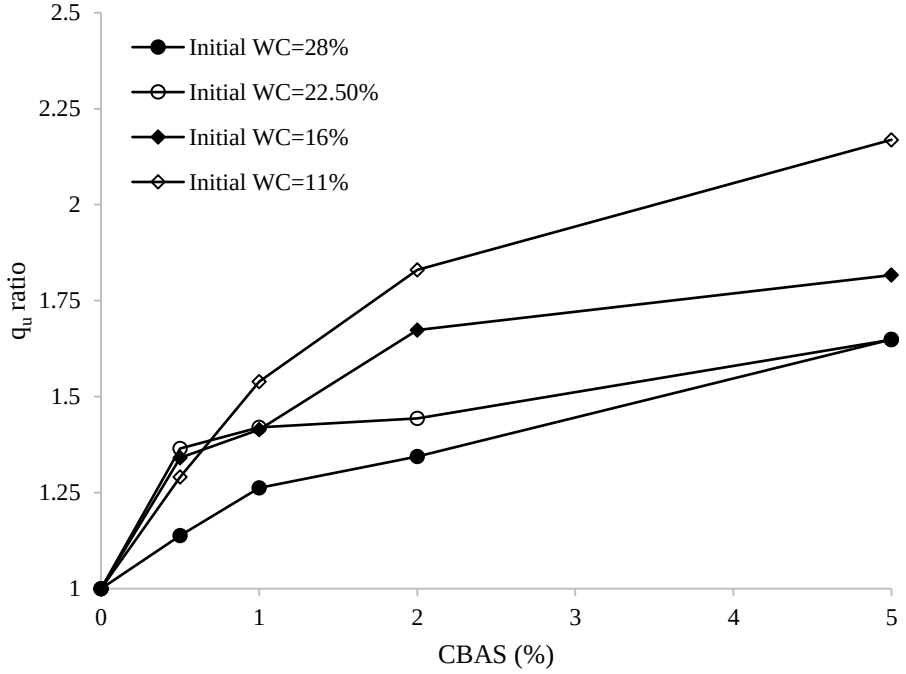


Figure 4.19. Comparison of the unconfined compressive strength of treated and untreated specimens

The strain at failure for all treated specimens is comparably greater, hence, indicating an increase in the ductility. The increase in the ductility of the treated specimens can be attributed to the development of polymeric chains in the clay fabric. Ductility is especially important for buried impermeable fills, such as landfill liners, which can undergo significant strains due to the weight of waste fill. An increased strain at failure can provide an advantage for such fills to retain their mass characteristics at higher strains, so that they can perform within the serviceability limits of their specification of hydraulic conductivity (Dixon and Jones 2005).

In order to assess the effect of polymer treatment on the ductility of specimens, the ductility ratio (DR) is plotted with respect to the amount of polymer treatment in Figure 4.20. The ductility ratio is simply defined as the ratio of axial strain at failure of the treated specimens ($\varepsilon_i$) to the axial strain at failure of untreated specimens ($\varepsilon_0$).

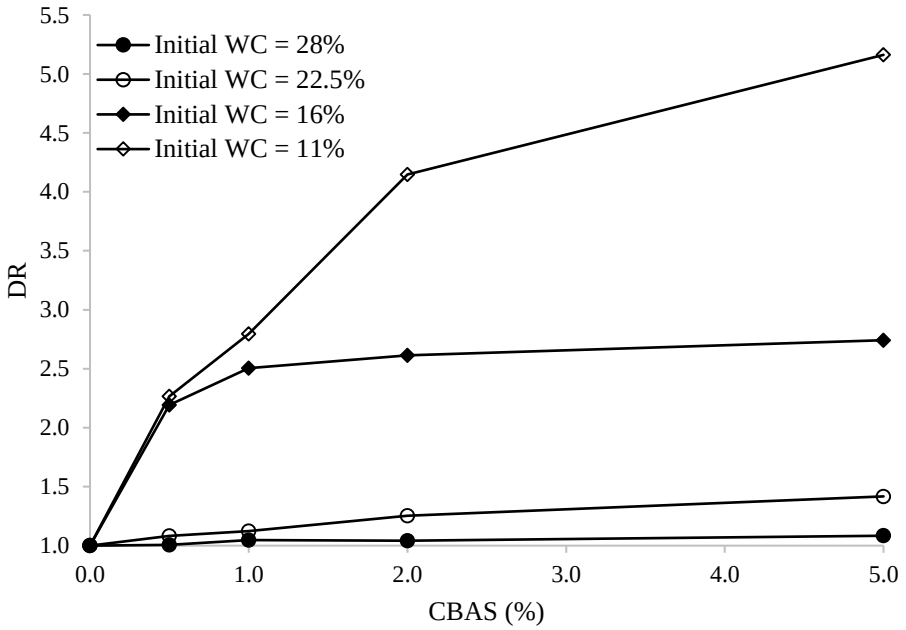


Figure 4.20. Ductility ratio with respect to CBAS content

The results indicate that the increase in the DR at 28% initial moisture content is approximately 10% regardless of the amount of polymer treatment. However, as the moisture content drops, the improvement in the DR is much more significant. It is also notable that the improvement in the DR for the dry side of the optimum moisture content can be assessed as approximately in the range of 10% to 50% depending on the amount of polymer treatment performed. As the results of this research is based on the Standard Proctor compaction effort, it is likely that an increased compaction effort (in the field) can provide even higher improvement for the DR due to a lower optimum moisture content.

The average elasticity modulus ($E_{50}$), evaluated for the treated and untreated specimens are presented in Figure 4.21. The average elasticity modulus is calculated by considering the slope of the compressive stress versus axial strain curve corresponding to the initial tangent line drawn through the half of the peak compressive stress.

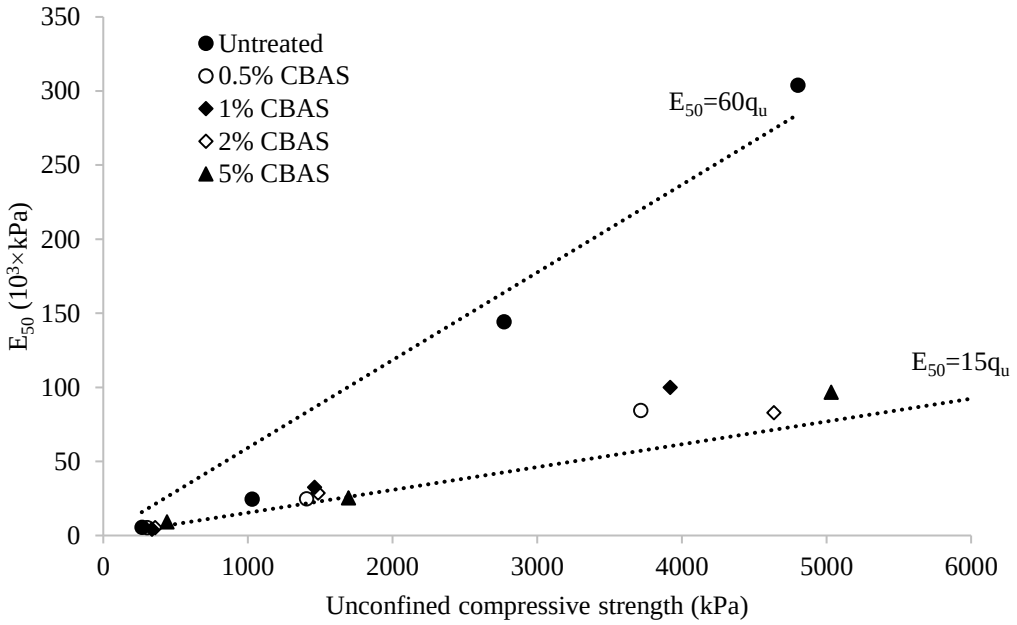


Figure 4.21. Average elasticity modulus versus unconfined compressive strength

The data indicates that there is a linear relationship between the average elasticity modulus and the unconfined compressive strength, which is in line with the well-known correlations in the literature (Stroud and Butler, 1975; Duncan and Buchignani, 1976). It is notable that the correlation coefficient for the untreated specimens is significantly greater than the treated specimens. As $E_{50}$ is a parameter for the average elasticity of the specimen, essentially capturing the behavior of the specimen during the early stages and mid-stages of the test prior to failure, it is reasonable to suggest that the increase in the ductility is not only limited to the failure state but it onsets from the initial stages of loading. The unconfined compressive strength parameters are presented in Table 4.4.

Table 4.4. Unconfined compressive strength parameters.

| CBAS (%) | UCS (kPa) | Shear strength (kPa) | Water content (%) | Secant modulus (MPa) | Strain at failure (%) | DR |
|---|---|---|---|---|---|---|
| 0 | 265 | 132 | 28.72 | 5.54 | 11.921 | 1 |
| 0.5 | 302 | 151 | 27.96 | 5.31 | 11.991 | 1.005 |
| 1 | 335 | 167 | 26.45 | 4.25 | 12.472 | 1.046 |
| 2 | 357 | 178 | 26.92 | 5.25 | 12.419 | 1.041 |
| 5 | 438 | 219 | 27.84 | 9.13 | 12.922 | 1.083 |
| 0 | 1028 | 514 | 21.99 | 24.48 | 10.0937 | 1 |
| 0.5 | 1403 | 701 | 22.07 | 24.63 | 10.931 | 1.082 |
| 1 | 1460 | 730 | 22.68 | 32.46 | 11.334 | 1.122 |
| 2 | 1484 | 742 | 22.21 | 28.53 | 12.660 | 1.254 |
| 5 | 1560 | 780 | 21.02 | 25.30 | 14.307 | 1.417 |
| 0 | 2769 | 1384 | 16.68 | 144.24 | 2.5614 | 1 |
| 0.5 | 3714 | 1857 | 16.70 | 84.43 | 5.617 | 2.193 |
| 1 | 3917 | 1958 | 16.86 | 99.93 | 6.415 | 2.504 |
| 2 | 4635 | 2317 | 15.17 | 82.77 | 6.695 | 2.613 |
| 5 | 5031 | 2515 | 16.08 | 96.75 | 7.023 | 2.741 |
| 0 | 4801 | 2400 | 10.92 | 303.91 | 1.585 | 1 |
| 0.5 | 6200 | 3100 | 8.99 | 231.37 | 3.592 | 2.266 |
| 1 | 7393 | 3696 | 10.63 | 227.97 | 4.433 | 2.796 |
| 2 | 8790 | 4395 | 10.16 | 159.82 | 6.574 | 4.147 |
| 5 | 10415 | 5207 | 10.73 | 150.95 | 8.181 | 5.161 |

## 4.6 Internal Stability Test Results

The results of the clay stability tests are presented in Table 4.5. The calculated K values indicate that the test specimens treated with CBAS have improved stability, with an increasing trend as the percentage addition of the CBAS is increased. Even with the minute amount added in Gr-2, the clay stability index is improved considerably for a given initial water content. The additional photos of the test are presented in Appendix B.

Table 4.5. Water stability test results

| Initial Moisture content | (%) | | 11 | 16 | 22.5 | 28 | | 11 | 16 | 22.5 | 28 |
|---|---|---|---|---|---|---|---|---|---|---|---|
| $K_{10}$ | (%) | GR - 1 | 81.6 | 75 | 73 | 70 | Percentage of explosive collapse | 10 | 8 | 0 | 0 |
| | | GR - 2 | 73.8 | 97.2 | 100 | 100 | | 50 | 42 | - | - |
| | | GR - 3 | 93.8 | 97.4 | 100 | 100 | | 100 | 33 | - | - |
| | | GR - 4 | 92.2 | 100 | 100 | 100 | | 100 | - | - | - |
| $K_{20}$ | (%) | GR - 1 | 63.9 | 61.5 | 57.2 | 53.7 | | 25 | 8 | 0 | 0 |
| | | GR - 2 | 59.1 | 90.6 | 100 | 100 | | 50 | 50 | - | - |
| | | GR - 3 | 83.5 | 92 | 100 | 100 | | 78 | 50 | - | - |
| | | GR - 4 | 87.7 | 100 | 100 | 100 | | 100 | - | - | - |
| $K_{30}$ | (%) | GR - 1 | 52.5 | 57 | 53.6 | 45.2 | | 29 | 8 | 0 | 0 |
| | | GR - 2 | 52.7 | 83.8 | 100 | 100 | | 60 | 0 | - | - |
| | | GR - 3 | 77 | 88.1 | 100 | 100 | | 78 | 60 | - | - |
| | | GR - 4 | 85.1 | 100 | 100 | 100 | | 100 | - | - | - |

GR - 1 (Untreated clay, GR - 2 (clay with %0.5 CBAS), GR - 3 (clay with %1 CBAS), GR - 4 (clay with %2 CBAS).

### 4.6.1 Evaluation of Water Stability Test Results

In order to highlight the degree of improvement for treated test specimens (Gr-2 to 4) with respect to control group (Gr-1) specimens, the ratio of clay stability index of

treated specimens to the clay stability index of the control group specimens are calculated. As depicted in Figure 4.22 to 4.24, the improvement is more prevalent as the time period at which K value calculated increases, confirming the improved long term stability of the treated test specimens.

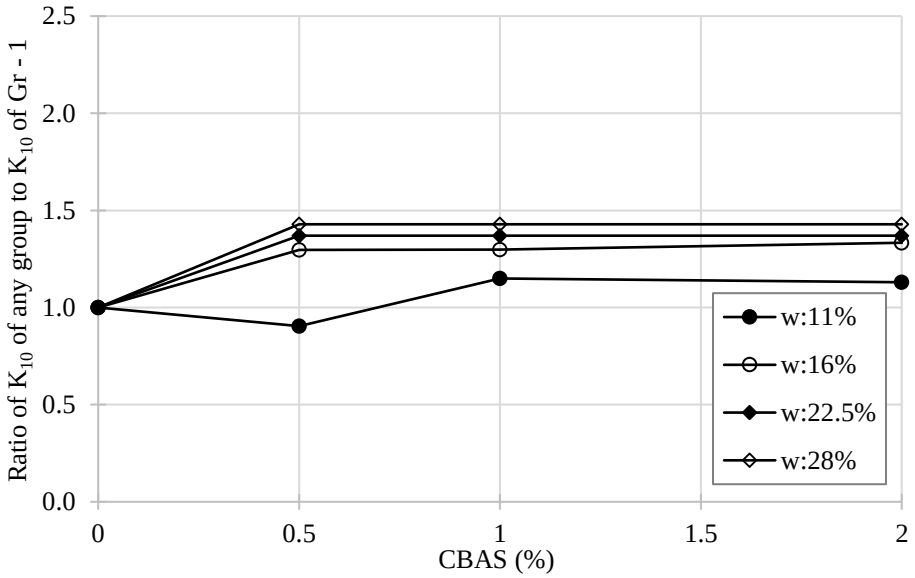


Figure 4.22. Variation of the water stability index at 10 mins with respect to CBAS

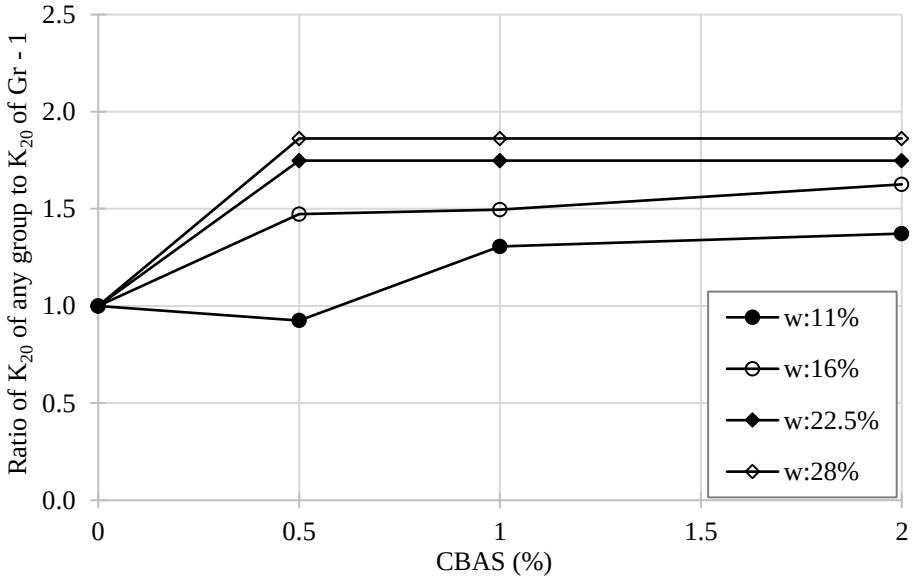


Figure 4.23. Variation of the water stability index at 20 mins with respect to CBAS

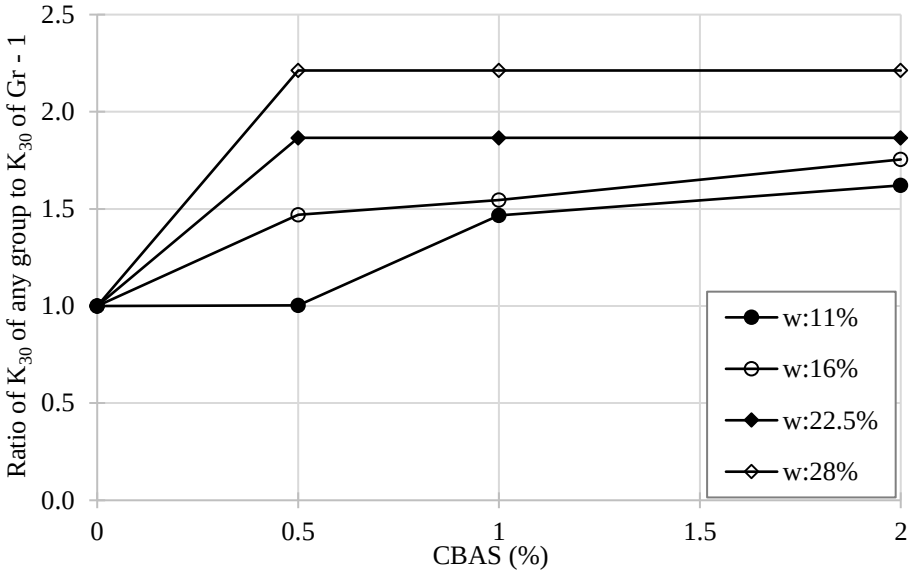


Figure 4.24. Variation of the water stability index at 30 mins with respect to CBAS

The impact of the initial water content on the test results is notable. In Figure 4.25 to 4.27, the plot of the test results indicates that the internal stability of all treated test specimens is improved with respect to increase in the initial water content prior to testing.

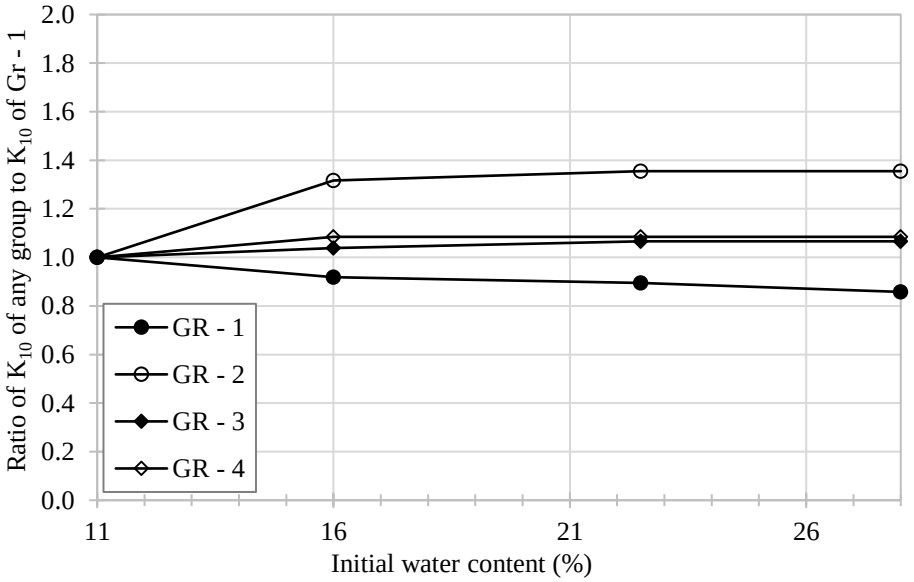


Figure 4.25. Variation of the water stability index at 10 mins with respect to initial water content

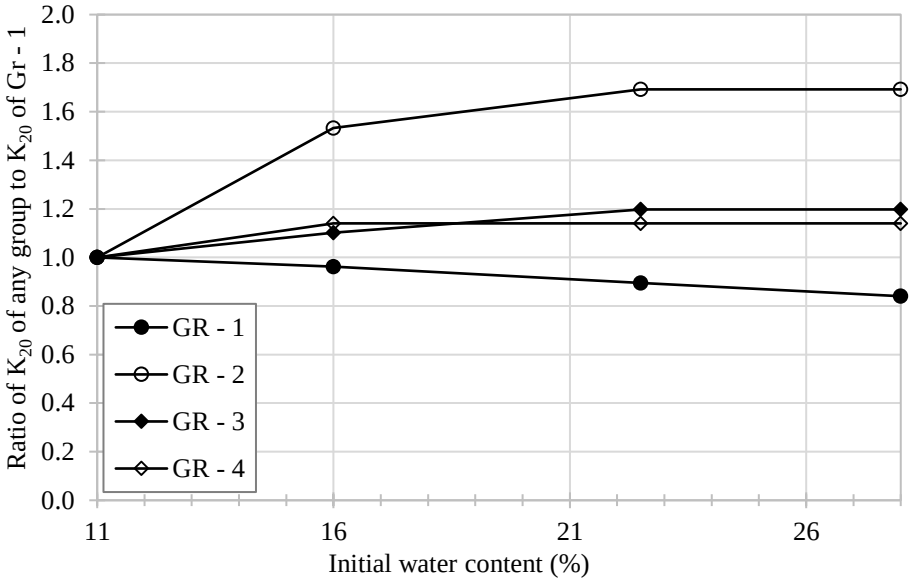


Figure 4.26. Variation of the water stability index at 20 mins with respect to initial water content

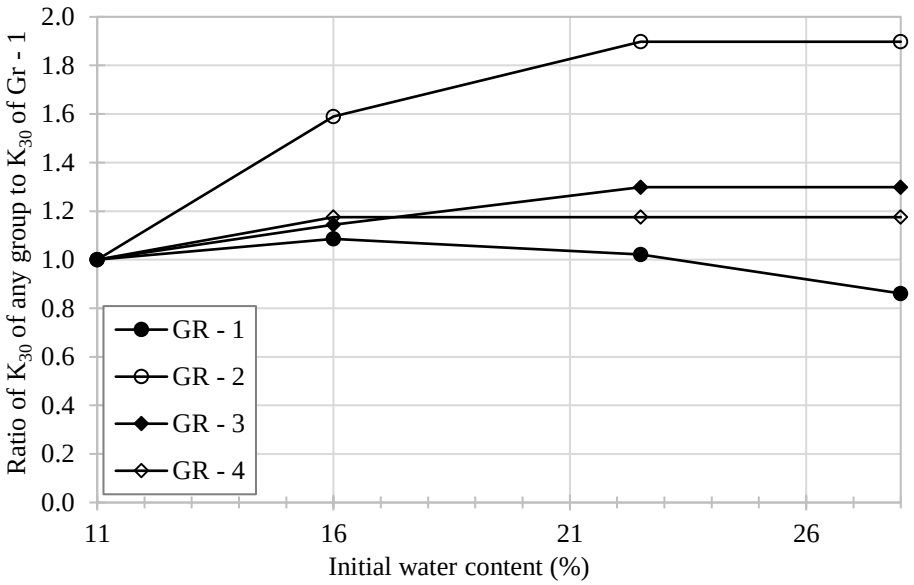


Figure 4.27. Variation of the water stability index at 30 mins with respect to initial water content

It is also interesting that CBAS seems to be most effective for Gr-2 test specimens, which only consists 0.5% of CBAS by dry mass of clay. As control specimens became less stable with increasing initial water content, the treated samples had an improved

performance, reflecting an improvement in resistance against inundation even at high initial water content levels.

When these results are examined from another point of view, i.e. with respect to decrease in the initial water content, it can be perceived that there is an improvement in internal stability for the control specimens. It can be stipulated that, the improvement in the performance of control specimens is due to the increase in the affinity of the clay mineral layers to absorb water which, initially, will be tolerated well by the clay microstructure causing an apparent stability in the clay-water electrolyte system. However, with the degree of saturation of the test specimens increasing, the absorbed ions on the diffuse double layer around the clay particles will lead to expansion of the inter-particle pore space and increase in the repulsion forces between clay particles (Mitchell and Soga 2005). This phenomenon reduces the stability of the clay structure as depicted by a drop in the clay stability index, when it is measured at various time periods as $K_{10}$, $K_{20}$ and $K_{30}$ in the clay stability test. For treated specimens, CBAS addition leads to a reduction in the interaction between the clay particles and particle associations with the water and, as a result, the clay fabric will be affected less. However, increase in the absorbed water will lead to an increased interaction between the clay-water-polymer electrolyte system. Hence, the increased interaction is reflected as a reduction in the clay stability index. In this mechanism, it is notable that the reduction in the clay stability index decreases as the polymer added increases, which would imply that, as the amount of polymer is increased, lower initial water contents can be tolerated for the same level of internal stability. This is especially important as the polymer treatment in civil engineering projects can be performed for superficial clays, which may be exposed to significant moisture changes.

A general trend was observed through the clay stability test in terms of mode of collapse, such that the test specimens with higher CBAS content tended to reflect the explosive mode of collapse more than the other test specimens. The initial water content of the specimens did not appear to have a clear impact on the mode of collapse. However, it is observed that explosive collapse is more common with the specimens having lower initial water content (11% and 16%). On the other hand, the time period at which the internal stability is evaluated seems to have a correlation with the collapse mode, such that most of the collapses observed after 10 minutes are recorded to be due to gradual cracking and slaking rather than explosive mode of collapse. It is observed that the interaction between CBAS and clay is effective on the collapse mode. It is envisaged that, for treated specimens, formation of a web of CBAS chains within the macropores may have generated an initial resistance against cracking and slaking immediately after the immersion of specimens in water. As the test progressed, the absorbed water induced volume increase in the specimens which created an increase in internal stress and caused the explosive mode of collapse in most of the treated specimens, confirming that an effective web of polymer chains was formed around clay fabric as well in most of the specimens.

### 4.6.2 Evaluation of Water Stability Test Results with Respect to One-Dimensional Swell Test Results

The results obtained in the one-dimensional swell tests are essentially linked to the water stability tests as in both of these tests the specimens are exposed to similar conditions (inundation in distilled water), with some differences in the boundary conditions (confined or unconfined). The interaction between CBAS and clay is considered to be effective on the collapse mode observed. It is envisaged that for treated specimens, formation of a web of CBAS chains around the clay mineral layers

may have generated an initial resistance against cracking and slaking immediately after immersion of specimens in water. When the one-dimensional swell test results are compared with the clay stability test results, it can be stated that the CBAS addition is very effective in the latter even at low levels of treatment. However, higher percentages of CBAS are required in order to observe a significant improvement in the former. The reason for this behavior can be explained as below.

a) the mechanism of internal stresses generated when swelling takes place in confined, one-dimensional form is different than the mechanism of internal stresses generated in the clay stability test where three dimensional swell is allowed in an unconfined manner, and

b) one-dimensional swell test results are interpreted at lower strain levels compared to the clay stability test results in which collapse of specimens was observed relating to a failure condition (large strain).

### 4.6.3 Analysis of Double Hydrometer Test Results

The results of the double hydrometer tests are presented in Figure 4.28 and 4.29. As it can be observed from the comparison of all test results, the polymer treated specimens, regardless of addition of dispersing agent, resulted to a coarser particle size distribution. This indicates that the polymer-soil-water interaction resulted to accumulation of fine soil particle clusters closer together leading to detection of a greater particle size as a result in the hydrometer test. Without the addition of the dispersing agent in the tests, the polymer became even more effective in the above process, leading to a greater difference, especially in the average particle size range corresponding to coarse-fine limit (eg. 60 μm based on USCS).

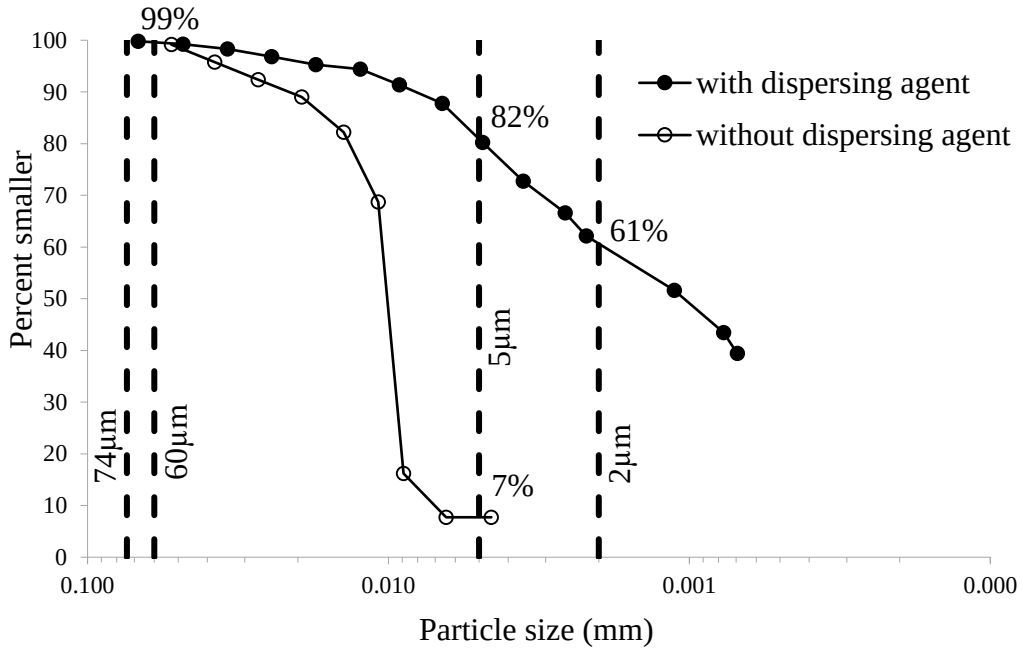


Figure 4.28. Double hydrometer test for untreated soil

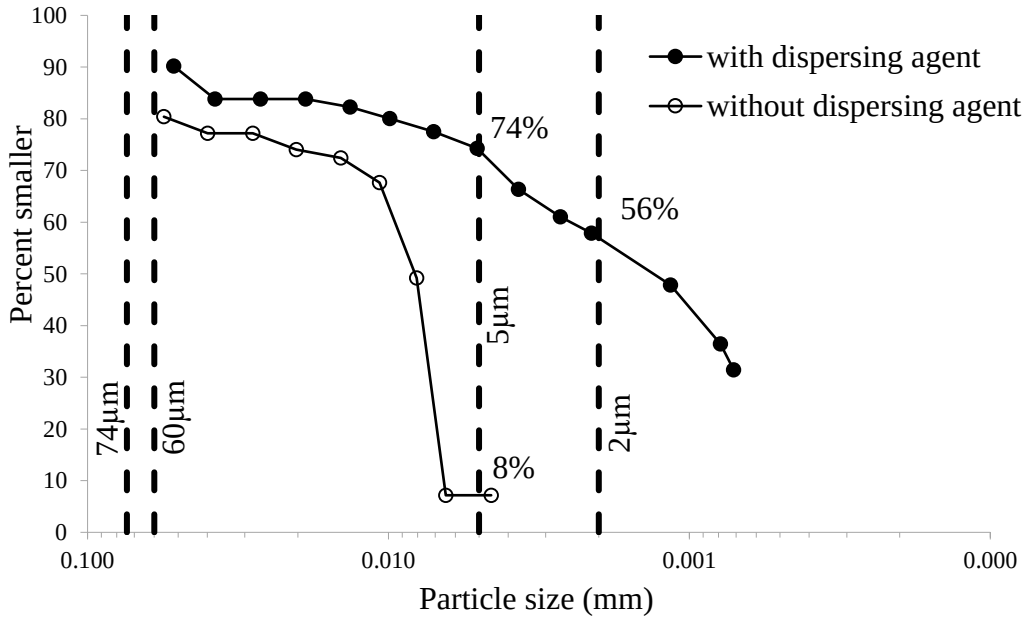


Figure 4.29. Double hydrometer test for 5% CBAS treated soil

There is approximately 20% less particles in suspension by weight for polymer treated specimen without dispersing agent (Figure 4.29) at this average particle size limit compared to the result of the control specimen (Figure 4.28). The difference in the

results becomes less pronounced for smaller particle sizes (5 µm and 2 µm) as during the waiting time in hydrometer test, naturally, there is already accumulation of particles leading to sedimentation. It is important to also note that due to effective polymer-soil-water interaction observed, it is likely that CBAS can also have a potential for improvement of the dispersibility characteristics of soils vulnerable against internal erosion. As this aspect of the use of CBAS was not intended to be tested as part of this thesis, other tests relating to more accurate measurement of the dispersibility characteristics are not performed.

## 4.7 Microstructure

### 4.7.1 X-Ray Diffraction Analysis (XRD)

The results of the XRD test is used to determine whether new crystals are formed in the treated clay. The results are presented in Figure 4.30 and Figure 4.31.

The results indicate only minute changes in the reflection intensity confirming that there isn't a new crystal formation. However, the minute changes in the reflection intensities may also mean that the mineral crystallite size is slightly affected after the treatment.

### 4.7.2 Fourier Infrared Spectronomy (FT-IR)

FT-IR test results are presented in Figurer 4.32. As depicted in this figure, at 1730 and 2958 wavenumber Carbonyl group and Carbon-Hydrogen bonds and other electrostatic bonds are formed in the treated clay. The additional test results are presented in Appendix E.

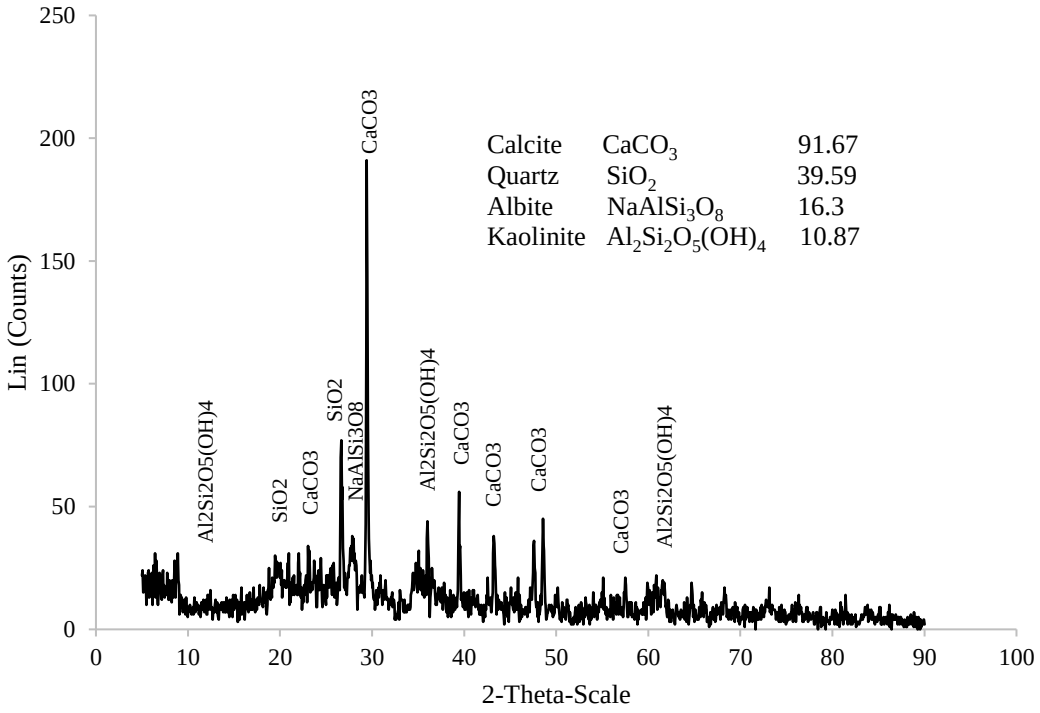


Figure 4.30. X-Ray Diffraction analysis of untreated clay. (Start: 5.0˚- End: 90.02˚ - Step time: 1.s – Temp: 25℃)

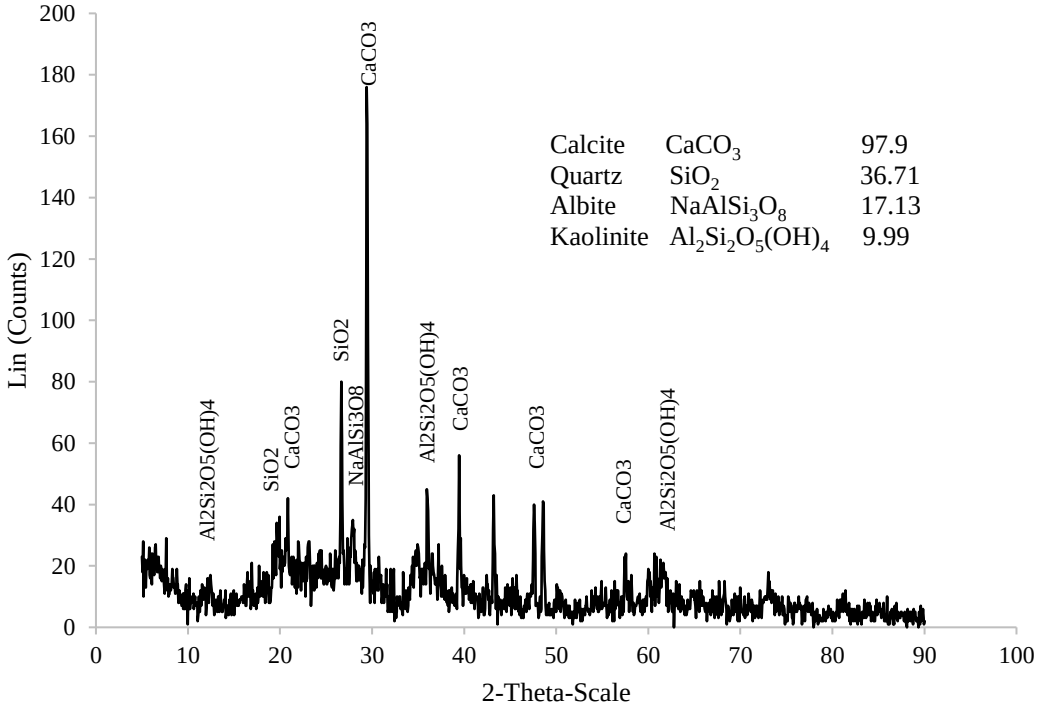


Figure 4.31. X-Ray Diffraction analysis of 5% CBAS treated clay. (Start: 5.0˚- End: 90.02˚ - Step time: 1.s – Temp: 25℃)

When CBAS is diluted in water and mixed with wet clay, hydrogen bonds are formed between the anionic polymer chains and the hydrogen atoms of the water molecules, creating a dipole. Then, the resulting negative charge on the other side of the dipole forms electrostatic bonds with the cations in the clay, which in turn, are attached to negatively charged clay minerals through further electrostatic bonding.

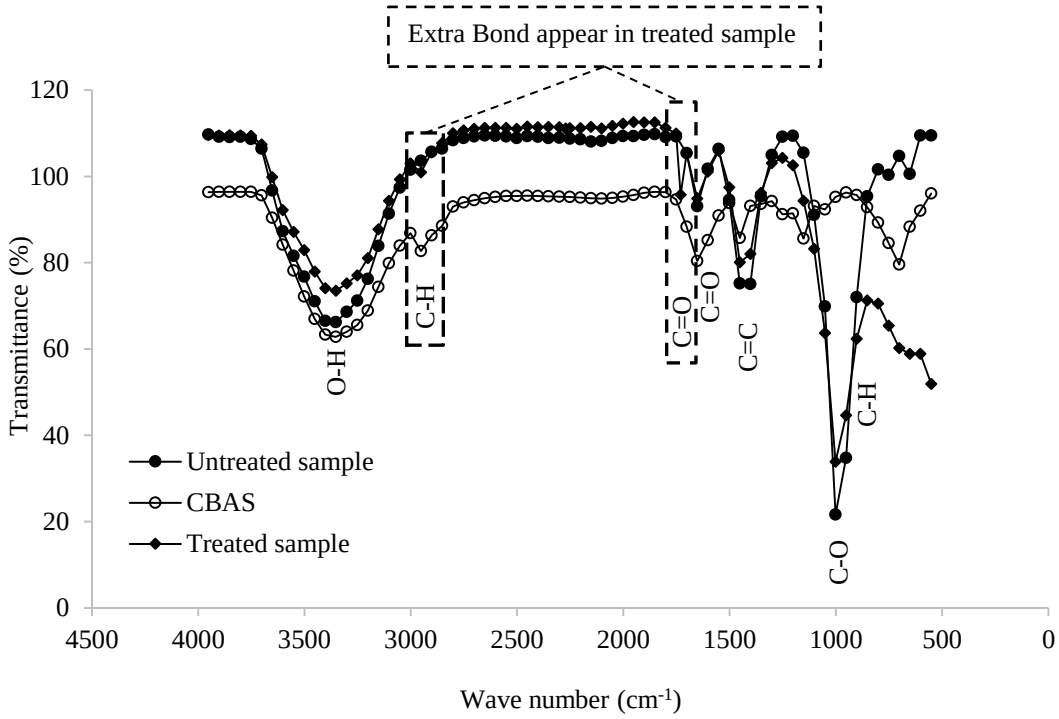


Figure 4.32. Fourier Transform Infrared spectrometer

Reduction in water content during drying causes the hydrogen bonds to detach as water molecules are removed from macro pores, however, bonds formed in micro pores remain attached at double diffuse layer at clay mineral layer surfaces. As a result, it can be stated that CBAS may interact with the clay mineral layers even when the treated clay loses moisture, providing improvement for water stability.

### 4.7.3 Scanning Electron Microscopy (SEM)

The effect of CBAS treatment in the microstructure of the soil is studied using scanning electron microscopy images, which are presented in Figure 4.33 to 4.35. The effectiveness of CBAS treatment on the microstructure is a function of the two main mechanisms which are; 1 – adsorption of the polymer chains to form bridges between the soil particle clusters and, 2 – ability of the polymer chains to form an enclosure around the particle clusters. Both of these mechanisms are demonstrated in Figure 4.33 to 4.35. The polymer treatment provides support to macropores, hence improving the swelling characteristics as well as compressibility by as measured also in one-dimensional swell and consolidation tests. Although both of these tests are applied when the specimens are in saturated condition, which is the case when the particle cluster spaces are significantly greater, the improvement observed is still significant confirming that the modification attained in the microstructure level is adequate. The additional SEM photos are presented in Appendix E.

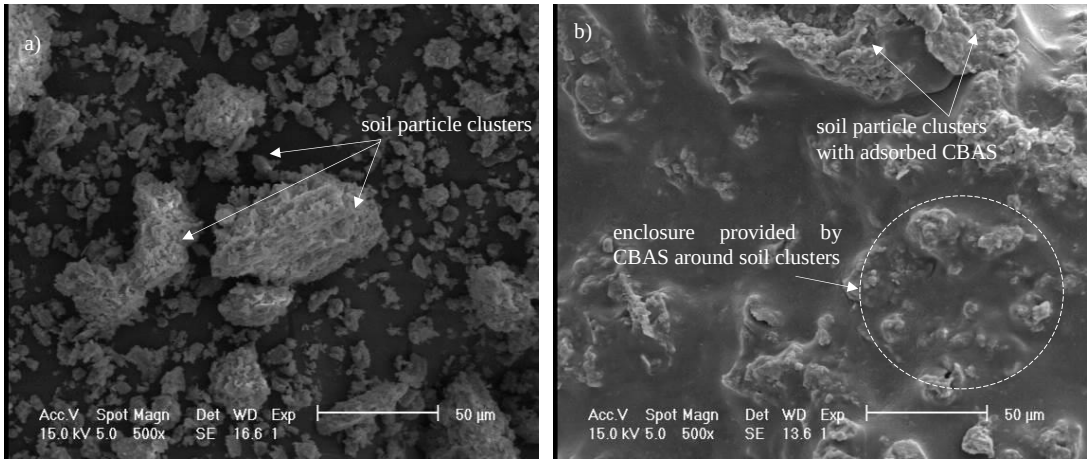

Figure 4.33. Scanning electron microscopy images; a- untreated soil, b- treated soil

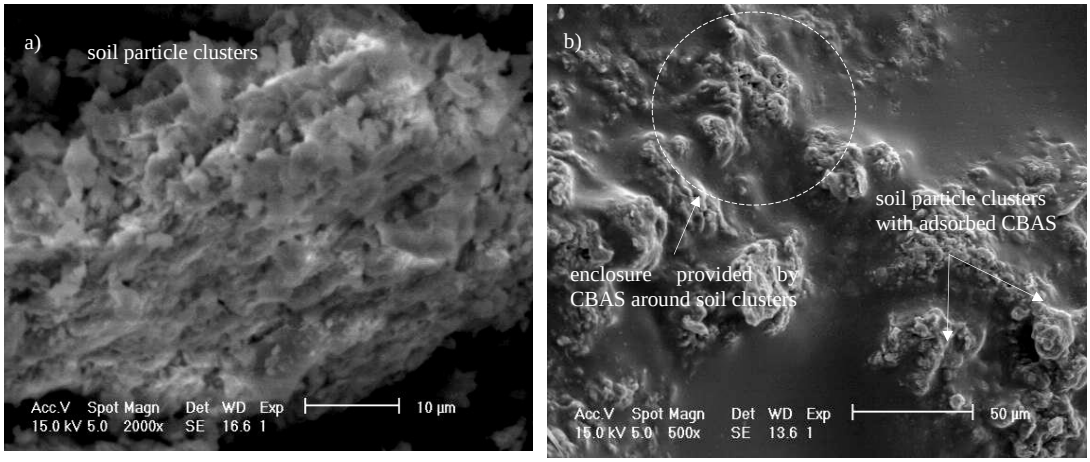


Figure 4.34. Scanning electron microscopy images; a- untreated soil, b- treated soil

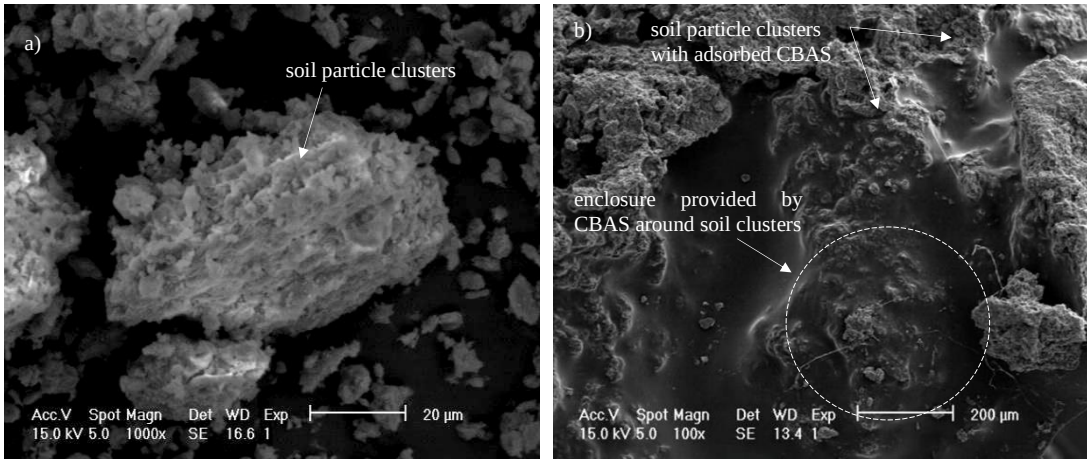


Figure 4.35. Scanning electron microscopy images; a- untreated soil, b- treated soil

# Chapter 5

# CONCLUSION

## 5.1 General

The aim of this research was to assess the effect of an aqueous polymer on hydro-mechanical properties of an alluvial clay sampled from Famagusta Bay North Cyprus, classified as highly expansive clay (CH). Although the research is focused on a certain type of aqueous polymer called co-polymer of butyl acrylate and styrene (CBAS), it is believed that the outcome of this research may help provide a guidance for the use of other types of aqueous polymers for stabilization of cohesive soils.

## 5.2 Conclusion

The outcomes of this research are concluded as presented in the following text:

- The specimens tested in slurry form for the measurement of clay-polymer-water electrolyte system properties, confirmed that the type of aqueous polymer used does not require a curing period. The interaction was detectable with the measurements carried out on the electrical conductivity and total dissolved solids data.

- The measurements taken during specimen preparation indicated that the drying curves of polymer treated specimens and control specimens differ such that the treated specimens allow for a greater void volume at the same water content. This is considered to be due to the support provided by polymer chains, within the treated specimens, against collapse of the macropores during drying, the

polymer chains lead to less shrinkage and fewer desiccation cracks, improving the internal stability of compacted clay upon inundation. Therefore, introducing CBAS provides and increased resistance to the volumetric shrinkage, reducing shrinkage cracking of cohesive fills such as impervious core of earth dams or levees, highway embankments and landfill capping fills, which might be under the influence of arid or semi-arid climates imposing significant seasonal moisture variations.

- The one-dimensional swelling behaviour results indicated that, CBAS did not reflect a significant improvement on the swelling behaviour when it is used at the same level of treatment. However, when the level of treatment is increased to be more than 5% swelling potential and the rate of swelling is improved significantly.

- Compared to the internal stability test results, a higher percentage of CBAS is required for effective treatment of volume change behaviour. This is likely due to the need for resistance against the internal tensile stresses generated by water absorption.

- The assessment of the compressibility of the tested specimens concluded that the CBAS addition provided a significant reduction in the compressibility when their initial state prior to effective stress increase is considered.

- The specimens which were dried to a moisture content lower than their shrinkage limit reflected a higher swelling potential and as a result a greater

void ratio was achieved prior to performing the one-dimensional consolidation tests.

- The compressibility of the test specimens is assessed by normalization of the change in void ratio upon increase in the effective stress with respect to their initial void ratio after swelling, which proved that there is a significant improvement in the compressibility.

- The long term compressibility behaviour is also investigated by assessing creep data, which indicated that the creep rate can be reduced to approximately 25% to 50% of its value for the untreated specimen.

- The increase attained in the undrained shear strength after stabilization of engineered fills is important to be provided with sufficient ductility to allow mobilization of the shear strength with reduction in the degradation of mass integrity within serviceability limits of stress, i e. with the least amount of cracking. It is concluded by the results that CBAS addition can provide a significant increase in the ductility not only at the failure state but also for the range of stresses prior to failure.

- The internal stability test results depend on the initial water content of the test specimens, because, as the initial water content increases, the internal stability also improves. Reduction in initial water content caused lower internal stability, both for untreated and treated test specimens. Most of the treated test specimens did not collapse in the clay stability tests.

- In the internal stability tests, treated specimens are significantly improved, even when the degree of treatment is as low as 0.5% by dry mass of the clay. The improvement in the clay stability index, K, is as high as two fold when the results are compared with the results from untreated test specimens.

- The internal stability test is performed by following a time-based methodology when calculating the clay stability index, K. The results indicated that the long term behaviour of the test specimens is determined more accurately by using computations of K at 10mins, 20mins and 30mins.

- In the internal stability tests, the mode of collapse is influenced by the water absorption rate, linked with the initial water content.

- Time dependent evaluation of the mode of collapse in the internal stability tests indicated that the specimens are more likely to collapse by gradual cracking for $K_{20}$ and $K_{30}$ measurements.

- In the internal stability tests, the specimens tended to reflect an increase in the explosive mode of collapse behaviour as the polymer content increased, which is considered to be associated with the effective entrapment of clay particles by polymer chains.

- XRD and FT-IR tests showed that, there are no chemical interaction between the Polymer and the clay, which indicates that the stability is improved through hydrogen and electrostatic bonding.

- SEM photos of the untreated and treated specimens are compared to observe significant changes in the soil structure. The results showed that the CBAS can be adsorbed into the soil fabric and also the polymer soil matrix is effectively formed with ease.

## 5.3 Limitations and Recommendations for Further Studies

The limitations and recommendations for future research are presented in the following text:

- For assessing the effectiveness of using CBAS, it would be better to perform the same testing program on various types of aqueous polymers for comparison.

- Data on the use of aqueous polymers in real scale soil stabilisation works is scarce, hence it can be very helpful to assess performance of a few types of aqueous polymers in an insitu application, e.g. for dust or erosion control.

- Dust control is one of the biggest issues in construction works. Since the CBAS is a non-hazardous material and it has additional benefits such as improvement it attains against erosion, it is worthy to do further research on the use of CBAS in construction sites and earthworks.

- For a better assessment of the role of CBAS as a soil stabilizer, it is recommended to do further research on shear strength under various stress states and drainage conditions. Unsaturated soil characteristics of the stabilised material can be tested to measure soil water retention curve.

- In this research, the durability of the CBAS treatment with respect to leaching of aggressive chemicals is not studied. The field applications requiring such resistance will need further research of the behaviour of CBAS treated soils under such conditions. As a preliminary approach, it is recommended to perform leaching tests using salt and acid solutions.

# REFERENCES


Abiodun, A. A., & Nalbantoglu, Z. (2014). Lime pile techniques for the improvement of clay soils. *Canadian Geotechnical Journal*, *52*(6), 760-768.

Aggarwal, L. K., Thapliyal, P. C., & Karade, S. R. (2007). Properties of polymer-modified mortars using epoxy and acrylic emulsions. *Construction and Building Materials*, *21*(2), 379-383.

Agus, S. M., Hung, J. (2006). Shear strength around soft clay surrounded by lime columns. Dept. of Construction Engrg: Univ. Muhammadiyah, Yogyakarta, Indonesia and National Taiwan Univ. of Sci. & Tech., Taiwan.

Akay, O., Özer, A. T., & Fox, G. A. (2012). Experimental investigation of failure mechanism of expanded polystyrene block geofoam slope system under seepage. In *European geosynthetics congress, EuroGeo5* (pp. 16-19).

Al-Homoud, A. S., Basma, A. A., Husein Malkawi, A. I., & Al Bashabsheh, M. A. (1995). Cyclic swelling behavior of clays. *Journal of geotechnical engineering*, *121*(7), 562-565.

Al-Mukhtar, M., Lasledj, A., & Alcover, J. F. (2010). Behaviour and mineralogy changes in lime-treated expansive soil at 20 C. *Applied clay science*, *50*(2), 191-198.

Anagnostopoulos, C. A. (2007). Cement–clay grouts modified with acrylic resin or methyl methacrylate ester: Physical and mechanical properties. *Construction and Building Materials*, *21*(2), 252-257.

Anagnostopoulos, C. A., & Papaliangas, T. T. (2011). Experimental investigation of epoxy resin and sand mixes. *Journal of Geotechnical and Geoenvironmental Engineering*, *138*(7), 841-849.

Arasan, S., Bagherinia, M., Akbulut, R. K., & Zaimoglu, A. S. (2017). Utilization of polymers to improve soft clayey soils using the deep mixing method. *Journal of Environmental & Engineering Geoscience*, *23*(1), 1-12.

ASTM Committee D-18 on Soil and Rock. (2017). *Standard practice for classification of soils for engineering purposes (Unified Soil Classification System)*. ASTM International.

ASTM Committee D-18 on Soil and Rock. (2017). *Standard test methods for liquid limit, plastic limit, and plasticity index of soils*. ASTM international.

ASTM, D. (2014). Standard test methods for one-dimensional swell or collapse of cohesive soils. *D4546-08*.

ASTM Committee D-18 on Soil and Rock. (2012). *Standard Test Methods for Laboratory Compaction Characteristics of Soil Using Standard Effort (12 400 Ft-lbf/ft3 (600 KN-m/m3)) 1*. ASTM International.

ASTM Committee D-18 on Soil and Rock. (2014). *Standard test methods for specific gravity of soil solids by water pycnometer*. ASTM International.

Atalar, C., & Das, B. M. (2009). Geotechnical properties of Nicosia soils, Cyprus. In *2nd International Conference on New Developments in Soil Mechanics and Geotechnical Engineering* (Vol. 28, p. 30).

Azhar, A. T. S., Fazlina, M. I. S., Nizam, Z. M., Fairus, Y. M., Hakimi, M. N. A., Riduan, Y., & Faizal, P. (2017). Shear Strength of Stabilized Kaolin Soil Using Liquid Polymer. In *IOP Conference Series: Materials Science and Engineering* (Vol. 226, No. 1, p. 012063). IOP Publishing.

Azzam, W. R. (2014). Utilization of polymer stabilization for improvement of clay microstructures. *Applied clay science*, *93*, 94-101.

Bae, S., Inyang, H. I., Galvão, T. D. B., & Mbamalu, G. E. (2006). Soil desiccation rate integration into empirical dust emission models for polymer suppressant evaluation. *Journal of hazardous materials*, *132*(1), 111-117.

Barbhuiya, S. A., Gbagbo, J. K., Russell, M. I., & Basheer, P. A. M. (2009). Properties of fly ash concrete modified with hydrated lime and silica fume. *Construction and Building Materials*, *23*(10), 3233-3239.

Barthes, B., & Roose, E. (2002). Aggregate stability as an indicator of soil susceptibility to runoff and erosion; validation at several levels. *Catena*, *47*(2), 133-149.

Basma, A. A., & Tuncer, E. R. (1991). Effect of lime on volume change and compressibility of expansive clays. *Transportation research record*, (1295).

Basma, A. A., Al-Homoud, A. S., Malkawi, A. I. H., & Al-Bashabsheh, M. A. (1996). Swelling-shrinkage behavior of natural expansive clays. *Applied Clay Science*, *11*(2-4), 211-227.

Basma, A. A., Al-Rawas, A. A., Al-Saadi, S. N., & Al-Zadjali, T. F. (1998). Stabilization of expansive clays in Oman. *Environmental & Engineering Geoscience*, *4*(4), 503-510.

Bell, F. G. (1996). Lime stabilization of clay minerals and soils. *Engineering geology*, *42*(4), 223-237.

Bilsel, H., & Tuncer, E. R. (1998). Cyclic swell-shrink behavior of Cyprus clays. In *Proceedings of the International Symposium on Problematic Soils* (Vol. 98, pp. 337-340).

Bozbey, I., & Garaisayev, S. (2010). Effects of soil pulverization quality on lime stabilization of an expansive clay. *Environmental Earth Sciences*, *60*(6), 1137-1151.

British Standards Institution. (1990). *British Standard Methods of Test for Soils for Civil Engineering Purposes: Part 5: Compressibility, Permeability and Durability Tests*. British Standards Institution.

Broms, B. B., & Boman, P. (1979). Lime columns-a new foundation method. *Journal of Geotechnical and Geoenvironmental Engineering*, *105*(ASCE 14543).

Craig, R. F. (2004). *Craig's soil mechanics*. CRC Press.

Cokca, E. (2001). Use of class c fly ashes for the stabilizationof an expansive soil. *Journal of Geotechnical and Geoenvironmental Engineering*, *127*(7), 568-573.

Das, B. M., & Sobhan, K. (2013). Principles of geotechnical engineering. Cengage *learning.*

Diamond, S., & Kinter, E. B. (1965). Mechanisms of soil-lime stabilization. *Highway Research Record*, *92*, 83-102.

Ding, X. (2018). Research and Application of Non-traditional Chemical Stabilizers on Bauxite 3 Residue (Red Sand) Dust Control (Doctoral dissertation, Curtin University).

Dixon, N., & Jones, D. R. V. (2005). Engineering properties of municipal solid waste. *Geotextiles and Geomembranes*, *23*(3), 205-233.

Dotto, J. M. R., De Abreu, A. G., Dal Molin, D. C. C., & Müller, I. L. (2004). Influence of silica fume addition on concretes physical properties and on corrosion behaviour of reinforcement bars. *Cement and concrete composites*, *26*(1), 31-39.

Duncan, J. M., & Buchignani, A. L. (1976). *An Engineering Manual for Settlement Studies: By JM Duncan and AL Buchignani*. Department of Civil Engineering, University of California.

Eades, J. L., & Grim, R. E. (1960). Reaction of hydrated lime with pure clay minerals in soil stabilization. *Highway Research Board Bulletin*, (262).

Eades, J. L., Nichols Jr, F. P., & Grim, R. E. (1962). Formation of new minerals with lime stabilization as proven by field experiments in Virginia. *Highway Research Board Bulletin*, (335).

Estabragh, A. R., Beytolahpour, I., & Javadi, A. A. (2010). Effect of resin on the strength of soil-cement mixture. *Journal of Materials in Civil Engineering*, *23*(7), 969-976.

Fannin, R. J., & Raju, D. M. (1993). On the pullout resistance of geosynthetics. *Canadian Geotechnical Journal*, *30*(3), 409-417.

Galán-Marín, C., Rivera-Gómez, C., & Petric, J. (2010). Clay-based composite stabilized with natural polymer and fibre. *Construction and Building Materials*, *24*(8), 1462-1468.

Gamble, B.R. (1971). Stabilization of Fine Sands Using Polyvinyl Acetate. *Canadian Geotechnical Journal*. 8(2). pp. 336-340.

Ganapathy, G. P., Gobinath, R., Akinwumi, I. I., Kovendiran, S., Thangaraj, M., Lokesh, N., Hema, S. (2017). Bio-enzymatic stabilization of a soil having poor engineering properties. *International Journal of Civil Engineering*, *15*(3), 401-409.

Ghavam Shirazi, S., Valipourian, K., Golhashem, M. R. (2017). Geomebrane Characteristics and Application in Geotechnical Engineering: A review. *19th International Conference on Civil, Environmental and Structural Engineering*, Vancouver, Canada, 11(8).

Glenn, G. R., & Handy, R. L. (1963). Lime-clay mineral reaction products. *Highway research record*, (29).

Golhashem, M. R., & Uygar, E. (2019). Improvement of Internal Stability of Alluvial Clay from Famagusta Bay, Cyprus, Using Copolymer of Butyl Acrylate and Styrene. *Environmental & Engineering Geoscience*, 1-12.

Goodarzi, A. R., Goodarzi, S. H., & Akbari, H. R. (2015). Assessing geo-mechanical and micro-structural performance of modified expansive clayey soil by silica fume as industrial waste. *Iranian Journal of Science and Technology Transactions of Civil Engineering*, 39(C2), 333-350.

Grim, R. E. (1968). The Clay Mineralogy 2nd edition Mac Graw Hill. *New York*, 596.

Guney, Y., Sari, D., Cetin, M., & Tuncan, M. (2007). Impact of cyclic wetting–drying on swelling behavior of lime-stabilized soil. *Building and Environment*, *42*(2), 681-688.

Heller, H., & Keren, R. (2002). Anionic polyacrylamide polymers effect on rheological behavior of sodium-montmorillonite suspensions. *Soil Science Society of America Journal*, *66*(1), 19-25.

Huang, H., Liu, L. (2012). Application of Water-Soluble Polymers in the Soil Quality Improvement. *Civil Engineering and Urban Planning 2012 American Society of Civil Engineers (ASCE) Yantai China,* 123-129.

Hudyma, N., Avar, B.B., (2006). Changes in swell behavior of expansive clay soils from dilution with sand. *Environmental & Engineering Geoscience, 12*(2), pp.137-145.

Inyang, H. I., & Bae, S. (2005). Polyacrylamide sorption opportunity on interlayer and external pore surfaces of contaminant barrier clays. *Chemosphere*, *58*(1), 19-31.

Inyang, H. I., Bae, S., Mbamalu, G., & Park, S. W. (2007). Aqueous polymer effects on volumetric swelling of Na-montmorillonite. *Journal of Materials in Civil Engineering*, *19*(1), 84-90.

Iyengar, S. R., Masad, E., Rodriguez, A. K., Bazzi, H. S., Little, D., & Hanley, H. J. (2012). Pavement subgrade stabilization using polymers: characterization and performance. *Journal of Materials in Civil Engineering*, *25*(4), 472-483.

Jafari, N. H., Stark, T. D., & Rowe, R. K. (2013). Service life of HDPE geomembranes subjected to elevated temperatures. *Journal of Hazardous, Toxic, and Radioactive Waste*, *18*(1), 16-26.

Kalkan, E. (2011). Impact of wetting–drying cycles on swelling behavior of clayey soils modified by silica fume. *Applied Clay Science*, *52*(4), 345-352.

Khatami, H. R., & O'Kelly, B. C. (2012). Improving mechanical properties of sand using biopolymers. *Journal of Geotechnical and Geoenvironmental Engineering*, *139*(8), 1402-1406.

Koteng, D. O., & Chen, C. T. (2015). Strength development of lime–pozzolana pastes with silica fume and fly ash. *Construction and Building Materials*, *84*, 294-300.

Lahalih, S. M., & Ahmed, N. (1998). Effect of new soil stabilizers on the compressive strength of dune sand. *Construction and Building Materials*, *12*(6-7), 321-328.

Langroudi, A. A., & Yasrobi, S. S. (2009). A micro-mechanical approach to swelling behavior of unsaturated expansive clays under controlled drainage conditions. *Applied Clay Science*, *45*(1-2), 8-19.

Li, M., Fang, C., Kawasaki, S., & Achal, V. (2018). Fly ash incorporated with biocement to improve strength of expansive soil. *Scientific Reports*, *8*(1), 2565.

Lima Júnior, N. R. (2000). *Soil-geosynthetic interaction study for environmental protection constructions using ramp test equipment* (Doctoral dissertation, MSc

Dissertation, Publication G. DM–071A/2000, Department of Civil and Environmental Engineering, University of Brasília, Brasília, DF, Brazil, 48 p (In Portuguese)).

Liu, J., Shi B., Jiang, H., Bae, S., & Huang, H. (2009). Improvement of water-stability of clay aggregates admixed with aqueous polymer soil stabilizers. *Catena*, *77*(3), 175-179.

Liu, J., Shi, B., Jiang, H., Huang, H., Wang, G., & Kamai, T. (2011). Research on the stabilization treatment of clay slope topsoil by organic polymer soil stabilizer. *Engineering Geology*, *117*(1-2), 114-120.

Maaitah, O. N. (2012). Soil stabilization by chemical agent. *Geotechnical and Geological Engineering*, *30*(6), 1345-1356.

Mahrous, M. A., Šegvić, B., Zanoni, G., Khadka, S. D., Senadheera, S., & Jayawickrama, P. W. (2018). The Role of Clay Swelling and Mineral Neoformation in the Stabilization of High Plasticity Soils Treated with the Fly Ash-and Metakaolin-Based Geopolymers. *Minerals*, *8*(4), 146.

Maghchiche, A., Haouam, A., & Immirzi, B. (2010). Use of polymers and biopolymers for water retaining and soil stabilization in arid and semiarid regions. *Journal of Taibah University for Science*, *4*(1), 9-16.

Miao, S., Shen, Z., Wang, X., Luo, F., Huang, X., & Wei, C. (2017). Stabilization of Highly Expansive Black Cotton Soils by Means of Geopolymerization. *Journal of Materials in Civil Engineering*, *29*(10), 04017170.

Mitchell, J. K., & Soga, K. (2005). *Fundamentals of soil behavior* (Vol. 3). New York: John Wiley & Sons.

Naeini, S. A., & Ghorbanalizadeh, M. (2010). Effect of wet and dry conditions on strength of silty sand soils stabilized with epoxy resin polymer. *Journal of Applied Sciences(Faisalabad)*, *10*(22), 2839-2846.

Nagaraj, H., Munnas, M., & Sridharan, A. (2010). Swelling behavior of expansive soils. *International Journal of Geotechnical Engineering*, *4*(1), 99-110.

Nalbantoğlu, Z. (2004). Effectiveness of class C fly ash as an expansive soil stabilizer. *Construction and Building Materials*, *18*(6), 377-381.

Nalbantoglu, Z., & Gucbilmez, E. (2002). Utilization of an industrial waste in calcareous expansive clay stabilization. *Geotechnical Testing Journal*, 25(1), 78-84.

Nalbantoglu, Z., & Tawfiq, S. (2006). Evaluation of the effectiveness of olive cake residue as an expansive soil stabilizer. *Environmental Geology*, 50(6), 803-807.

Nalbantoglu, Z., & Tuncer, E. R. (2001). Compressibility and hydraulic conductivity of a chemically treated expansive clay. *Canadian Geotechnical Journal*, *38*(1), 154-160.

Niewczas, J., & Witkowska-Walczak, B. (2005). The soil aggregates stability index (ASI) and its extreme values. *Soil and Tillage Research*, *80*(1-2), 69-78.

Öncü, Ş., & Bilsel, H. (2017). Influence of Polymeric Fiber Reinforcement on Strength Properties of Sand-stabilized Expansive Soil. *Polymer-Plastics Technology and Engineering*, *56*(4), 391-399.

Orts, W. J., Roa-Espinosa, A., Sojka, R. E., Glenn, G. M., Imam, S. H., Erlacher, K., & Pedersen, J. S. (2007). Use of synthetic polymers and biopolymers for soil stabilization in agricultural, construction, and military applications. *Journal of materials in civil engineering*, *19*(1), 58-66.

Panova, I. G., Sybachin, A. V., Spiridonov, V. V., Kydralieva, K., Jorobekova, S., Zezin, A. B., & Yaroslavov, A. A. (2017). Non-stoichiometric interpolyelectrolyte complexes: Promising candidates for protection of soils. *Geoderma*, 307, 91-97.

Park, S. J., & Seo, M. K. (2011). Interface science and composites (Vol. 18). Academic Press.

Popescu, M. (1980). Behaviour of expansive soils with a crumb structure. In Proceeding. of *the 4th International Conference on Expansive Soils* (Vol. 1, pp. 158-171).

Pu, S., Hou, Y., Ma, J., Zou, Y., Xu, L., Shi, Q., ... & Pei, X. (2019). Stabilization Behavior and Performance of Loess Using a Novel Biomass-based Polymeric Soil Stabilizer. *Environmental & Engineering Geoscience*, *25*(2), 103-114.

Rezaeimalek, S., Nasouri, R., Huang, J., & Bin-Shafique, S. (2018). Curing Method and Mix Design Evaluation of a Styrene-Acrylic Based Liquid Polymer for Sand and Clay Stabilization. *Journal of Materials in Civil Engineering*, *30*(9), 04018200.

Rogers, L. C. G., & Zane, O. (1997). Valuing moving barrier options. *Journal of Computational Finance*, *1*(1), 5-11.

Rowe, B. W., Freeman, B. D., & Paul, D. R. (2009). Physical aging of ultrathin glassy polymer films tracked by gas permeability. *Polymer*, 50(23), 5565-5575.

Seco, A., Ramírez, F., Miqueleiz, L., & García, B. (2011). Stabilization of expansive soils for use in construction. *Applied Clay Science*, *51*(3), 348-352.

Shukla, S. K. (Ed.). (2002). *Geosynthetics and their applications*. Thomas Telford.

Soltani-Jigheh, H. (2016). Compressibility and shearing behavior of clayey soil reinforced by plastic waste. *International Journal of Civil Engineering*, *14*(7), 479-489.

Soltani-Jigheh, H., & Azarnia, A. (2017). Effect of Liquid Polymeric and Lime Additives on the Behavior of Fine-Grained Soil at Unfrozen and Freeze–Thaw Conditions. *Indian Geotechnical Journal*, *47*(4), 529-536.

Stroud, M. A., & Butler, F. G. (1975). The standard penetration test and the engineering properties of glacial materials. In *Symposium on Engineering Properties of Glacial Materials, Midland Geotechnical Society*.

Tajdini, M., Nabizadeh, A., Taherkhani, H., & Zartaj, H. (2017). Effect of added waste rubber on the properties and failure mode of kaolinite clay. *International Journal of Civil Engineering*, *15*(6), 949-958.

Tingle, J., Newman, J., Larson, S., Weiss, C., & Rushing, J. (2007). Stabilization mechanisms of nontraditional additives. *Transportation Research Record: Journal of the Transportation Research Board*, (1989), 59-67.

Uygar, E. (1999). *An Investigation on Internal Erosion Characteristics of Various Earth Dams in Turkish Republic of Northern Cyprus* (Doctoral dissertation, Eastern Mediterranean University).

Williams, B. G., Greenland, D. J., & Quirk, J. P. (1968). The water stability of natural clay aggregates containing polyvinyl alcohol. *Soil Research*, *6*(1), 59-66.

Xiao, H., Liu, G., Liu, P., Zheng, F., Zhang, J., & Hu, F. (2017). Developing equations to explore relationships between aggregate stability and erodibility in Ultisols of subtropical China. *Catena*, *157*, 279-285.

Xu, G., Ding, X., Kuruppu, M., Zhou, W., & Biswas, W. (2018). Research and application of non-traditional chemical stabilizers on bauxite residue (red sand) dust control, a review. *Science of the Total Environment*, 616, 1552-1565.

Yazdandoust, F., & Yasrobi, S. S. (2010). Effect of cyclic wetting and drying on swelling behavior of polymer-stabilized expansive clays. *Applied Clay Science*, *50*(4), 461-468.

Yılmaz, O., Cheaburu, C. N., Gülümser, G., & Vasile, C. (2012). On the stability and properties of the polyacrylate/Na-MMT nanocomposite obtained by seeded emulsion polymerization. *European Polymer Journal*, *48*(10), 1683-1695.

Zezin, A. B., Mikheikin, S. V., Rogacheva, V. B., Zansokhova, M. F., Sybachin, A. V., & Yaroslavov, A. A. (2015). Polymeric stabilizers for protection of soil and ground against wind and water erosion. *Advances in Colloid and Interface Science*, 226, 17-23.

# APPENDICES

# Appendix A: Soil Classification

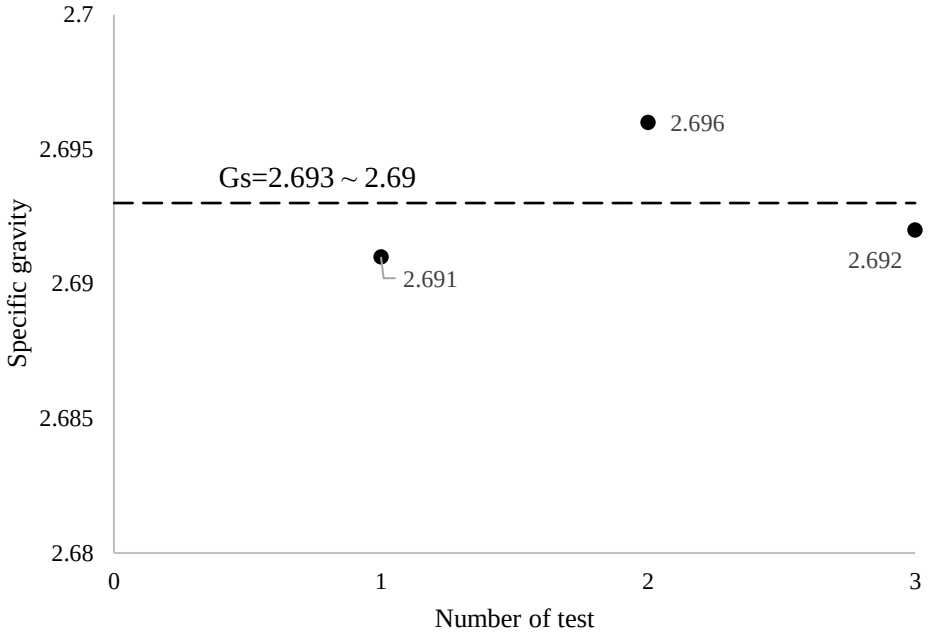


Figure A.1. Specific gravity

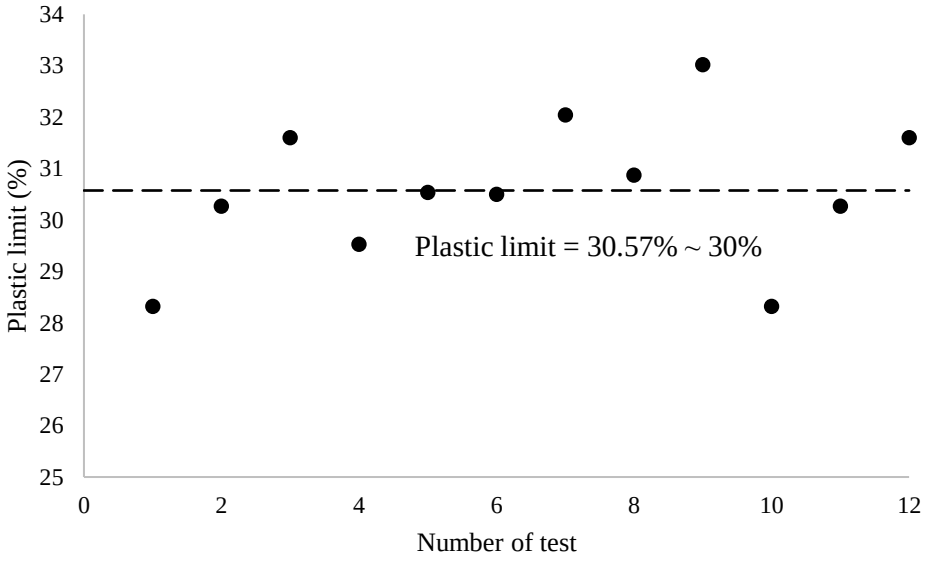


Figure A.2. Plastic limit

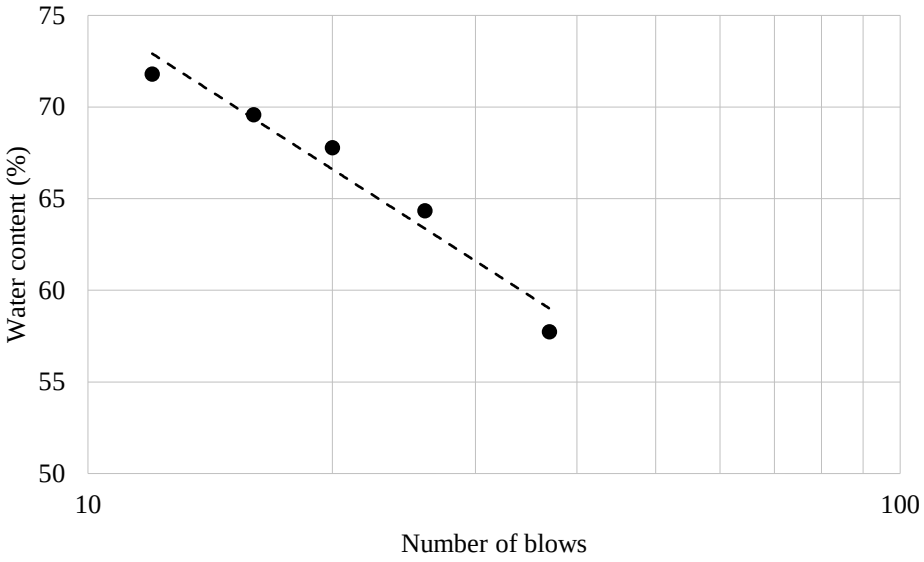


Figure A.3. Water content versus number of blows for untreated specimens

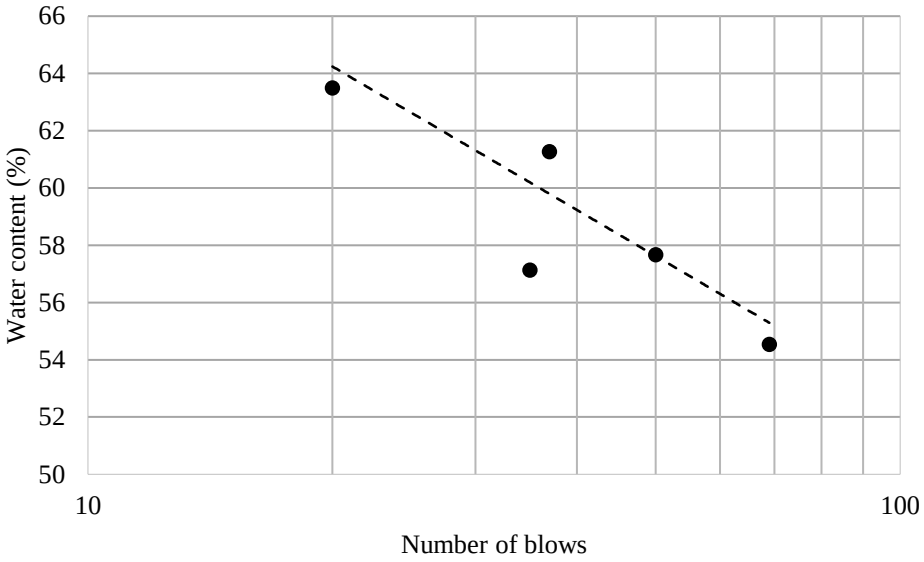


Figure A.4. Water content versus number of blows for 0.1% CBAS

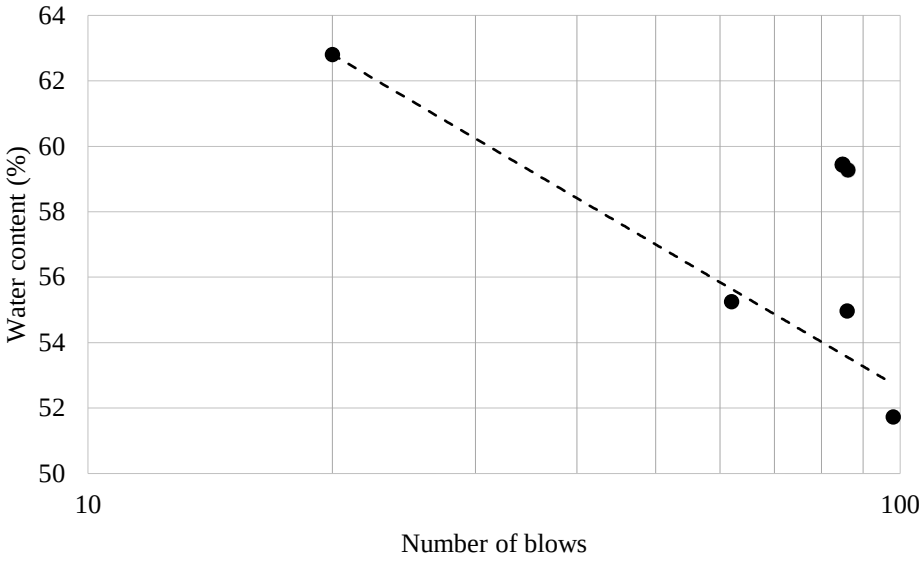


Figure A.5. Water content versus number of blows for 0.25% CBAS

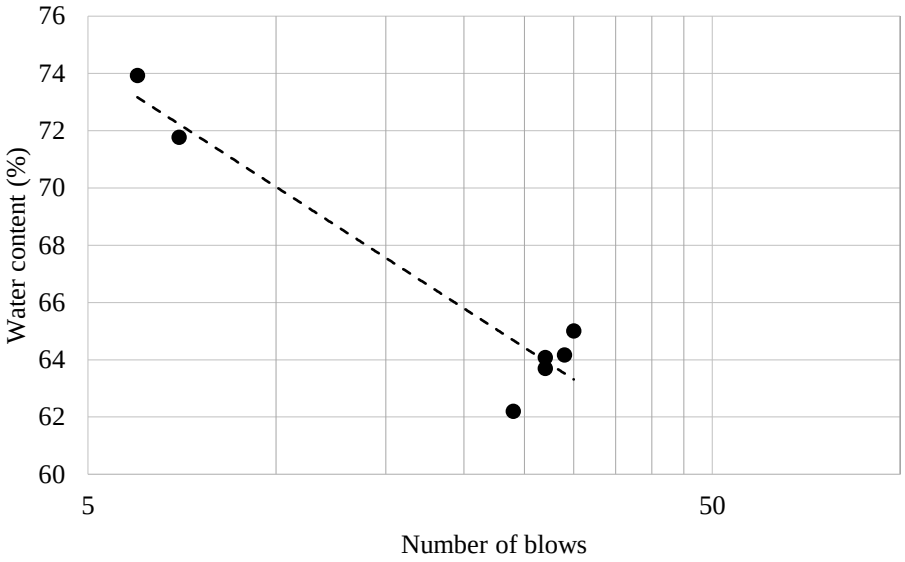


Figure A.6. Water content versus number of blows for 0.5% CBAS

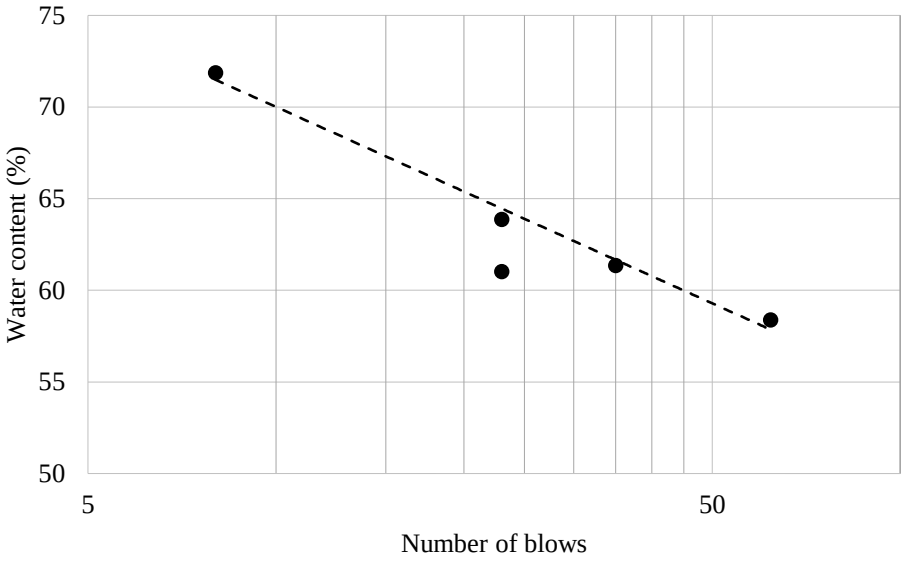


Figure A.7. Water content versus number of blows for 0.75% CBAS

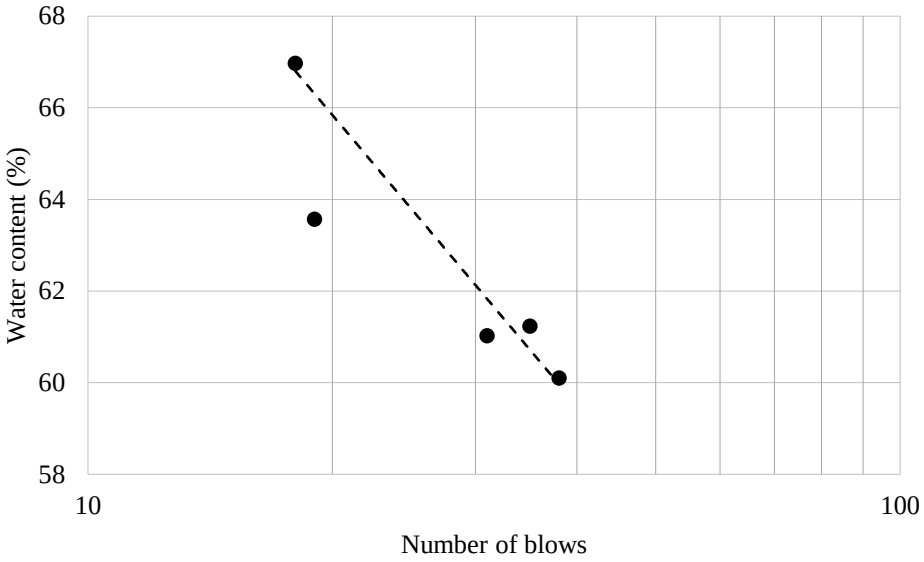


Figure A.8. Water content versus number of blows for 1% CBAS

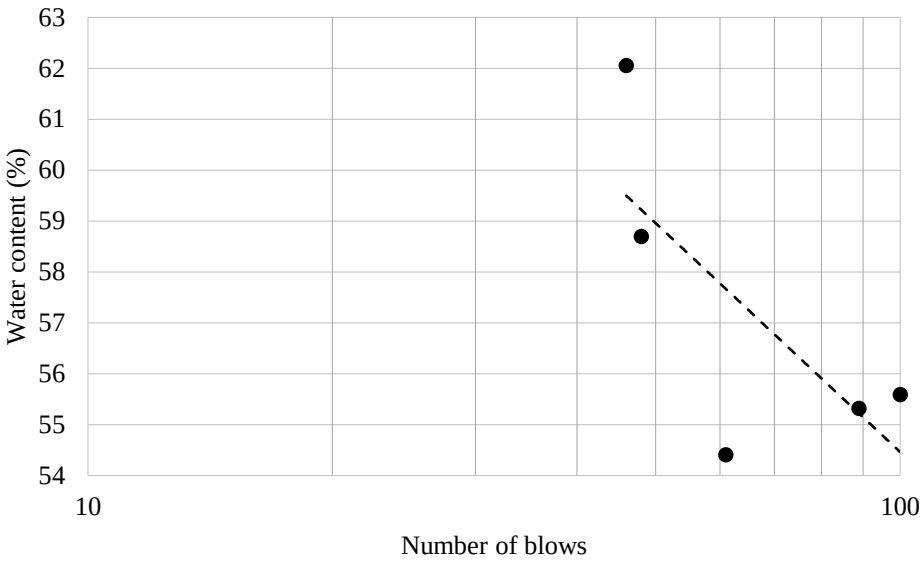


Figure A.9. Water content versus number of blows for 2% CBAS

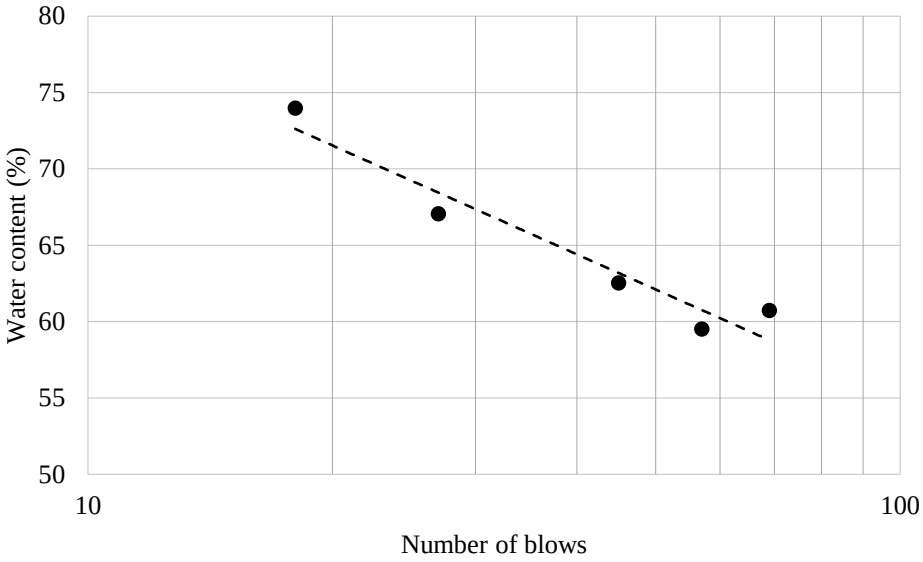


Figure A.10. Water content versus number of blows for 4% CBAS

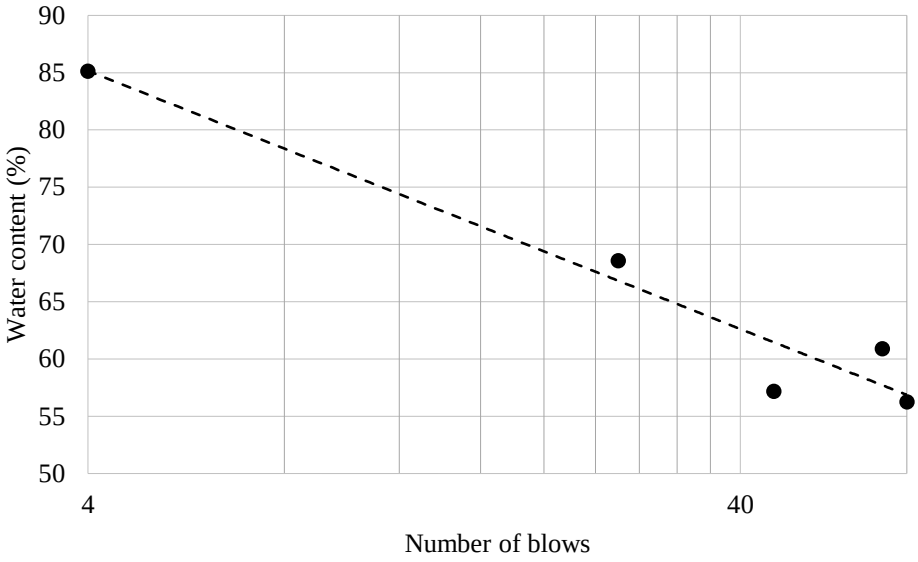


Figure A.11. Water content versus number of blows for 6% CBAS

## Appendix B: Internal Stability

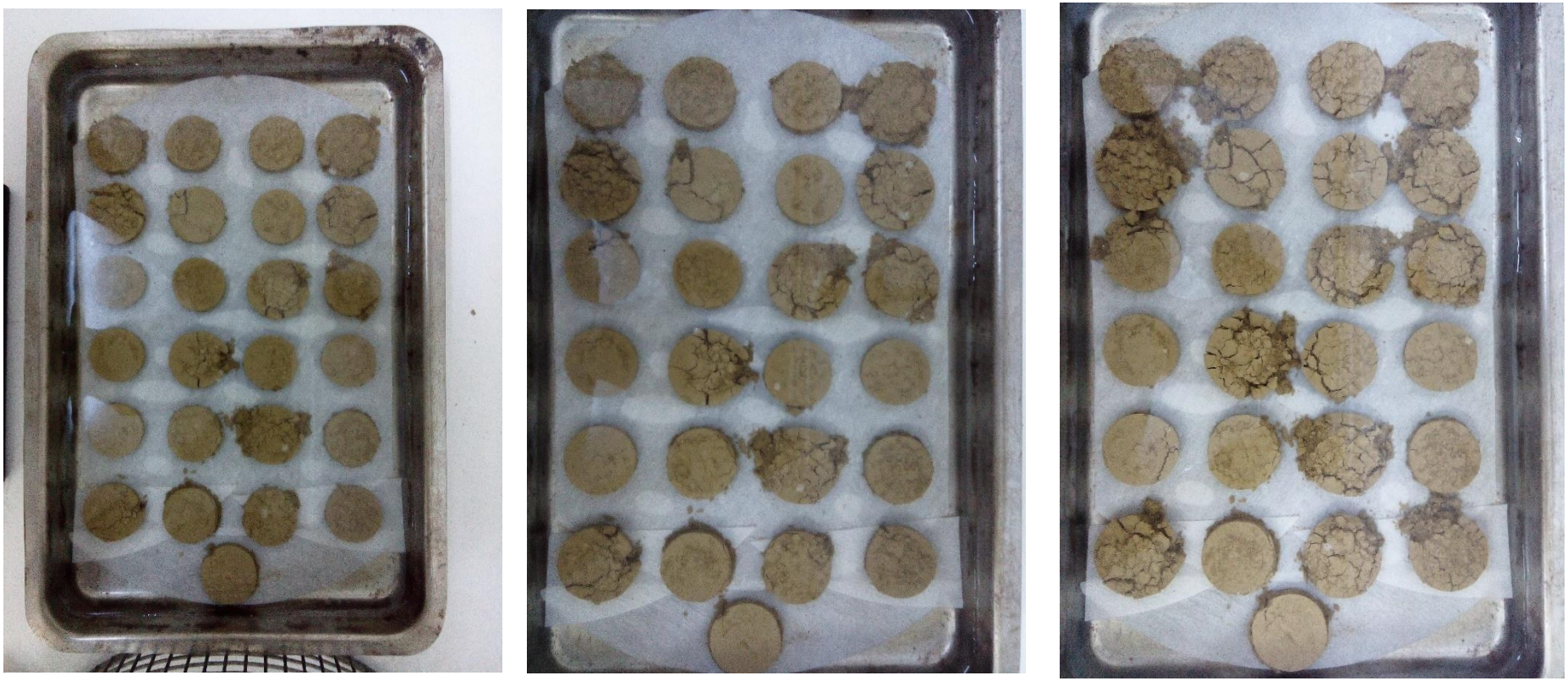

(a) (b) (c)

Figure A.12. Internal stability for untreated specimens with 28% initial water content at the end of a) 10 min, b) 20 min, C) 30 min

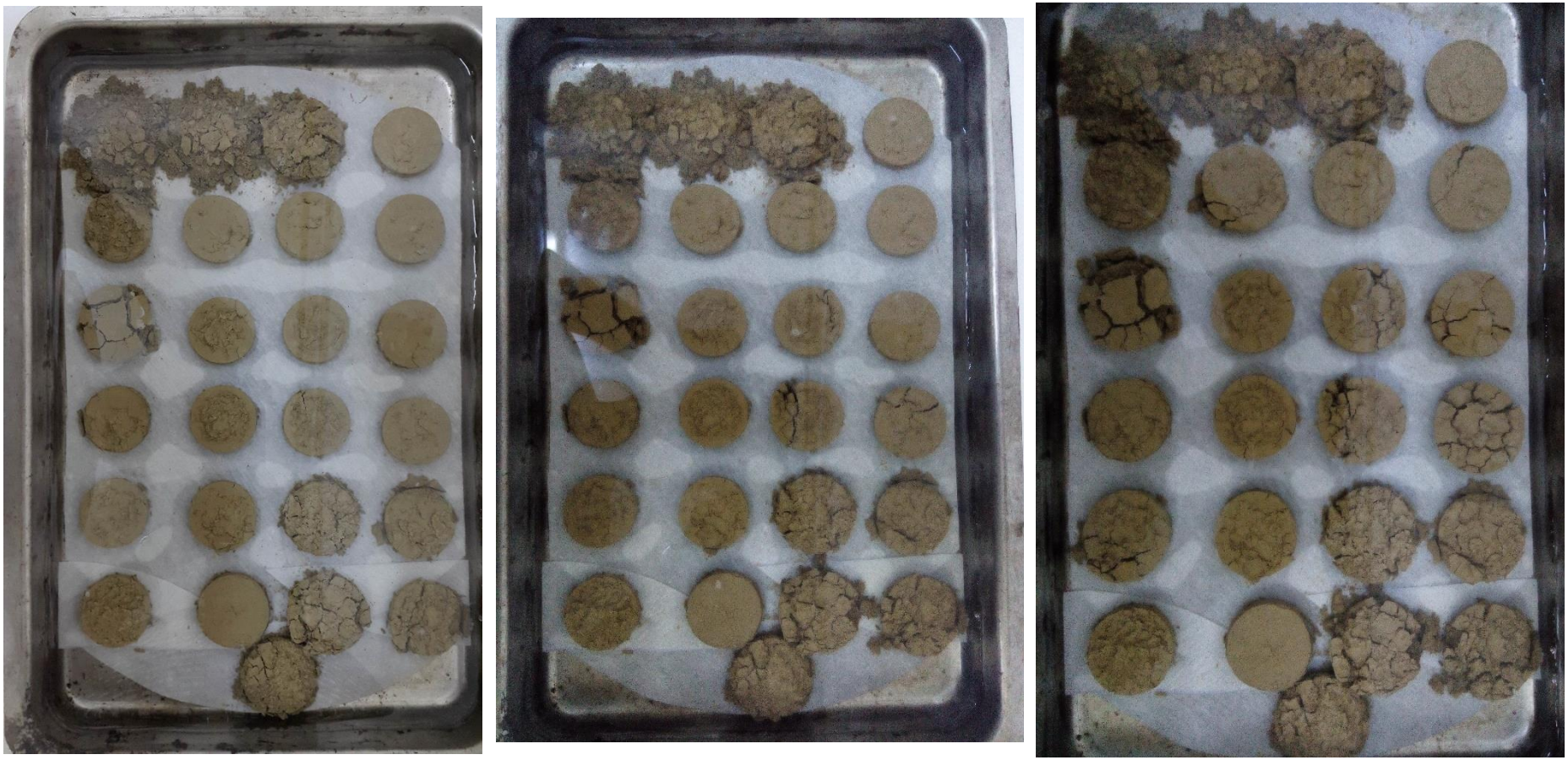

(a) (b) (c)

Figure A.13. Internal stability for untreated specimens with 22.5% initial water content at the end of a) 10 min, b) 20 min, C) 30 min

(a) (b) (c)

Figure A.14. Internal stability for untreated specimens with 16% initial water content at the end of a) 10 min, b) 20 min, C) 30 min

(a) (b) (c)

Figure A.15. Internal stability for untreated specimens with 11% initial water content at the end of a) 10 min, b) 20 min, C) 30 min

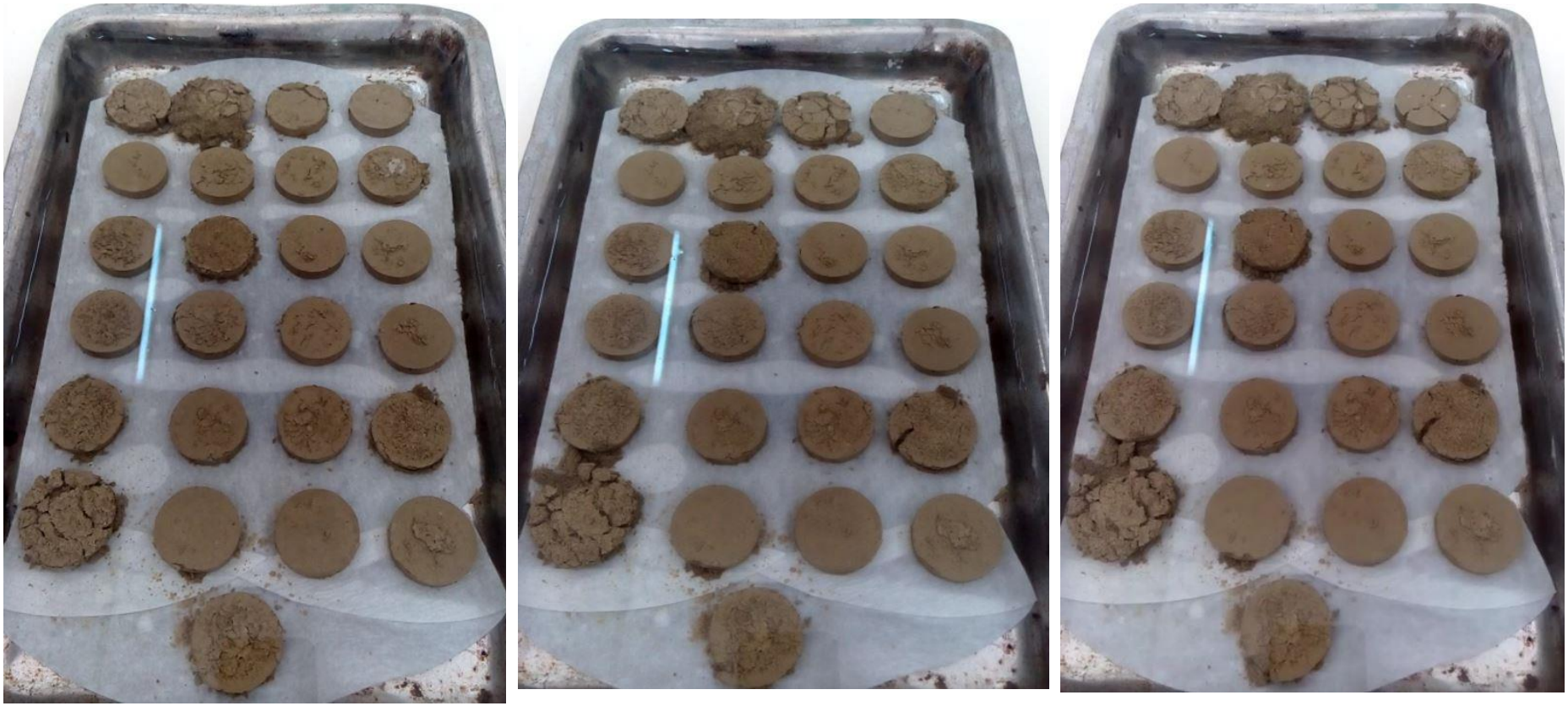

(a) (b) (c)

Figure A.16. Internal stability for 0.5% CBAS treated specimens with 16% initial water content at the end of a) 10 min, b) 20 min, C) 30 min

(a) (b) (c)

Figure A.17. Internal stability for 0.5% CBAS treated specimens with 11% initial water content at the end of a) 10 min, b) 20 min, C) 30 min

(a) (b) (c)

Figure A.18. Internal stability for 1% CBAS treated specimens with 16% initial water content at the end of a) 10 min, b) 20 min, C) 30 min

(a) (b) (c)

Figure A.19. Internal stability for 1% CBAS treated with 11% initial water content specimens at the end of a) 10 min, b) 20 min, C) 30 min

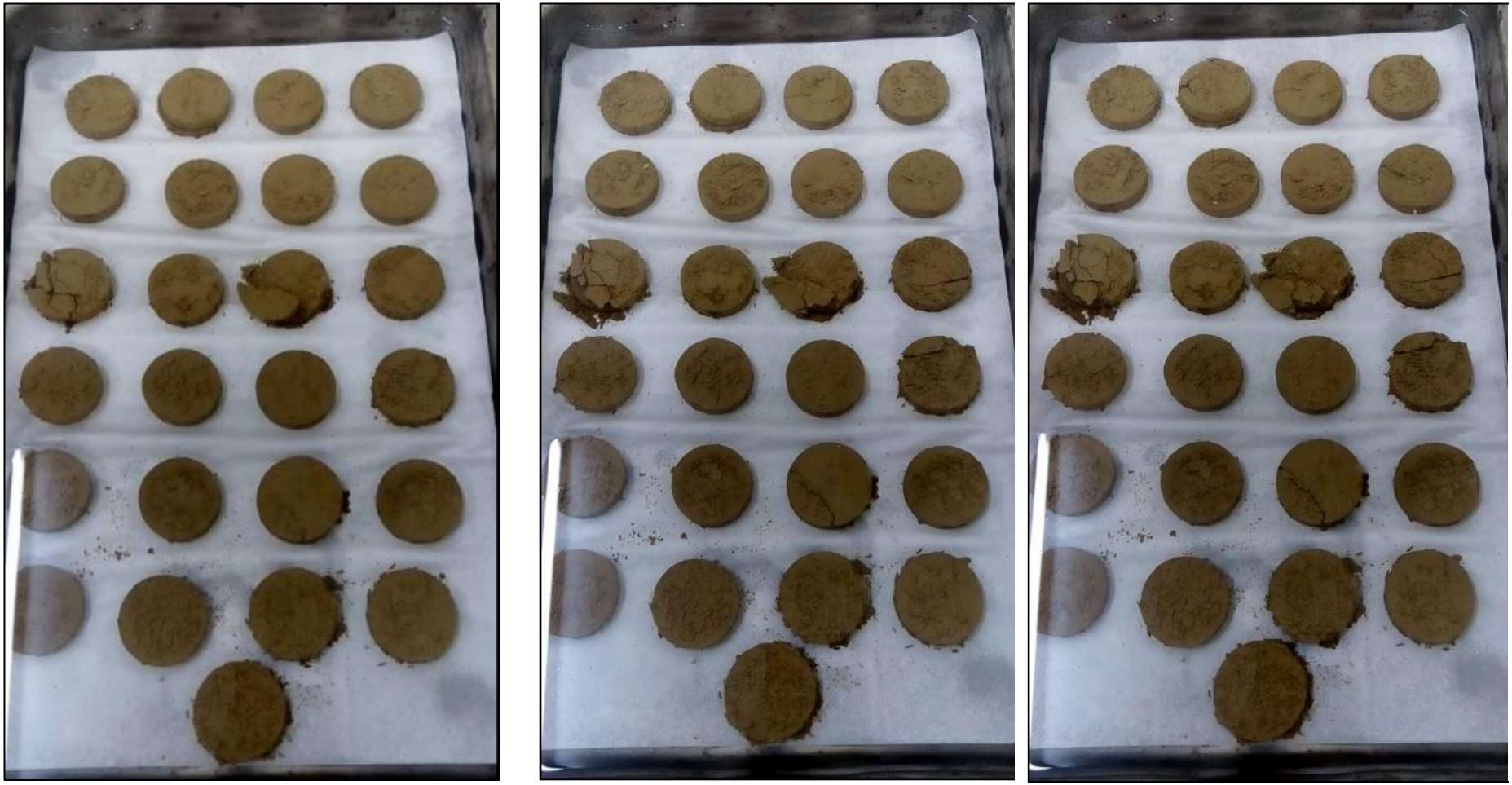

(a) (b) (c)

Figure A.20. Internal stability for 2% CBAS treated with 11% initial water content specimens at the end of a) 10 min, b) 20 min, C) 30 min

## Appendix C: UCS Results and Photos of Failure Mode Observed for Representative Specimens from Unconfined Compressive Strength Tests

Table A.1. Unconfined compressive strength results

| CBAS (%) | $q_u$ (kPa) | $C_u$ (kPa) | Water content% | Elasticity modulus (MPa) | Strain at failure (%) |
|---|---|---|---|---|---|
| 0 | 265.9 | 133.0 | 28.7 | 5.5 | 11.9 |
| 0 | 1028.3 | 514.2 | 22.0 | 24.5 | 10.1 |
| 0 | 2769.5 | 1384.7 | 16.7 | 144.2 | 2.6 |
| 0 | 4801.9 | 2400.9 | 10.9 | 303.9 | 1.6 |
| 0.5 | 302.8 | 151.4 | 28.0 | 5.3 | 12.0 |
| 0.5 | 1403.9 | 702.0 | 22.1 | 24.6 | 10.9 |
| 0.5 | 3715.0 | 1857.5 | 16.7 | 84.4 | 5.6 |
| 0.5 | 6200.9 | 3100.4 | 9.0 | 228.0 | 3.6 |
| 1 | 335.8 | 167.9 | 26.5 | 4.3 | 12.5 |
| 1 | 1460.8 | 730.4 | 22.7 | 32.5 | 11.3 |
| 1 | 3917.5 | 1958.8 | 16.9 | 99.9 | 6.4 |
| 1 | 7393.3 | 3696.7 | 10.6 | 243.2 | 4.4 |
| 2 | 357.5 | 178.8 | 26.9 | 5.3 | 12.4 |
| 2 | 1484.1 | 742.0 | 22.2 | 28.5 | 12.7 |
| 2 | 4635.3 | 2317.6 | 15.2 | 82.8 | 6.7 |
| 2 | 8790.1 | 4395.1 | 10.2 | 159.8 | 6.6 |
| 5 | 438.6 | 219.3 | 27.8 | 9.1 | 12.9 |
| 5 | 1695.3 | 847.6 | 21.0 | 25.3 | 14.3 |
| 5 | 5031.4 | 2515.7 | 16.1 | 96.8 | 7.0 |
| 5 | 10415.6 | 5207.8 | 10.7 | 151.0 | 8.2 |

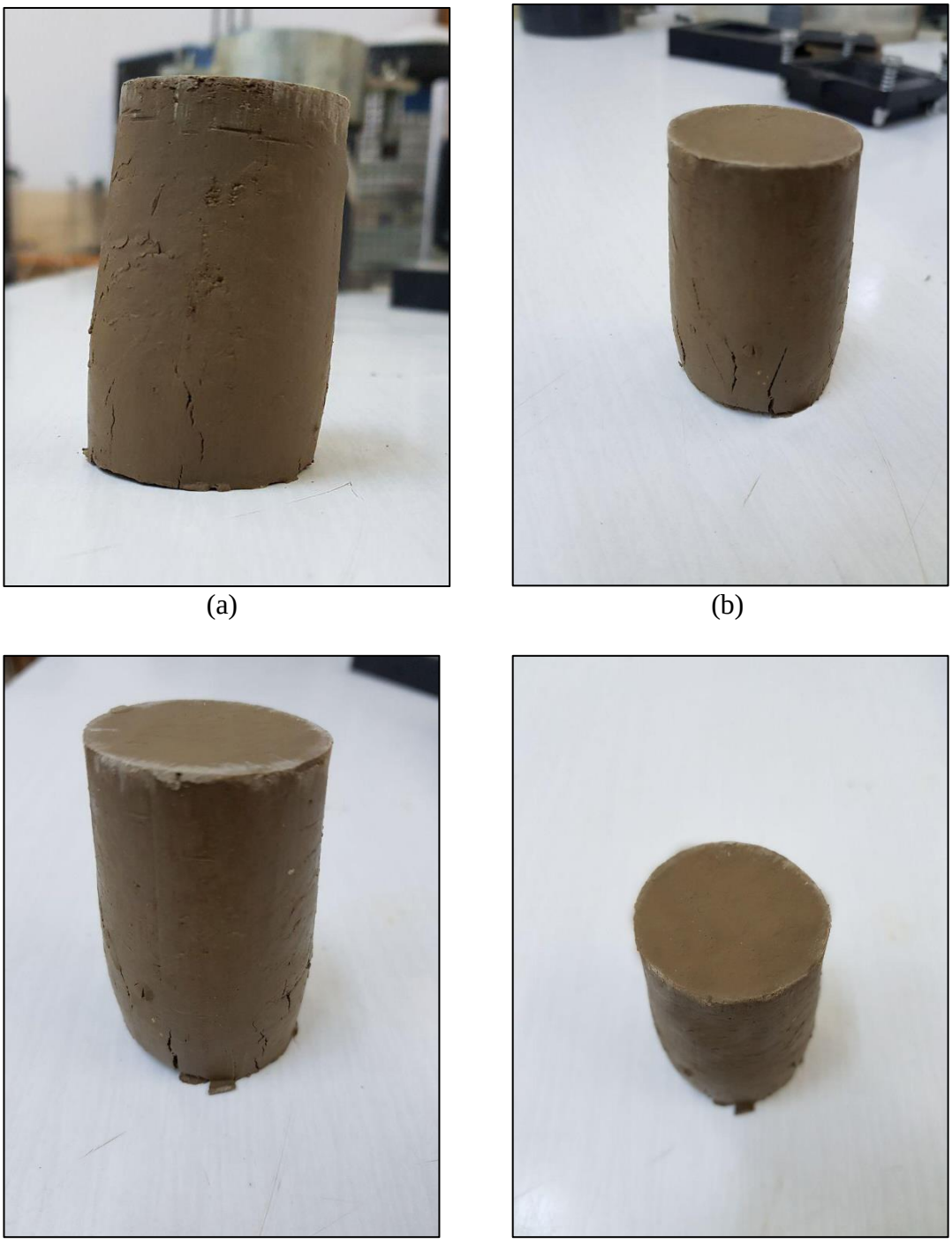

(a) (b)

(c) (d)

Figure A.21. Failure pattern of specimens at 28% initial water content

(a)

(b)

(c)

(d)

Figure A.22. Failure pattern of specimens at 22.5% initial water content

(a)

(b)

(b)

(d)

Figure A.23. Failure pattern of specimens at 16% initial water content

(a)

(b)

(c)

(d)

Figure A.24. Failure pattern of specimens at 11% initial water content

# Appendix D: Sample Preparation and Raw Data of Compressibility

Figure A.25. Oedometer apparatus

Figure A.26. Sample preparation of one dimensional consolidation test at 28% initial water content

Figure A.27. Sample preparation of one dimensional consolidation test at 22.5% initial water content

Figure A.28. Sample preparation of one dimensional consolidation test at 16% initial water content

Figure A.29. Sample preparation of one dimensional consolidation test at 11% initial water content

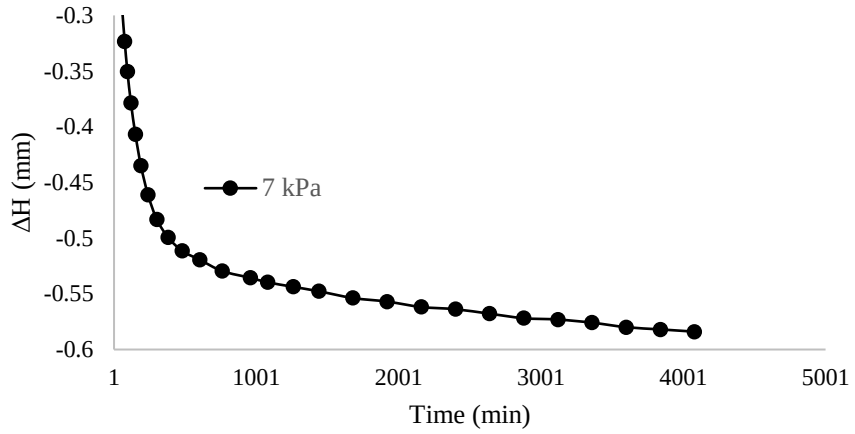


Figure A.30. ΔH versus time prior to compressibility test for untreated specimen at 28% initial water content

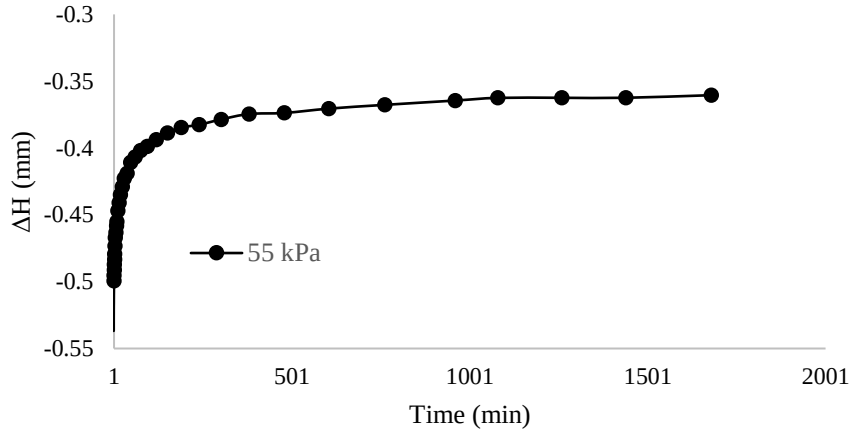


Figure A.31. ΔH versus time at 55 kPa (loading) for untreated specimen at 28% initial water content

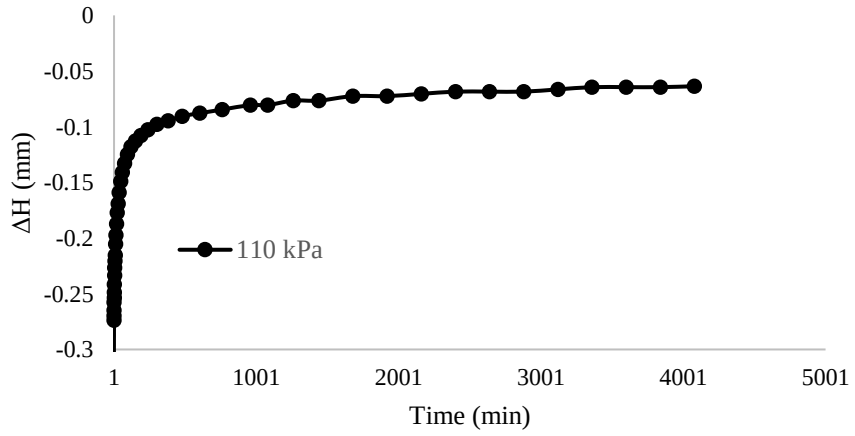


Figure A.32. ΔH versus time at 110 kPa (loading) for untreated specimen at 28% initial water content

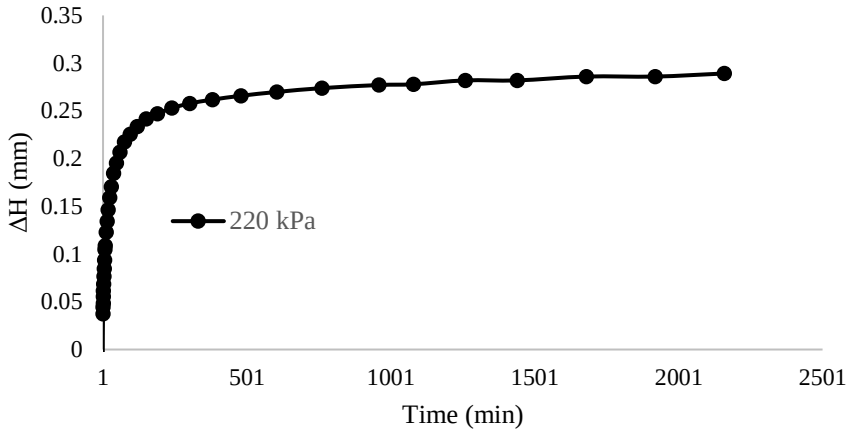


Figure A.33. ΔH versus time at 220 kPa (loading) for untreated specimen at 28% initial water content

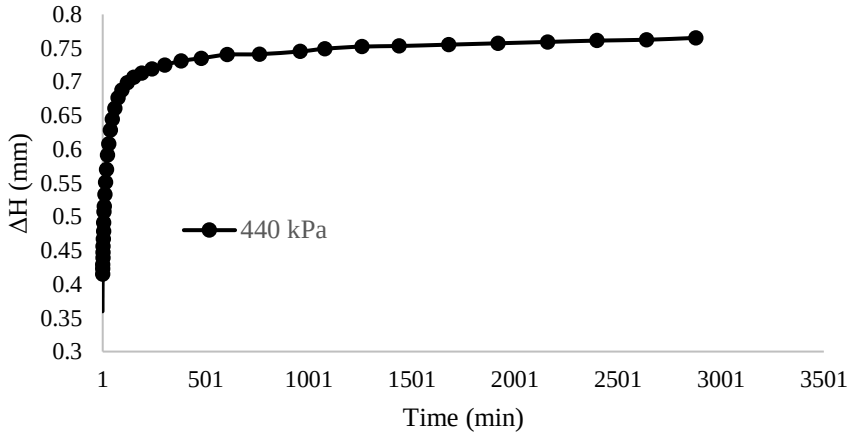


Figure A.34. ΔH versus time at 440 kPa (loading) for untreated specimen at 28% initial water content

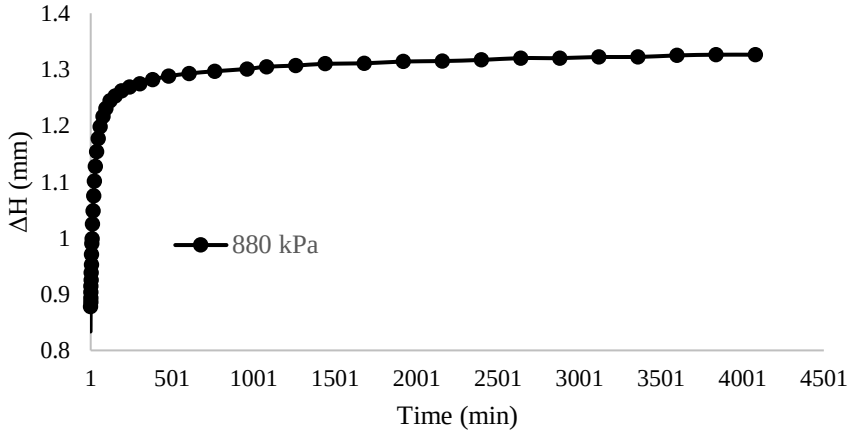


Figure A.35. ΔH versus time at 880 kPa (loading) for untreated specimen at 28% initial water content

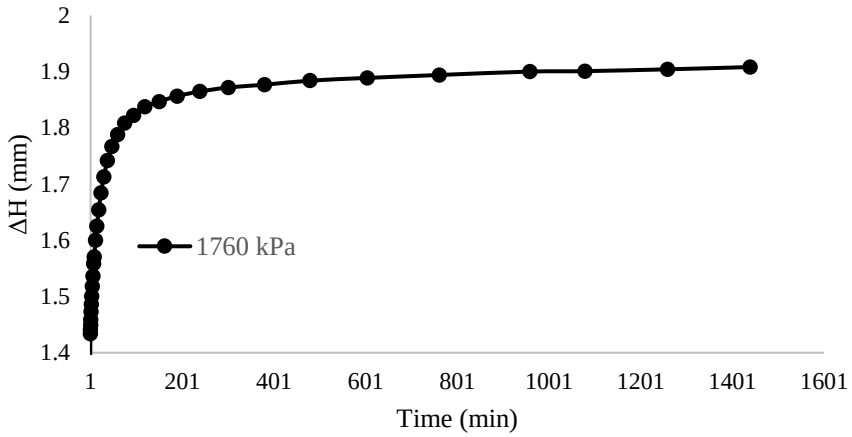


Figure A.36. ΔH versus time at 1760 kPa (loading) for untreated specimen at 28% initial water content

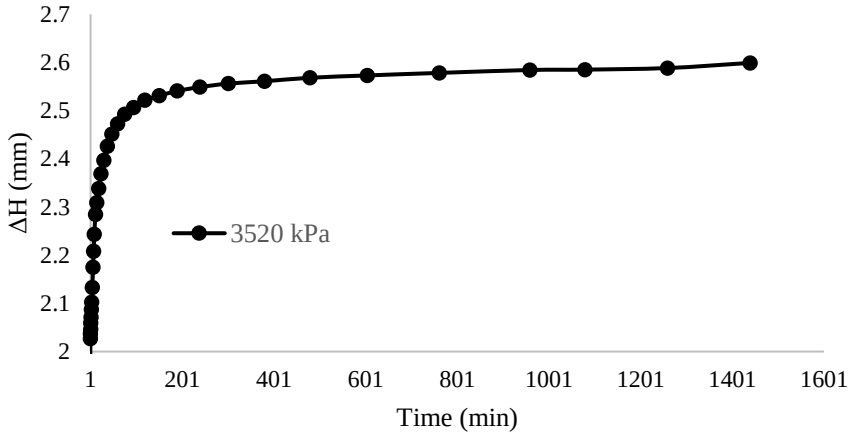


Figure A.37. ΔH versus time at 3520 kPa (loading) for untreated specimen at 28% initial water content

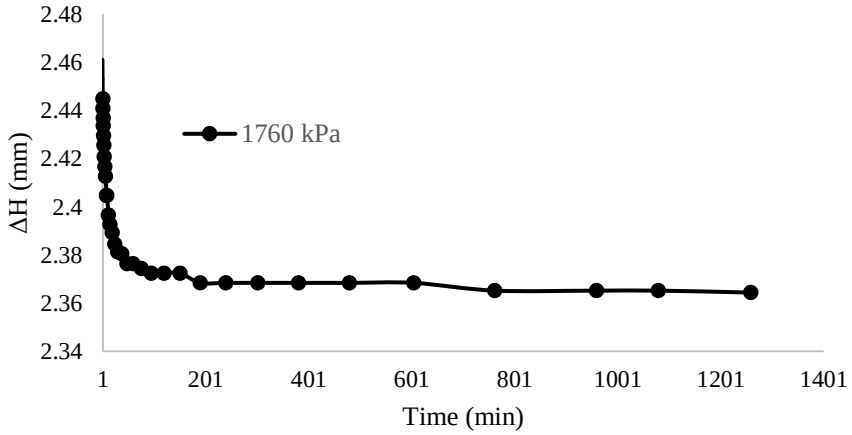


Figure A.38. ΔH versus time at 1760 kPa (unloading) for untreated specimen at 28% initial water content

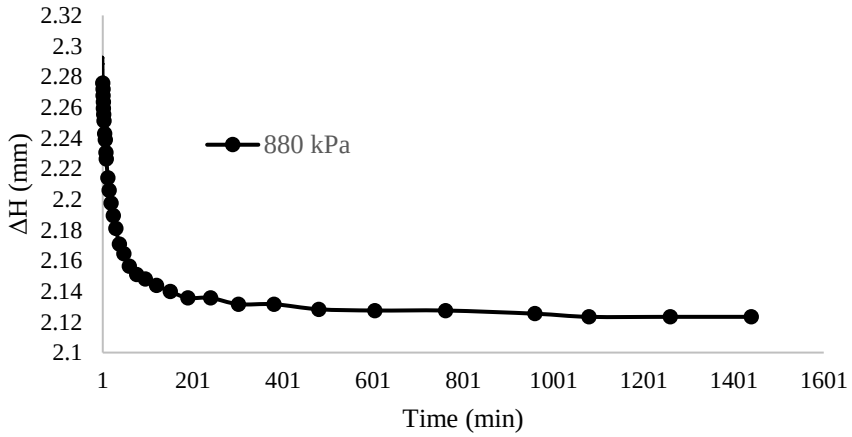


Figure A.39. ΔH versus time at 880 kPa (unloading) for untreated specimen at 28% initial water content

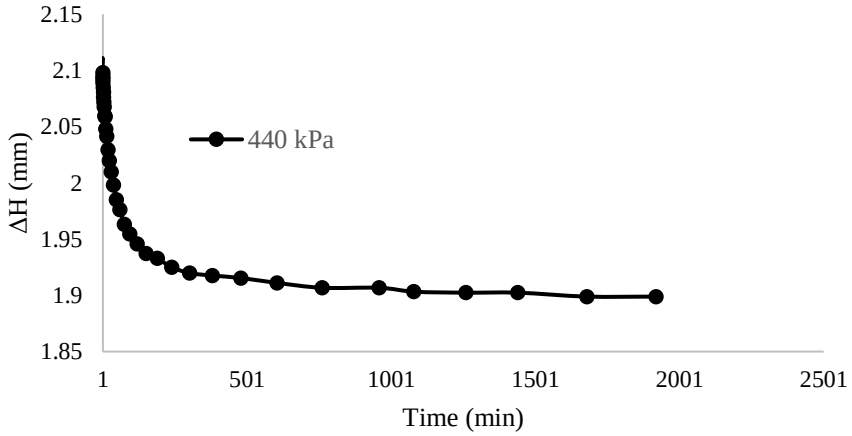


Figure A.40. ΔH versus time at 440 kPa (unloading) for untreated specimen at 28% initial water content

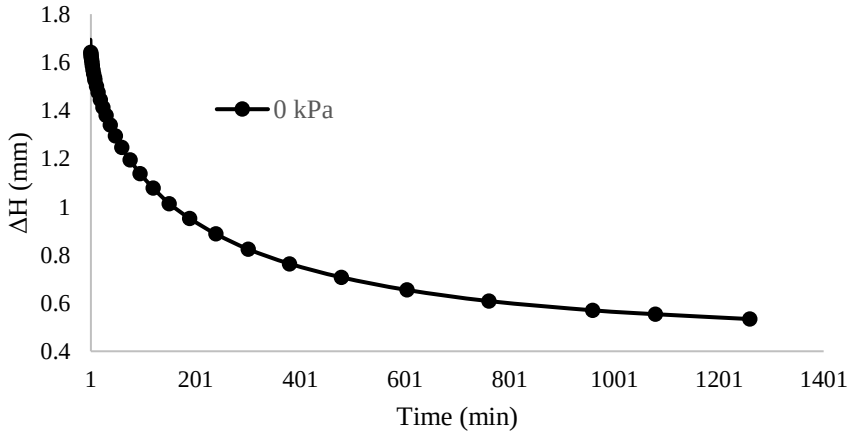


Figure A.41. ΔH versus time at 0 kPa (unloading) for untreated specimen at 28% initial water content

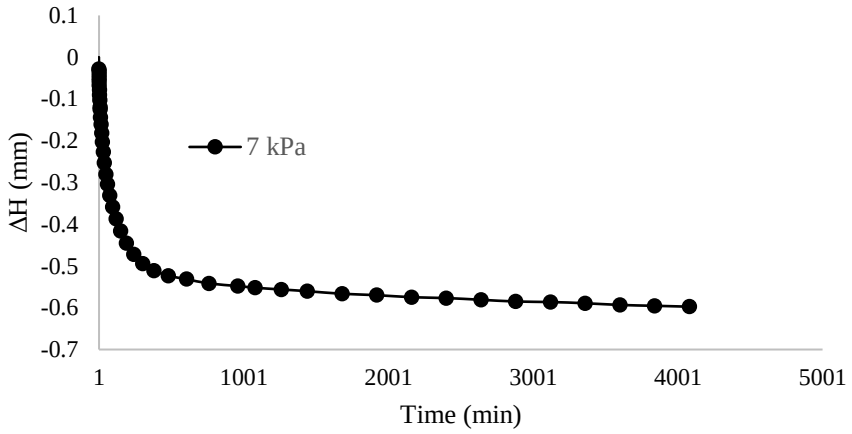


Figure A.42. ΔH versus time prior to compressibility test for untreated specimen at 22.5% initial water content

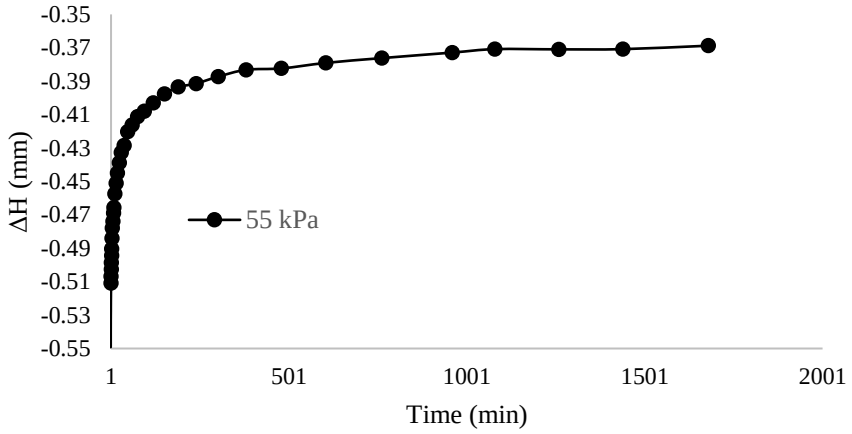


Figure A.43. ΔH versus time at 55 kPa (loading) for untreated specimen at 22.5% initial water content

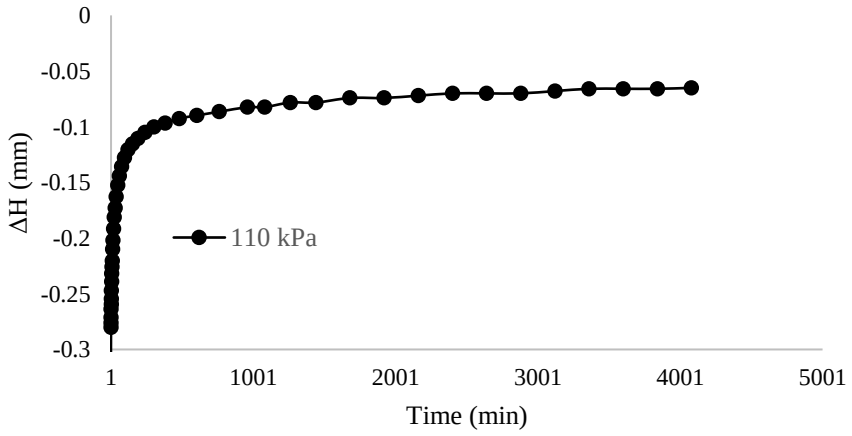


Figure A.44. ΔH versus time at 110 kPa (loading) for untreated specimen at 22.5% initial water content

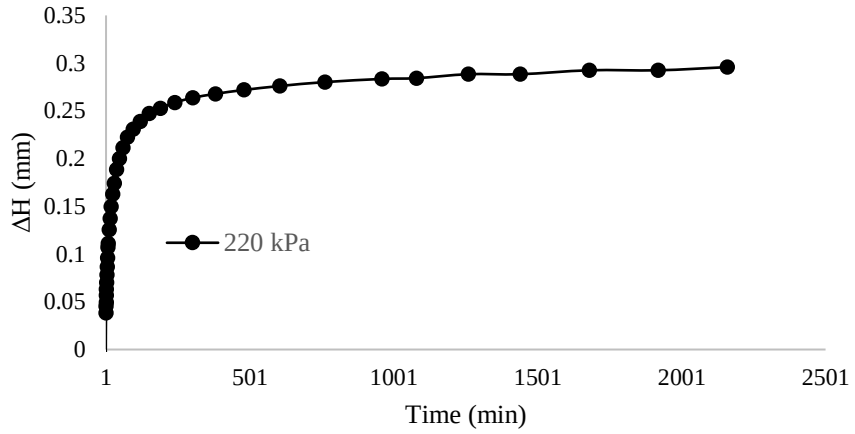


Figure A.45. ΔH versus time at 220 kPa (loading) for untreated specimen at 22.5% initial water content

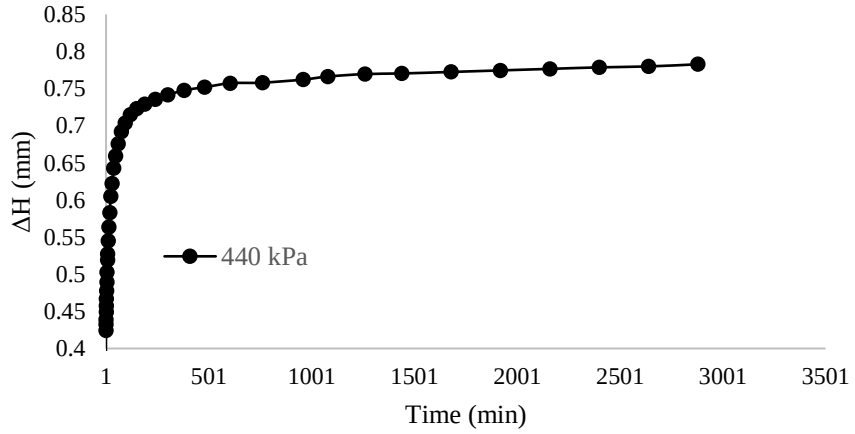


Figure A.46. ΔH versus time at 440 kPa (loading) for untreated specimen at 22.5% initial water content

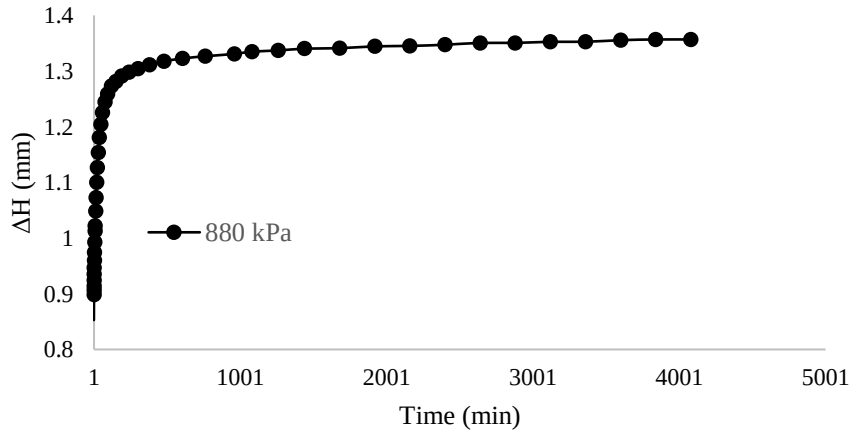


Figure A.47. ΔH versus time at 880 kPa (loading) for untreated specimen at 22.5% initial water content

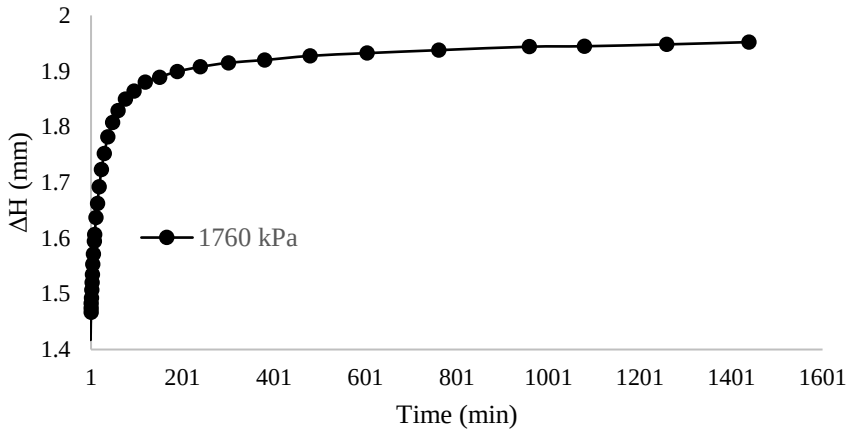


Figure A.48. ΔH versus time at 1760 kPa (loading) for untreated specimen at 22.5% initial water content

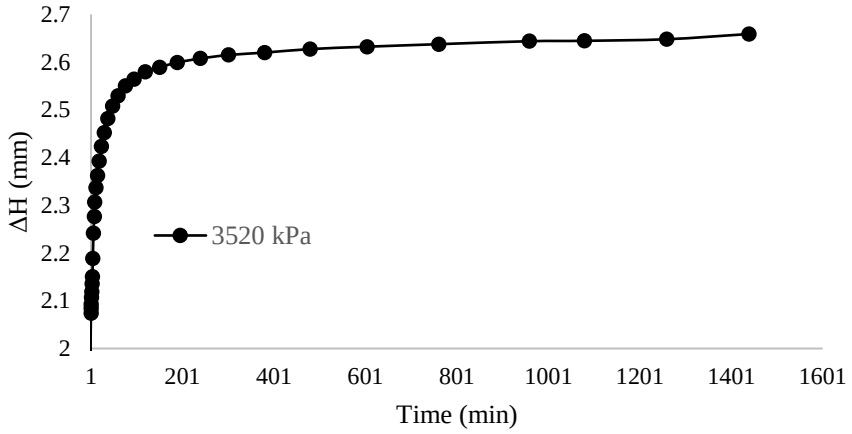


Figure A.49. ΔH versus time at 3520 kPa (loading) for untreated specimen at 22.5% initial water content

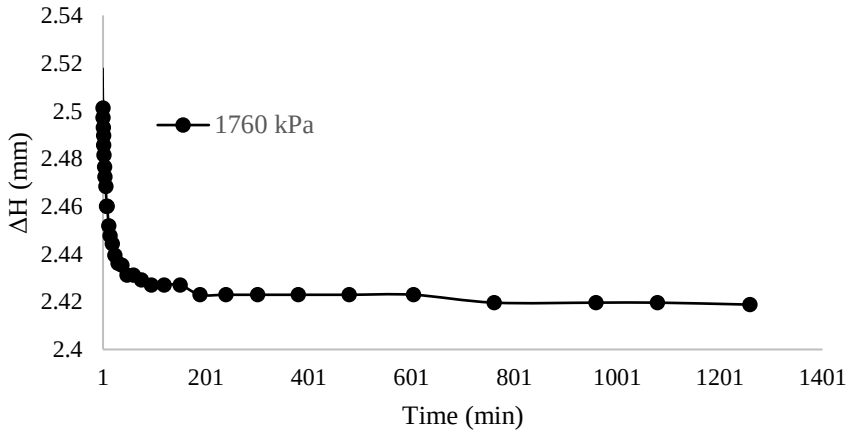


Figure A.50. ΔH versus time at 1760 kPa (unloading) for untreated specimen at 22.5% initial water content

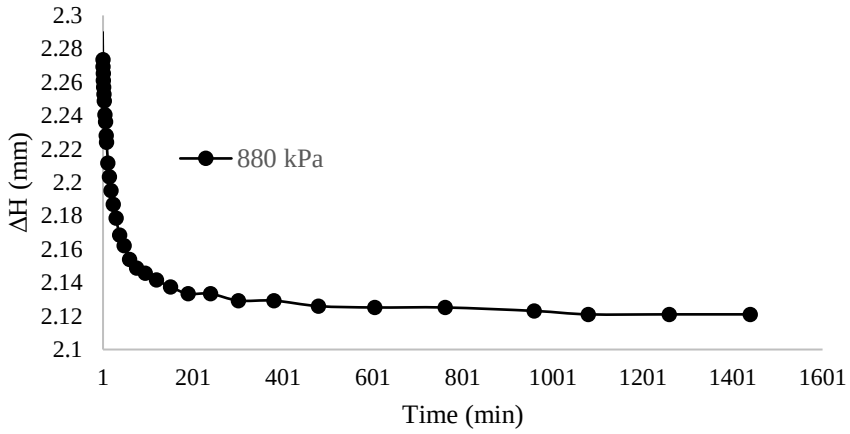


Figure A.51. ΔH versus time at 880 kPa (unloading) for untreated specimen at 22.5% initial water content

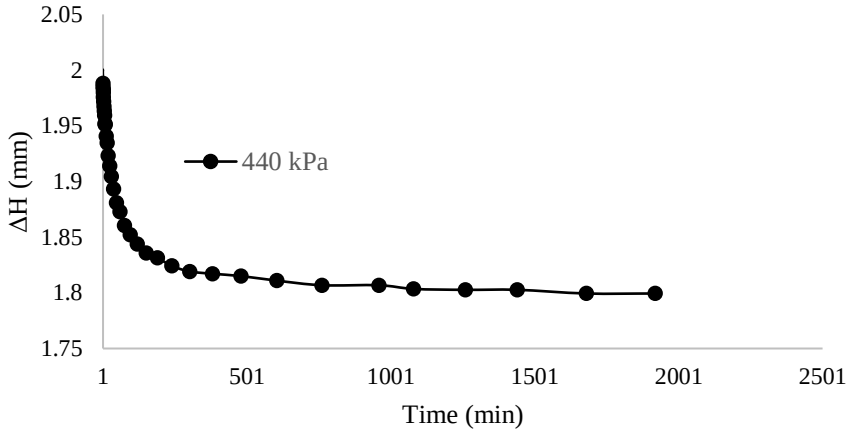


Figure A.52. ΔH versus time at 440 kPa (unloading) for untreated specimen at 22.5% initial water content

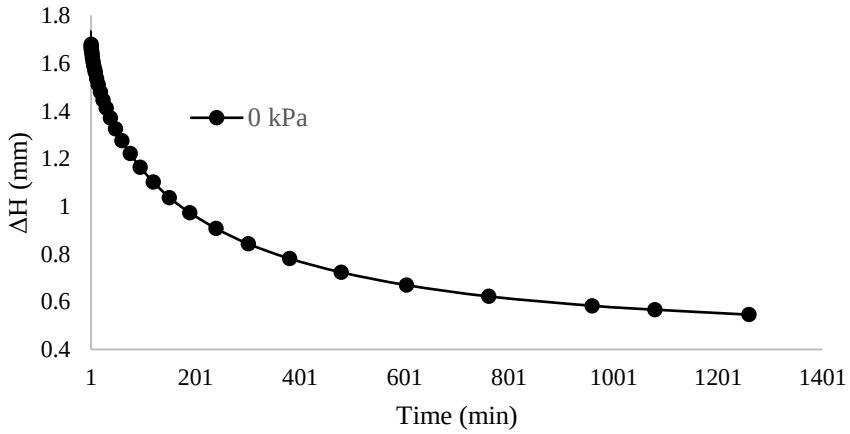


Figure A.53. ΔH versus time at 0 kPa (unloading) for untreated specimen at 22.5% initial water content

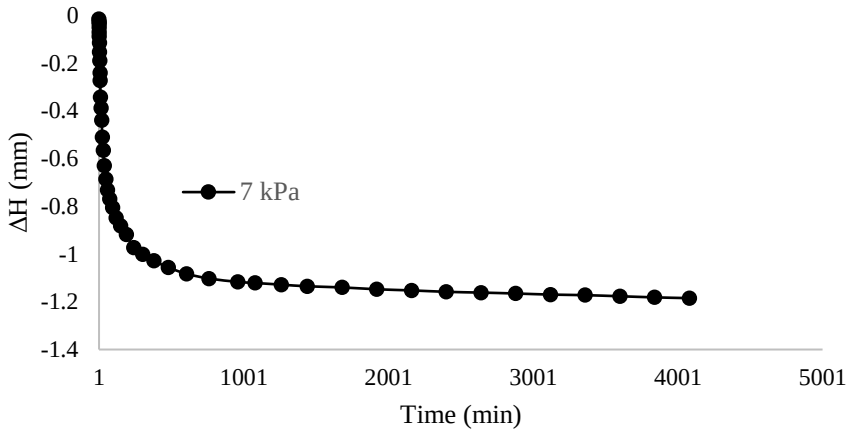


Figure A.54. ΔH versus time prior to compressibility test for untreated specimen at 16% initial water content

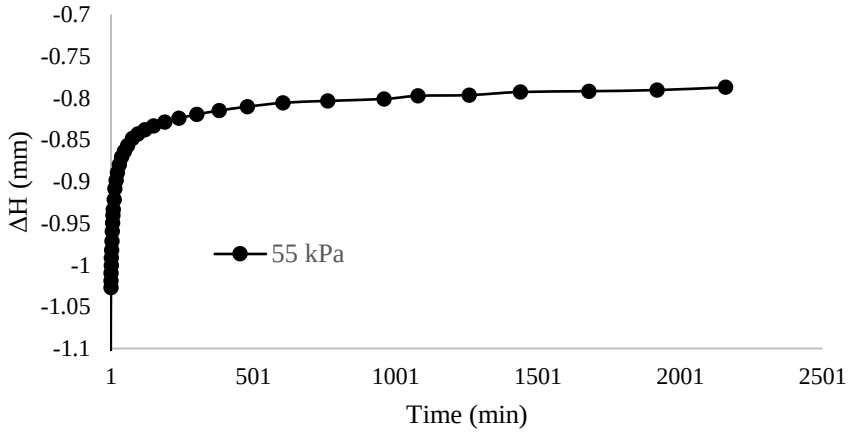


Figure A.55. ΔH versus time at 55 kPa (loading) for untreated specimen at 16% initial water content

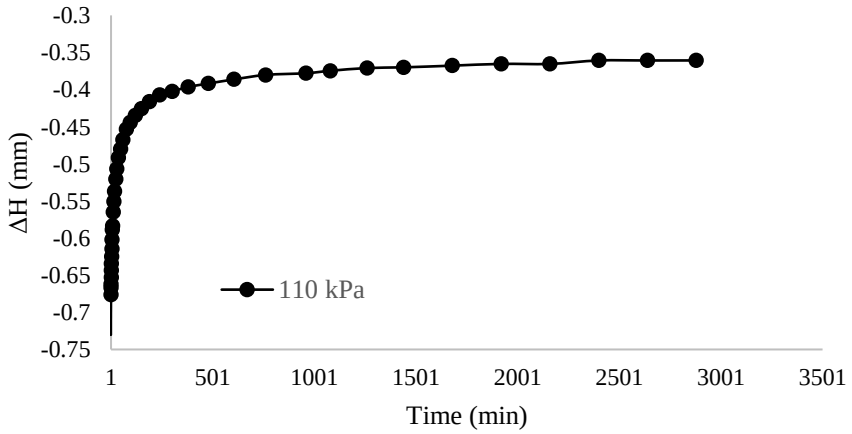


Figure A.56. ΔH versus time at 110 kPa (loading) for untreated specimen at 16% initial water content

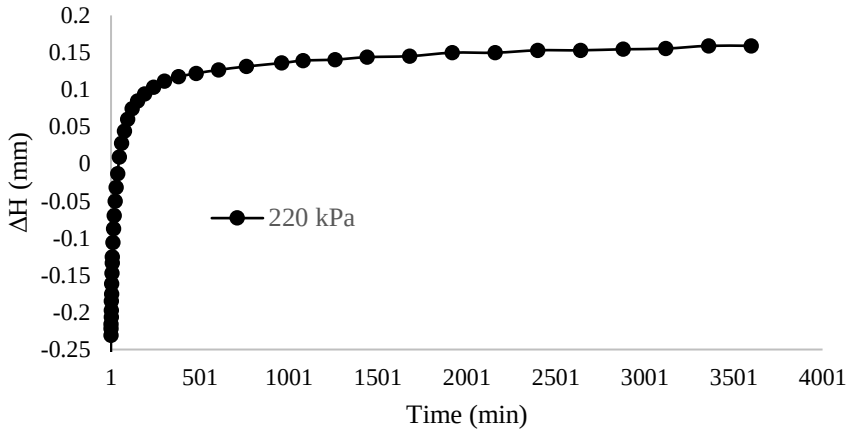


Figure A.57. ΔH versus time at 220 kPa (loading) for untreated specimen at 16% initial water content

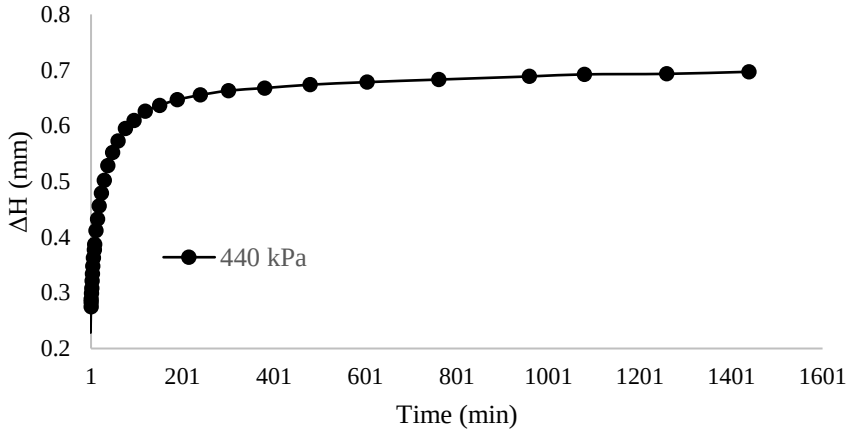


Figure A.58. ΔH versus time at 440 kPa (loading) for untreated specimen at 16% initial water content

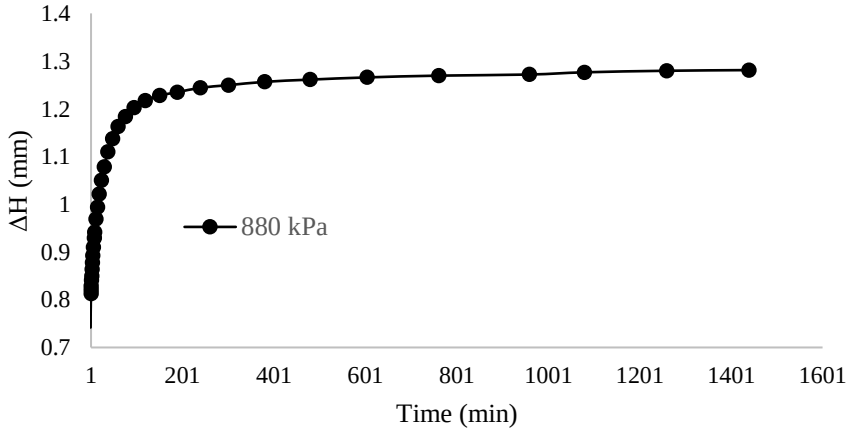


Figure A.59. ΔH versus time at 880 kPa (loading) for untreated specimen at 16% initial water content

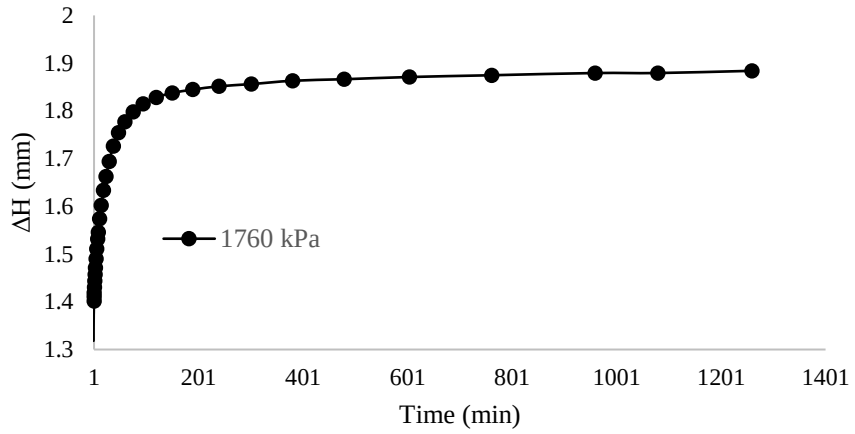


Figure A.60. ΔH versus time at 1760 kPa (loading) for untreated specimen at 16% initial water content

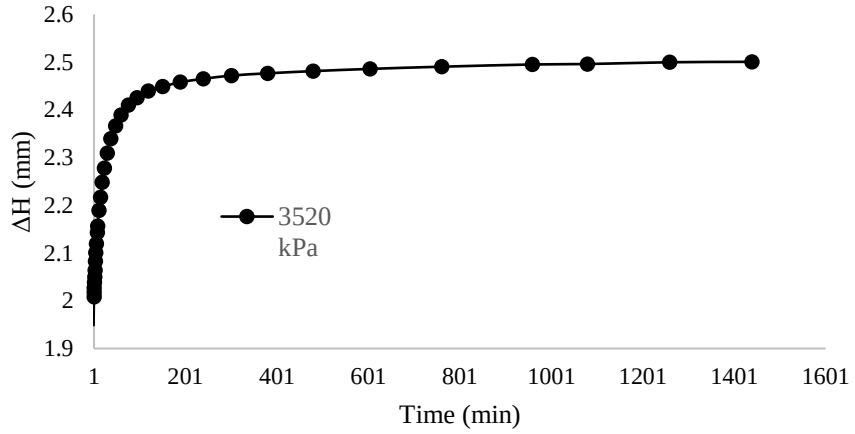


Figure A.61. ΔH versus time at 3520 kPa (loading) for untreated specimen at 16% initial water content

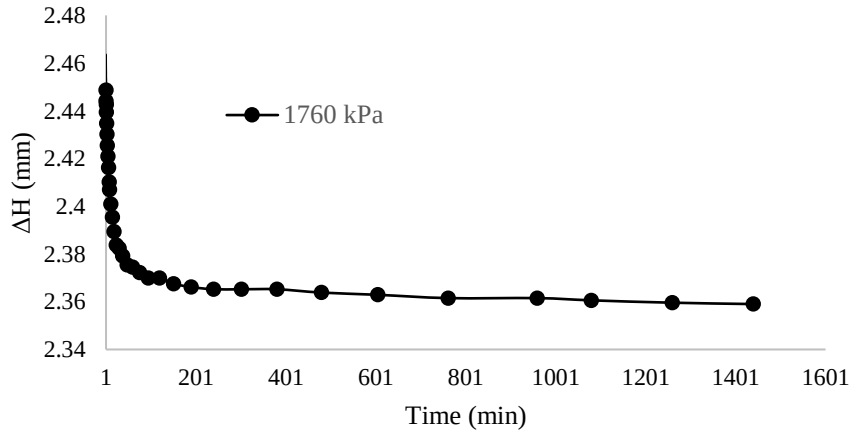


Figure A.62. ΔH versus time at 1760 kPa (unloading) for untreated specimen at 16% initial water content

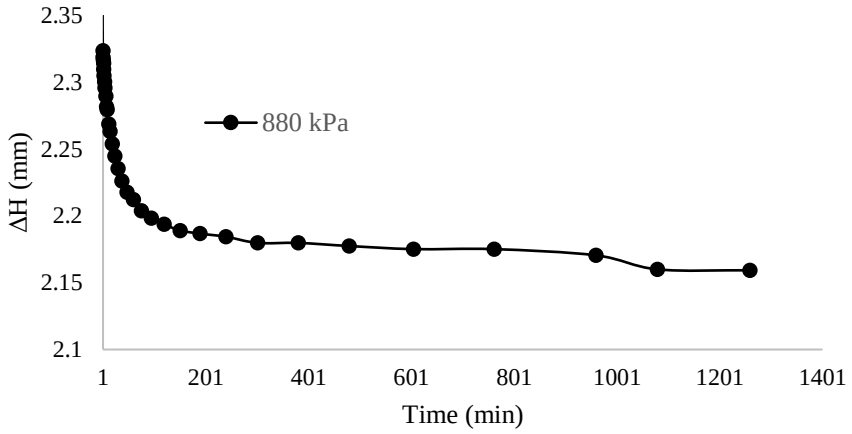


Figure A.63. ΔH versus time at 880 kPa (unloading) for untreated specimen at 16% initial water content

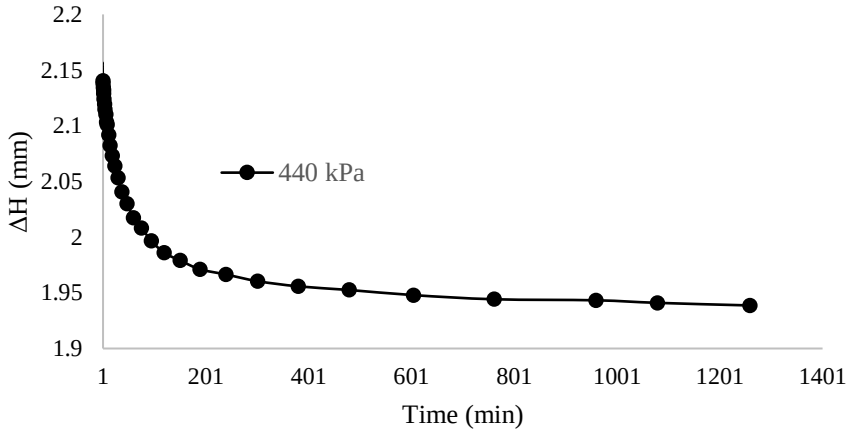


Figure A.64. ΔH versus time at 440 kPa (unloading) for untreated specimen at 16% initial water content

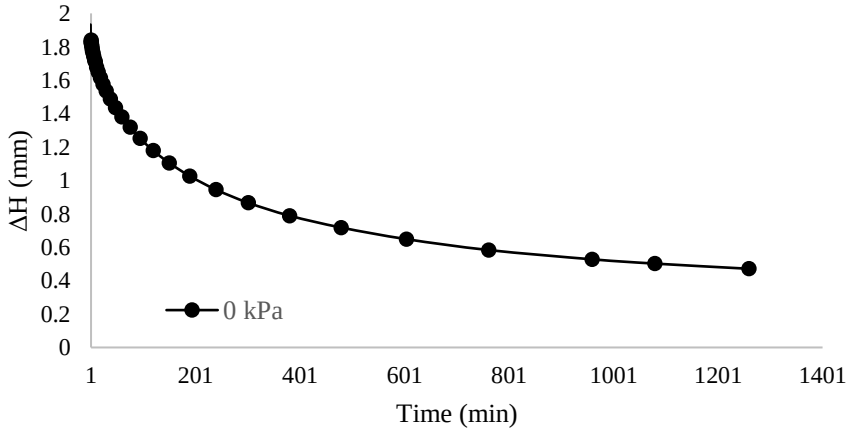


Figure A.65. ΔH versus time at 0 kPa (unloading) for untreated specimen at 16% initial water content

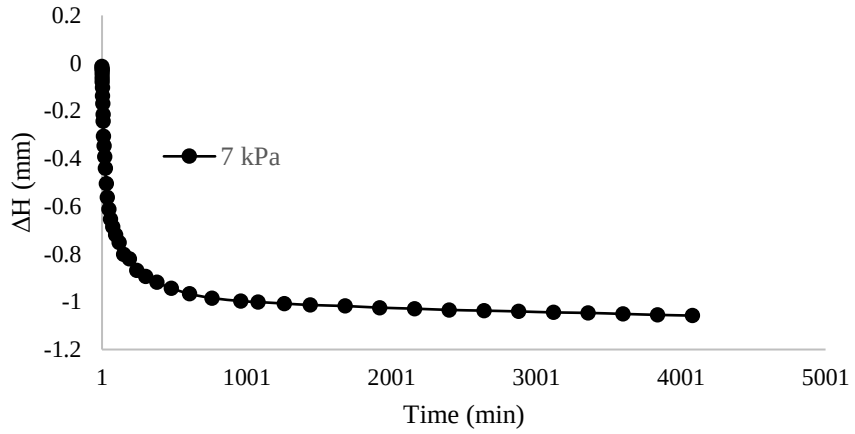


Figure A.66. ΔH versus time prior to compressibility test for untreated specimen at 11% initial water content

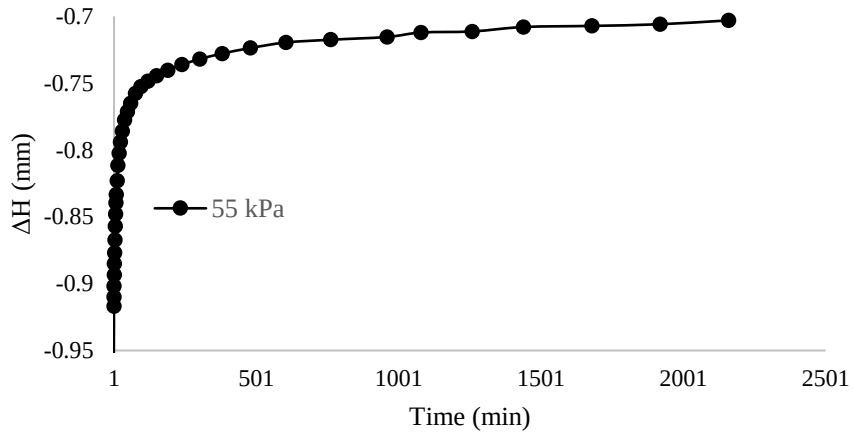


Figure A.67. ΔH versus time at 55 kPa (loading) for untreated specimen at 11% initial water content

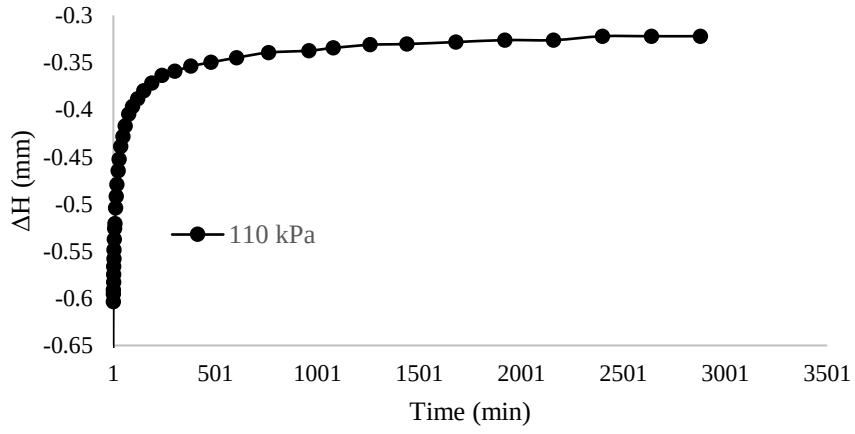


Figure A.68. ΔH versus time at 110 kPa (loading) for untreated specimen at 11% initial water content

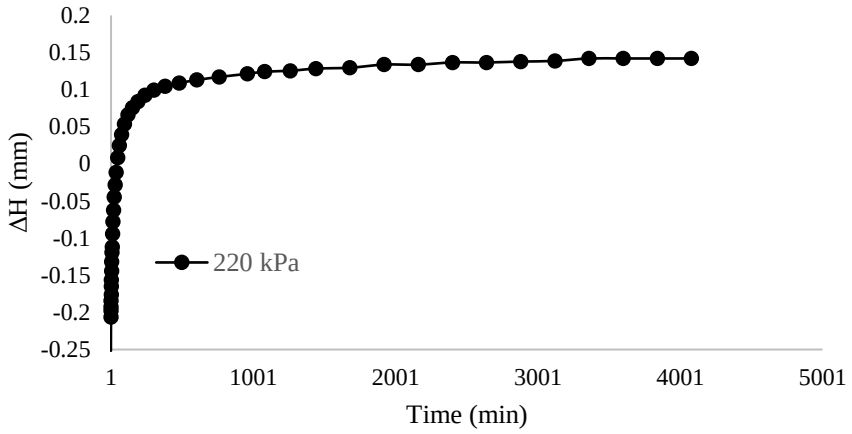


Figure A.69. ΔH versus time at 220 kPa (loading) for untreated specimen at 11% initial water content

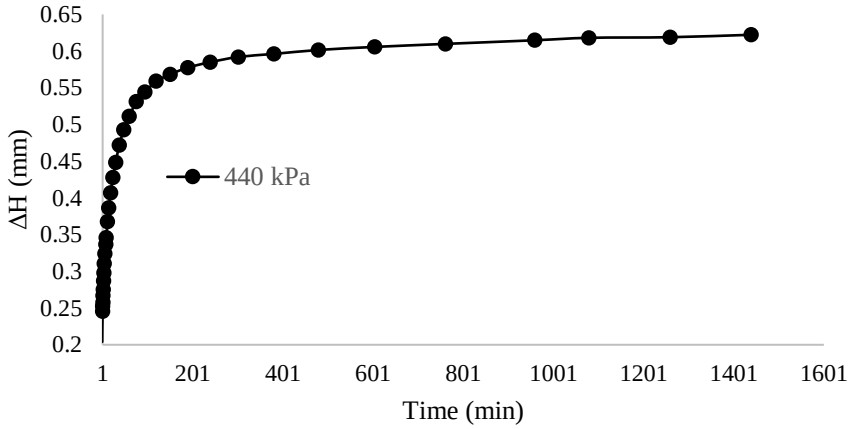


Figure A.70. ΔH versus time at 440 kPa (loading) for untreated specimen at 11% initial water content

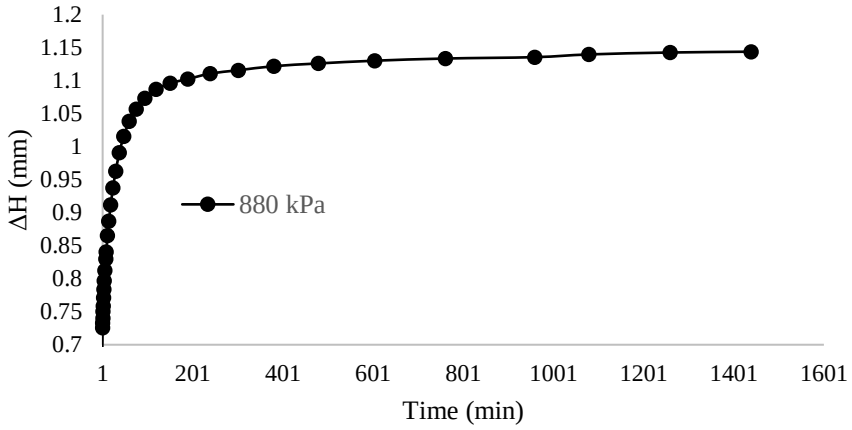


Figure A.71. ΔH versus time at 880 kPa (loading) for untreated specimen at 11% initial water content

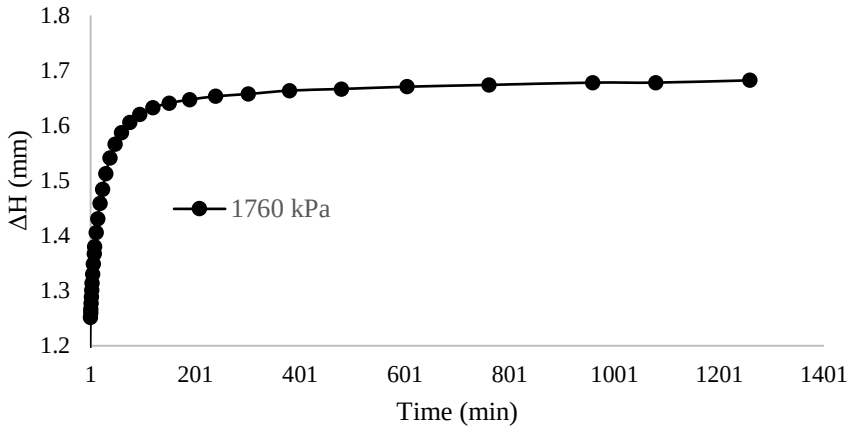


Figure A.72. ΔH versus time at 1760 kPa (loading) for untreated specimen at 11% initial water content

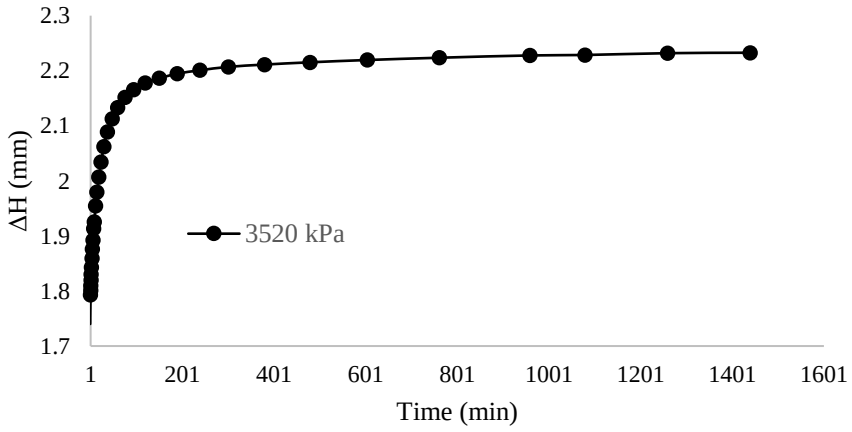


Figure A.73. ΔH versus time at 3520 kPa (loading) for untreated specimen at 11% initial water content

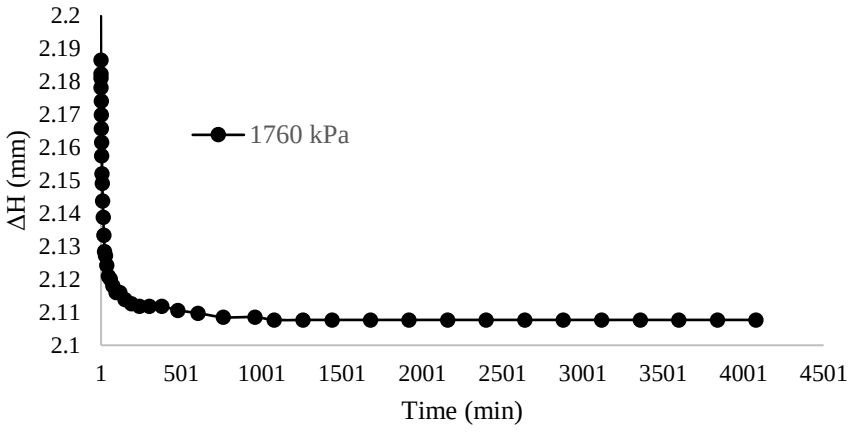


Figure A.74. ΔH versus time at 1760 kPa (unloading) for untreated specimen at 11% initial water content

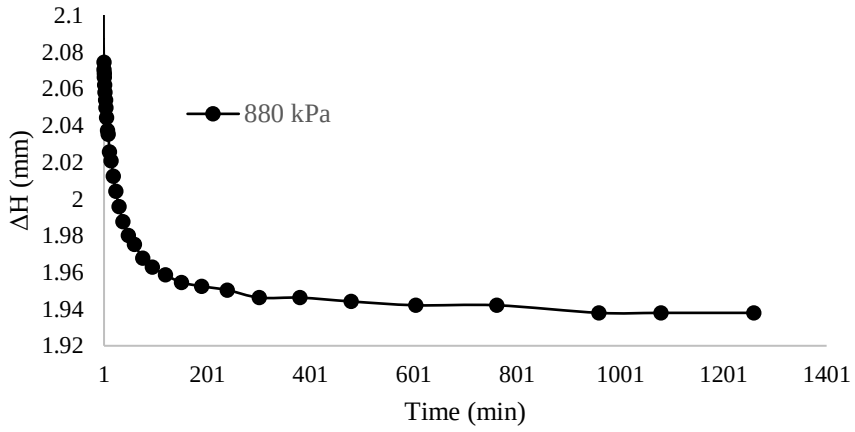


Figure A.75. ΔH versus time at 880 kPa (unloading) for untreated specimen at 11% initial water content

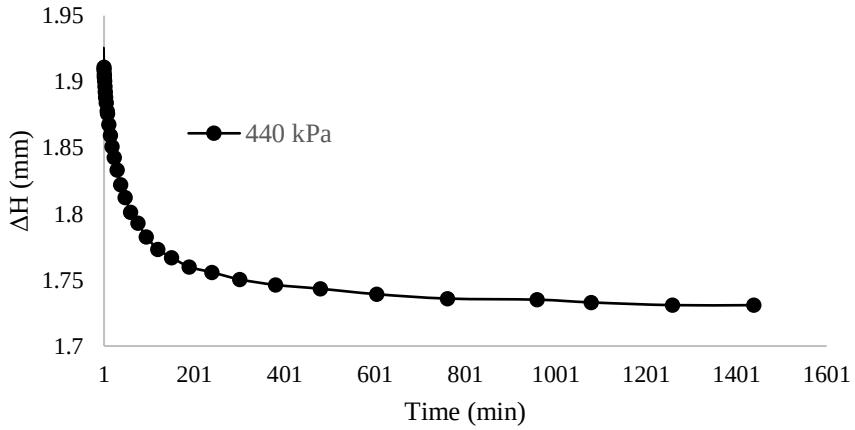


Figure A.76. ΔH versus time at 440 kPa (unloading) for untreated specimen at 11% initial water content

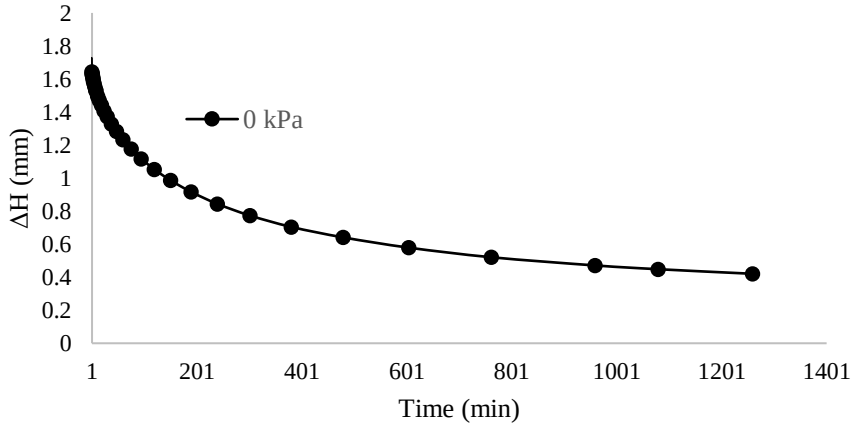


Figure A.77. ΔH versus time at 0 kPa (unloading) for untreated specimen at 11% initial water content

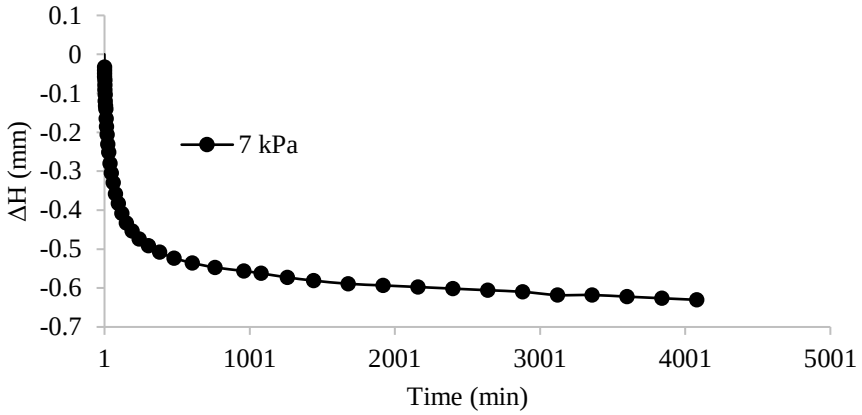


Figure A.78. ΔH versus time prior to compressibility test for 2% CBAS treated specimen at 28% initial water content

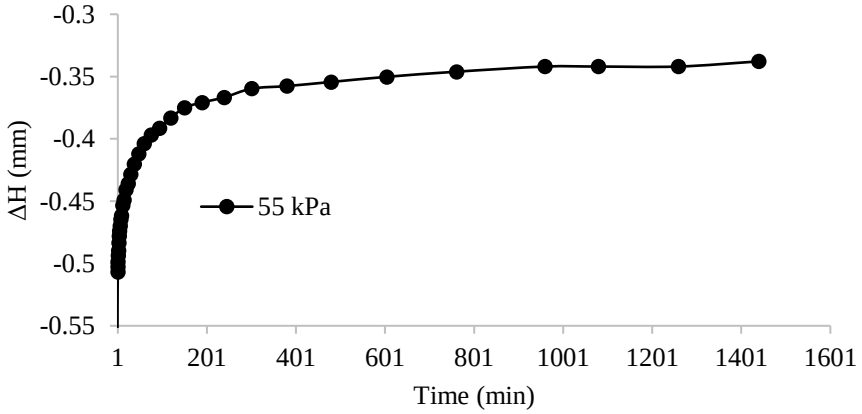


Figure A.79. ΔH versus time at 55 kPa (loading) for 2% CBAS treated specimen at 28% initial water content

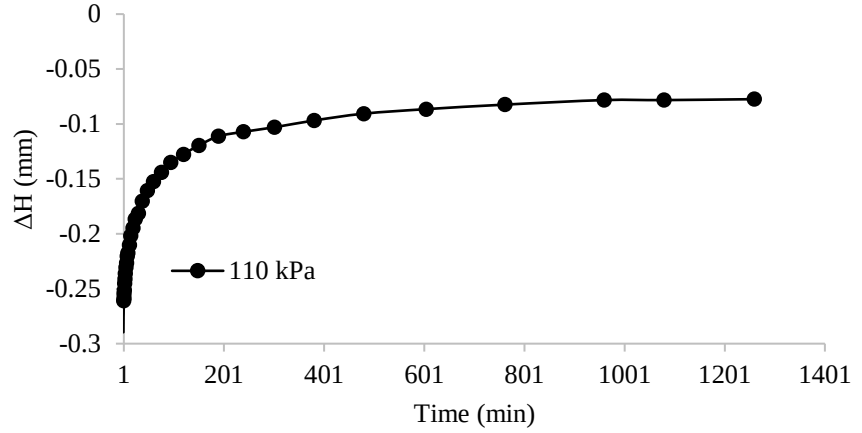


Figure A.80. ΔH versus time at 110 kPa (loading) for 2% CBAS treated specimen at 28% initial water content

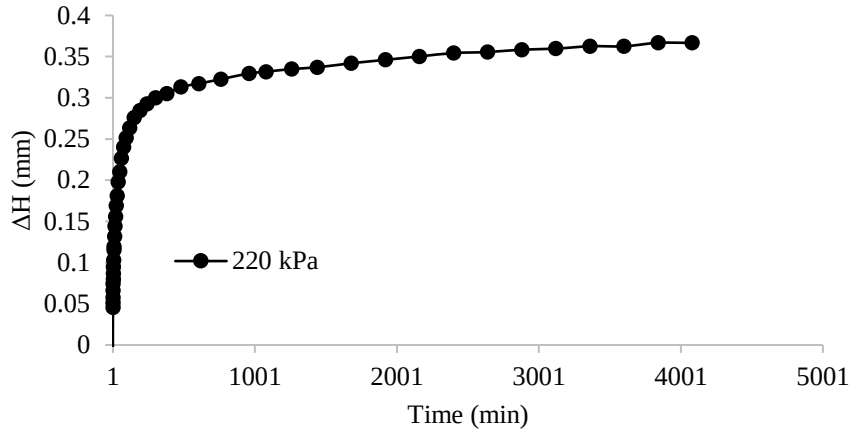


Figure A.81. ΔH versus time at 220 kPa (loading) for 2% CBAS treated specimen at 28% initial water content

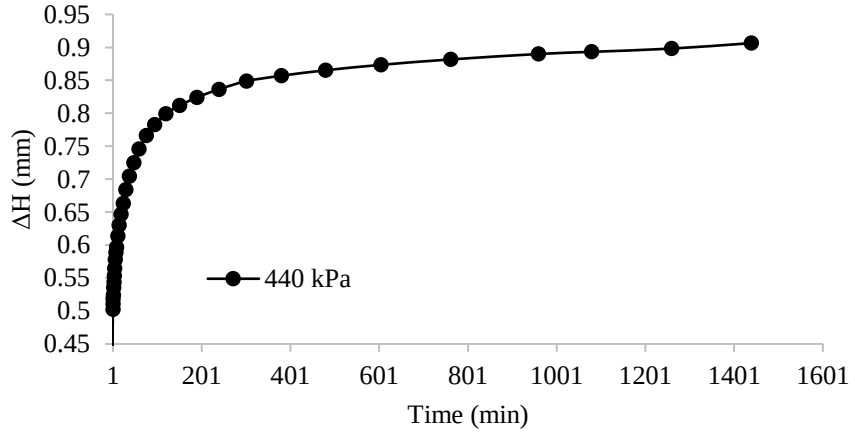


Figure A.82. ΔH versus time at 440 kPa (loading) for 2% CBAS treated specimen at 28% initial water content

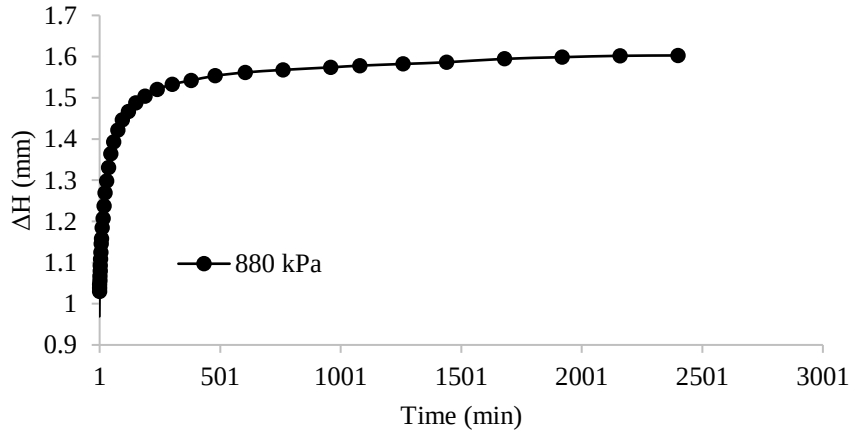


Figure A.83. ΔH versus time at 880 kPa (loading) for 2% CBAS treated specimen at 28% initial water content

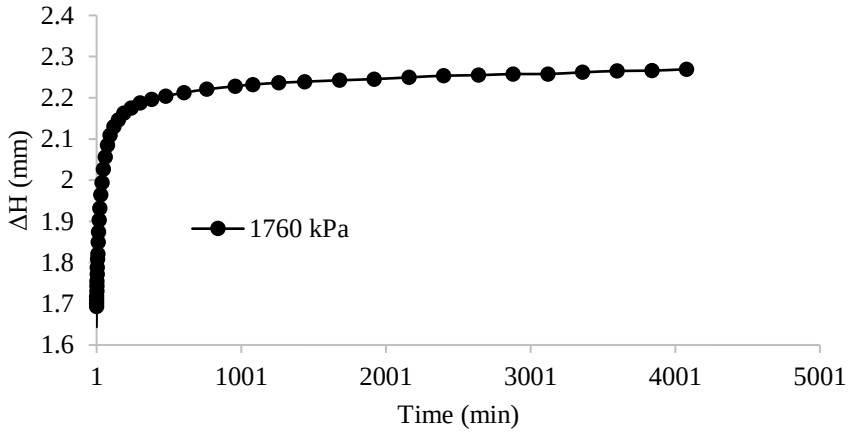


Figure A.84. ΔH versus time at 1760 kPa (loading) for 2% CBAS treated specimen at 28% initial water content

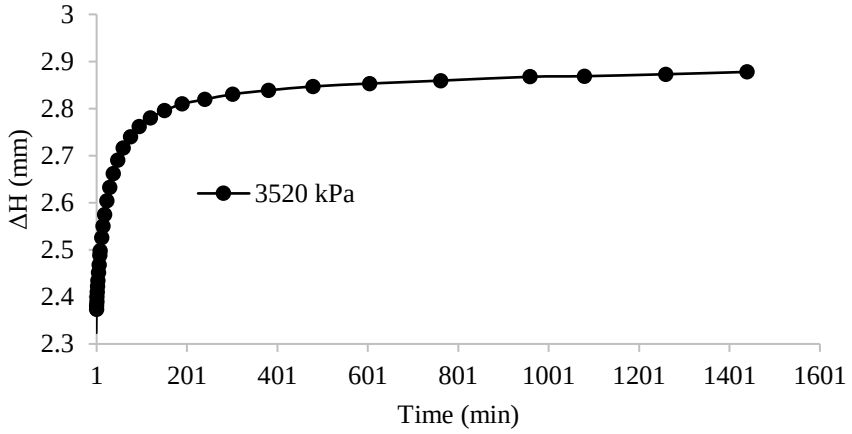


Figure A.85. ΔH versus time at 3520 kPa (loading) for 2% CBAS treated specimen at 28% initial water content

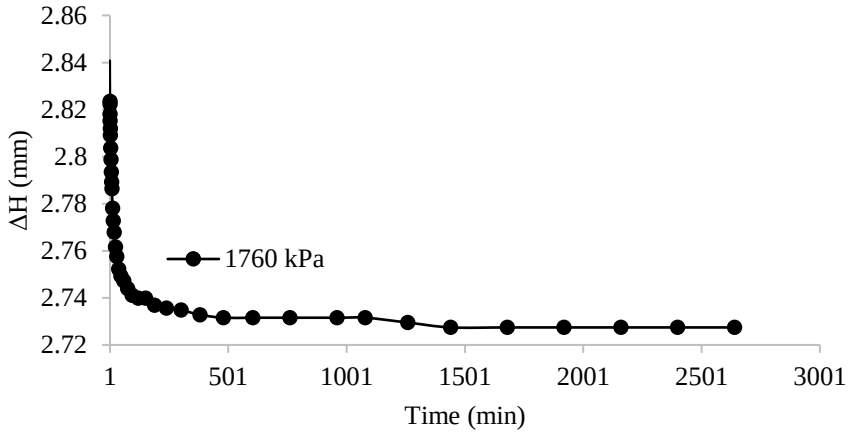


Figure A.86. ΔH versus time at 1760 kPa (unloading) for 2% CBAS treated specimen at 28% initial water content

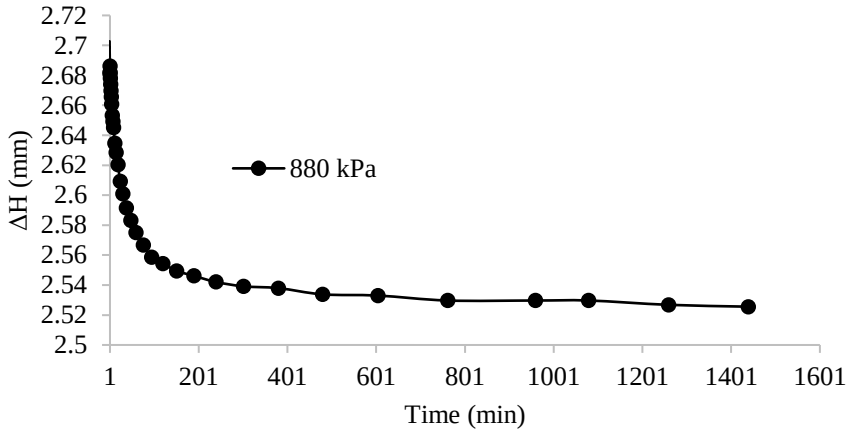


Figure A.87. ΔH versus time at 880 kPa (unloading) for 2% CBAS treated specimen at 28% initial water content

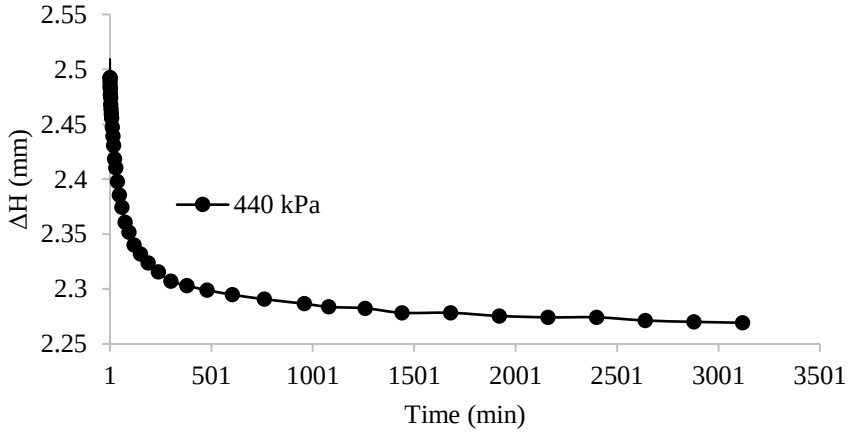


Figure A.88. ΔH versus time at 440 kPa (unloading) for 2% CBAS treated specimen at 28% initial water content

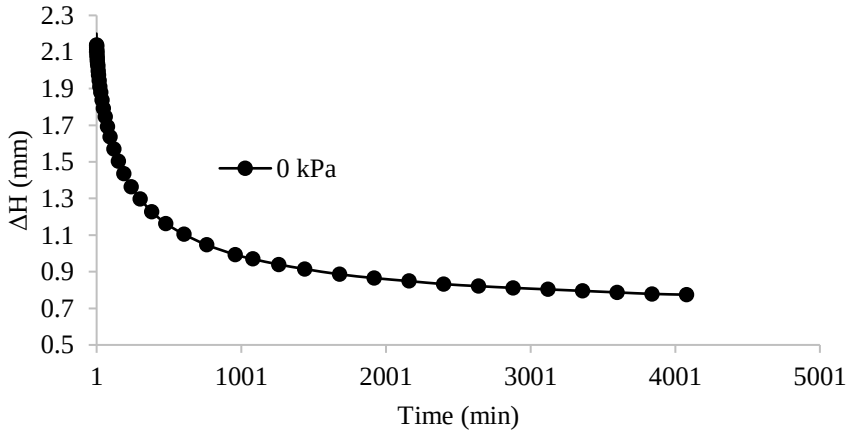


Figure A.89. ΔH versus time at 0 kPa (unloading) for 2% CBAS treated specimen at 28% initial water content

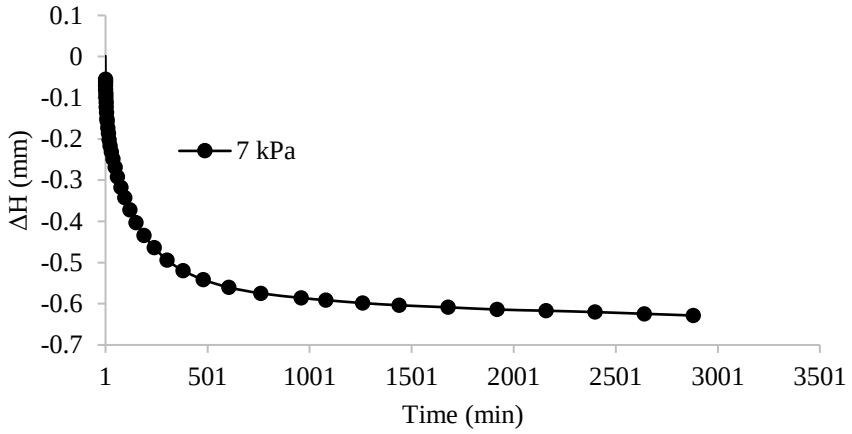


Figure A.90. ΔH versus time prior to compressibility test for 2% CBAS treated specimen at 22.5% initial water content

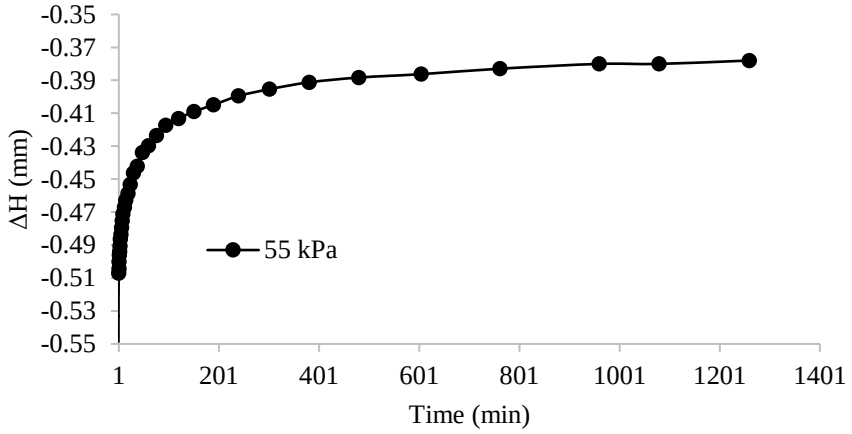


Figure A.91. ΔH versus time at 55 kPa (loading) for 2% CBAS treated specimen at 22.5% initial water content

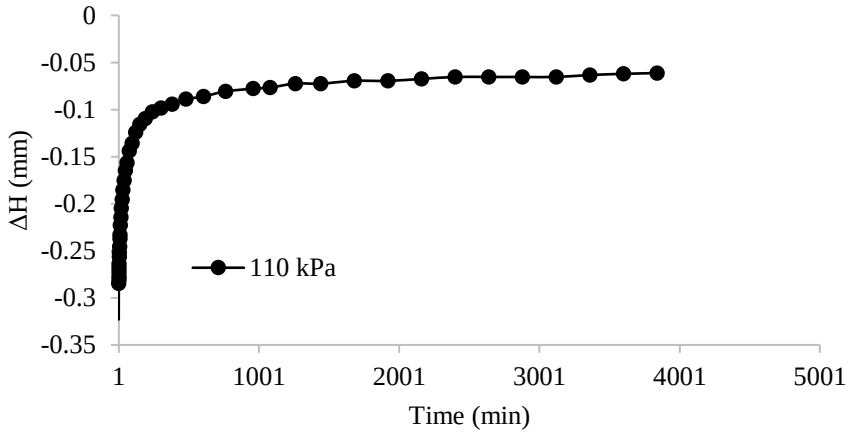


Figure A.92. ΔH versus time at 110 kPa (loading) for 2% CBAS treated specimen at 22.5% initial water content

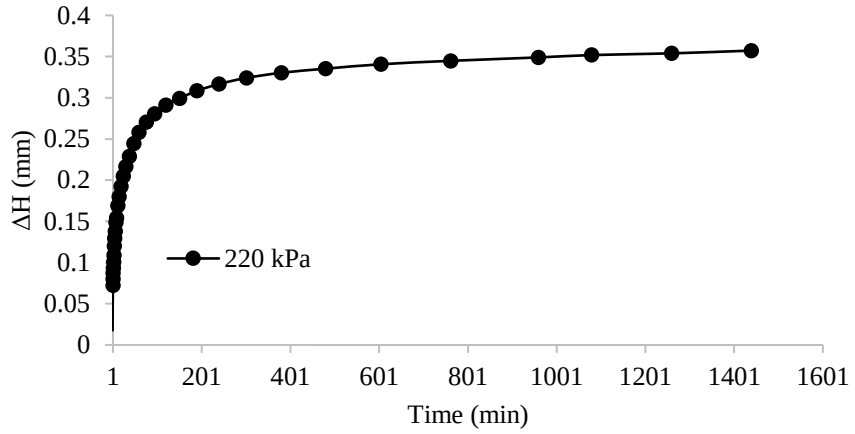


Figure A.93. ΔH versus time at 220 kPa (loading) for 2% CBAS treated specimen at 22.5% initial water content

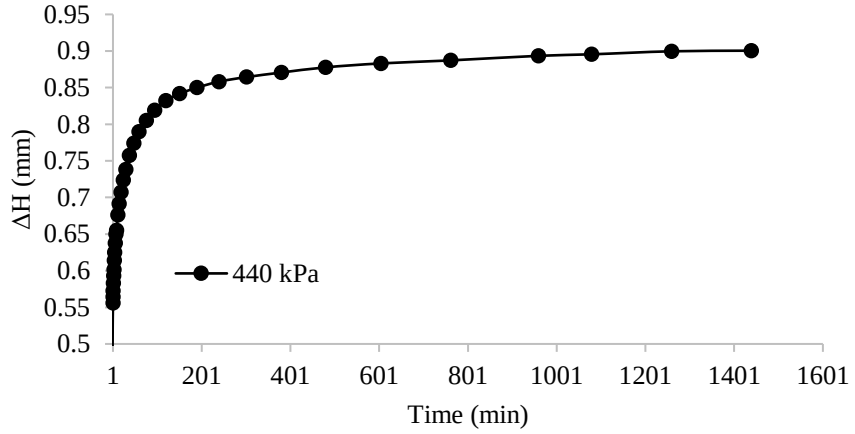


Figure A.94. ΔH versus time at 440 kPa (loading) for 2% CBAS treated specimen at 22.5% initial water content

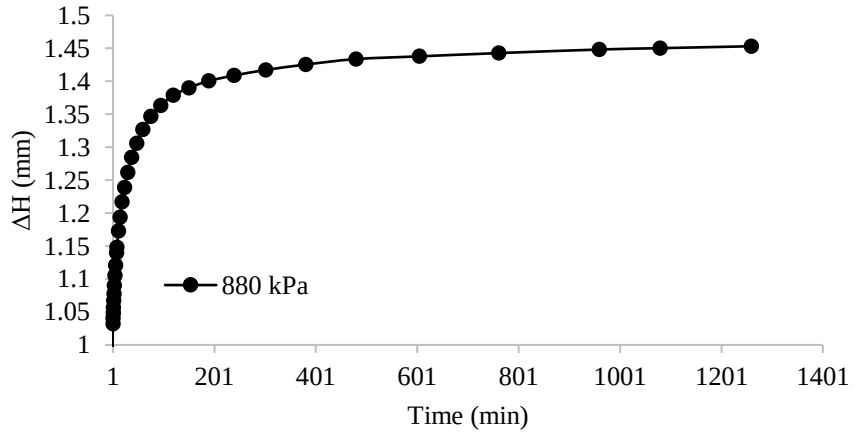


Figure A.95. ΔH versus time at 880 kPa (loading) for 2% CBAS treated specimen at 22.5% initial water content

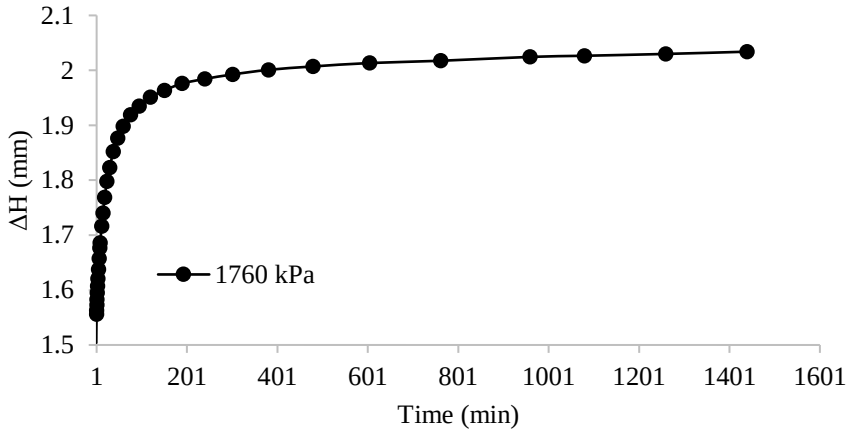


Figure A.96. ΔH versus time at 1760 kPa (loading) for 2% CBAS treated specimen at 22.5% initial water content

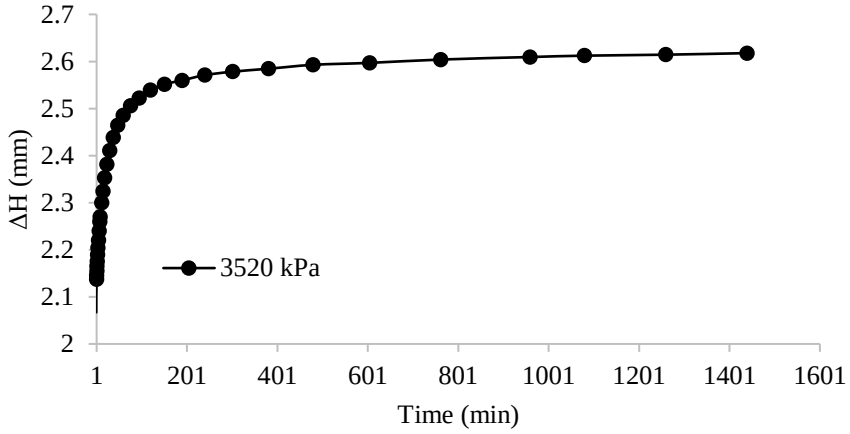


Figure A.97. ΔH versus time at 3520 kPa (loading) for 2% CBAS treated specimen at 22.5% initial water content

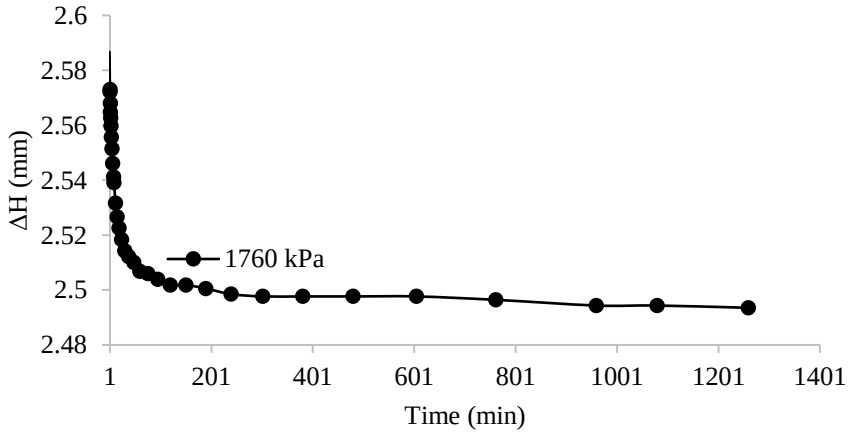


Figure A.98. ΔH versus time at 1760 kPa (unloading) for 2% CBAS treated specimen at 22.5% initial water content

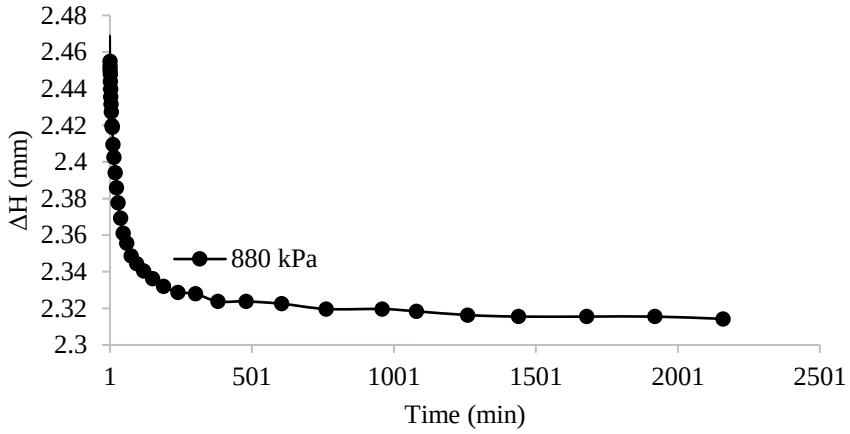


Figure A.99. ΔH versus time at 880 kPa (unloading) for 2% CBAS treated specimen at 22.5% initial water content

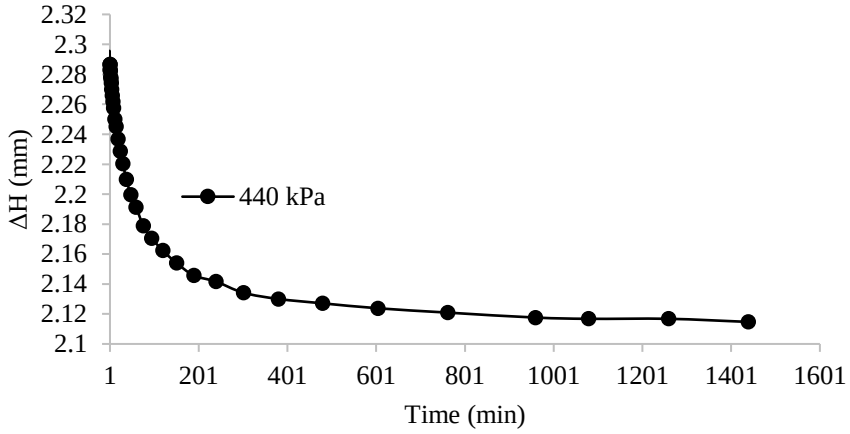


Figure A.100. ΔH versus time at 440 kPa (unloading) for 2% CBAS treated specimen at 22.5% initial water content

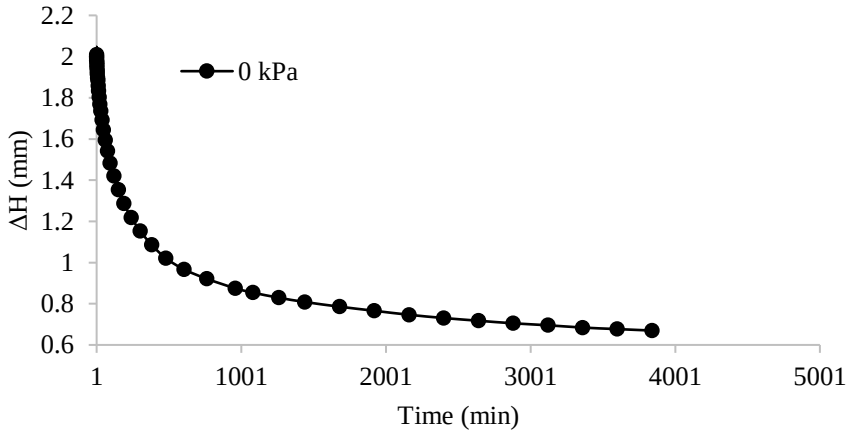


Figure A.101. ΔH versus time at 0 kPa (unloading) for 2% CBAS treated specimen at 22.5% initial water content

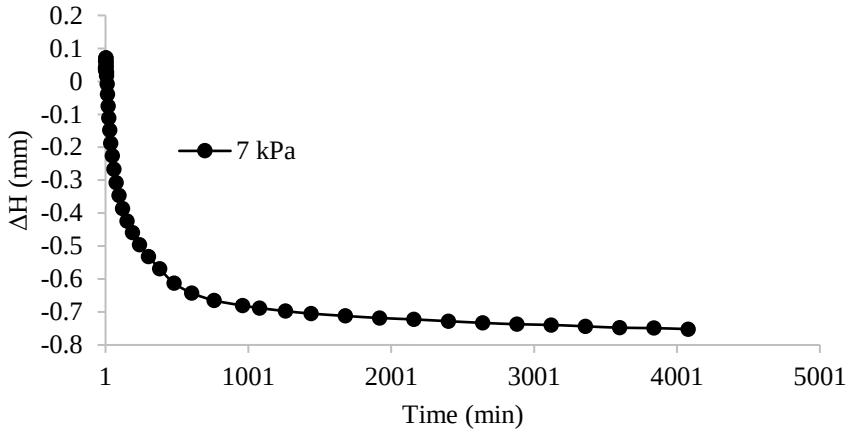


Figure A.102. ΔH versus time prior to compressibility test for 2% CBAS treated specimen at 16% initial water content

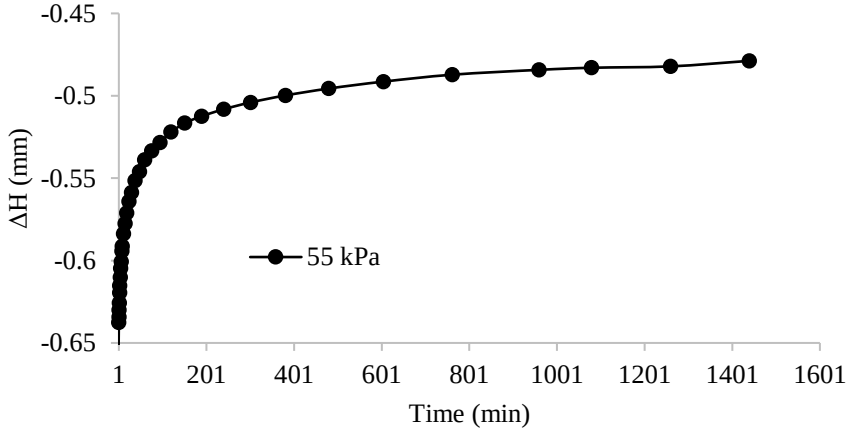


Figure A.103. ΔH versus time at 55 kPa (loading) for 2% CBAS treated specimen at 16% initial water content

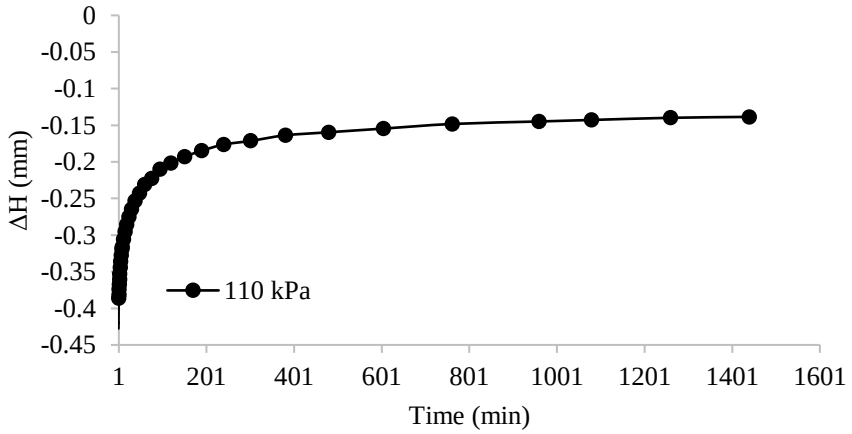


Figure A.104. ΔH versus time at 110 kPa (loading) for 2% CBAS treated specimen at 16% initial water content

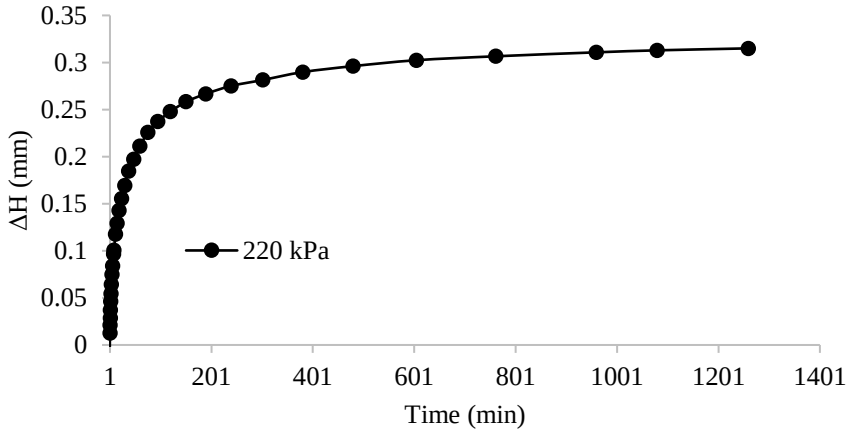


Figure A.105. ΔH versus time at 220 kPa (loading) for 2% CBAS treated specimen at 16% initial water content

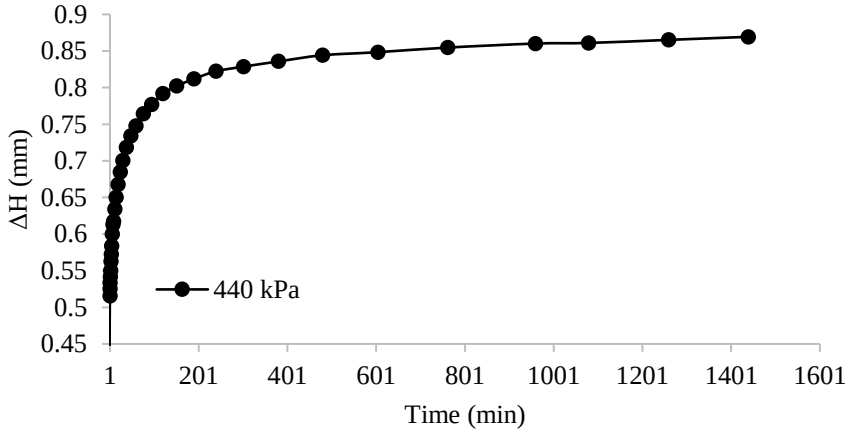


Figure A.106. ΔH versus time at 440 kPa (loading) for 2% CBAS treated specimen at 16% initial water content

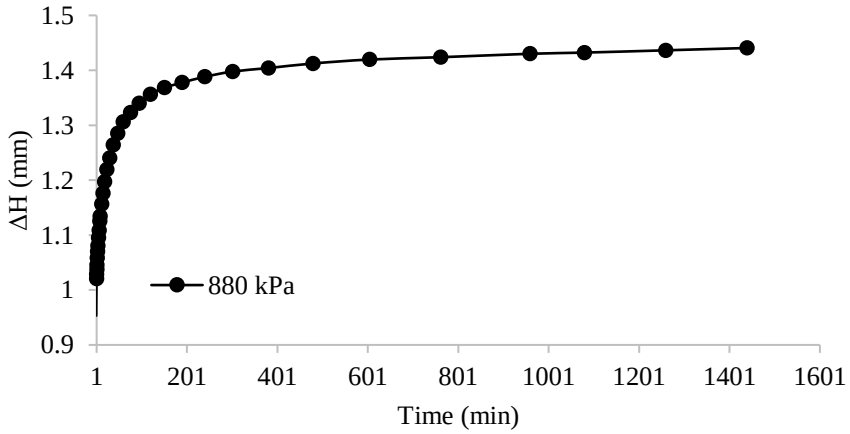


Figure A.107. ΔH versus time at 880 kPa (loading) for 2% CBAS treated specimen at 16% initial water content

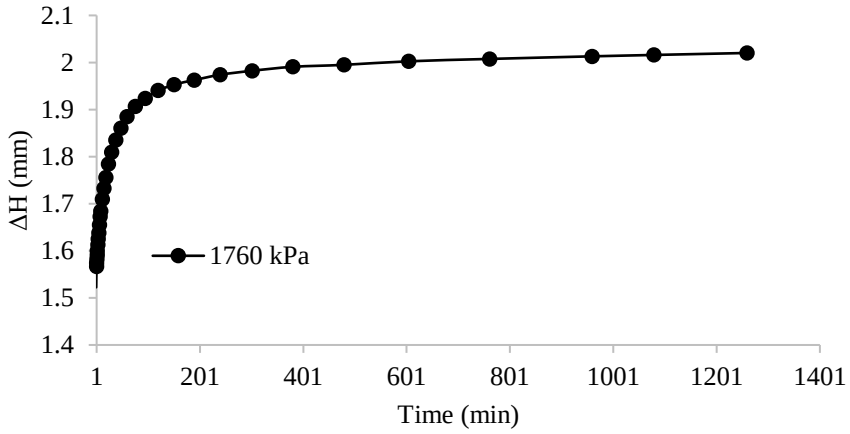


Figure A.108. ΔH versus time at 1760 kPa (loading) for 2% CBAS treated specimen at 16% initial water content

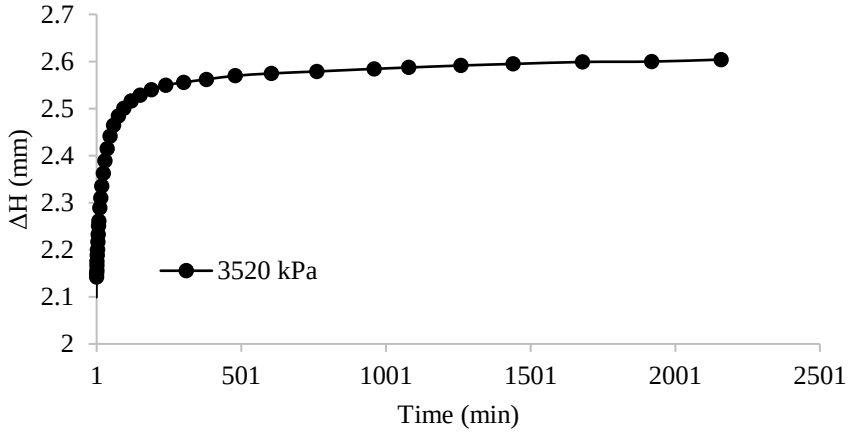


Figure A.109. ΔH versus time at 3520 kPa (loading) for 2% CBAS treated specimen at 16% initial water content

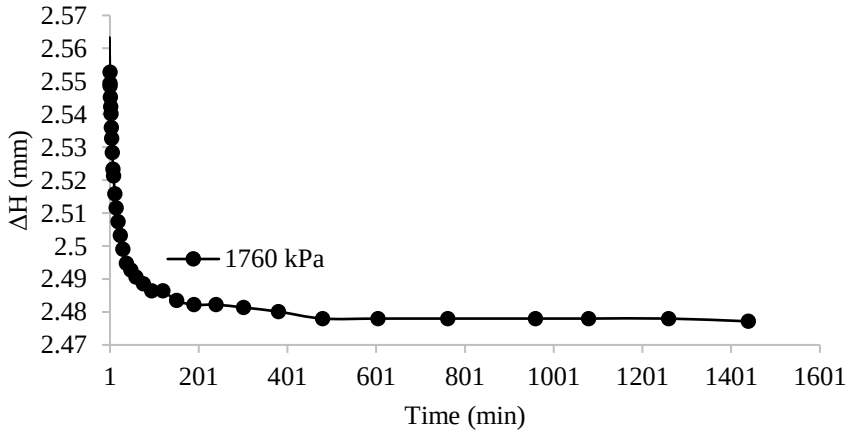


Figure A.110. ΔH versus time at 1760 kPa (unloading) for 2% CBAS treated specimen at 16% initial water content

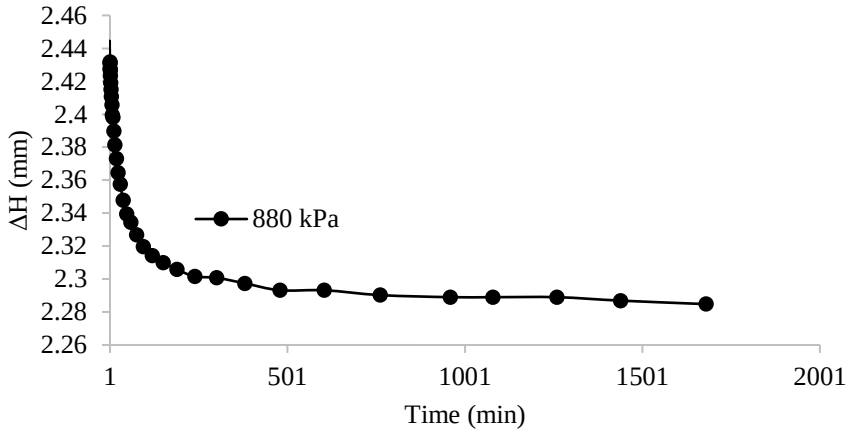


Figure A.111. ΔH versus time at 880 kPa (unloading) for 2% CBAS treated specimen at 16% initial water content

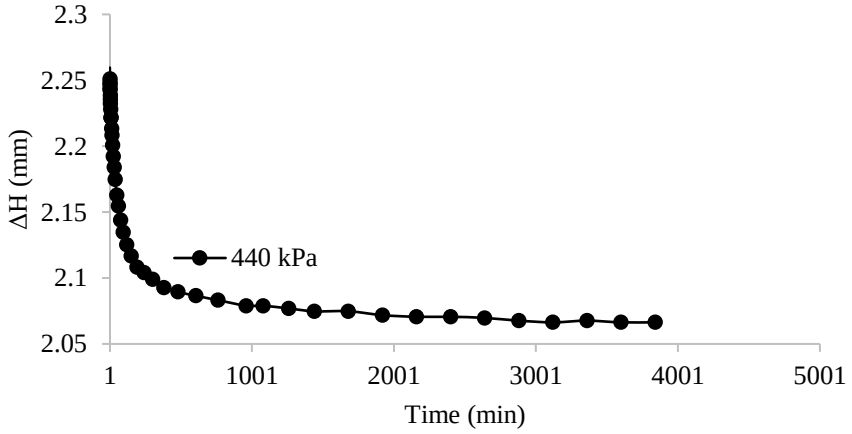


Figure A.112. ΔH versus time at 440 kPa (unloading) for 2% CBAS treated specimen at 16% initial water content

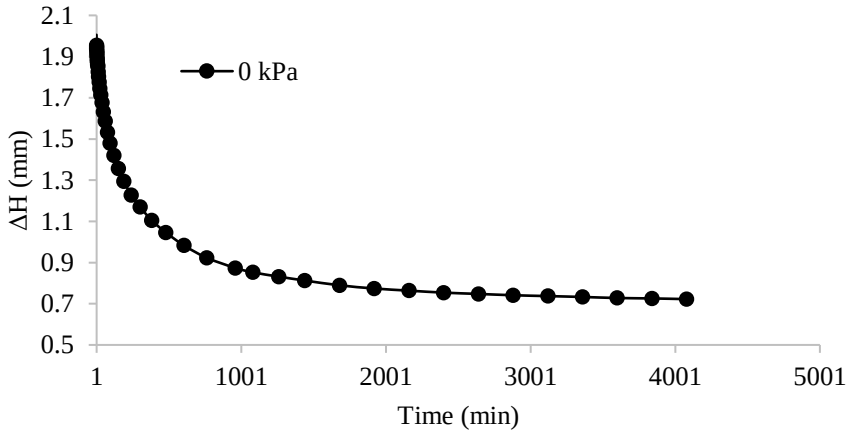


Figure A.113. ΔH versus time at 0 kPa (unloading) for 2% CBAS treated specimen at 16% initial water content

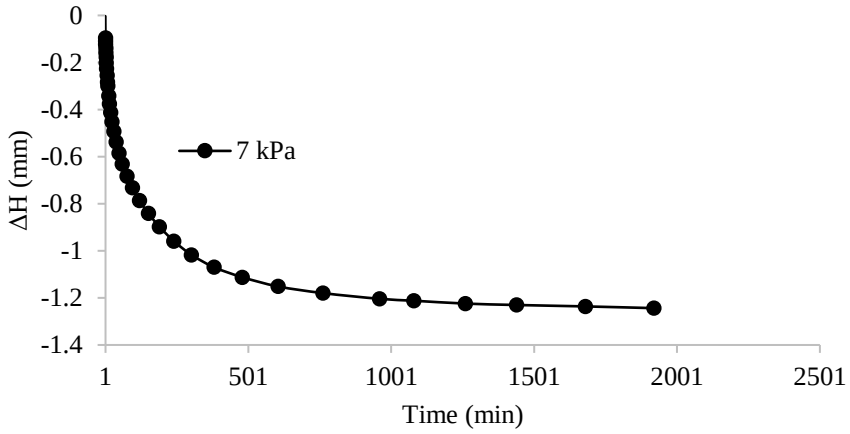


Figure A.114. ΔH versus time prior to compressibility test for 2% CBAS treated specimen at 11% initial water content

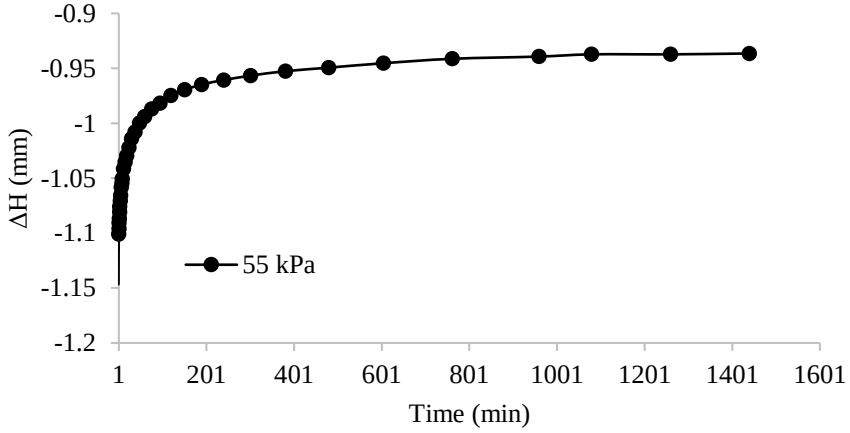


Figure A.115. ΔH versus time at 55 kPa (loading) for 2% CBAS treated specimen at 11% initial water content

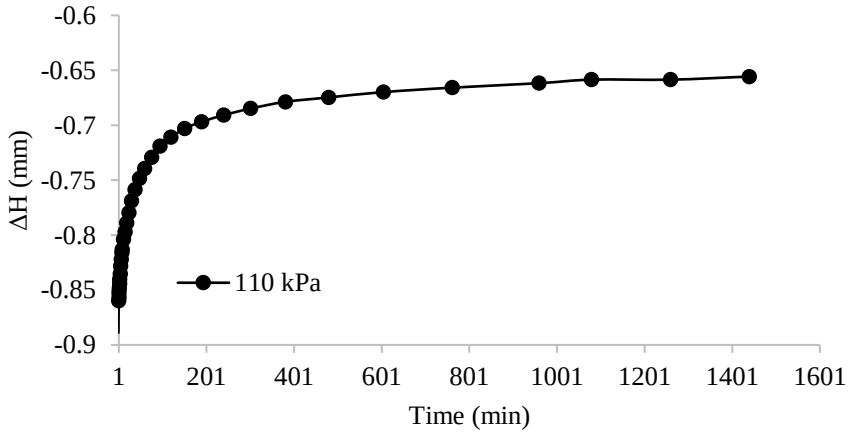


Figure A.116. ΔH versus time at 110 kPa (loading) for 2% CBAS treated specimen at 11% initial water content

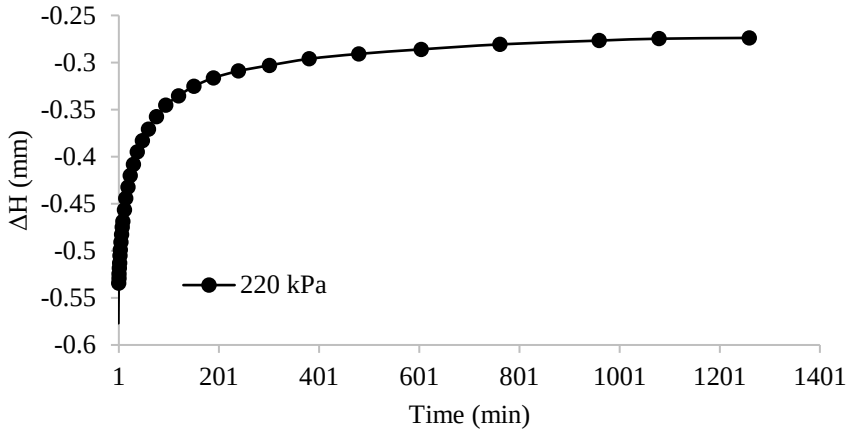


Figure A.117. ΔH versus time at 220 kPa (loading) for 2% CBAS treated specimen at 11% initial water content

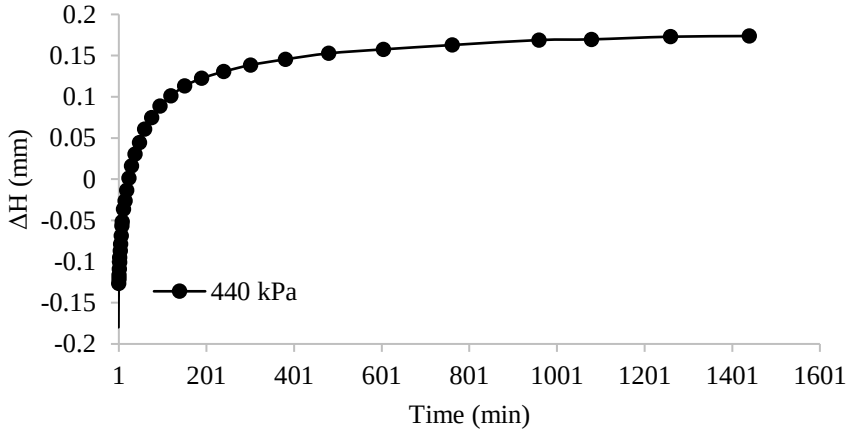


Figure A.118. ΔH versus time at 440 kPa (loading) for 2% CBAS treated specimen at 11% initial water content

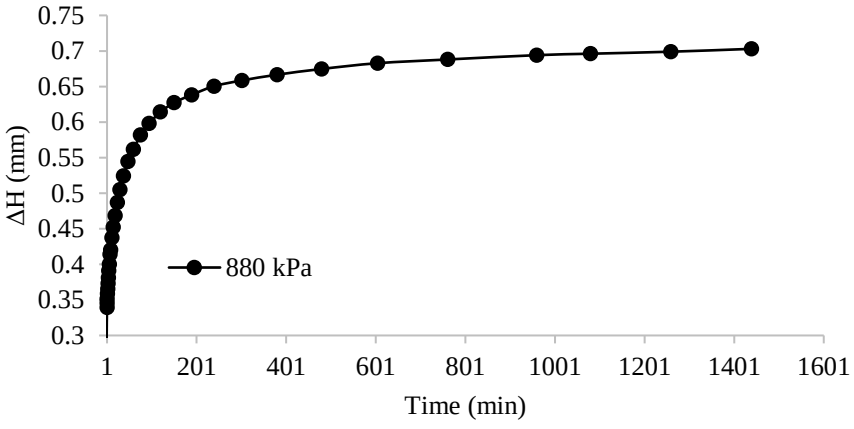


Figure A.119. ΔH versus time at 880 kPa (loading) for 2% CBAS treated specimen at 11% initial water content

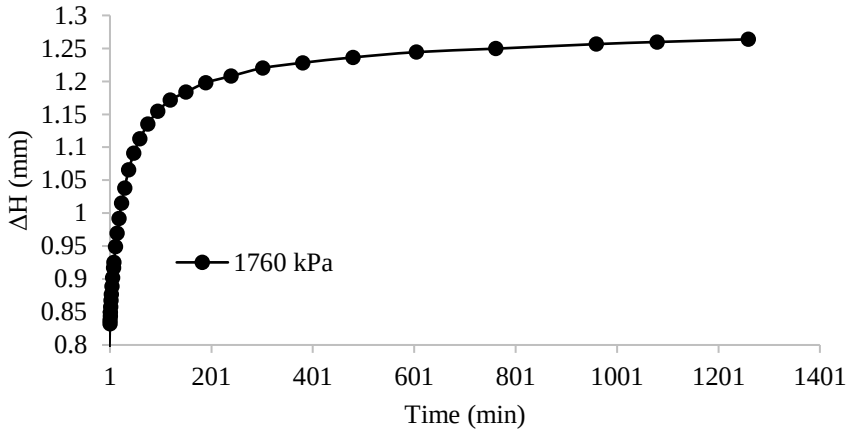


Figure A.120. ΔH versus time at 1760 kPa (loading) for 2% CBAS treated specimen at 11% initial water content

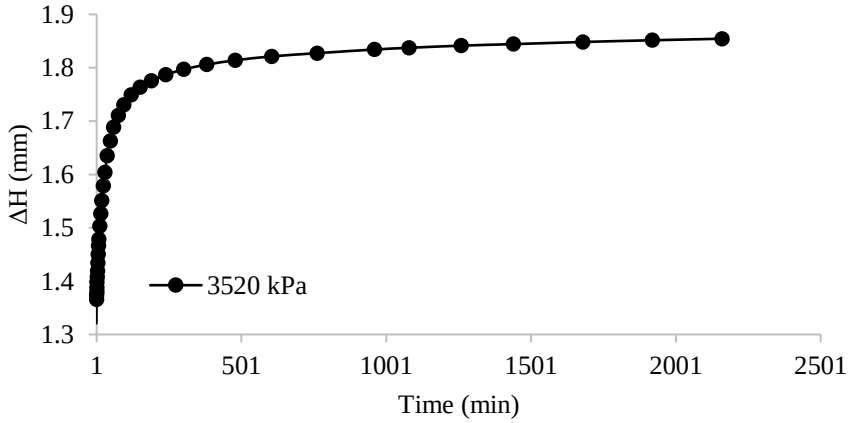


Figure A.121. ΔH versus time at 3520 kPa (loading) for 2% CBAS treated specimen at 11% initial water content

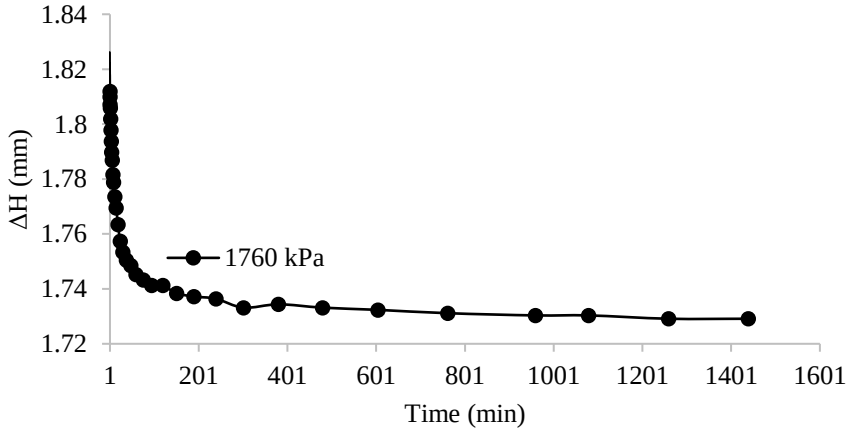


Figure A.122. ΔH versus time at 1760 kPa (unloading) for 2% CBAS treated specimen at 11% initial water content

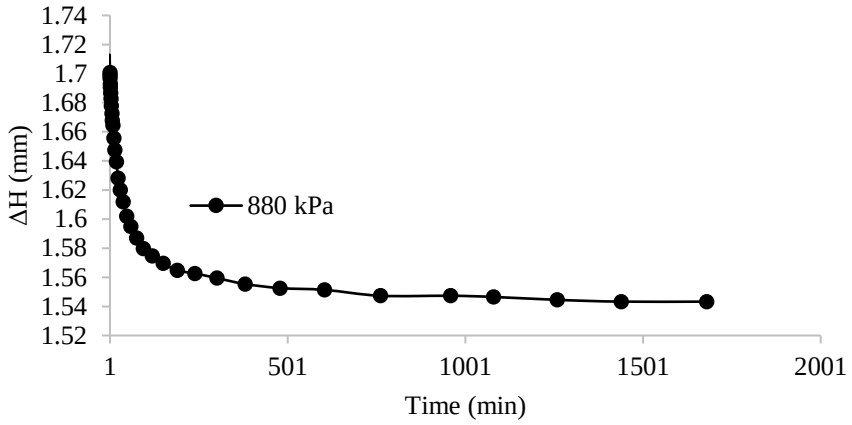


Figure A.123. ΔH versus time at 880 kPa (unloading) for 2% CBAS treated specimen at 11% initial water content

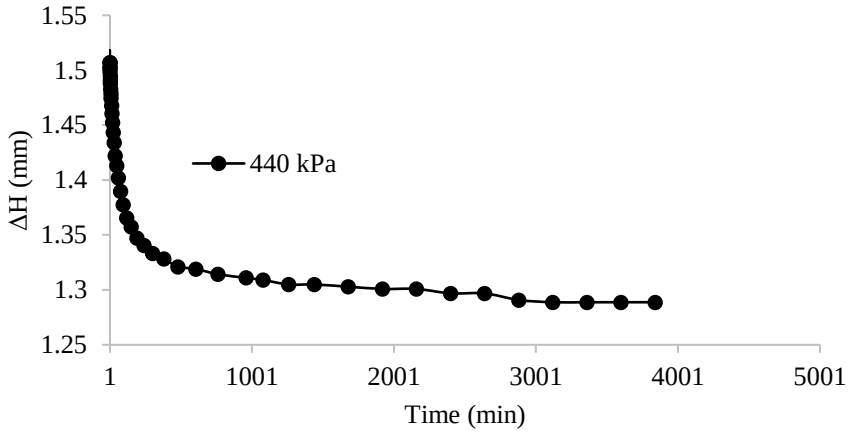


Figure A.124. ΔH versus time at 440 kPa (unloading) for 2% CBAS treated specimen at 11% initial water content

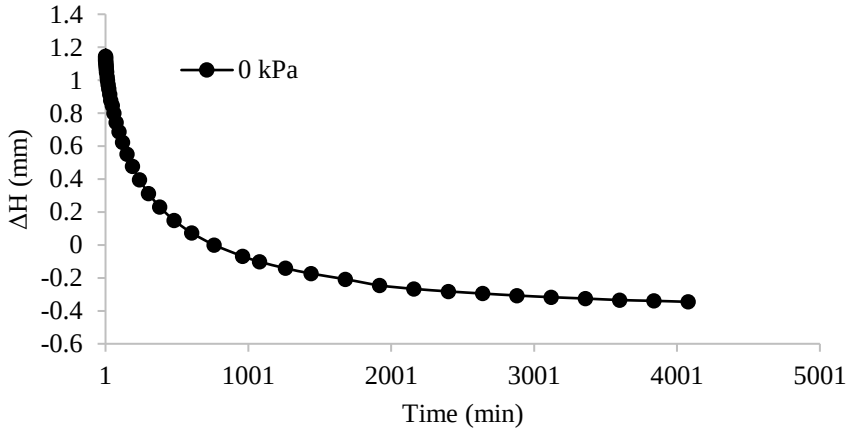


Figure A.125. ΔH versus time at 0 kPa (unloading) for 2% CBAS treated specimen at 11% initial water content

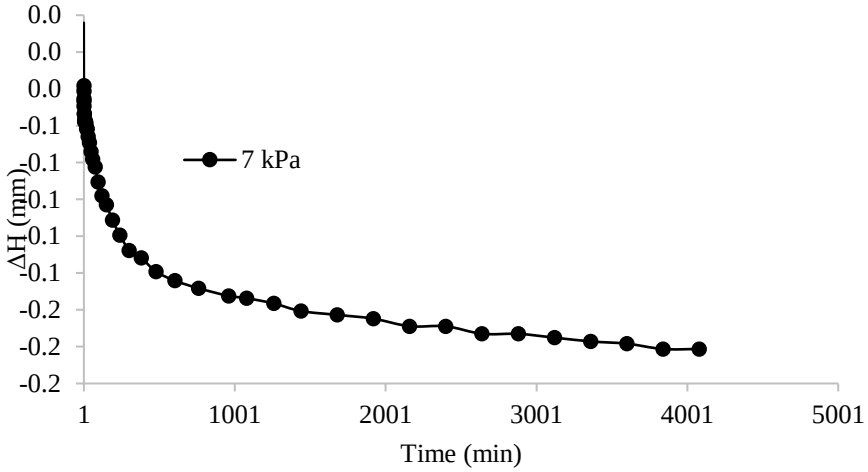


Figure A.126. ΔH versus time prior to compressibility test for 5% CBAS treated specimen at 28% initial water content

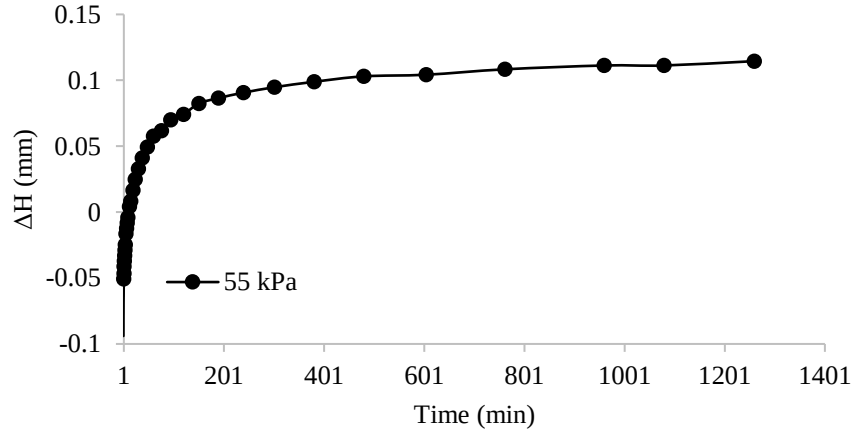


Figure A.127. ΔH versus time at 55 kPa (loading) for 5% CBAS treated specimen at 28% initial water content

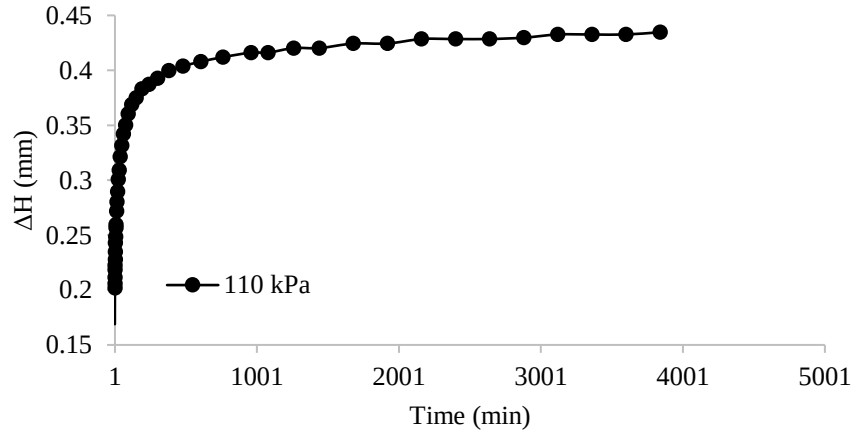


Figure A.128. ΔH versus time at 110 kPa (loading) for 5% CBAS treated specimen at 28% initial water content

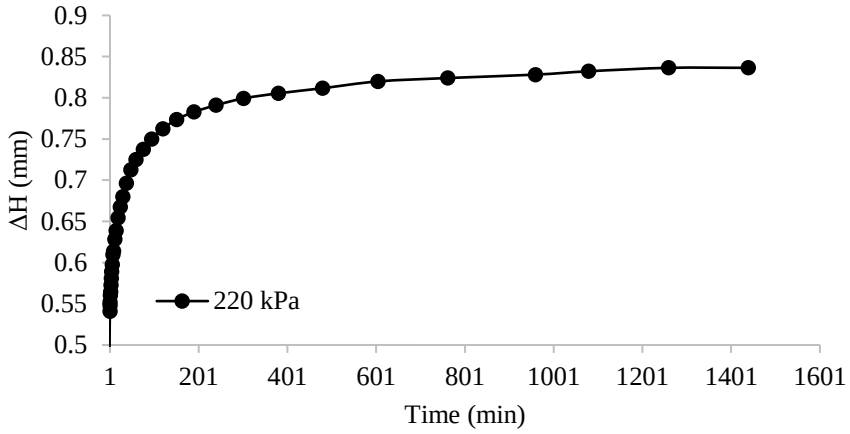


Figure A.129. ΔH versus time at 220 kPa (loading) for 5% CBAS treated specimen at 28% initial water content

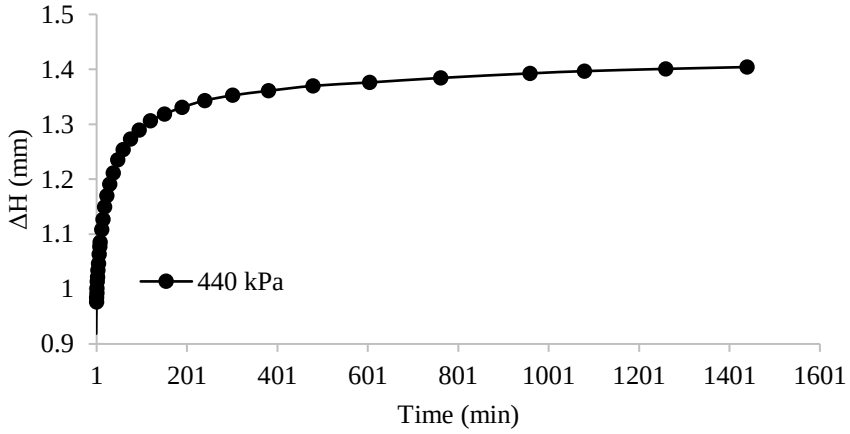


Figure A.130. ΔH versus time at 440 kPa (loading) for 5% CBAS treated specimen at 28% initial water content

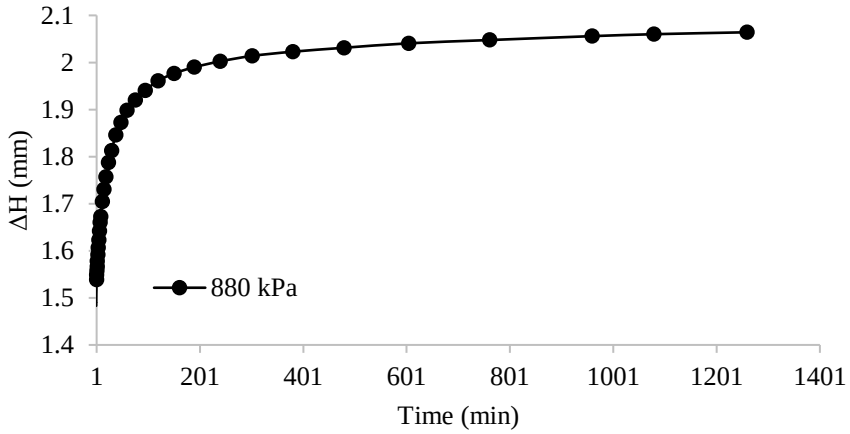


Figure A.131. ΔH versus time at 880 kPa (loading) for 5% CBAS treated specimen at 28% initial water content

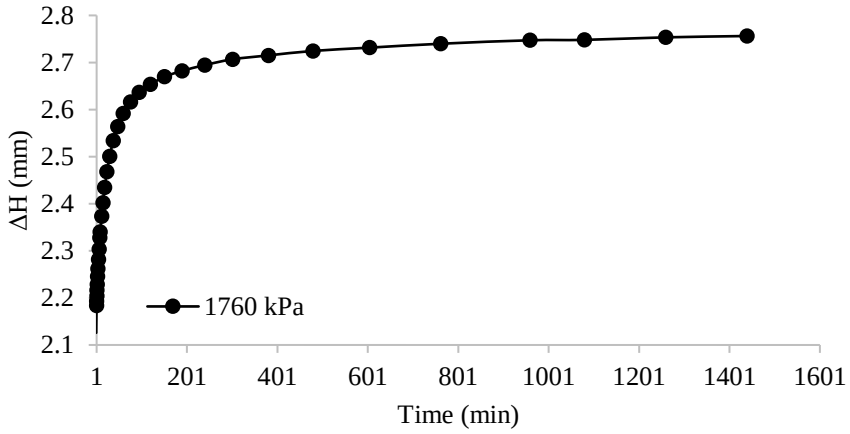


Figure A.132. ΔH versus time at 1760 kPa (loading) for 5% CBAS treated specimen at 28% initial water content

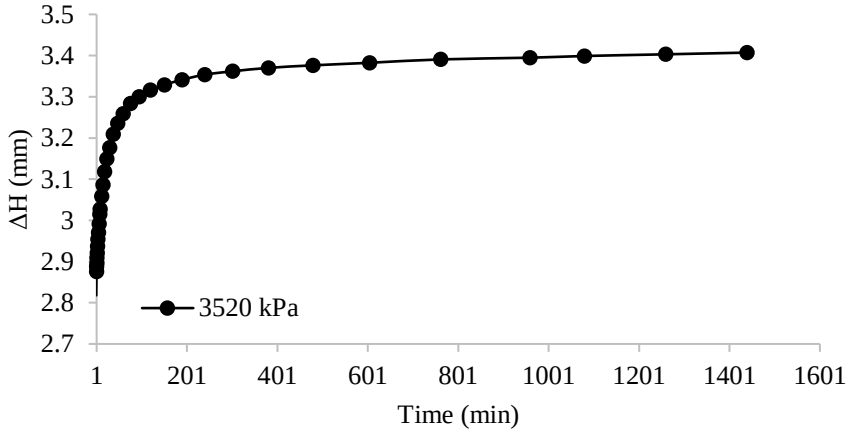


Figure A.133. ΔH versus time at 3520 kPa (loading) for 5% CBAS treated specimen at 28% initial water content

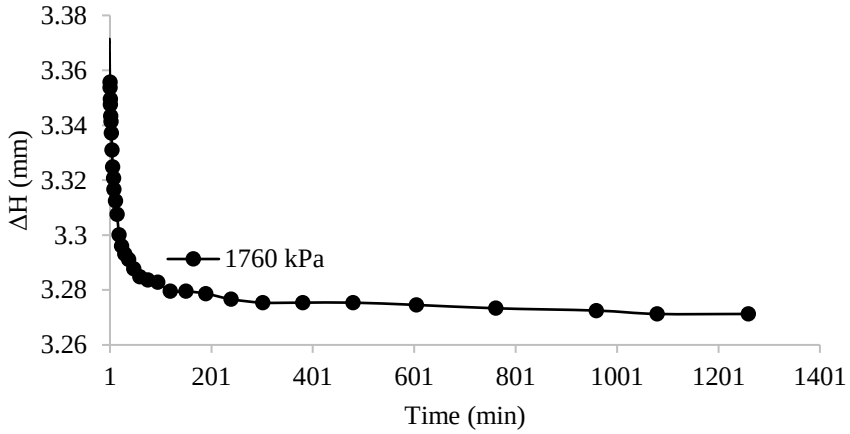


Figure A.134. ΔH versus time at 1760 kPa (unloading) for 5% CBAS treated specimen at 28% initial water content

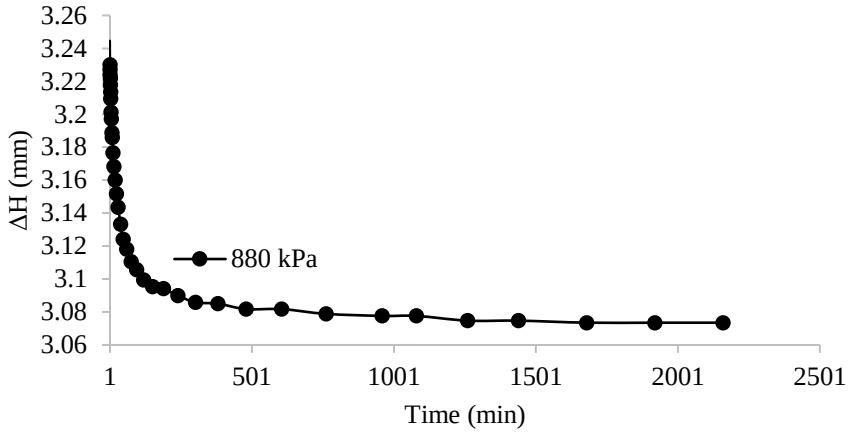


Figure A.135. ΔH versus time at 880 kPa (unloading) for 5% CBAS treated specimen at 28% initial water content

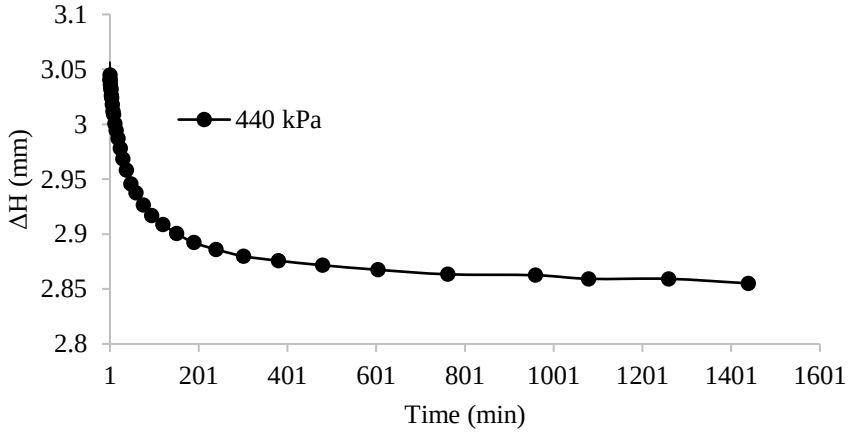


Figure A.136. ΔH versus time at 440 kPa (unloading) for 5% CBAS treated specimen at 28% initial water content

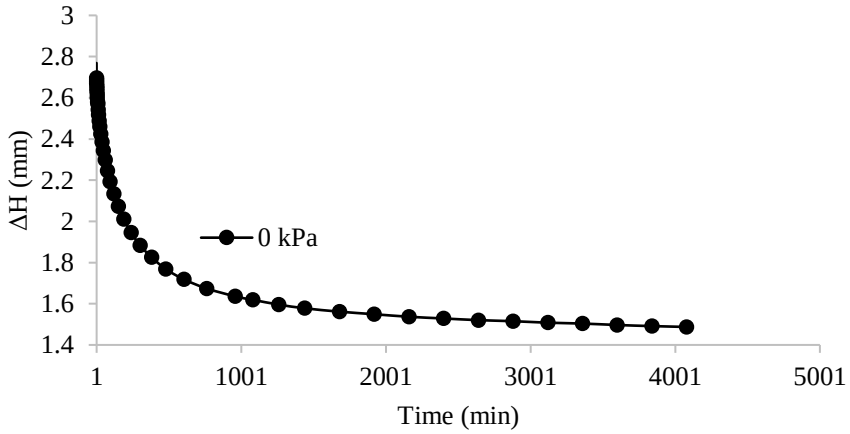


Figure A.137. ΔH versus time at 0 kPa (unloading) for 5% CBAS treated specimen at 28% initial water content

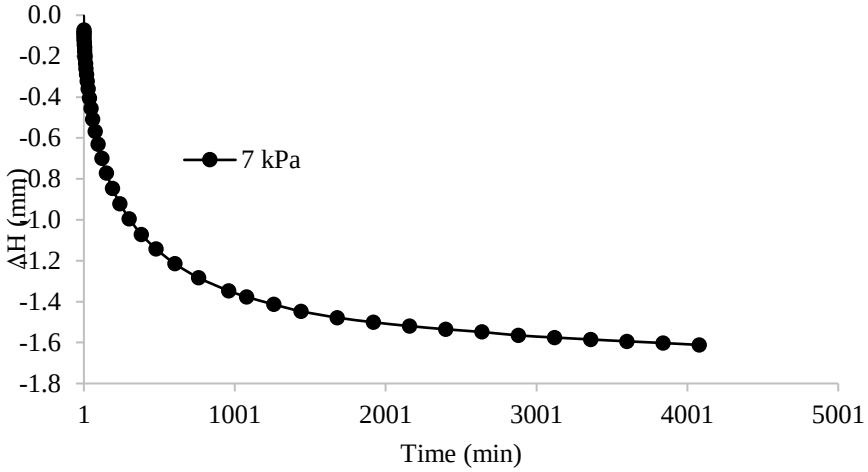


Figure A.138. ΔH versus time prior to compressibility test for 5% CBAS treated specimen at 22.5% initial water content

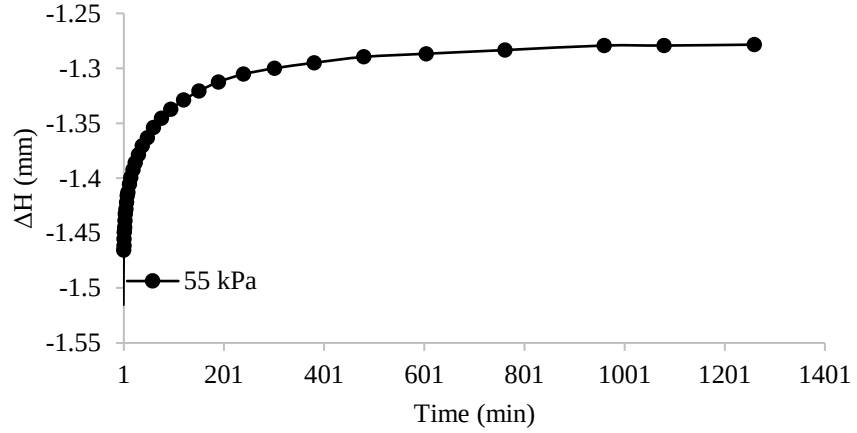


Figure A.139. ΔH versus time at 55 kPa (loading) for 5% CBAS treated specimen at 22.5% initial water content

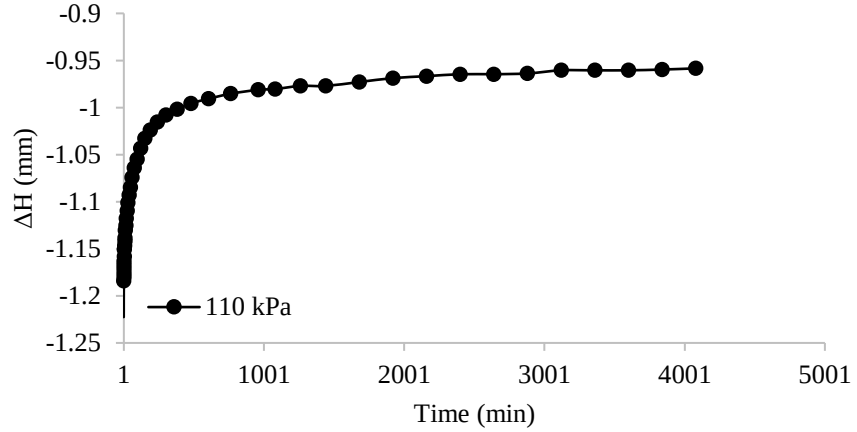


Figure A.140. ΔH versus time at 110 kPa (loading) for 5% CBAS treated specimen at 22.5% initial water content

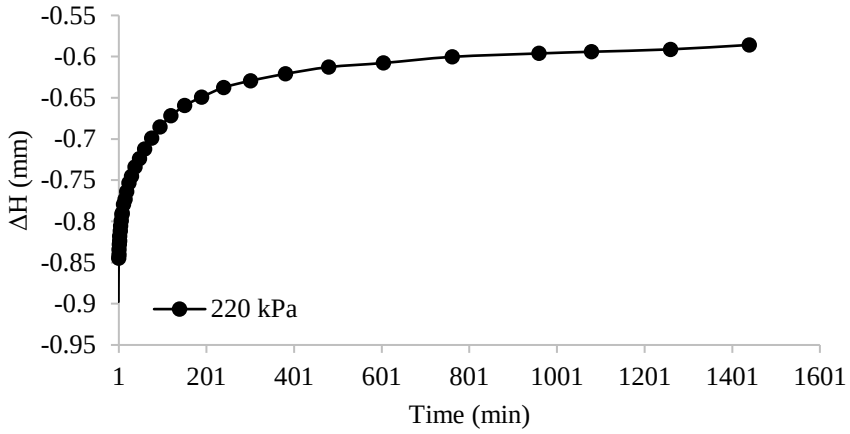


Figure A.141. ΔH versus time at 220 kPa (loading) for 5% CBAS treated specimen at 22.5% initial water content

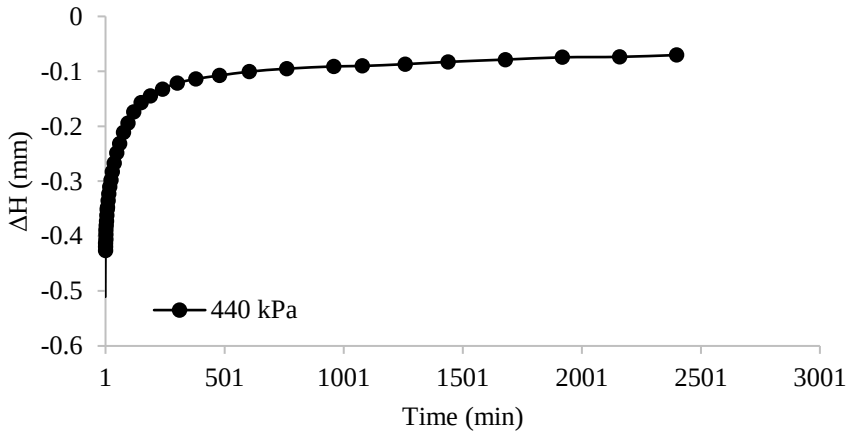


Figure A.142. ΔH versus time at 440 kPa (loading) for 5% CBAS treated specimen at 22.5% initial water content

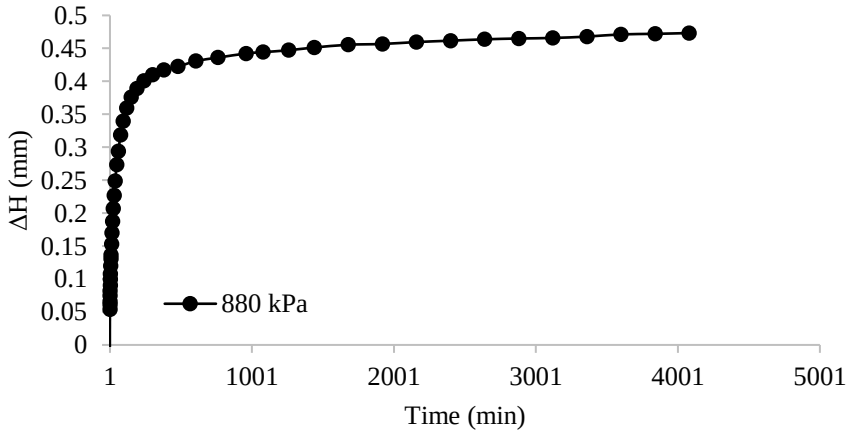


Figure A.143. ΔH versus time at 880 kPa (loading) for 5% CBAS treated specimen at 22.5% initial water content

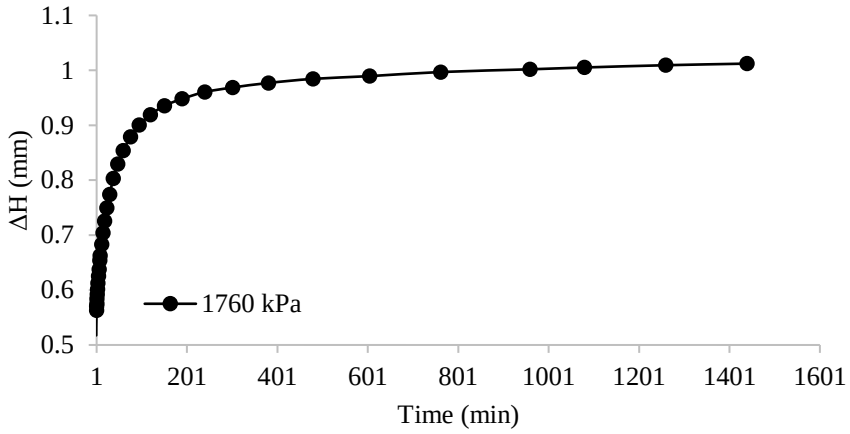


Figure A.144. ΔH versus time at 1760 kPa (loading) for 5% CBAS treated specimen at 22.5% initial water content

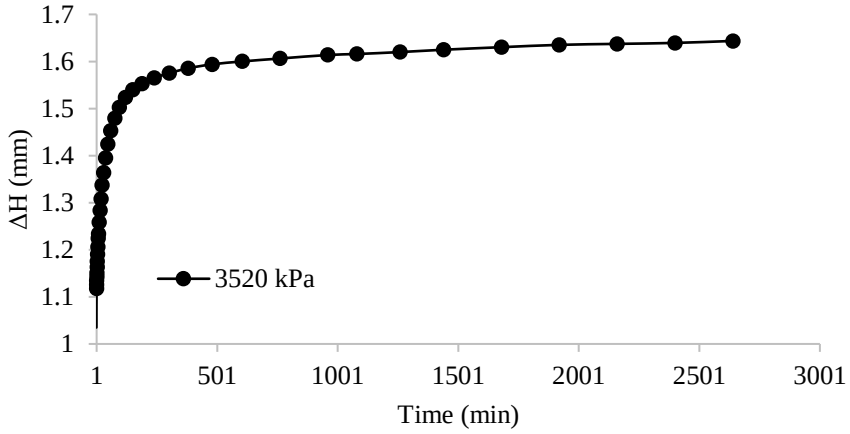


Figure A.145. ΔH versus time at 3520 kPa (loading) for 5% CBAS treated specimen at 22.5% initial water content

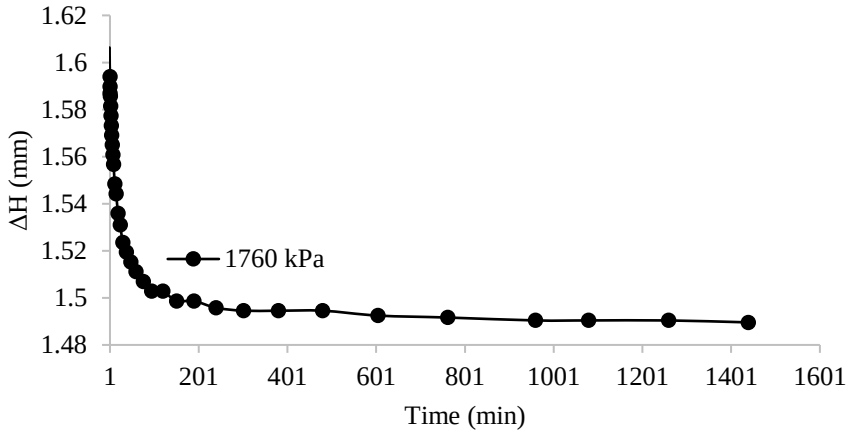


Figure A.146. ΔH versus time at 1760 kPa (unloading) for 5% CBAS treated specimen at 22.5% initial water content

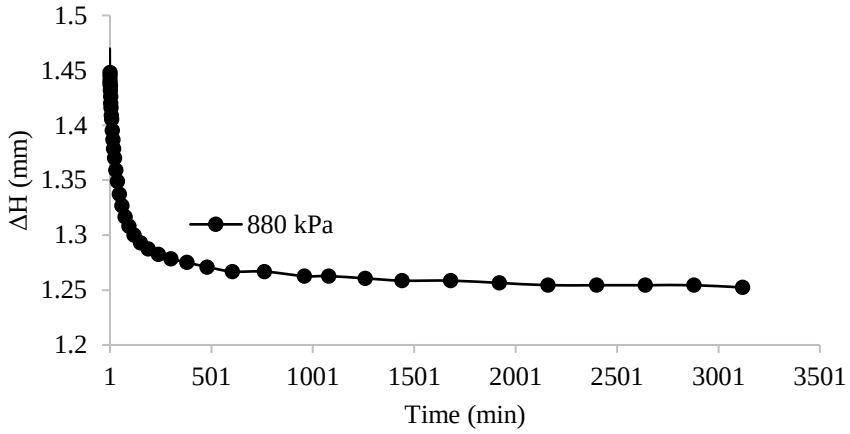


Figure A.147. ΔH versus time at 880 kPa (unloading) for 5% CBAS treated specimen at 22.5% initial water content

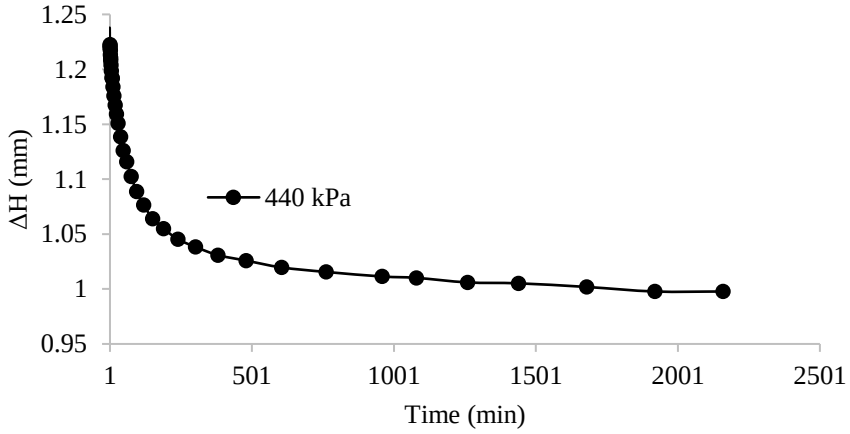


Figure A.148. ΔH versus time at 440 kPa (unloading) for 5% CBAS treated specimen at 22.5% initial water content

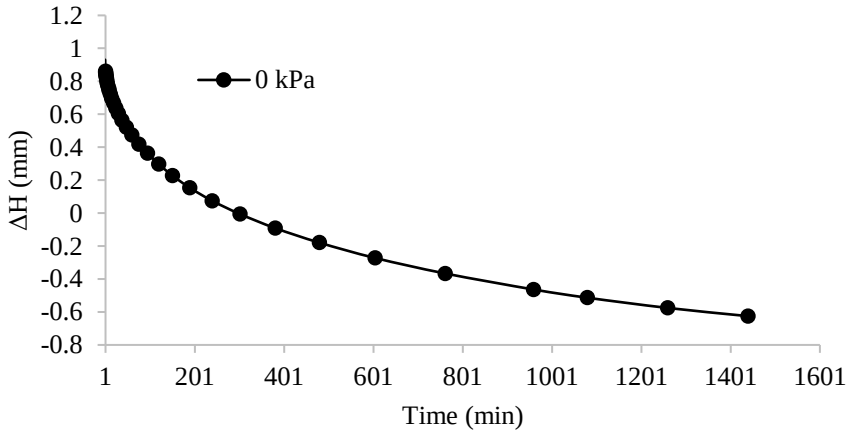


Figure A.149. ΔH versus time at 0 kPa (unloading) for 5% CBAS treated specimen at 22.5% initial water content

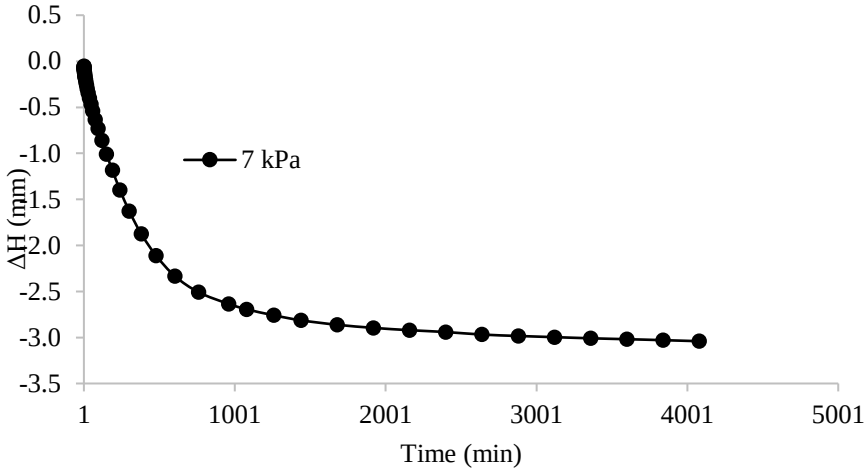


Figure A.150. ΔH versus time prior to compressibility test for 5% CBAS treated specimen at 16% initial water content

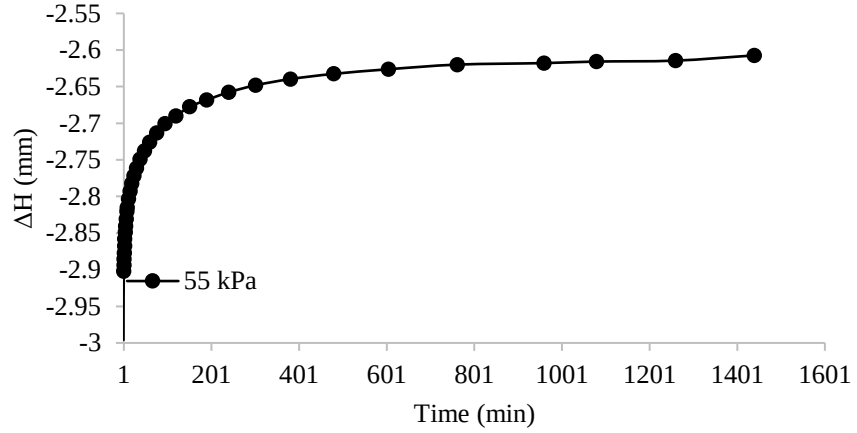


Figure A.151. ΔH versus time at 55 kPa (loading) for 5% CBAS treated specimen at 16% initial water content

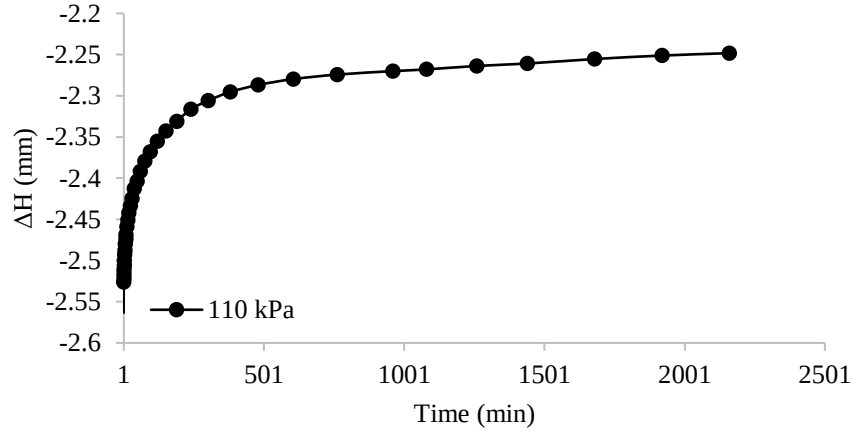


Figure A.152. ΔH versus time at 110 kPa (loading) for 5% CBAS treated specimen at 16% initial water content

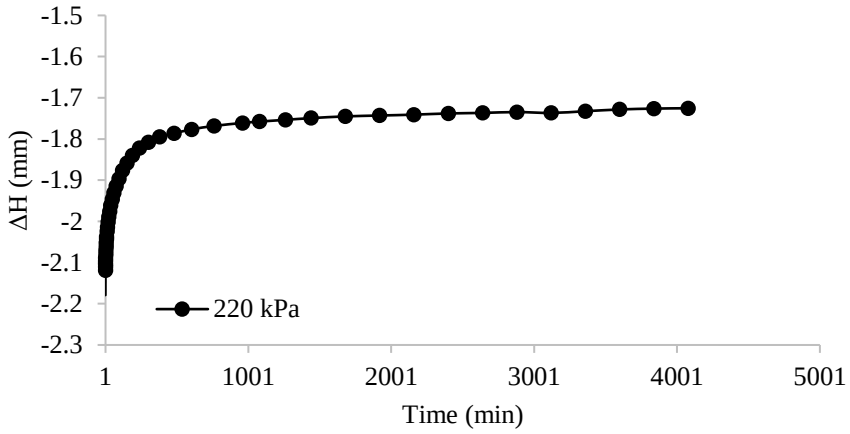


Figure A.153. ΔH versus time at 220 kPa (loading) for 5% CBAS treated specimen at 16% initial water content

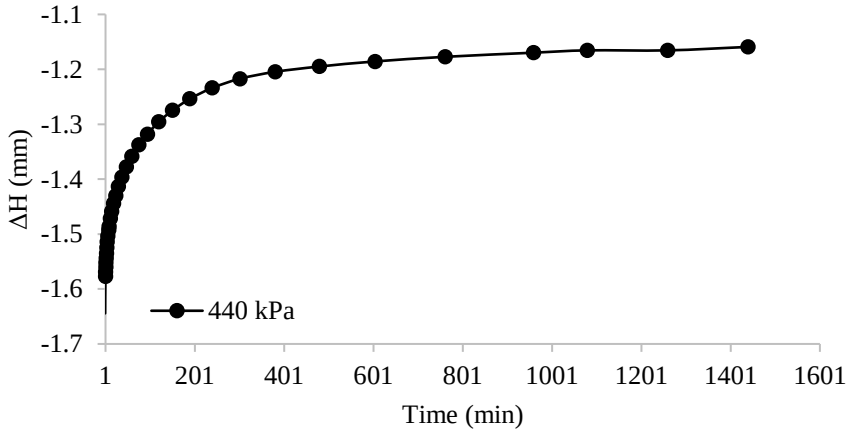


Figure A.154. ΔH versus time at 440 kPa (loading) for 5% CBAS treated specimen at 16% initial water content

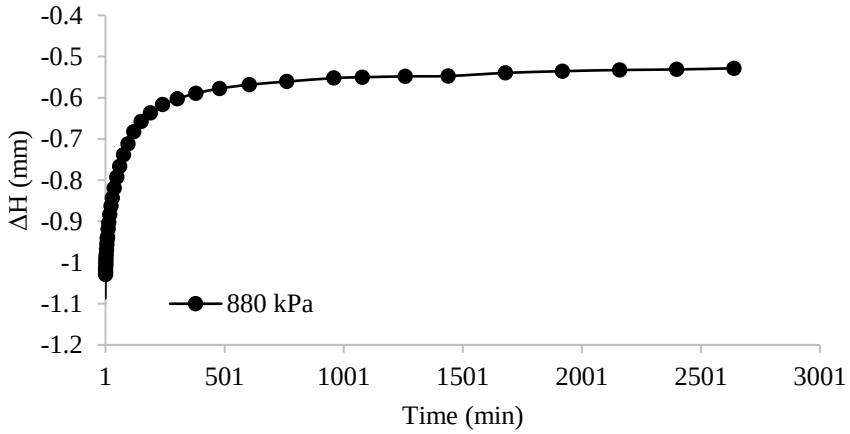


Figure A.155. ΔH versus time at 880 kPa (loading) for 5% CBAS treated specimen at 16% initial water content

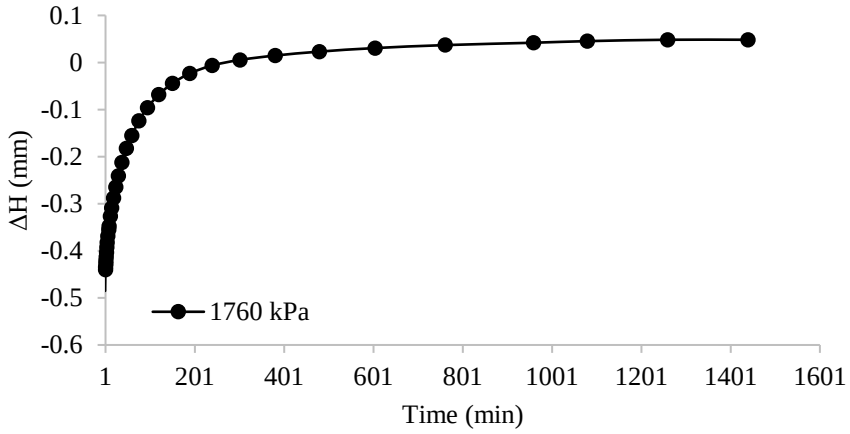


Figure A.156. ΔH versus time at 1760 kPa (loading) for 5% CBAS treated specimen at 16% initial water content

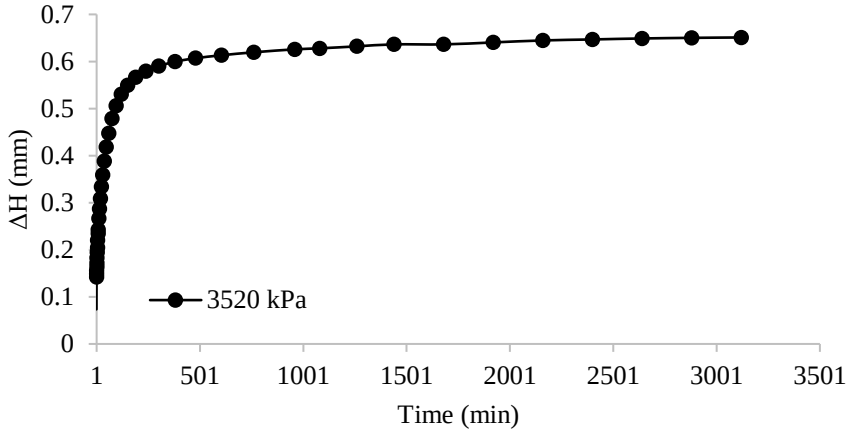


Figure A.157. ΔH versus time at 3520 kPa (loading) for 5% CBAS treated specimen at 16% initial water content

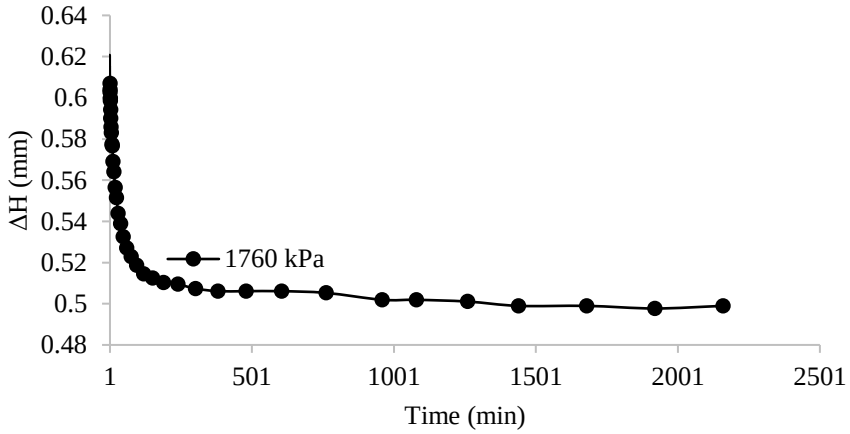


Figure A.158. ΔH versus time at 1760 kPa (unloading) for 5% CBAS treated specimen at 16% initial water content

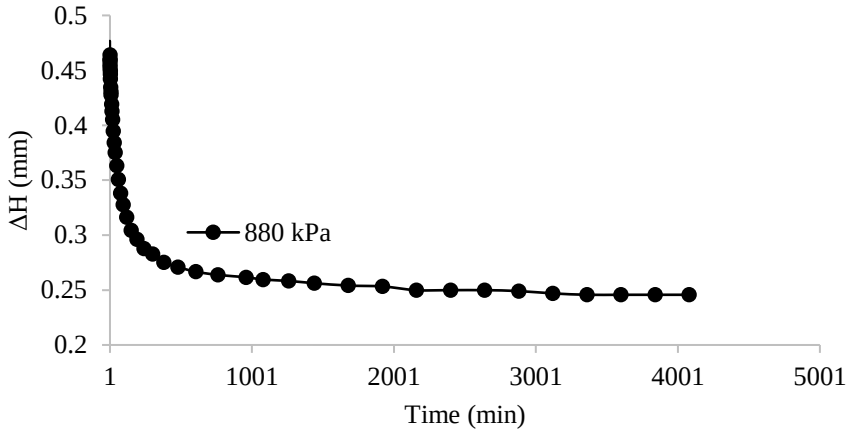


Figure A.159. ΔH versus time at 880 kPa (unloading) for 5% CBAS treated specimen at 16% initial water content

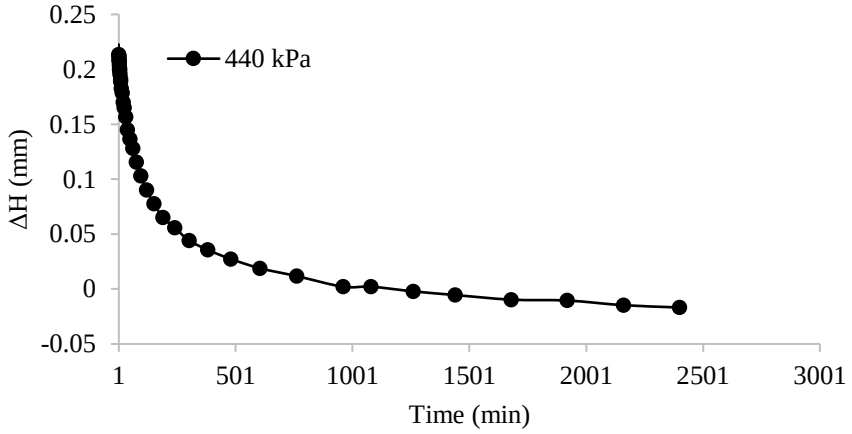


Figure A.160. ΔH versus time at 440 kPa (unloading) for 5% CBAS treated specimen at 16% initial water content

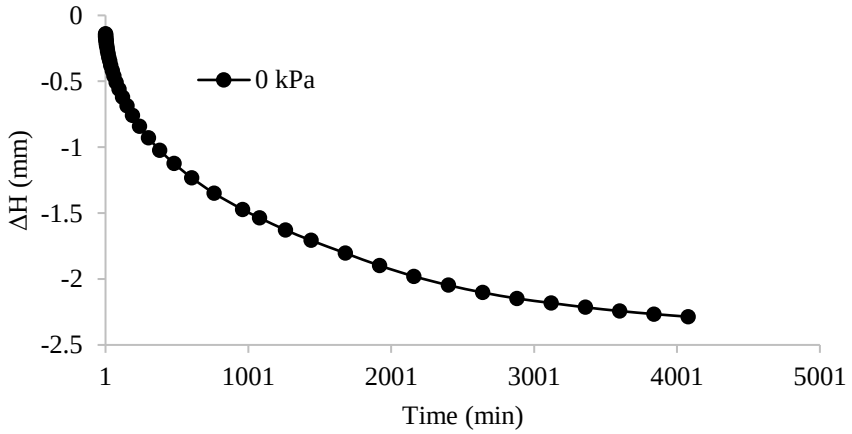


Figure A.161. ΔH versus time at 0 kPa (unloading) for 5% CBAS treated specimen at 16% initial water content

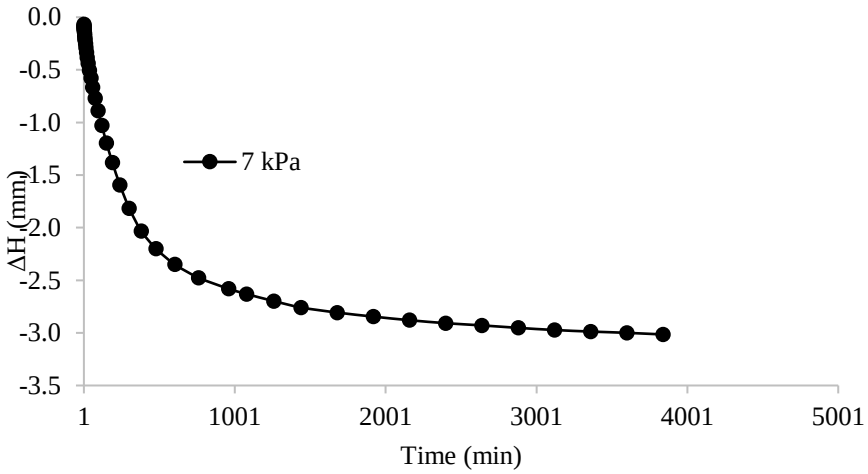


Figure A.162. ΔH versus time prior to compressibility test for 5% CBAS treated specimen at 11% initial water content

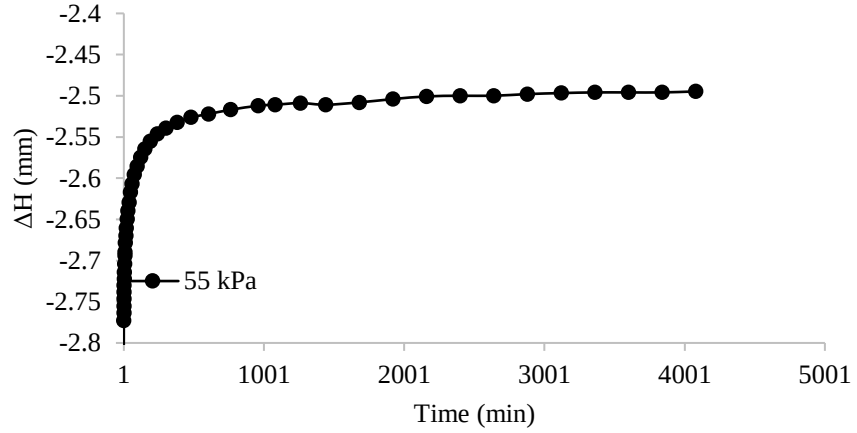


Figure A.163. ΔH versus time at 55 kPa (loading) for 5% CBAS treated specimen at 11% initial water content

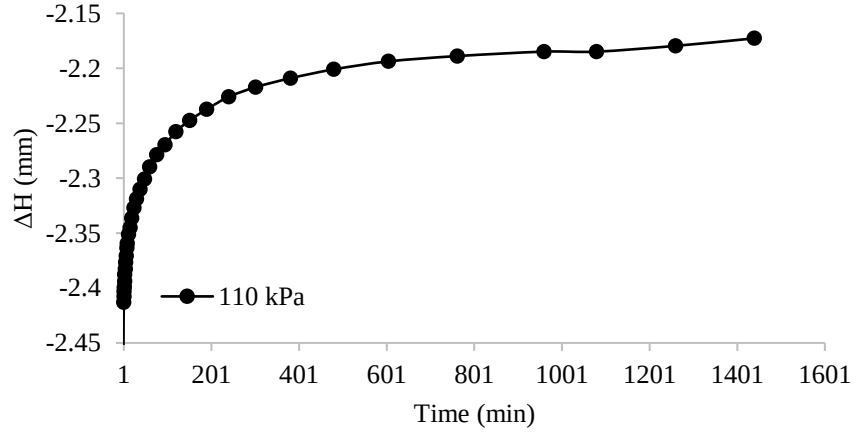


Figure A.164. ΔH versus time at 110 kPa (loading) for 5% CBAS treated specimen at 11% initial water content

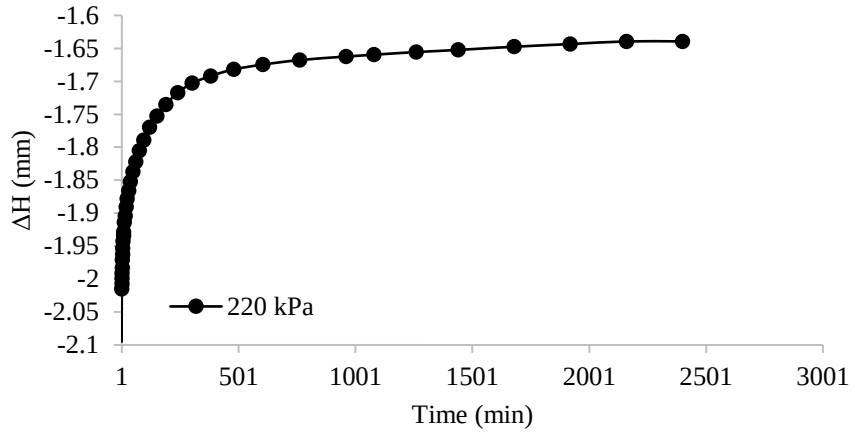


Figure A.165. ΔH versus time at 220 kPa (loading) for 5% CBAS treated specimen at 11% initial water content

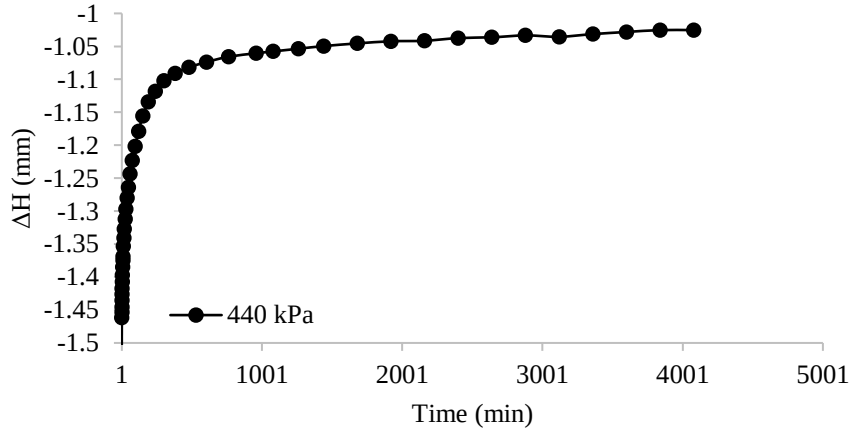


Figure A.166. ΔH versus time at 440 kPa (loading) for 5% CBAS treated specimen at 11% initial water content

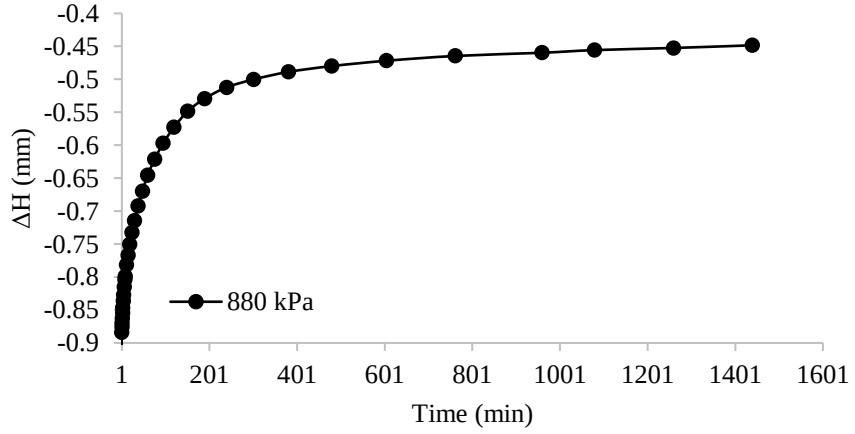


Figure A.167. ΔH versus time at 880 kPa (loading) for 5% CBAS treated specimen at 11% initial water content

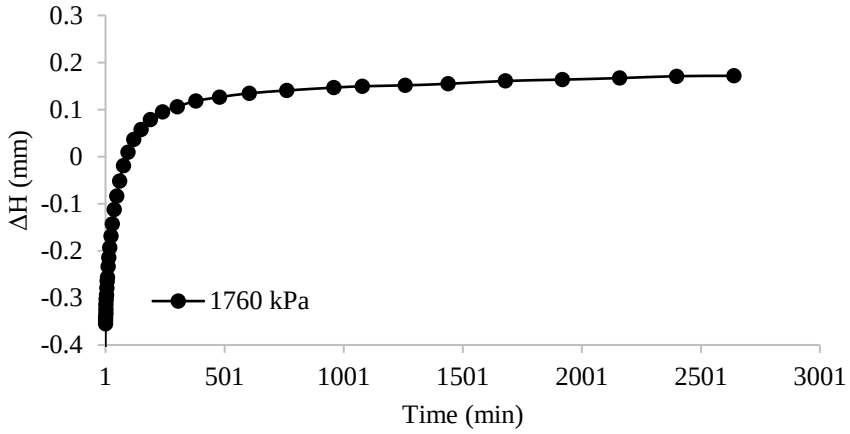


Figure A.168. ΔH versus time at 1760 kPa (loading) for 5% CBAS treated specimen at 11% initial water content

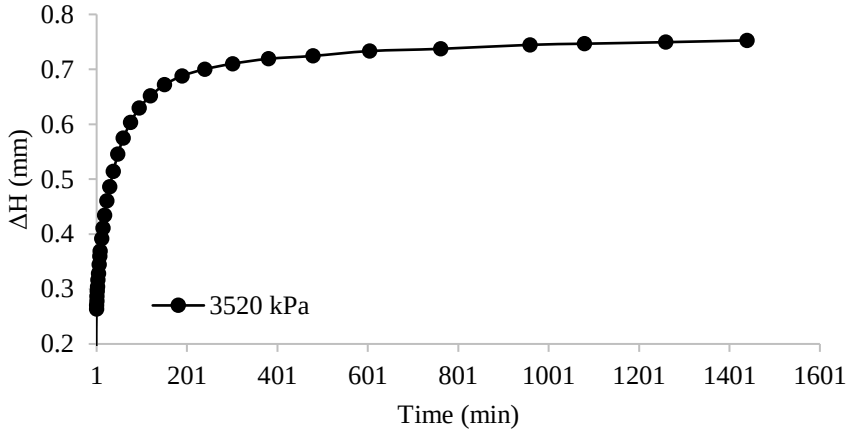


Figure A.169. ΔH versus time at 3520 kPa (loading) for 5% CBAS treated specimen at 11% initial water content

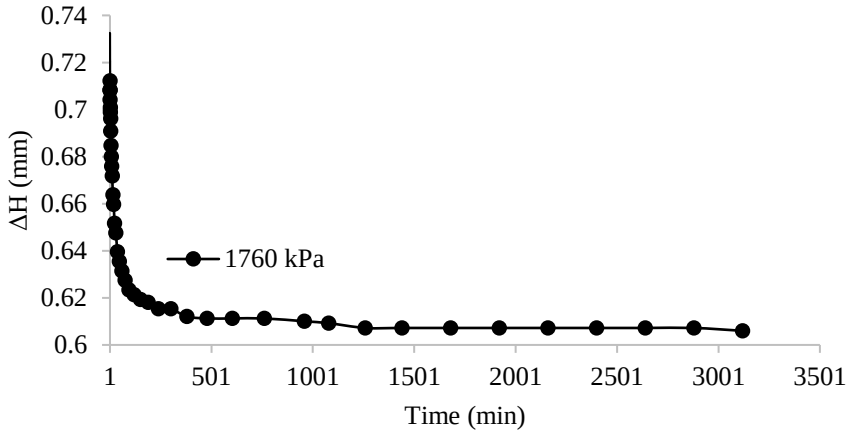


Figure A.170. ΔH versus time at 1760 kPa (unloading) for 5% CBAS treated specimen at 11% initial water content

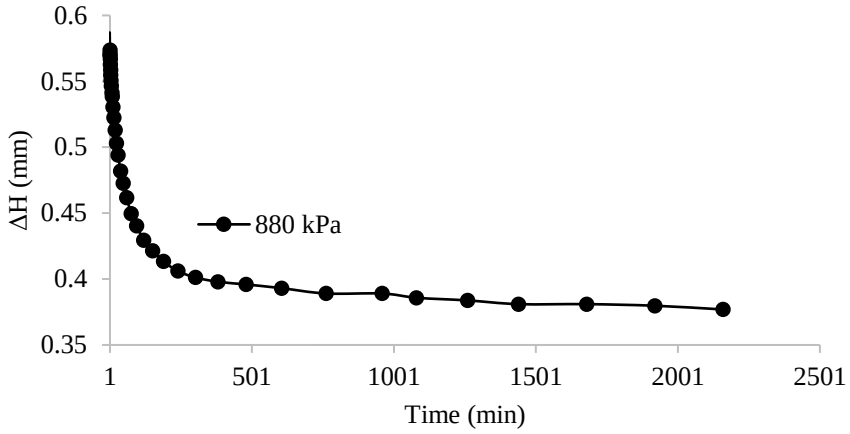


Figure A.171. ΔH versus time at 880 kPa (unloading) for 5% CBAS treated specimen at 11% initial water content

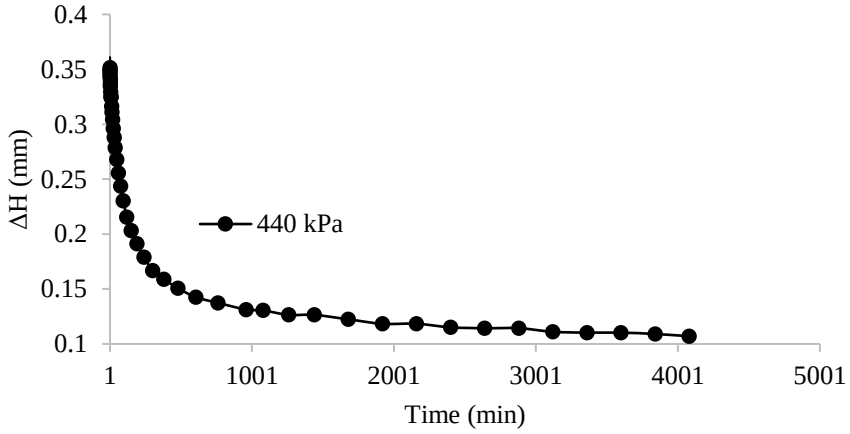


Figure A.172. ΔH versus time at 440 kPa (unloading) for 5% CBAS treated specimen at 11% initial water content

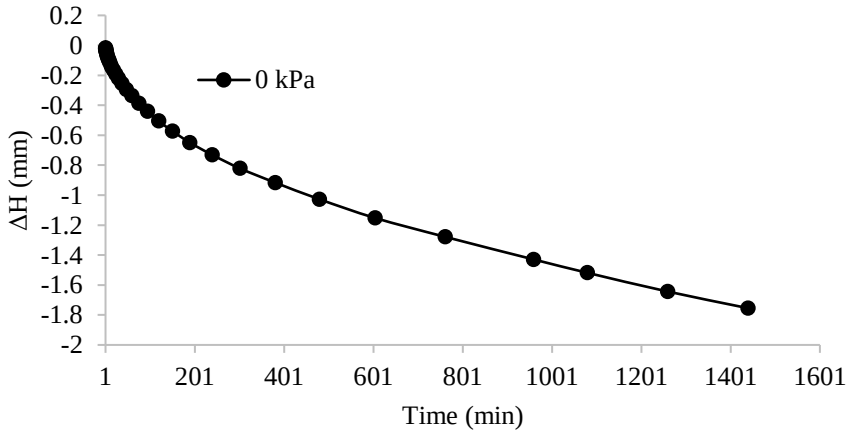


Figure A.173. ΔH versus time at 0 kPa (unloading) for 5% CBAS treated specimen at 11% initial water content

## Appendix E: Microstructural Observation

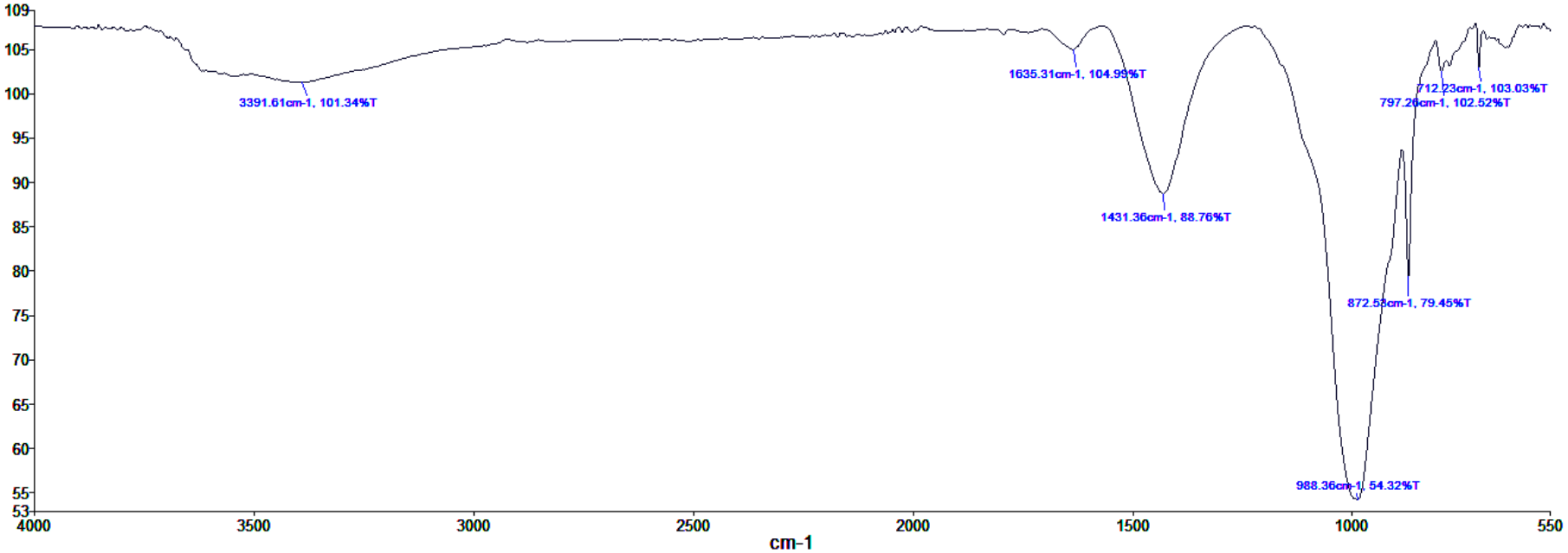


Figure A.174. FT-IR result of dry untreated specimen

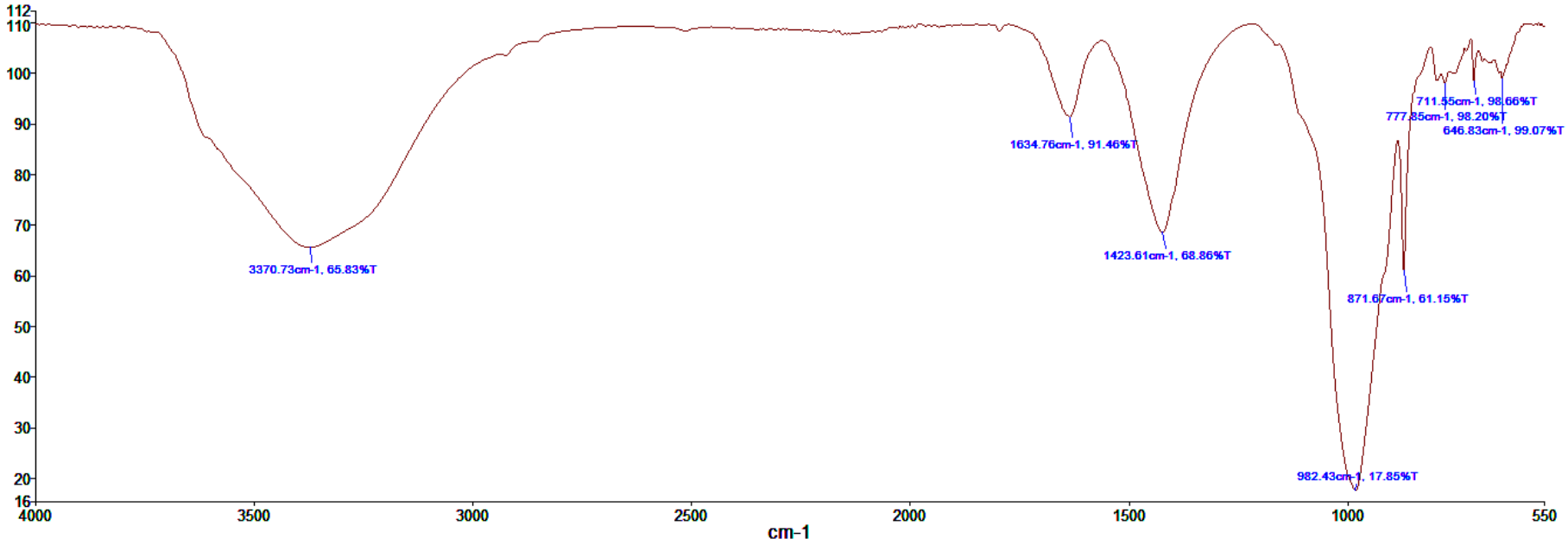


Figure A.175. FT-IR result of slurry untreated specimen

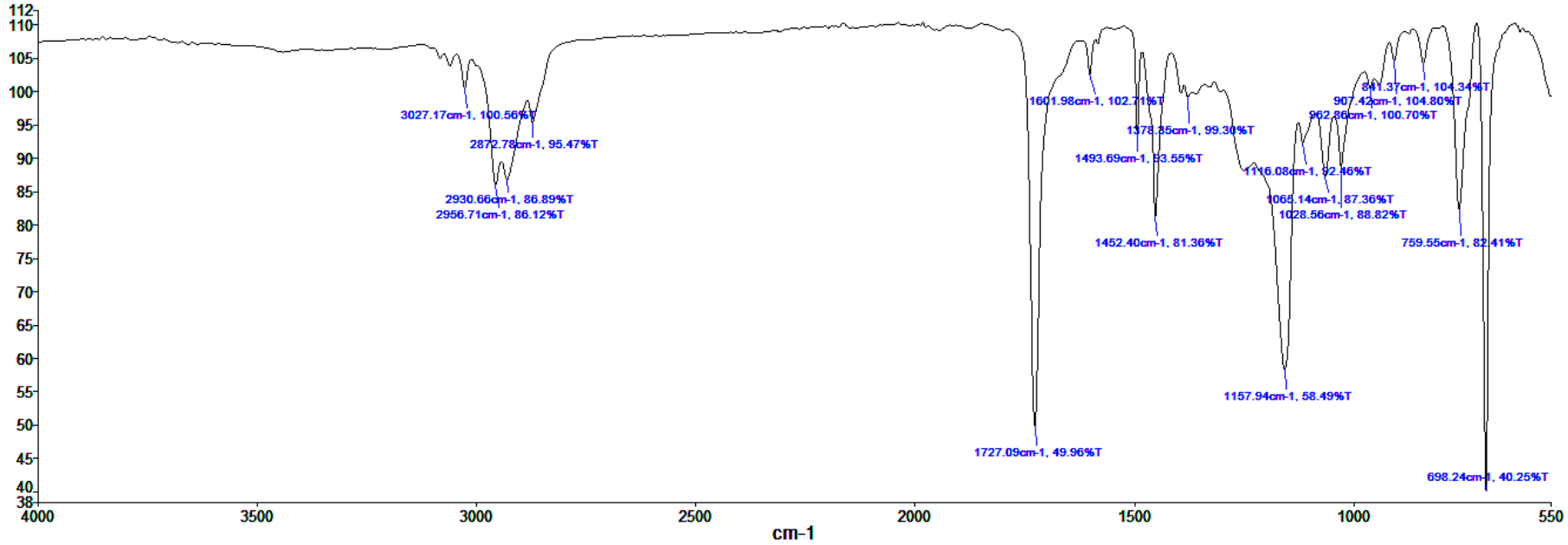


Figure A.176. FT-IR result of dry CBAS

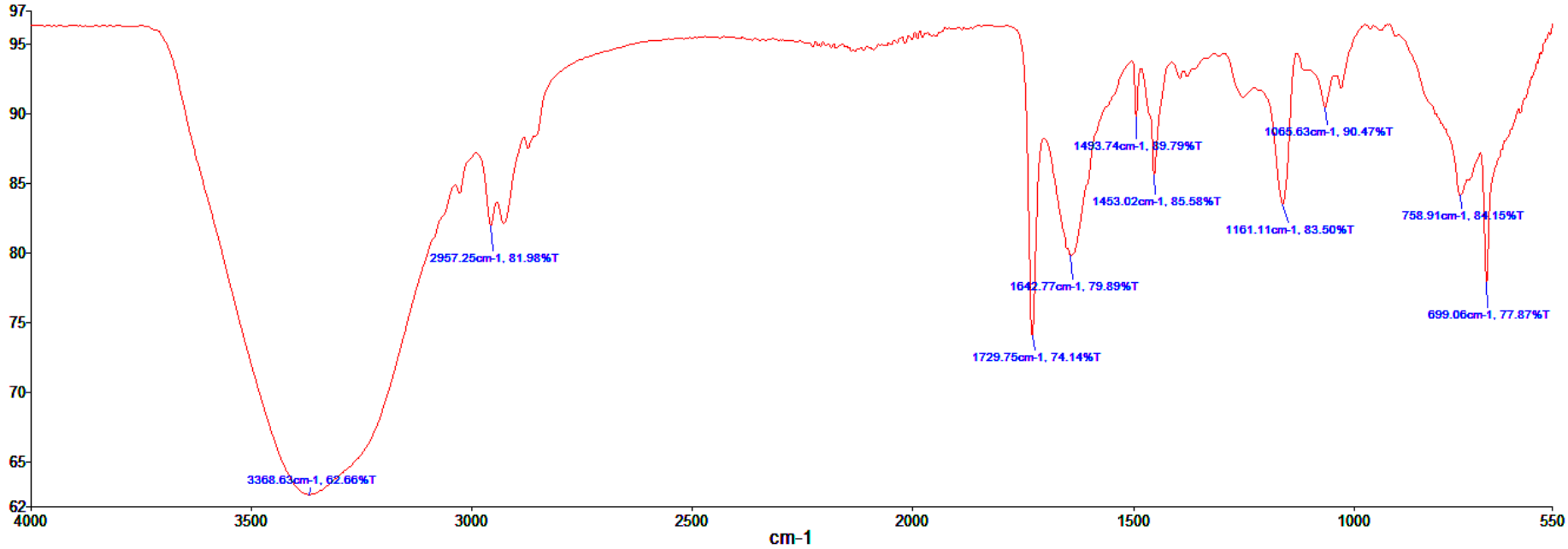


Figure A.177. FT-IR result of slurry CBAS

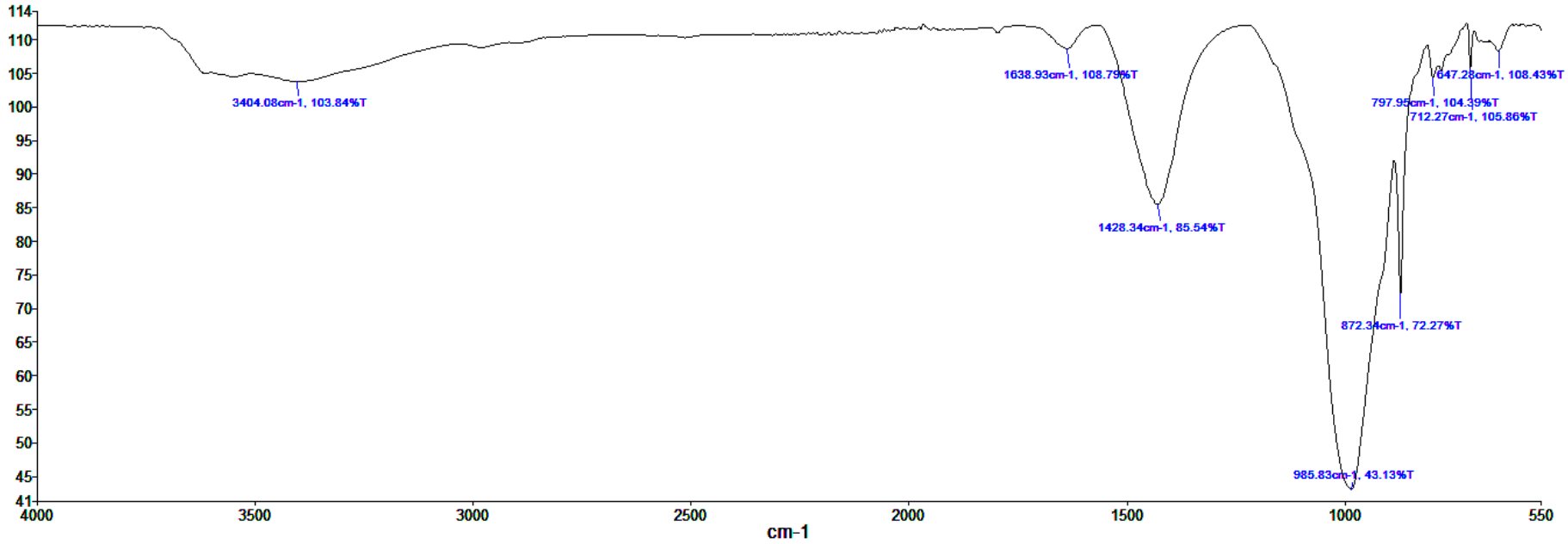


Figure A.178. FT-IR result of dry 0.5% CBAS treated specimen

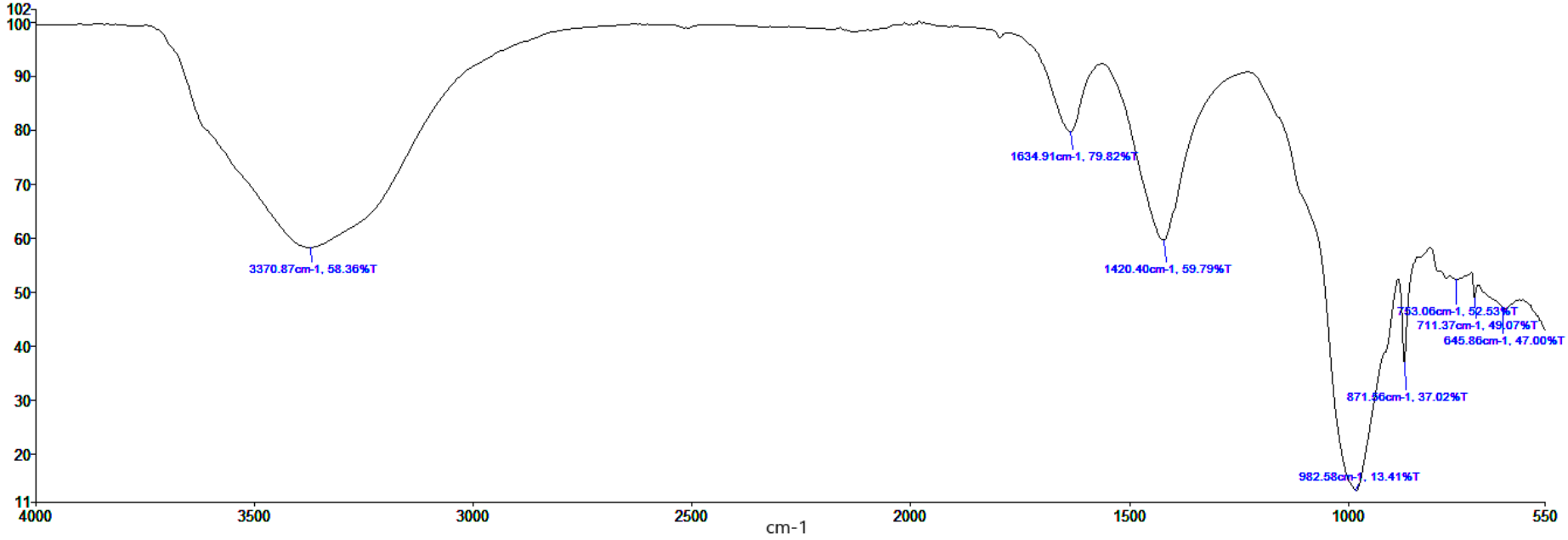


Figure A.179. FT-IR result of slurry 0.5% CBAS treated specimen

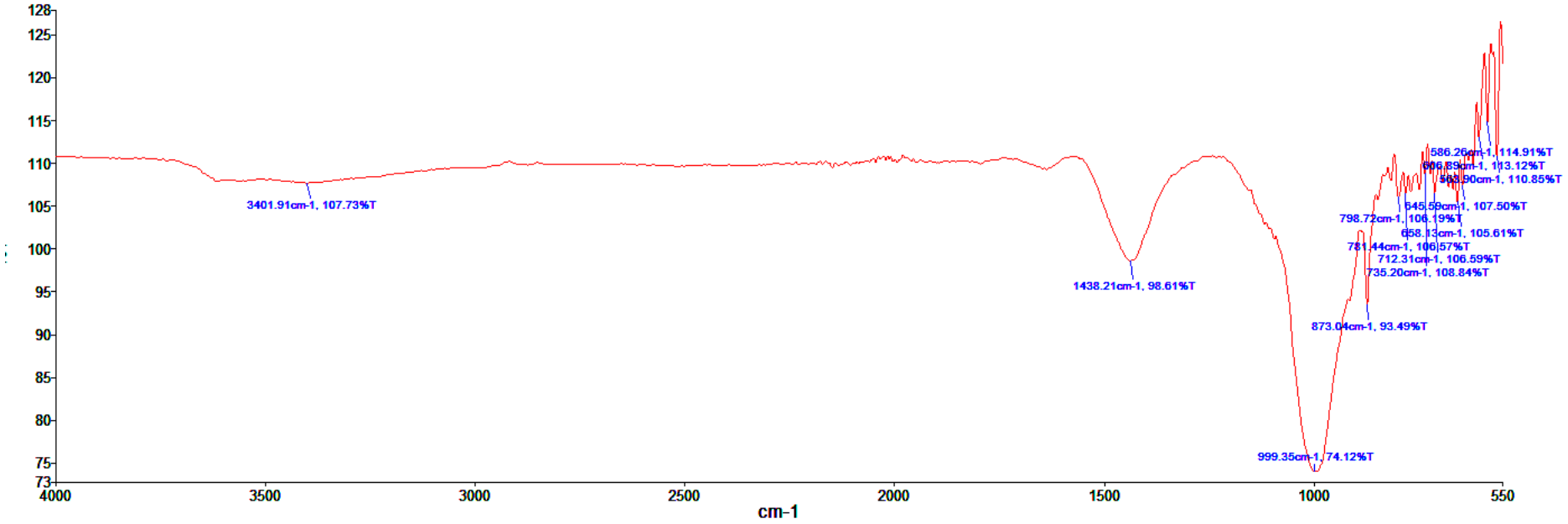


Figure A.180. FT-IR result of dry 1% CBAS treated specimen

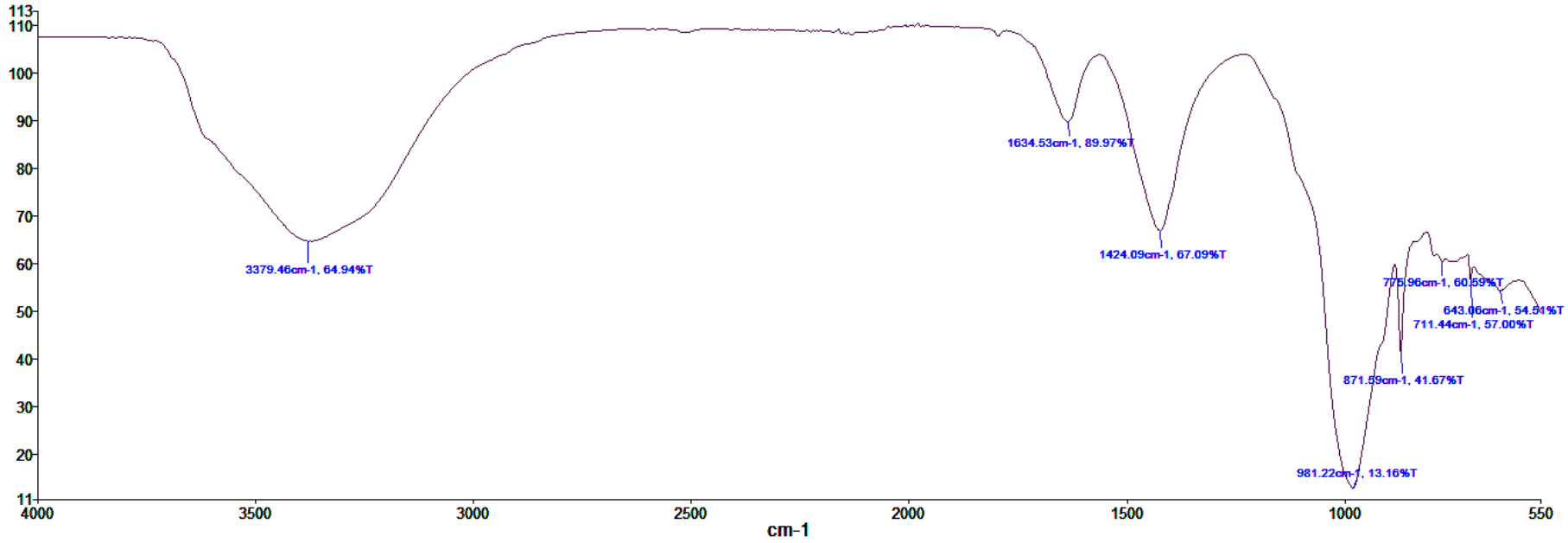


Figure A.181. FT-IR result of slurry 1% CBAS treated specimen

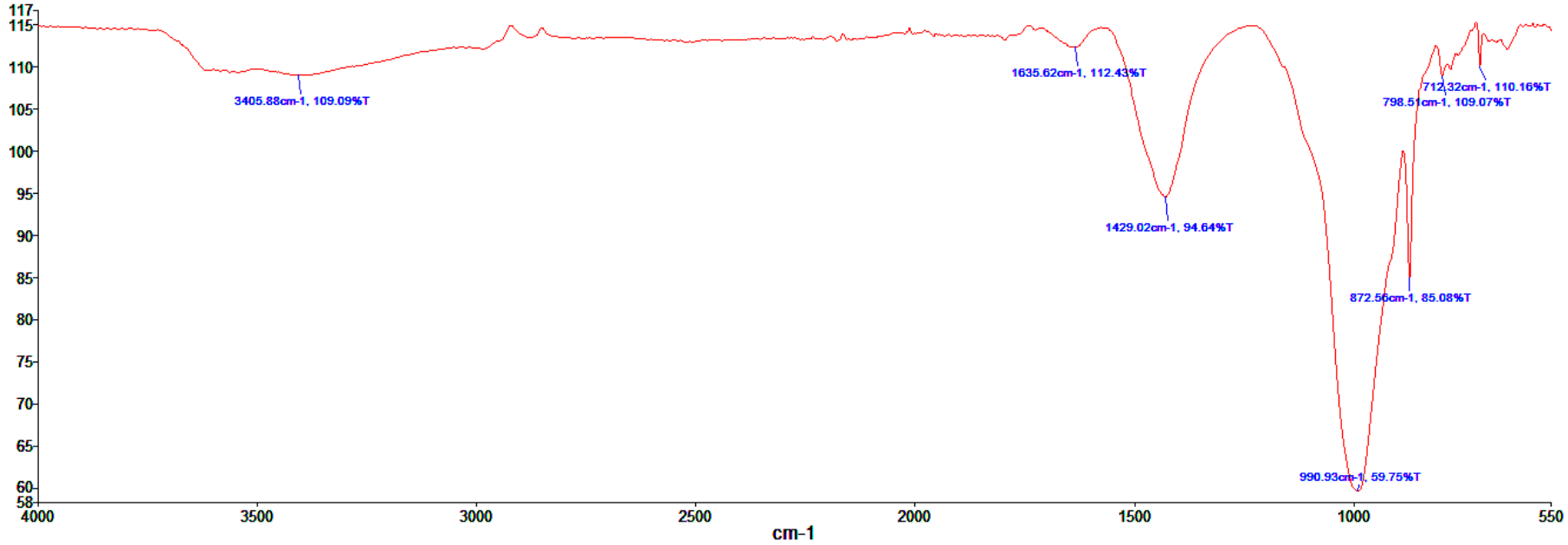


Figure A.182. FT-IR result of dry 2% CBAS treated specimen

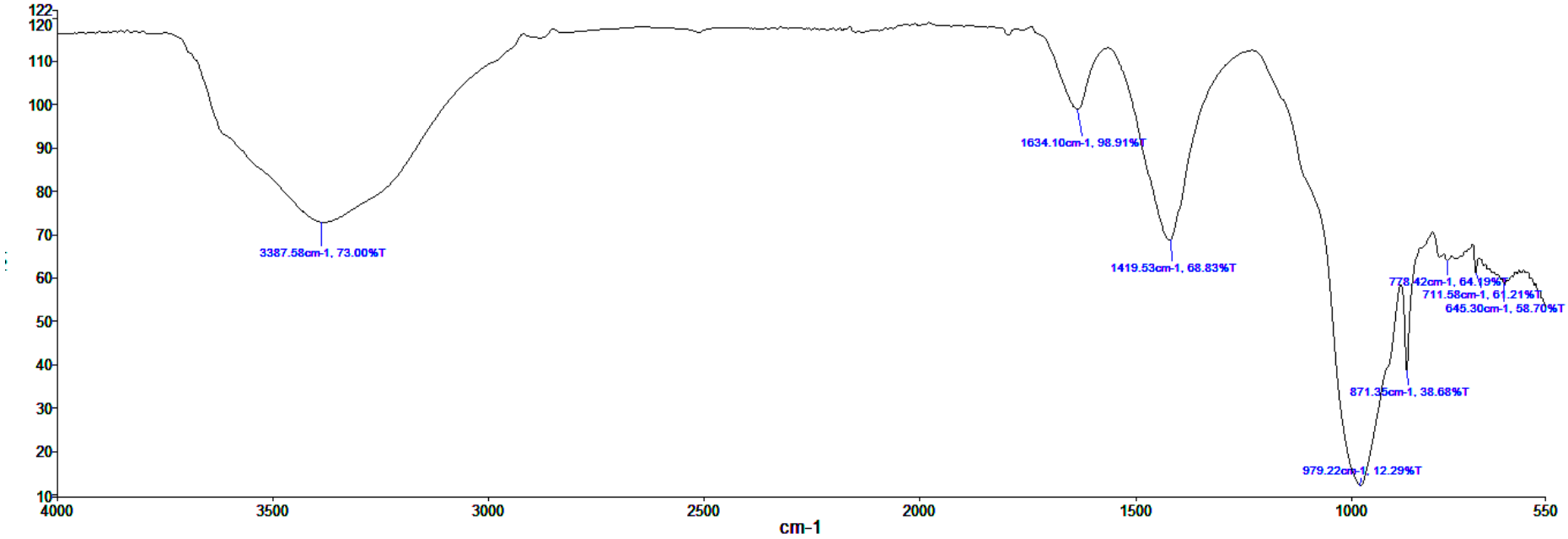


Figure A.183. FT-IR result of slurry 2% CBAS treated specimen

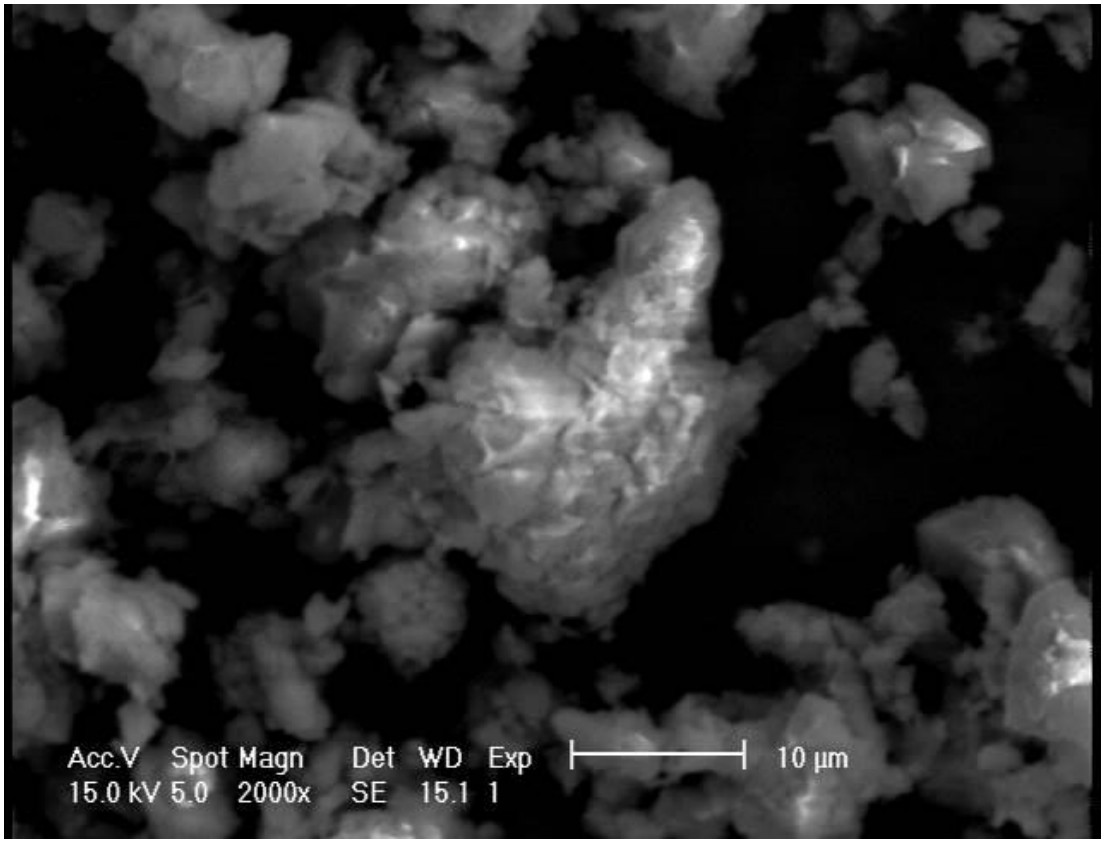

Figure A.184. Scanning electron microscopy of untreated specimen (2000x)

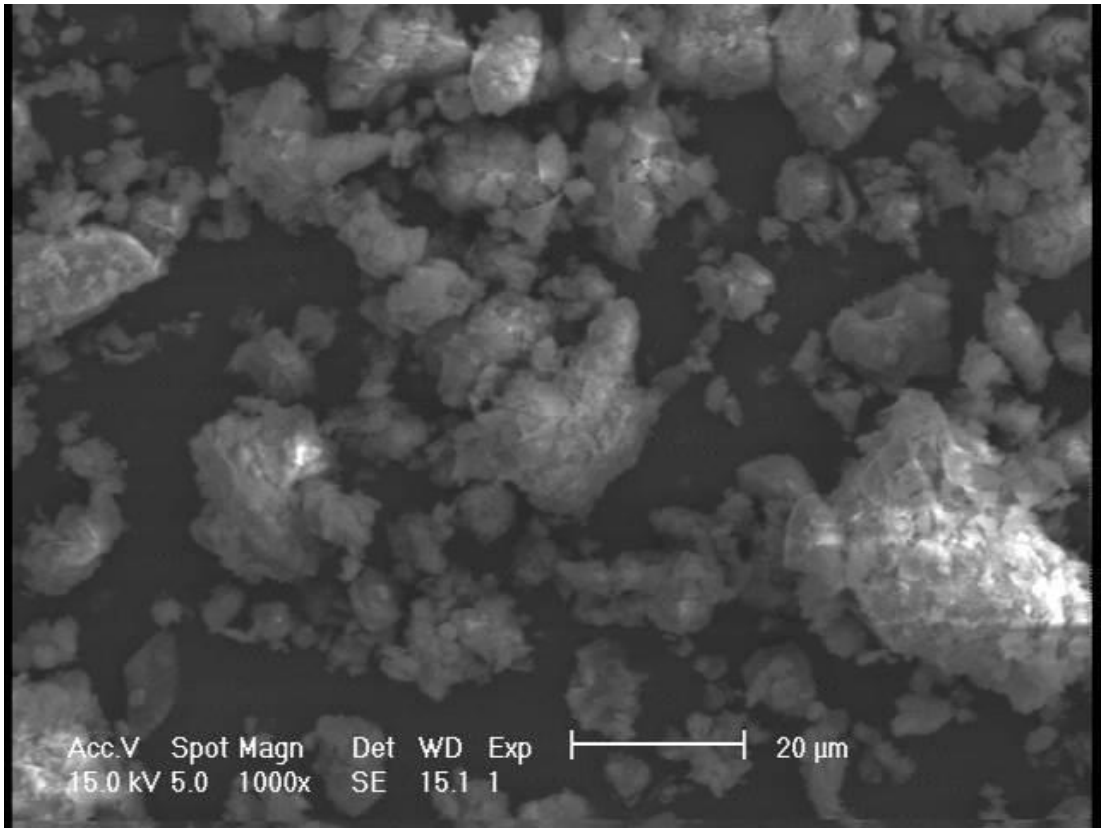

Figure A.185. Scanning electron microscopy of untreated specimen (1000x)

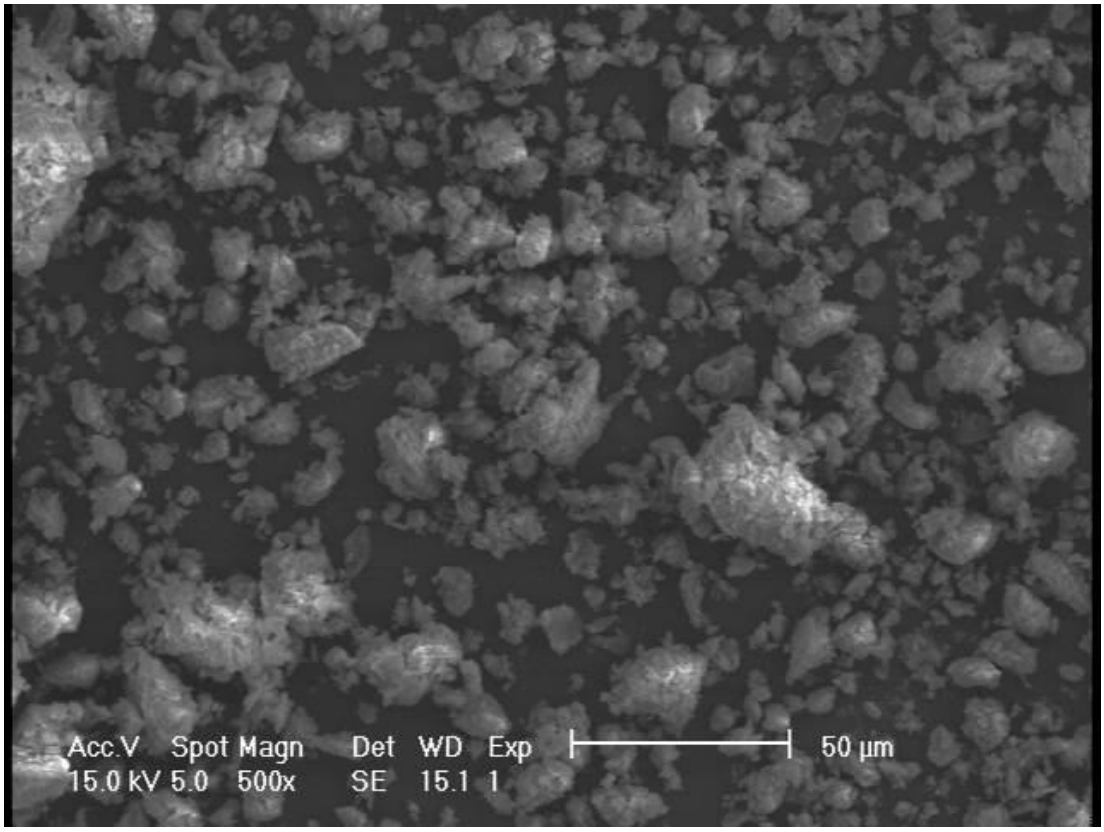


(a)

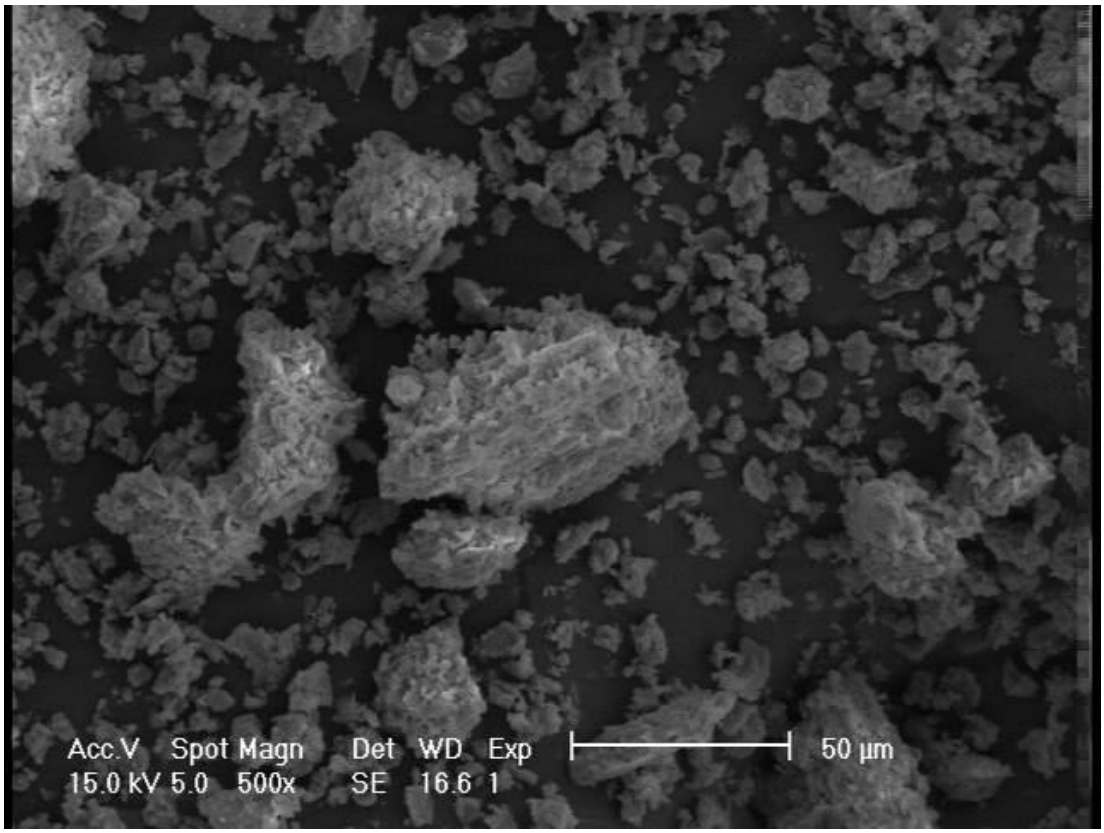


(b)

Figure A.186. Scanning electron microscopy of untreated specimen (500x)

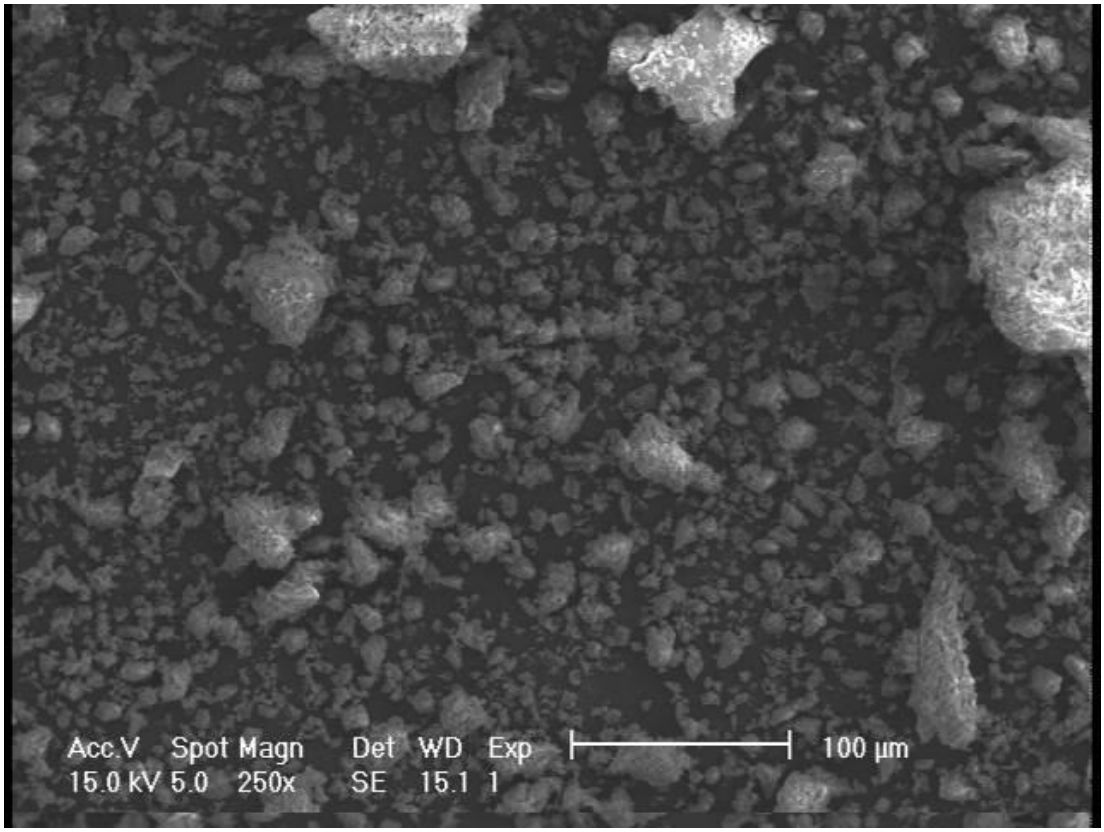

Figure A.187. Scanning electron microscopy of untreated specimen (250x)

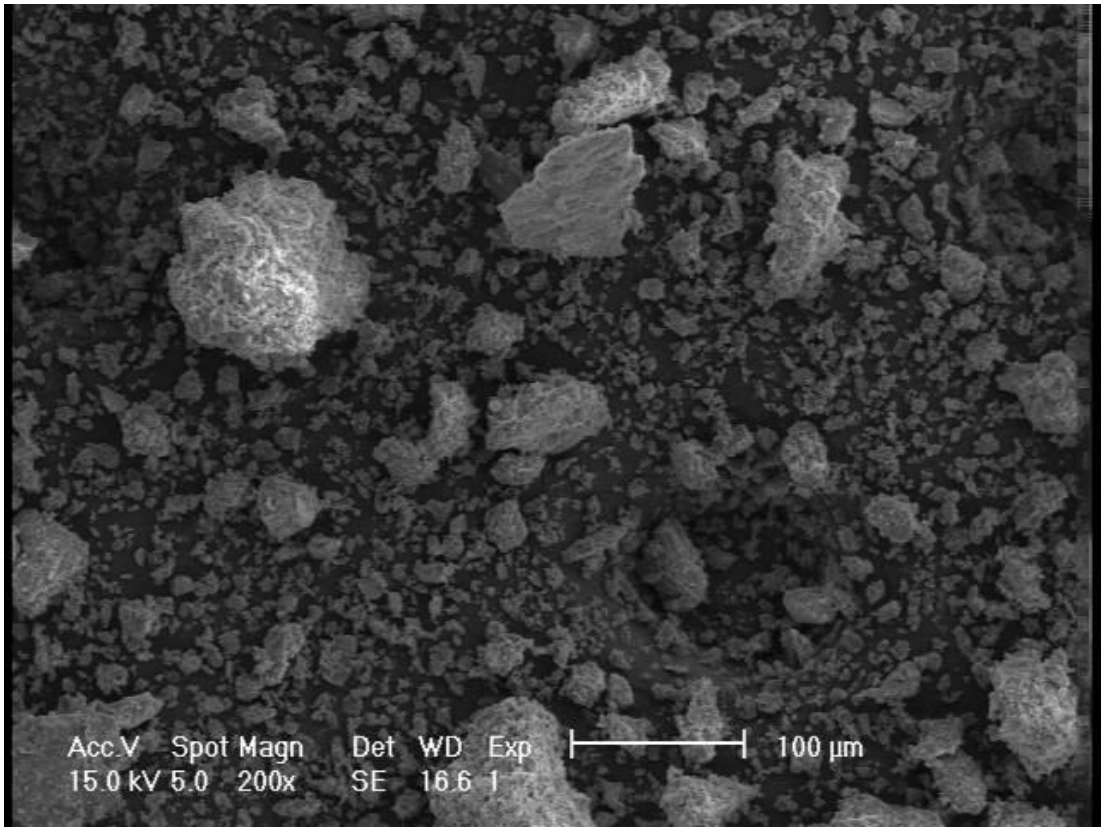

Figure A.188. Scanning electron microscopy of untreated specimen (200x)

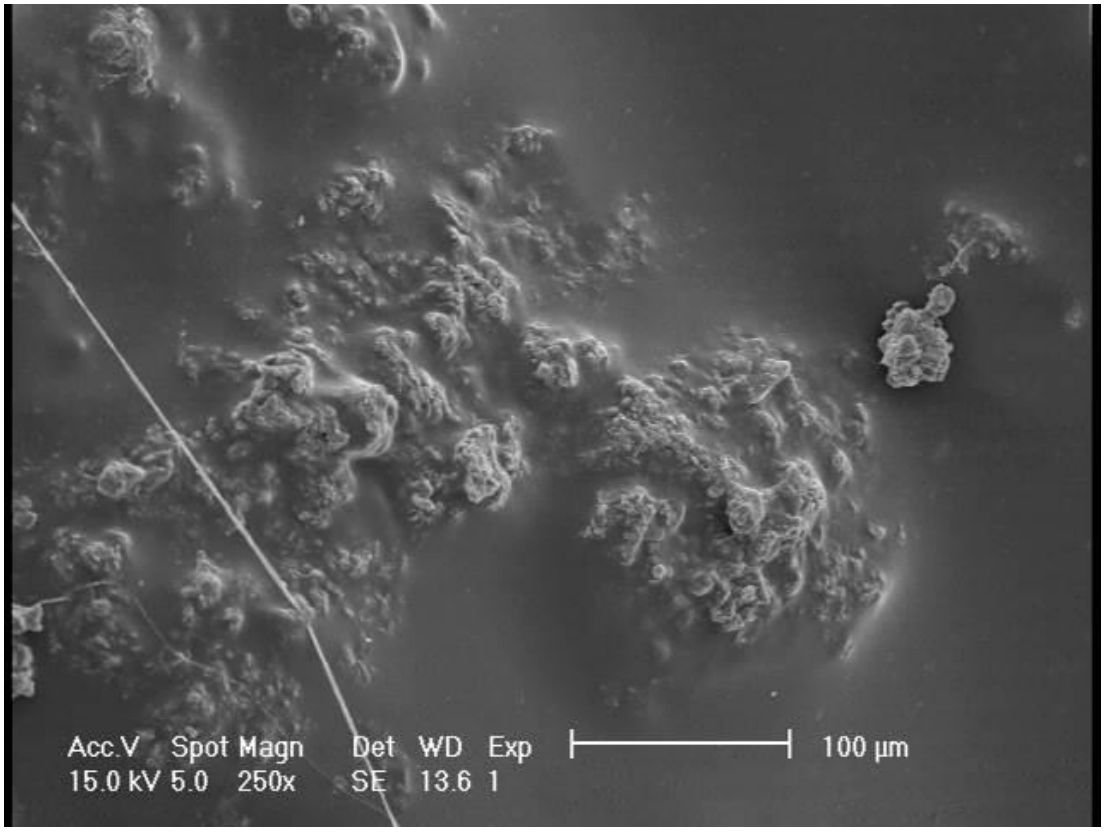

Figure A.189. Scanning electron microscopy of CBAS treated specimen (250x)

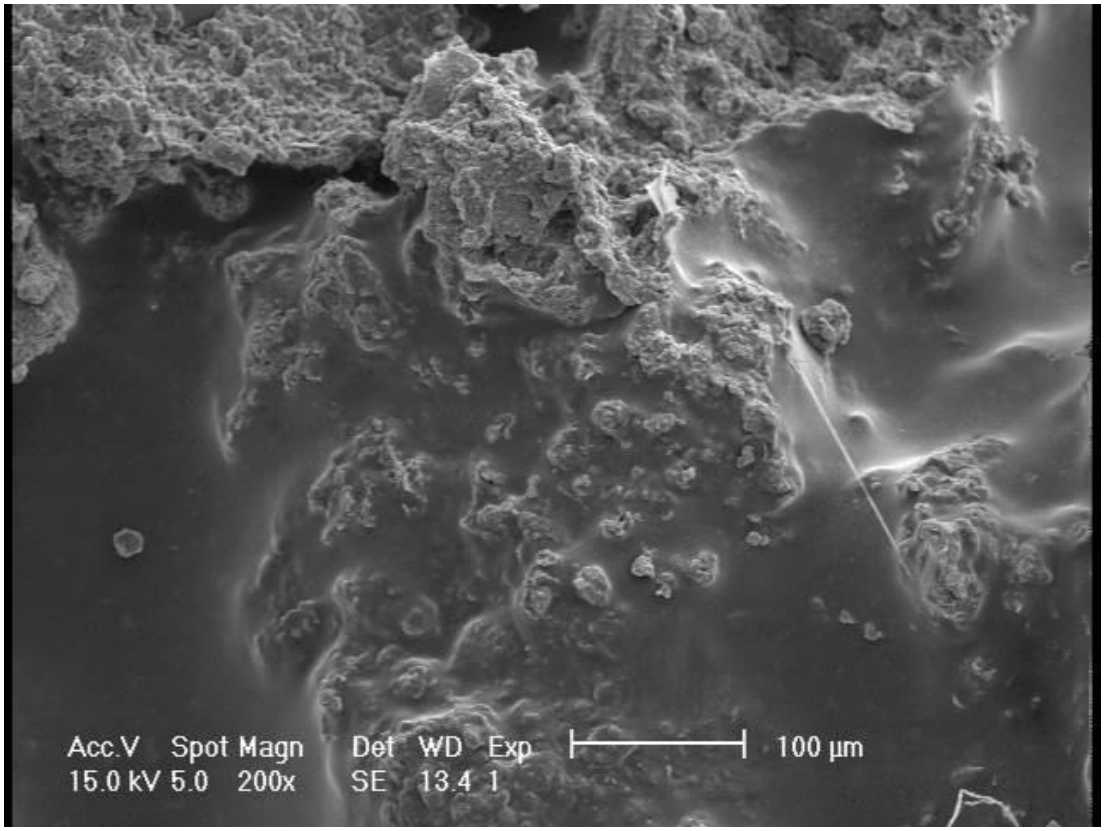

Figure A.190. Scanning electron microscopy of CBAS treated specimen (200x)

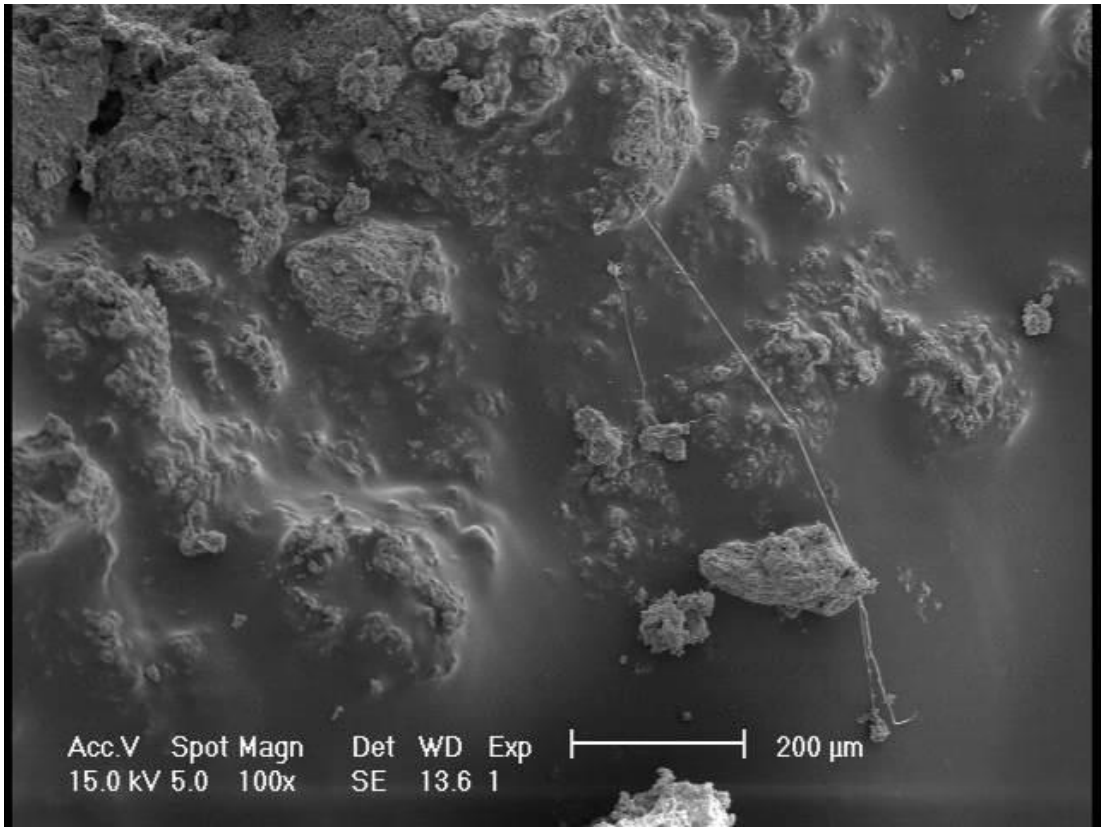


(a)

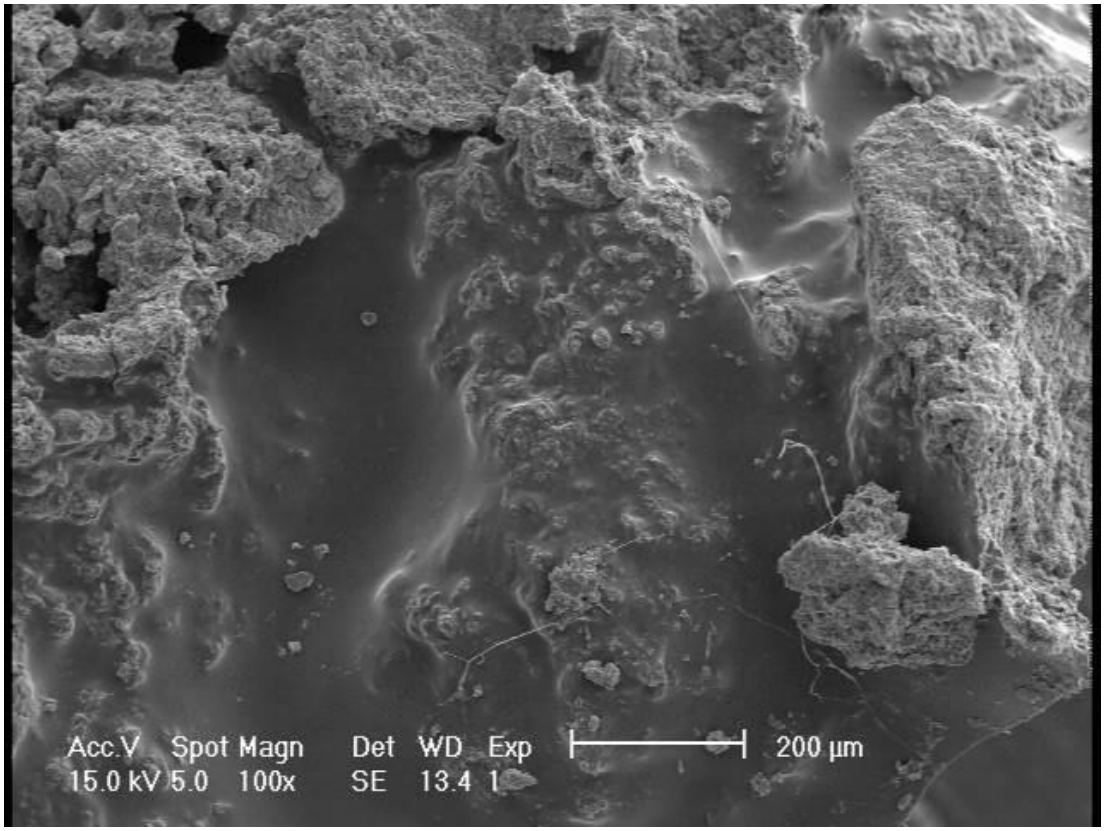


(b)

Figure A.191. Scanning electron microscopy of CBAS treated specimen (100x)